

## A large, dense pile of uncooked, golden-brown lentils. The lentils are small, oval-shaped, and have a slightly wrinkled texture. They are piled together, creating a mound that fills most of the frame. The background is a plain, light-colored surface.

S=C=NCC(C)CSC(=O)C  
S=C=NCC(C)CSC(=O)C  
S=C=NCC(C)CSC(=O)C  
S=C=NCC(C)CSC(=O)C  
S=C=NCC(C)c1ccccc1



## Propositions

1. Isothiocyanates (ITCs) with methylsulfinyl or methylsulfonyl groups represent ITCs with a good antimicrobial activity ( $\text{MIC} \leq 25 \mu\text{g/mL}$ ).  
(this thesis)
2. Total amino acid content of growth media influences the antimicrobial activity of ITCs.  
(this thesis)
3. The saying "eat your breakfast like an empress, lunch like a queen, and dine like a pauper" only applies for obese women to lose body weight. (Key refs: Jakubowicz *et al.* (2013) *Obesity* **21**, 2504-2512; Andersen *et al.* (2004) *Int. J. Obes.* **28**, 1338-1343)
4. Agroforestry with a financial compensation is a solution to reduce deforestation in Indonesia.
5. Dutch colonization of Indonesia has caused a false perception of typical Indonesian foods, including *sate ayam*, *ketjap manis*, and *sambal oelek*.
6. Social media addiction should be viewed as an illness and requires an appropriate rehabilitation treatment.

Propositions belonging to the thesis entitled:

Antimicrobial isothiocyanates from Brassicaceae glucosinolates

*Analysis, reactivity, and quantitative structure-activity relationships*

Silvia Andini

Wageningen, 06 November 2020





# **Antimicrobial isothiocyanates from Brassicaceae glucosinolates**

*Analysis, reactivity, and quantitative structure-  
activity relationships*

**Silvia Andini**

## **Thesis committee**

### **Promotor**

Prof. Dr J.-P. Vincken  
Professor of Food Chemistry  
Wageningen University & Research

### **Co-promotor**

Dr C. Araya-Cloutier  
Assistant professor, Laboratory of Food Chemistry  
Wageningen University & Research

### **Other members**

Prof. Dr V. Fogliano, Wageningen University & Research  
Dr N. Agerbirk, University of Copenhagen, Denmark  
Dr J.-W. Sanders, Unilever R&D, Wageningen  
Dr A.B.G. Bonnema, Wageningen University & Research

This research was conducted under the auspices of the Graduate School VLAG (Advanced studies in Food Technology, Agrobiotechnology, Nutrition and Health Sciences).

# **Antimicrobial isothiocyanates from Brassicaceae glucosinolates**

***Analysis, reactivity, and quantitative structure-  
activity relationships***

**Silvia Andini**

## **Thesis**

submitted in fulfilment of the requirements for the degree of doctor  
at Wageningen University  
by the authority of the Rector Magnificus,  
Prof. Dr A.P.J. Mol,  
in the presence of the  
Thesis Committee appointed by the Academic Board  
to be defended in public  
on Friday 6 November 2020  
at 1:30 pm in the Aula.

Silvia Andini

Antimicrobial isothiocyanates from Brassicaceae glucosinolates

*Analysis, reactivity, and quantitative structure-activity relationships*

208 pages.

PhD thesis, Wageningen University, Wageningen, The Netherlands (2020)

With references, with summary in English

ISBN 978-94-6395-454-9

DOI <https://doi.org/10.18174/526437>

---

# Abstract

---

Isothiocyanates (ITCs) are electrophilic phytochemicals naturally originating from glucosinolates (GSLs), the major phytochemicals in the plant family of Brassicaceae. ITCs are released when GSLs come in contact with myrosinase. This is part of the Brassicaceae defence system against their natural enemies. The aim of this thesis was to explore the potential of ITCs as natural antimicrobials, e.g. as food preservatives. For this, their production, analysis, reactivity, and (quantitative) structure-activity relationships were studied.

Fungal elicitation was studied as an attempt to increase content and structural diversity of GSLs. (Non-)pathogenic fungal elicitation, during Brassicaceae seed germination, did not increase structural diversity nor content of GSLs further than what could be obtained by germination alone. Meanwhile, non-elicited seedlings contained higher or equal GSL content compared to the untreated seeds. As GSLs were present in high abundance in Brassicaceae seeds, the seeds were employed as the source of antimicrobial ITCs via extraction of GSLs, followed by a myrosinase treatment. For this, a method to analyze GSLs and ITCs simultaneously using RP-UHPLC-ESI-MS<sup>n</sup> was developed and validated with 14 GSLs and 15 ITCs, consisting of 8 subclasses differing in side chain configuration. The method enabled monitoring the *in vitro* enzymatic conversion of GSLs to ITCs. Due to their electrophilicity, antimicrobial activity of ITCs was negatively affected by nucleophile richness of growth media. In nucleophile-poor growth media, antimicrobial activity of ITCs, particularly  $\alpha$ -(methylsulfinyl)alkyl ITC (MSITC) and  $\alpha$ -(methylsulfonyl)alkyl ITC (MSoITC), was remarkably improved by a factor of at least 4, compared to that in the nucleophile-rich. Of 9 ITC subclasses tested, MSITC and MSoITC were the most promising ones. Antimicrobial activity of MSITC and MSoITC was dependent on chain length. The short-chained MSITC and MSoITC had good antimicrobial activity (minimum inhibitory concentration, MIC  $\leq$  25  $\mu$ g/mL) against Gram<sup>-</sup> bacteria and Gram<sup>+</sup> bacteria, whereas the long-chained ones had good antimicrobial activity against Gram<sup>+</sup> bacteria and fungi. A QSAR study revealed that partial charge, polarity, reactivity, and shape were the main physicochemical properties defining the antimicrobial activity of ITCs. The developed QSAR models had good internal prediction power ( $Q^2_{adj} > 0.80$ ) and successfully predicted activity of ITC-rich Brassicaceae extracts.



---

## Table of contents

---

<b>Chapter 1</b>	General introduction	<b>1</b>
<b>Chapter 2</b>	Modulation of glucosinolate composition in Brassicaceae seeds by germination and fungal elicitation	<b>27</b>
<b>Chapter 3</b>	Simultaneous analysis of glucosinolates and isothiocyanates by RP-UHPLC-ESI-MS <sup>n</sup>	<b>71</b>
<b>Chapter 4</b>	The interplay between antimicrobial activity and reactivity of isothiocyanates	<b>103</b>
<b>Chapter 5</b>	QSAR-based physicochemical properties of isothiocyanate antimicrobials against Gram-negative and Gram-positive bacteria	<b>123</b>
<b>Chapter 6</b>	General discussion	<b>167</b>
<b>Summary</b>		<b>197</b>
<b>Acknowledgements</b>		<b>201</b>
<b>About the author</b>		<b>205</b>





# CHAPTER

# 1

---

## General Introduction

---

There is an urgent call to continuously discover new antimicrobial compounds, especially derived from nature. Plant secondary metabolites, so-called phytochemicals, involved in plant defense, potentially are new natural antimicrobial candidates, which can be useful to healthcare systems and food industries, as well as other industries. Isothiocyanates (ITCs) are typical phytochemicals involved in the defense system of the Brassicaceae family, a widely cultivated and economically important plant family. ITCs are released upon degradation of glucosinolates (GSLs) by the activity of myrosinase. ITCs, likewise GSLs, are structurally diverse. Reports on antimicrobial activity of ITCs and their potential application are limited to just a few ITCs. Considering the large structural diversity of ITCs, systematic investigations of structure-activity relationship of ITCs as antimicrobials are scarce. Furthermore, ITCs are electrophilic making them reactive towards nucleophiles, which are abundantly present in many food products and microbial growth media. The consequences of this have been relatively underexposed in scientific literature. This chapter addresses (i) the need for new natural antimicrobial compounds, (ii) structural diversity of GSLs and ITCs, including their analysis, (iii) occurrence of GSLs and ITCs, (iv) approaches to modulate structural diversity and content of GSLs in Brassicaceae seedlings, and (v) ITCs as potential natural antimicrobial candidates, also considering their reactivity.

## 1.1. The need for new natural antimicrobial compounds

Food industries are facing a continuous challenge to develop clean label and mildly processed, as well as safe and convenient food products, to meet consumer demands.<sup>1-3</sup> Furthermore, secondary shelf life of food products is an underestimated issue and receives less attention than primary shelf life.<sup>4</sup> Primary shelf life, often referred to as just shelf life, is the length of time after production and packaging during which a food product in the enclosed state stays at the required level of quality and safety under a well-defined storage condition. Secondary shelf life, so-called period after opening or open shelf life, is the length of time after opening of a food product during which it may be consumed at an acceptable quality and safety level. Released from manufacturers, food products should be microbiologically safe with zero or very low microbial contamination. Once opened, food products acquire microbial contamination from the environment and upon handling by consumers. Vinegar, sugar, and salt are often added to food products, not only for taste and flavor, but also for extending the secondary shelf life. Alternative ingredients for extending secondary shelf life of various food products (heated and raw) without influencing their sensory attributes are of great interest.

At the same time the world is facing the problem of antimicrobial resistance (AMR) and persistence causing the treatment of microbial infections to become more difficult, with a concomitant increase in the number of casualties.<sup>5</sup> In 2016, 700,000 deaths globally caused by AMR infections were estimated.<sup>6</sup> This number is predicted to grow to 10 million in 2050, along with a global economic cost of 100 trillion USD, if no action is taken to tackle the global AMR problem.<sup>6</sup>

Altogether, there is an urgent call to continuously discover new antimicrobial compounds to address challenges faced by food industries for obtaining natural food preservatives, and by healthcare systems for combatting AMR pathogens.

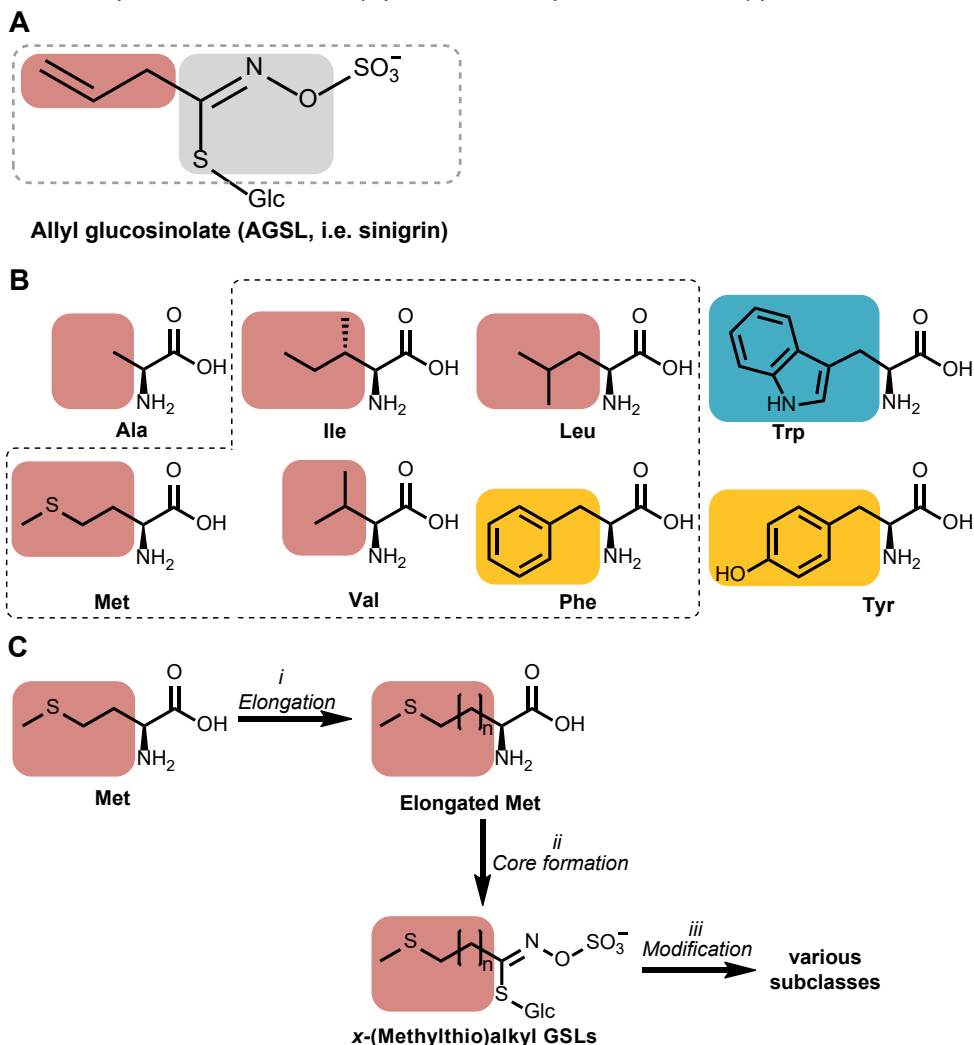
## 1.2. Structural diversity of GSLs and ITCs

ITCs have been known to have antifungal and antibacterial properties since 1946.<sup>7</sup> Although antimicrobial properties of ITCs have been documented in many reports since then,<sup>8-20</sup> many ITCs with different structures remain uninvestigated. In nature, ITCs are generated from their precursors, namely GSLs, which will be discussed first.

### 1.2.1. Classification of GSLs

A GSL is a (Z)-thiohydroximate with a sulfate ester group at the oxygen and a glucosyl residue at the sulfur (**Figure 1.1A**).<sup>21</sup> GSLs are biosynthesized from amino acids. Based on the side chain variation of the amino acids (**Figure 1.1B**), GSLs

are simply classified into 3 classes: aliphatic (derived from Ala, Ile, Leu, Met, Val), benzenic (derived from Phe, Tyr), and indolic (derived from Trp).<sup>21-23</sup>

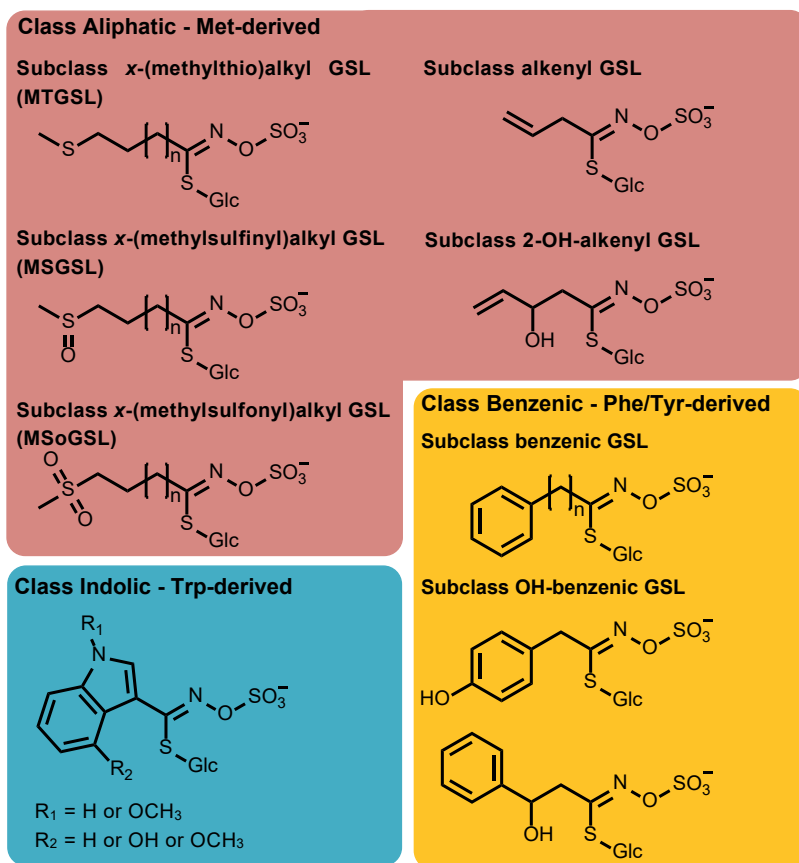


**Figure 1.1.** The most widely studied GSL, namely allyl GSL (AGSL, i.e. sinigrin). The moieties in grey shade, red shade, and grey-dotted-line box represent the (Z)-thiohydroximate, the side chain, and the aglucone, respectively (A). Amino acid precursors of GSLs. The moieties in colored boxes represent the side chains of GSLs from the aliphatic (red), benzenic (yellow), and indolic (blue) class. Amino acids indicated in the black-dotted-line box are those which can be elongated, and the rest are those which cannot be elongated (B). Simplified biosynthesis pathway of aliphatic GSLs, as a representative class, illustrated by Met-derived GSLs (C).

Biosynthesis of GSLs consists of three major stages (**Figure 1.1C**).<sup>22-26</sup> The first stage is chain elongation of amino acids. Only Met, Val, Leu or homoVal, Ile, and Phe can be elongated. Met can undergo extraordinary chain elongation up to

C11 (undecyl).<sup>27</sup> The second stage is formation of the core GSL structure. The third stage comprises secondary modifications of the side chain, including oxidation, desaturation, hydroxylation, and methoxylation.<sup>24,28</sup> In addition, esterification at the thioglucosyl (S-Glc) moiety with sinapic acid has been reported.<sup>29-31</sup> By mid-2018, 88 GSLs were well characterized by nuclear magnetic resonance (NMR) spectroscopy and mass spectrometry (MS), and 49 GSLs had been partially characterized.<sup>21</sup> Most GSLs are derived from Met, Phe/Tyr, and Trp.

It is clear that variation in GSLs originates from their amino acid precursors and modification to the side chains. The 3 GSL classes can be divided into various subclasses as shown in **Figure 1.2** for common GSLs. It should be noted that combinations of secondary modification can occur resulting in more subclasses, which are not displayed, for example x-(methylsulfinyl)alkenyl GSL (MS-en-GSL).



**Figure 1.2.** Classification of the most common GSLs (Met-, Phe/Tyr-, and Trp-derived). Different color shadings indicate different classes.

### 1.2.2. Enzymatic degradation products of GSLs

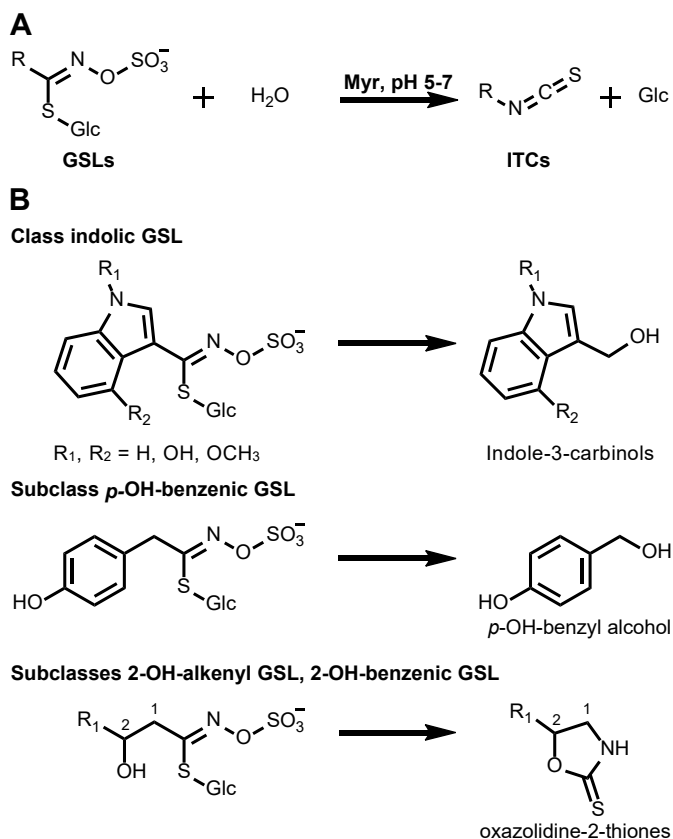
In all Brassicaceae plant tissues, GSLs co-exist with myrosinase, so-called thioglucosidase (EC 3.2.1.147). Myrosinase is expressed in myrosin cells, located next to the GSL containing cells.<sup>32</sup> Consequently, upon cell damage, GSLs come in contact with myrosinase and are then degraded to form ITCs, as shown in **Figure 1.3A**. Therefore, the (sub)classification of ITCs is similar to that of GSLs, except for the indolic class and subclasses that have been modified by hydroxylation.<sup>33-37</sup> Indolic GSLs and *p*-OH-benzyl GSL (*p*-OH-BGSL, i.e. glucosinalbin) form unstable ITCs, which react spontaneously with water, forming indol-3-carbinols and *p*-OH-benzyl alcohol, respectively, whereas GSLs hydroxylated at the C2-position form unstable ITCs, which undergo spontaneous cyclization, forming oxazolidine-2-thiones (**Figure 1.3B**).<sup>33-35,38</sup> *p*-OH-Benzyl ITC (*p*-OH-BITC) can coexist with *p*-OH-benzyl alcohol, but the majority of the unstable ITCs are untraceable. Overall, the side chain of GSLs determines whether an ITC is formed, with the majority of GSLs forming ITCs. Besides this, other factors determine the kind of degradation products, but for this thesis research the other products are not relevant. Briefly, pH, ferrous ion (Fe<sup>2+</sup>), specifier proteins (endogenous proteins that alter the arrangement of aglucones into nitriles, epithionitriles, or thiocyanates) determine the degradation products.<sup>39-40</sup> Under controlled conditions at pH 5-7, in the absence of Fe<sup>2+</sup> and specifier proteins, ITCs are the dominant degradation products.<sup>24,41-42</sup> The GSL-myrosinase system, also known as the “mustard oil bomb”, provides plants with an effective defense against pathogens,<sup>43-44</sup> and ITCs are considered to be the most potent degradation products.<sup>45-46</sup>

### 1.2.3. Analysis of GSLs and ITCs

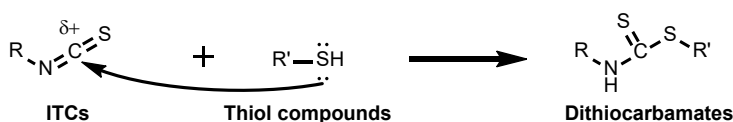
To advance the investigation of ITCs as potential natural antimicrobials, reliable and efficient analysis of GSLs and ITCs is important. The analysis of GSLs and ITCs is often performed in two separate analyses: GSLs by liquid chromatography (LC), and ITCs by gas chromatography (GC) due to their volatility.<sup>21,27,47</sup> However, ITCs, including the most widely studied allyl ITC (AITC), 4-(methylsulfinyl)butyl ITC (4-MSITC, i.e. sulforaphane), and benzyl ITC (BITC), are thermally unstable, and consequently LC is preferred.<sup>48-50</sup> In this respect, LC analysis seems more robust. Nevertheless, LC analysis requires a pre-column derivatization step, which often involves thiol compounds (e.g. *N*-acetyl-L-cysteine, *N*-(*tert*-butoxycarbonyl)-L-cysteine methylester), employing the electrophilic property of ITCs and the nucleophilic property of thiol groups (**Figure 1.4**).

The electrophilic carbon makes ITCs readily react with nucleophiles, such as thiol (–SH), amine (–NH<sub>2</sub>), and hydroxyl (–OH) groups, which thereafter form dithiocarbamates, thioureas, and *O*-thiocarbamates, respectively.<sup>51-52</sup> The reaction with thiol groups is 10<sup>3</sup> to 10<sup>4</sup> times faster than that with amine or hydroxyl groups.<sup>51</sup> Reaction between ITCs and nucleophiles is pH dependent. Conditions at pH higher than the p*K*<sub>a</sub> of the nucleophiles promote the reaction. In general, the

reaction equilibrium between ITCs and thiol compounds, e.g. glutathione (GSH,  $pK_a$  (-SH) 9.42), cysteine (Cys,  $pK_a$  (-SH) 8.14), and *N*-acetyl-L-cysteine (NAC,  $pK_a$  (-SH) 9.53), is reached within 15 min, at 37 °C and physiological pH (i.e. pH 7.4).<sup>53</sup> This indicates that Cys residues can spontaneously react with ITCs, even under relatively mild conditions, due to the high polarizability and accessibility of the low-energy “d orbitals” of the cysteinyl sulfur and the delocalization of electrons over the  $-N=C=S$   $\pi$ -bond system.<sup>54</sup> In contrast, amines are more difficult to polarize and, thus, the potential energy barrier associated with the reaction of the  $-N=C=S$  moiety and  $-NH_2$  is relatively higher.<sup>54</sup>



**Figure 1.3.** Enzymatic degradation of GSLs by myrosinase (Myr) forming ITCs at pH 5-7 (**A**) or other degradation products (in grey) depending on the side chain of GSLs (**B**).



**Figure 1.4.** Reaction scheme of electrophilic ITCs and nucleophilic thiol compounds.

Derivatization gives ITCs a distinct UV absorption maximum and enhances their ionization upon MS.<sup>55-56</sup> Few LC methods with UV detection or MS detection for simultaneous analysis of GSLs and ITCs have been developed.<sup>57-59</sup> Those methods were limited to just a few pairs of GSLs and ITCs present in certain plant species. Simultaneous analysis of GSLs and ITCs enhances efficiency in sample and instrument preparation, as well as the analysis itself. Considering the large structural diversity of GSLs and ITCs, the simultaneous analysis should be developed for a more diverse set of GSLs and ITCs. Furthermore, the new method should be compatible with degradation by myrosinase, so that it would support studies on understanding *in vitro* enzymatic GSL conversion to ITCs, both in standard mixtures and in plant extracts, under controlled conditions.

### 1.3. Occurrence of GSLs and ITCs

GSLs are typical phytochemicals of the Brassicaceae (i.e. Cruciferae) family, including plant species such as *Sinapis alba* (yellow mustard), *Brassica napus* (rapeseed), and *B. oleraceae* (broccoli, cauliflower, etc.), and related families within the order Capparales.<sup>28</sup> GSL profiles of Brassicaceae plants vary widely between species and, within the species, between varieties. Often, a plant variety contains only few (1-4) GSLs in high abundance.<sup>42,60</sup> Five widely consumed Brassicaceae species were used as representatives in this PhD study, each having their own specific GSL profile (structural diversity) and GSL content (**Table 1.1**).




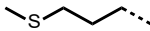
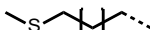
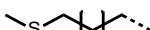
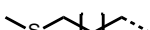
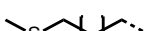


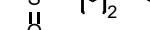
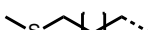



**Table 1.1.** GSL composition of several Brassicaceae seeds studied in this thesis.

Plant species	Subclass of GSL	Predominant GSL, trivial name	Content (μmol/g DW)	Ref.
<i>Sinapis alba</i> (yellow mustard)	OH-Benzenic GSL	<i>p</i> -OH-Benzyl GSL, <u>glucosinabin</u>	110-210	61
<i>Brassica napus</i> (rapeseed)	OH-Indolic GSL	4-OH-Indol-3-ylmethyl GSL, <u>4-OH-glucobrassicin</u>	4	62
	2-OH-Alkenyl GSL	( <i>R</i> )-2-OH-Butenyl GSL, <u>progoitrin</u>	3	
<i>B. juncea</i> var. <i>rugosa rugosa</i> (amsoy)	Alkenyl GSL	3-Butenyl GSL, <u>Gluconapin</u>	66-90	63
	Alkenyl GSL	Allyl GSL, <u>sinigrin</u>	20-37	
<i>B. oleracea</i> var. <i>botrytis</i> (broccoli)	MSGSL	4-(Methylsulfinyl)butyl GSL, <u>glucoraphanin</u>	83	64
<i>Camelina sativa</i> (German sesame)	MSGSL	10-(Methylsulfinyl)decyl GSL, <u>glucocamelinin</u>	10-19	65

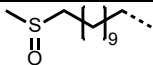
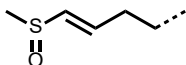
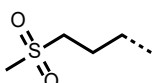
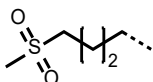
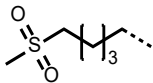
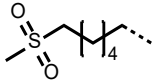
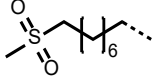
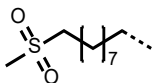
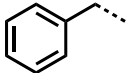
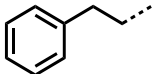
In some widely consumed Brassicaceae species, the predominant GSLs do not form ITCs as the major degradation product (e.g. *Brassica napus*). In contrast, many ITCs with potential as antimicrobials are formed from GSLs present in wild and/or ornament (flowering) Brassicaceae species (e.g. *Arabis* spp., *Rorippa* spp.).<sup>66</sup> **Table 1.2** lists ITCs of interest in this thesis and their occurrence in nature.

The authentic ITC standards of the majority of these are commercially available and the characterization of their GSL precursors has been reviewed.<sup>21,27</sup>

**Table 1.2.** Diverse ITCs and the Brassicaceae sources of their GSL precursors.

R-group	ITC <sup>a</sup>	Occurrence <sup>b</sup>	Ref.
<b>Class Aliphatic ITC</b>			
<b>Subclass Alkenyl ITC</b>			
	Allyl ITC (AlTC)	<i>B. juncea</i> , <i>B. nigra</i> , <i>B. oleracea</i> , <i>R. amphibia</i> , <i>R. sylvestris</i>	63,67-69
	3-Butenyl ITC (BuITC)	<i>B. napus</i> , <i>B. rapa</i> , <i>R. amphibia</i>	62,67,69-70
	4-Pentenyl ITC (PeITC)	<i>B. napus</i> , <i>R. amphibia</i>	69,71-72
<b>Subclass x-(Methylthio)alkyl ITC (MTITC)</b>			
	3-(Methylthio)propyl ITC (3-MTITC), <u>iberverin</u>	<i>I. sempervirens</i>	73
	4-(Methylthio)butyl ITC (4-MTITC), <u>erucin</u>	<i>D. borealis</i> , <i>E. sativa</i> , <i>Ra. raphanistrum</i>	67-68,74-77
	5-(Methylthio)pentyl ITC (5-MTITC), <u>berteroin</u>	<i>A. sinuata</i> , <i>Be. incana</i> , <i>D. borealis</i> , <i>De. velebitica</i>	77-80
	6-(Methylthio)hexyl ITC (6-MTITC), <u>lesquerellin</u>	<i>D. borealis</i> , <i>L. lasiocarpa</i> , <i>Lo. maritima</i> , <i>W. japonica</i>	77,81-83
	9-(Methylthio)nonyl ITC (9-MTITC)	<i>Ar. purpurea</i>	84-85
<b>x-(Methylsulfinyl)alkyl ITC (MSITC)</b>			
	3-(Methylsulfinyl)propyl ITC (3-MSITC), <u>iberin</u>	<i>B. oleracea</i> , <i>I. amara</i> , <i>L. fendleri</i> , <i>Ra. raphanistrum</i>	67-68,76,83,86-89
	4-(Methylsulfinyl)butyl ITC (4-MSITC), <u>sulforaphane</u>	<i>B. oleracea</i> , <i>Er. allionii</i> , <i>Le. draba</i> , <i>Ra. raphanistrum</i>	67-68,76,83,88,90-91
	5-(Methylsulfinyl)pentyl ITC (5-MSITC), <u>allysin</u>	<i>Alyssum</i> spp, <i>A. sinuata</i> , <i>B. napus</i> , <i>W. japonica</i>	76,78,92-95
	6-(Methylsulfinyl)hexyl ITC (6-MSITC), <u>hesperin</u>	<i>D. borealis</i> , <i>Di. wislizenii</i> , <i>Er. cheiri</i> , <i>H. matronalis</i> , <i>Ra. raphanistrum</i> , <i>W. japonica</i>	76-77,83,92,96-97
	8-(Methylsulfinyl)octyl ITC (8-MSITC), <u>hirsutin</u>	<i>Ar. hirsuta</i> , <i>D. borealis</i> , <i>R. amphibia</i> , <i>R. sylvestris</i> , <i>R. indica</i>	69,77,98-99
	9-(Methylsulfinyl)nonyl ITC (9-MSITC), <u>arabin</u>	<i>Ar. alpina</i> , <i>C. sativa</i> , <i>D. borealis</i> , <i>R. indica</i>	65,77,99-100
	10-(Methylsulfinyl)decyl ITC (10-MSITC), <u>camelinin</u>	<i>C. dentata</i> ( <i>C. alyssum</i> ), <i>C. microcarpa</i> , <i>C. sativa</i> , <i>Ca. bursa-pastoris</i>	65,69,83,99,101



R-group	ITC <sup>a</sup>	Occurrence <sup>b</sup>	Ref.
	11-(Methylsulfinyl)undecyl ITC (11-MSITC)	<i>C. sativa</i> , <i>N. paniculata</i>	65,102
<b>x-(Methylsulfinyl)alkenyl ITC (MS-en-ITC)</b>			
	4-(Methylsulfinyl)-3-butenyl ITC (4-MS-3-en-ITC), <u>sulforaphene</u>	<i>Ra. raphanistrum</i> , <i>Ra. sativus</i>	67,76,103 -105
<b>x-(Methylsulfonyl)alkyl ITC (MSolTC)</b>			
	3-(Methylsulfonyl)propyl ITC (3-MSolTC), <u>cheirolin</u>	<i>Ch. cheiri</i> ( <i>Er. cheiri</i> )	83,106
	4-(Methylsulfonyl)butyl ITC (4-MSolTC), <u>erysolin</u>	<i>Er. allionii</i> , <i>Er. perowskianum</i>	83
	5-(Methylsulfonyl)pentyl ITC (5-MSolTC)	n.e.e. <sup>c</sup>	21
	6-(Methylsulfonyl)hexyl ITC (6-MSolTC)	<i>Ar. drummondii</i> , <i>Is. microcarpa</i>	107-108
	8-(Methylsulfonyl)octyl ITC (8-MSolTC)	<i>Ar. turrita</i> , <i>B. juncea</i> , <i>He. amplexicaulis</i> , <i>R. amphibia</i> , <i>R. dubia</i> , <i>R. indica</i> , <i>R. sylvestris</i> , <i>S. arvensis</i>	66,69,99, 109
	9-(Methylsulfonyl)nonyl ITC (9-MSolTC)	<i>Ar. turrita</i> , <i>B. juncea</i> , <i>Ca. bursa-pastoris</i> , <i>He. amplexicaulis</i> , <i>R. dubia</i> , <i>R. indica</i> , <i>S. arvensis</i>	66,99,109
<b>(Sub)class Benzenic ITC</b>			
	Benzyl ITC (BITC)	<i>Le. sativum</i> , <i>Ra. raphanistrum</i> , <i>S. alba</i>	67,76
	Phenethyl ITC (PhEITC)	<i>B. napus</i> , <i>B. nigra</i> , <i>Ba. verna</i> , <i>Coincya</i> spp., <i>Hi. incana</i> , <i>Hm. fruticulosa</i> , <i>Le. sativum</i> , <i>Na. officinale</i> , <i>Sinapis</i> spp	67-68

<sup>a</sup> The names of ITCs are given as full (semi)systematic names, the abbreviations in brackets, and trivial names (when available) in an underlined style.

<sup>b</sup> Plant genus: *Aurinia* (A.), *Arabis* (Ar.), *Brassica* (B.), *Berteroa* (Be.), *Barbarea* (Ba.), *Camelina* (C.), *Capsella* (Ca.), *Cheiranthus* (Ch), *Draba* (D.), *Degenia* (De.), *Dithyrea* (Di.), *Eruca* (E.), *Erysimum* (Er.), *Hesperis* (H.), *Heliophila* (He.), *Hirschfeldia* (Hi.), *Hemicrambe* (Hm.), *Iberis* (I.), *Isatis* (Is.), *Lesquerella* (L.), *Lepidium* (Le.), *Neslia* (N.), *Nasturtium* (Na.), *Rorippa* (R.), *Raphanus* (Ra.), *Sinapis* (S.).

<sup>c</sup> n.e.e. refers to an ITC for which there is no experimental evidence (n.e.e.) of the occurrence in nature of its GSL precursor, although theoretically the GSL could be biosynthesized.

## 1.4. Approaches to modulate GSL composition in Brassicaceae

Germination has been employed as a common natural process to enrich the content of phytochemicals.<sup>110</sup> To enrich the content of phytochemicals and enhance their structural diversity further, elicitation is often employed along with germination.<sup>111-116</sup> Elicitation refers to application of biotic materials, chemical substances, or physical treatments acting as stressors to the plants and, thus, activating an array of defense mechanisms.<sup>117-118</sup> As a result, elicitation changes plant metabolism and enhances the biosynthesis of phytochemicals.

To obtain a high amount of ITCs, a high amount of GSLs is required. GSL content in Brassicaceae seedlings can be enhanced by elicitation using phytohormones (i.e. methyl jasmonate, MeJA; jasmonic acid, JA), amino acids (e.g. Met), sugars (e.g. sucrose), salts (e.g. ZnSO<sub>4</sub>, CaCl<sub>2</sub>), and other substances (e.g. mannitol).<sup>115,117,119-122</sup> **Table 1.3** provides an overview of the increase of total GSL content, up to 3.8 fold in the most widely studied Brassicaceae species (i.e. *B. oleracea*, broccoli; *Raphanus sativus*, radish) by various chemical elicitors. The increased GSL content included GSLs from MSGSL, MS-en-GSL, MTGSL, and indolic GSL subclasses, which were already present in the seed(ling)s. MeJA seems to be more efficient than the other chemicals. MeJA is known to stimulate the biosynthesis of phytochemicals, as it plays an important role in signal transduction processes, which regulate defense genes in plants.<sup>123</sup>

Elicitation is often done by using microorganisms, e.g. fungi. The effect of fungal elicitation on the compositional changes of phytochemicals, particularly isoflavonoids and stilbenoids, in various legume seed(ling)s was studied previously in the Laboratory of Food Chemistry.<sup>111-114</sup> Not only was the content of isoflavonoids of the seedlings improved considerably (up to 5 fold, compared to the non-elicited seedlings) by *Rhizopus oryzae* elicitation, but also the structural diversity was considerably enhanced.<sup>111-112,114</sup> The fungal-elicited seedlings contained a higher amount of antimicrobial compounds than the non-elicited seedlings.<sup>124-125</sup> Furthermore, fungal elicitation seemed to be more efficient than chemical elicitation.<sup>123,126</sup> Meanwhile, research on the effect of fungal elicitation on GSL composition of Brassicaceae seedlings is scarce. Only one study is available in literature on the fungal elicitation, using a pathogenic fungus, applied onto Brassicaceae seeds of one species.<sup>127</sup> However, that study indicated no clear trend on the compositional changes of GSLs. Therefore, it remains to be investigated whether the simultaneous germination and *R. oryzae* (a non-pathogenic and food-grade fungus) elicitation applied onto Leguminosae seed(ling)s can be extrapolated to Brassicaceae seed(ling)s.

**Table 1.3.** The effect of chemical elicitation of Brassicaceae seedlings on the GSL composition.

Plant species (variety)	Main GSL <sup>a</sup>	Increase GSL content <sup>b</sup>	Elicitor	Ref.
<i>B. oleracea</i> L. (Italica)	4-(Methylsulfinyl)butyl	1.6×	MeJA, JA, or sugars	115
<i>B. oleracea</i> L. (Italica)	3-(Methylsulfinyl)propyl 4-(Methylsulfinyl)butyl Indol-3-ylmethyl (I3M) Methoxylated I3M	2.1×	MeJA	117
<i>B. oleracea</i> L. (Italica)	3-(Methylsulfinyl)propyl 4-(Methylsulfinyl)butyl I3M Methoxylated I3M	1.8×	Met	117
<i>B. oleracea</i> L. (Italica)	4-(Methylsulfinyl)butyl	1.3×	Met	120
<i>B. oleracea</i> L. (Italica)	4-(Methylsulfinyl)butyl	1.6×	ZnSO <sub>4</sub>	121
<i>B. oleracea</i> L. (Italica)	4-(Methylsulfinyl)butyl 4-(Methylthio)butyl I3M 4-OH-I3M 4-OCH <sub>3</sub> -I3M	1.7×	CaCl <sub>2</sub>	122
<i>B. oleracea</i> L. (Botrytis)	3-(Methylthio)propyl 4-(Methylthio)butyl 3-(Methylsulfinyl)propyl 4-(Methylsulfinyl)butyl 5-(Methylsulfinyl)pentyl I3M 4-OH-I3M Methoxylated I3M	1.8×	sucrose or mannitol	119
<i>R. sativus</i> (China rose)	4-(Methylsulfinyl)-3-butenyl	3.8×	MeJA	115
<i>R. sativus</i> (Rambo)	4-(Methylsulfinyl)-3-butenyl 4-(Methylthio)-3-butenyl I3M 4-OH-I3M	2.2×	MeJA	117
<i>R. sativus</i> (Rambo)	4-(Methylsulfinyl)-3-butenyl I3M 4-OH-I3M Methoxylated I3M	1.7×	JA	117
<i>R. sativus</i> (Rambo)	4-(Methylsulfinyl)-3-butenyl 4-(Methylthio)-3-butenyl 4-OH-I3M	1.7×	Met	117

<sup>a</sup> The names of main GSLs are presented as the names of their side chains.<sup>b</sup> The increased total GSL content was compared to that of the untreated seedlings.

## 1.5. ITCs as potential natural antimicrobials

### 1.5.1. Measuring antimicrobial activity of ITCs

Variation in the structure of ITCs results in differences in their antimicrobial effect.<sup>9-13,19,128-133</sup> **Table 1.4** shows the antimicrobial activity, expressed as minimum inhibitory concentration (MIC, µg/mL), of some ITCs against various food spoilage and pathogenic microbial strains, including Gram<sup>-</sup> bacteria, Gram<sup>+</sup>

bacteria, and fungi. MIC is defined as the minimum concentration of a compound to cause no visible microbial growth at the end of an incubation period. MIC was determined by using different assays, namely broth microdilution assays and agar dilution assay. In previous studies using the broth microdilution assays, the parameter was measured from either only the turbidity (OD<sub>600</sub>) measurement or in combination of OD<sub>600</sub> measurement and cell viability count by agar plating. Different assays can result in different MICs.

The discrepancy between broth micro- and macrodilution assays can be up to 0.3 fold for fluconazole in one study (laboratory) using the same microbial strain.<sup>134</sup> However, **Table 1.4** indicates that the discrepancy between broth micro- and macrodilution assays between studies for the same ITC (e.g. AITC) and microbial species (e.g. *Escherichia coli*) can be up to 8 fold.<sup>8,19</sup> The discrepancy between broth macrodilution and agar dilution assays can be up to 20 fold.<sup>10</sup> Moreover, a discrepancy of up to 4 fold can still be found between studies for the same assay (e.g. broth macrodilution), growth media (e.g. TSB), ITC (e.g. AITC), and microbial strain (e.g. *E. coli* B34).<sup>14,20</sup> For those two studies, only one parameter was noticed to be different, namely temperature (30 °C<sup>14</sup> and 37 °C<sup>20</sup>). Consequently, it is difficult to compare the potency of antimicrobial ITCs, as many MICs were determined in different studies (laboratories), against different microorganisms, by using different assays and conditions. Furthermore, for compounds which have relatively low solubility and low antimicrobial activity, a defined MIC value cannot be obtained. Therefore, another parameter to express the growth inhibitory effect caused by a compound, regardless of its potency, would be very valuable to better rank the antimicrobial effect of ITCs. Overall, there is a need for a systematic study on the antimicrobial activity of ITCs, using many ITC representatives.

### 1.5.2. Antimicrobial activity of ITCs

**Table 1.4** indicates that AITC, benzyl ITC (BITC), and phenethyl ITC (PhEITC) are the most extensively studied ITCs. Among the tested microorganisms, *Helicobacter pylori* seems to be the most susceptible towards ITCs, and among the ITCs tested, 4-MSITC seems to be the most effective (MIC 0.06-8 µg/mL or  $3 \times 10^{-4}$  – 0.05 mM). Against *H. pylori* (a Gram<sup>-</sup> bacterium), MSITC seems to be a more potent subclass than the other subclasses, but there was no clear trend on the effect of chain length on the potency.<sup>11</sup> Against different microbial species, the potency of ITCs from other subclasses can be higher than that of ITCs from the subclass MSITC. For instance, 4-MTITC and BITC had higher activity than 3-MSITC and 4-MSITC against *S. aureus* (a Gram<sup>+</sup> bacterium) and *C. albicans* (a fungus).<sup>12</sup>

Considering the large structural diversity of ITCs (**Table 1.2**), many other ITCs have not been investigated with respect to their antimicrobial effects, especially the long-chained MTITC, MSITC, and MSoITC. The relatively large number of ITCs that have not been tested for their antimicrobial potency, together with the variations in antimicrobial assays as mentioned above, calls for a

systematic determination of (quantitative) structure-antimicrobial activity relationships ((Q)SAR) of ITCs. QSAR studies are performed *in silico* and provide mathematical models relating the observed activity of molecules to their structural properties.<sup>135</sup> QSAR models can reveal the molecular requirements of ITCs as antimicrobials. To date, there is no QSAR study on antimicrobial ITCs available.

**Table 1.4.** Antimicrobial activity of several ITCs.

ITC <sup>a</sup>	Target mo <sup>b</sup>	Type of mo <sup>c</sup>	Spoilage/pathogen	MIC <sup>d</sup>	Assay <sup>e</sup>	Ref.
<b>Class Aliphatic ITC</b>						
<b>Subclass Alkenyl ITC</b>						
AITC	<i>B. cereus</i>	Gram <sup>+</sup>	Pathogen	128	Bmi	13
	<i>Bacillus spp.</i>	Gram <sup>+</sup>	Spoilage	90	Bma	8
	<i>B. subtilis</i>	Gram <sup>+</sup>	Spoilage	50	Bma	14
	<i>C. albicans</i> KCTC 7965	Fungus	Pathogen	219	Bmi	12
	<i>C. jejuni</i>	Gram <sup>-</sup>	Pathogen	10	Bma	10
	<i>E. coli</i> 84	Gram <sup>-</sup>	Pathogen	50	Bma	8
	<i>E. coli</i> B34	Gram <sup>-</sup>	Pathogen	50	Bma	14
	<i>E. coli</i> B34	Gram <sup>-</sup>	Pathogen	200	Bma	20
	<i>E. coli</i> K-12, O157:H7	Gram <sup>-</sup>	Pathogen	400	Bmi	19
	<i>E. coli</i> O157:H7	Gram <sup>-</sup>	Pathogen	250	Bma	17
	<i>E. coli</i> O157:H7	Gram <sup>-</sup>	Pathogen	81	Bma	16
	<i>L. monocytogenes</i>	Gram <sup>+</sup>	Pathogen	142	Bma	16
	<i>L. monocytogenes</i>	Gram <sup>+</sup>	Pathogen	200	Bma	14
	<i>S. cerevisiae</i>	Fungus	Spoilage	50	Bma	8
	<i>S. cerevisiae</i>	Fungus	Spoilage	4	Bma	14
	<i>S. Montevideo</i>	Gram <sup>-</sup>	Pathogen	121	Bma	16
	<i>S. Typhimurium</i>	Gram <sup>-</sup>	Pathogen	100	Bma	14
	MRSA	Gram <sup>+</sup>	Pathogen	28-220	Bmi	9
	<i>S. aureus</i> B31	Gram <sup>+</sup>	Pathogen	100	Bma	14
	<i>S. aureus</i> KCOM 1492	Gram <sup>+</sup>	Pathogen	3000	Bmi	12
<b>Subclass x-(Methylthio)alkyl ITC (MTITC)</b>						
4-MTITC	<i>C. albicans</i> KCTC 7965	Fungus	Pathogen	63	Bmi	12
	<i>H. pylori</i>	Gram <sup>-</sup>	Pathogen	8-32	Agd	11
	<i>S. aureus</i> KCOM 1492	Gram <sup>+</sup>	Pathogen	625	Bmi	12
5-MTITC	<i>H. pylori</i>	Gram <sup>-</sup>	Pathogen	1-16	Agd	11
<b>Subclass x-(Methylsulfinyl)alkyl ITC (MSITC)</b>						
3-MSITC	<i>C. albicans</i> KCTC 7965	Fungus	Pathogen	188	Bmi	12
	<i>H. pylori</i>	Gram <sup>-</sup>	Pathogen	16-32	Agd	11
	<i>S. aureus</i> KCOM 1492	Gram <sup>+</sup>	Pathogen	1000	Bmi	12
4-MSITC	<i>C. albicans</i> KCTC 7965	Fungus	Pathogen	1000	Bmi	12
	<i>E. coli</i> K-12, O157:H7	Gram <sup>-</sup>	Pathogen	350-710	Bmi	19
	<i>H. pylori</i>	Gram <sup>-</sup>	Pathogen	0.06-8	Agd	11
	<i>S. aureus</i> KCOM 1492	Gram <sup>+</sup>	Pathogen	1000	Bmi	12
5-MSITC	<i>H. pylori</i>	Gram <sup>-</sup>	Pathogen	8-16	Agd	11
8-MSITC	<i>H. pylori</i>	Gram <sup>-</sup>	Pathogen	2-8	Agd	11

ITC <sup>a</sup>	Target mo <sup>b</sup>	Type of mo <sup>c</sup>	Spoilage/pathogen	MIC <sup>d</sup>	Assay <sup>e</sup>	Ref.
<b>Subclass x-(Methylsulfinyl)alkenyl ITC (MS-en-ITC)</b>						
4-MS-3-en-ITC	<i>C. albicans</i> KCTC 7965	Fungus	Pathogen	344	Bmi	12
	<i>H. pylori</i>	Gram <sup>-</sup>	Pathogen	1-16	Agd, Bma	11,15
	MRSA	Gram <sup>+</sup>	Pathogen	13-25	Bmi	15
	<i>S. aureus</i> KCOM 1492	Gram <sup>+</sup>	Pathogen	1000	Bmi	12
<b>Subclass x-(Methylsulfonyl)alkyl ITCs (MSolTC)</b>						
3-MSolTC	<i>H. pylori</i>	Gram <sup>-</sup>	Pathogen	4-32	Agd	11
4-MSolTC	<i>H. pylori</i>	Gram <sup>-</sup>	Pathogen	4-32	Agd	11
<b>(Sub)class Benzenic ITC</b>						
BITC	<i>B. cereus</i>	Gram <sup>+</sup>	Pathogen	16	Bmi	13
	<i>C. albicans</i> KCTC 7965	Fungus	Pathogen	47	Bmi	12
	<i>C. jejuni</i>	Gram <sup>-</sup>	Pathogen	1.25	Bma	10
	<i>E. coli</i>	Gram <sup>-</sup>	Pathogen	64	Bmi	13
	<i>E. coli</i> K-12, O157:H7	Gram <sup>-</sup>	Pathogen	70	Bmi	19
	<i>H. pylori</i>	Gram <sup>-</sup>	Pathogen	8-16	Agd	11
	MRSA	Gram <sup>+</sup>	Pathogen	3-110	Bmi	9
	<i>S. aureus</i> KCOM 1492	Gram <sup>+</sup>	Pathogen	500	Bmi	12
PhEITC	<i>B. cereus</i>	Gram <sup>+</sup>	Pathogen	16	Bmi	13
	<i>C. albicans</i> KCTC 7965	Fungus	Pathogen	250	Bmi	12
	<i>E. coli</i> K-12, O157:H7	Gram <sup>-</sup>	Pathogen	8	Bmi	18
	<i>H. pylori</i>	Gram <sup>-</sup>	Pathogen	8-32	Agd	11
	MRSA	Gram <sup>+</sup>	Pathogen	7-183	Bmi	9
	<i>S. aureus</i> KCOM 1492	Gram <sup>+</sup>	Pathogen	750	Bmi	12

<sup>a</sup> The names of ITCs are presented as their abbreviations (see **Table 1.2**).

<sup>b</sup> Target mo (microorganisms): *B. cereus*, *Bacillus cereus*; *B. subtilis*, *Bacillus subtilis*; *Bacillus* spp., *Bacillus subtilis*; *B. stearothermophilus*; *C. jejuni*, *Campylobacter jejuni*; *C. albicans*, *Candida albicans*; *E. coli*, *Escherichia coli*; *H. pylori*, *Helicobacter pylori*; *L. monocytogenes*, *Listeria monocytogenes*; MRSA, methicillin-resistant *Staphylococcus aureus*; *S. cerevisiae*, *Saccharomyces cerevisiae*; *S. Montevideo*, *Salmonella Montevideo*; *S. Typhimurium*, *Salmonella Typhimurium*; *S. aureus*, *Staphylococcus aureus*.

<sup>c</sup> Types of microorganisms include Gram<sup>-</sup> bacteria, Gram<sup>+</sup> bacteria, and fungi.

<sup>d</sup> MIC values are in a standard unit of µg/mL.

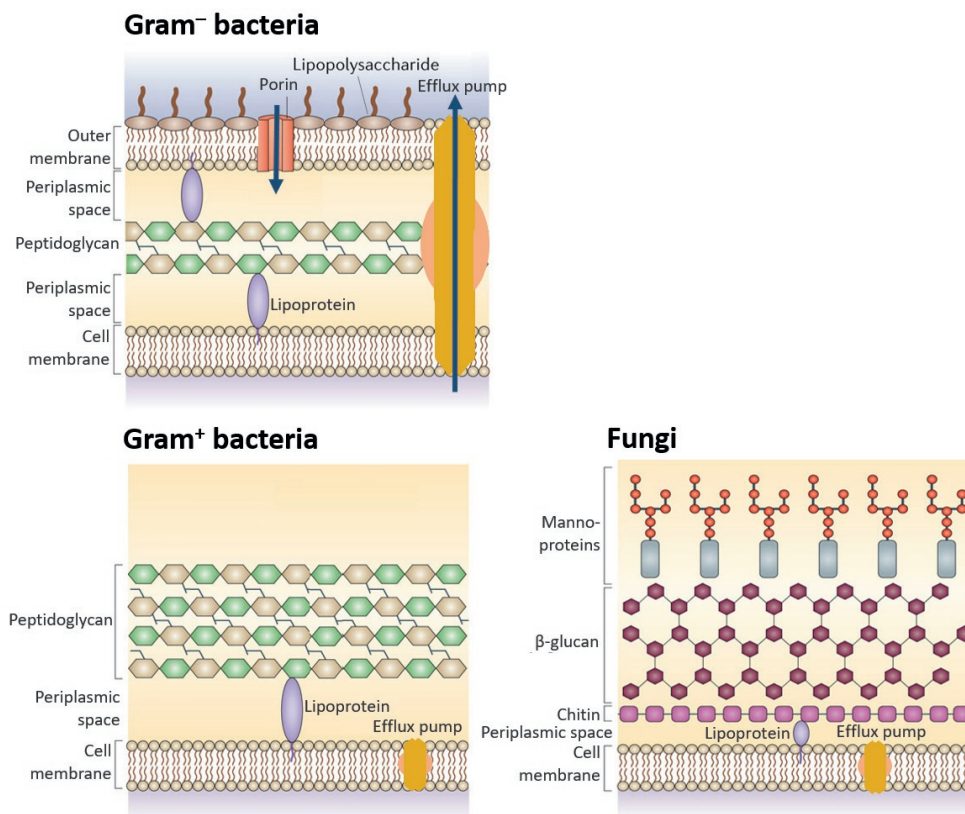
<sup>e</sup> Antimicrobial assays: Bmi, broth microdilution; Bma, broth macrodilution; and Agd, agar dilution.

### 1.5.3. Mode of antimicrobial action of ITCs

The mode of antimicrobial action of ITCs is not clear until now. Nevertheless, it has been speculated that the mode of action is related to the reactivity of ITCs towards thiol groups of Cys residues in particular (**Figure 1.4**). Microbial low-molecular-weight (LMW) thiol compounds and Cys-containing proteins, important for redox homeostasis and other functions of cells, might be the targets of ITCs.<sup>136-137</sup> Such (macro)molecules are present not only in the cytoplasm, but also in the cell envelope.

The cell envelope is indeed the first barrier for ITCs to reach their target, either in the cell envelope itself or in the cytoplasm. Although all ITCs have an electrophilic carbon, their antimicrobial potency can be different, because the side chains modulate ITC's physicochemical properties. These properties should be

compatible with that of the cell envelope, so that ITCs can pass through it. Each type of microorganism, i.e. Gram<sup>-</sup> bacteria, Gram<sup>+</sup> bacteria, and fungi has a different cell envelope architecture (**Figure 1.5**). This is one of the factors influencing the antimicrobial potency of ITCs against different types of microorganisms.



**Figure 1.5.** Cell envelope architectures of Gram<sup>-</sup> bacteria, Gram<sup>+</sup> bacteria, and fungi, modified from Brown *et al.*<sup>138</sup>

The cell envelope of Gram<sup>-</sup> bacteria consists of two phospholipid membranes, namely the outer membrane and the inner membrane (or cell membrane). At the outer side of the outer membrane, there are lipopolysaccharides (LPS) forming an impermeable barrier. These complex structures prevent passive diffusion of hydrophobic molecules,<sup>139</sup> which might include long-chained ITCs. In spite of that, water-filled protein channels (porins) are present to assist the influx of small hydrophilic molecules,<sup>140</sup> which might include short-chained ITCs. Furthermore, spanning through the outer and inner membranes, efflux pumps contribute an intrinsic resistance of Gram<sup>-</sup> bacteria by pumping toxic molecules directly out to the environment.<sup>141</sup> Previous studies indicated in **Table 1.4** did not use any efflux pump inhibitor in their antimicrobial assays for ITCs. Therefore, it is speculated

that the action of ITCs is not significantly affected by efflux pumps. The cell envelopes of Gram<sup>+</sup> bacteria and fungi share similarities. They consist of thick layers of polysaccharide-protein structures: peptidoglycan in Gram<sup>+</sup> bacteria, manno-proteins,  $\beta$ -glucan, and chitin in fungi. Thick cell walls of Gram<sup>+</sup> bacteria and fungi are porous, usually allowing the diffusion of various molecules,<sup>142-143</sup> which might also include ITCs with long chain length. Gram<sup>+</sup> bacteria and fungi have only one phospholipid membrane, i.e. the cell membrane.<sup>138,144</sup> In the cell membrane, efflux pumps are present.<sup>145-146</sup> The efflux pumps in Gram<sup>+</sup> bacteria (except mycobacteria, a Gram<sup>+</sup> bacterial class having two phospholipid membranes, but irrelevant in this thesis) and fungi can only pump out the toxic molecules to the periplasm, instead of to the environment.<sup>147-148</sup> Overall, the intrinsic antimicrobial resistance of Gram<sup>-</sup> bacteria is higher than that of Gram<sup>+</sup> bacteria and fungi.

One study showed *in vitro* inhibition of enzymes which contain Cys at the active site, i.e. *E. coli* thioredoxin reductase and acetate kinase, by AITC at 0.10-1.01 mM (10-100  $\mu$ g/mL).<sup>17</sup> Both enzymes are abundant in the cytoplasm of microorganisms.<sup>149-150</sup> Another study showed *in vitro* inhibition of *H. pylori* urease, a Cys-rich enzyme important for virulence of the bacterium, by ITCs at 0.01-5 mM (1.6-885  $\mu$ g/mL).<sup>151</sup> Furthermore, an *in vivo* study confirmed that ITCs inhibited nucleic acids synthesis in various bacteria species, which led to growth inhibition of some bacteria.<sup>152</sup> However, to date the actual target(s) of ITCs in microbial cells remains unclear. Due to their electrophilicity, ITCs might be non-specific antimicrobials, i.e. having multiple cellular targets, due to their ability to react with Cys residing at the active site of various enzymes and LMW thiol compounds.

Although the electrophilicity of ITCs might be important for their antimicrobial action, it also makes them sensitive to nucleophiles present in the environment, e.g. growth media, which can attack ITCs before they can reach their microbial target. Previous studies described that ITCs lost their antimicrobial activity in the presence of GSH and Cys, as well as when pre-incubated for a few hours in a rich microbial growth medium at 37 °C.<sup>13,153</sup> However, most studies on the antimicrobial activity of ITCs do not account for their potential reactivity towards constituents in growth media.



## 1.6. Aim and outline of thesis

The main aim of this thesis research was to explore the potential of ITCs as natural antimicrobials. For this, the production, the analysis, the reactivity, and the (quantitative) structure-activity relationships of ITCs were studied, with consideration of their electrophilicity.

**Chapter 2** addresses the effect of fungal elicitation during germination on the GSL compositions of three different Brassicaceae species, namely *S. alba*, *B. napus*, and *B. juncea*. Three different fungal species having different level of pathogenicity, i.e. *R. oryzae*, *Fusarium graminearum*, and *F. oxysporum*, were applied to evaluate whether the simultaneous germination and *R. oryzae* elicitation protocol for Leguminosae could be extrapolated as such or would require different fungi. **Chapter 3** describes the development of an RP-UHPLC-ESI-MS<sup>n</sup> analytical method to analyze GSLs and ITCs simultaneously. In this method, ITCs were derivatized with a thiol compound, namely NAC, which did neither affect GSL analysis, nor the enzymatic process to degrade GSLs into ITCs. This method was validated with 14 GSLs and 15 ITCs and applied to simultaneously monitor the increase of ITC concentrations and the decrease of GSL concentrations during the enzymatic hydrolysis of GSLs. **Chapter 4** addresses the antimicrobial activity of 10 ITCs from 5 subclasses, each with a short and a long alkyl chain representative, against Gram<sup>+</sup> bacteria (*B. cereus*, *L. monocytogenes*, and *S. aureus*), Gram<sup>-</sup> bacteria (*E. coli*, *S. Typhimurium*, and *P. aeruginosa*), and fungi (*S. cerevisiae*, *C. holmii*, and *A. niger* spores). The antimicrobial assays were performed in nucleophile-rich and nucleophile-poor growth media. Furthermore, the reactivity of ITCs with the growth media was investigated under conditions applied in the antimicrobial assays to determine the reaction rate of ITCs with nucleophiles present in the growth media. **Chapter 5** describes a QSAR study with 26 ITCs against Gram<sup>-</sup> *E. coli* and Gram<sup>+</sup> *B. cereus*. To be able to use ITCs with a complete range of activity from poor to good antimicrobial, a new parameter of bacterial growth inhibition of ITCs was introduced and used as an activity input for the QSAR modeling. The developed QSAR models were applied to predict the activity of ITC-rich Brassicaceae seed extracts. The most important findings of these four chapters were discussed integrally in **Chapter 6** to define the prospects of isothiocyanates as novel natural antimicrobials.

## 1.7. References

1. Tiwari, B. K.; ValDRAMIDIS, V. P.; O'Donnell, C. P.; Muthukumarappan, K.; Bourke, P.; Cullen, P. J., Application of natural antimicrobials for food preservation. *J. Agric. Food Chem.* **2009**, *57*, 5987-6000.
2. Jensen, K. O. D.; Denver, S.; Zanolli, R., Actual and potential development of consumer demand on the organic food market in Europe. *NJAS - Wageningen J. Life Sci.* **2011**, *58*, 79-84.
3. Zink, D. L., The impact of consumer demands and trends on food processing. *Emerging Infect. Dis.* **1997**, *3* (4), 467-469.
4. Nicoli, M. C.; Calligaris, S., Secondary shelf life: An underestimated issue. *Food Eng. Rev.* **2018**, *10*, 57-65.
5. WHO, Antimicrobial resistance: global report on surveillance 2014. World Health Organization: **2014**; p 257.
6. O'Neill, J. *Tackling drug-resistant infections globally: Final report and recommendations*; The United Kingdom Government: London, **2016**; p 84.
7. Gilliver, K., The inhibitory action of antibiotics on plant pathogenic bacteria and fungi. *Ann. Bot.* **1946**, *10*, 271.
8. Brabban, A. D.; Edwards, C., The effects of glucosinolates and their hydrolysis products on microbial growth. *J. Appl. Bacteriol.* **1995**, *79*, 171-177.
9. Dias, C.; Aires, A.; Saavedra, M. J., Antimicrobial activity of isothiocyanates from cruciferous plants against methicillin-resistant *Staphylococcus aureus* (MRSA). *Int. J. Mol. Sci.* **2014**, *15*, 19552-19561.
10. Dufour, V.; Alazzam, B.; Ermel, G.; Thepaut, M.; Rossero, A.; Tresse, O.; Baysse, C., Antimicrobial activities of isothiocyanates against *Campylobacter jejuni* isolates. *Front. Cell. Infect. Microbiol.* **2012**, *2*, 53.
11. Haristoy, X.; Fahey, J. W.; Scholtus, I.; Lozniewski, A., Evaluation of the antimicrobial effects of several isothiocyanates on *Helicobacter pylori*. *Planta Med.* **2005**, *71*, 326-330.
12. Ko, M. O.; Kim, M. B.; Lim, S. B., Relationship between chemical structure and antimicrobial activities of isothiocyanates from cruciferous vegetables against oral pathogens. *J. Microbiol. Biotechnol.* **2016**, *26*, 2036-2042.
13. Kurepina, N.; Kreiswirth, B. N.; Mustaev, A., Growth-inhibitory activity of natural and synthetic isothiocyanates against representative human microbial pathogens. *J. Appl. Microbiol.* **2013**, *115*, 943-954.
14. Kyung, K. H.; Fleming, H. P., Antimicrobial activity of sulfur compounds derived from cabbage. *J. Food Prot.* **1997**, *60*, 67-71.
15. Lim, S.; Han, S.-W.; Kim, J., Sulforaphene identified from radish (*Raphanus sativus* L.) seeds possesses antimicrobial properties against multidrug-resistant bacteria and methicillin-resistant *Staphylococcus aureus*. *J. Funct. Foods* **2016**, *24*, 131-141.
16. Lin, C. M.; Preston, J. F., 3rd; Wei, C. I., Antibacterial mechanism of allyl isothiocyanate. *J. Food Prot.* **2000**, *63*, 727-34.
17. Luciano, F. B.; Holley, R. A., Enzymatic inhibition by allyl isothiocyanate and factors affecting its antimicrobial action against *Escherichia coli* O157:H7. *Int. J. Food Microbiol.* **2009**, *131*, 240-5.
18. Nowicki, D.; Maciag-Dorszynska, M.; Kobiela, W.; Herman-Antosiewicz, A.; Wegrzyn, A.; Szalewska-Palasz, A.; Wegrzyn, G., Phenethyl isothiocyanate inhibits shiga toxin production in enterohemorrhagic *Escherichia coli* by stringent response induction. *Antimicrob. Agents Chemother.* **2014**, *58*, 2304-15.
19. Nowicki, D.; Rodzik, O.; Herman-Antosiewicz, A.; Szalewska-Palasz, A., Isothiocyanates as effective agents against enterohemorrhagic *Escherichia coli*: Insight to the mode of action. *Sci. Rep.* **2016**, *6*, 22263.
20. Shofran, B. G.; Purrington, S. T.; Breidt, F.; Fleming, H. P., Antimicrobial properties of sinigrin and its hydrolysis products. *J. Food Sci.* **1998**, *63*, 621-624.

21. Blažević, I.; Montaut, S.; Burčul, F.; Olsen, C. E.; Burow, M.; Rollin, P.; Agerbirk, N., Glucosinolate structural diversity, identification, chemical synthesis and metabolism in plants. *Phytochemistry* **2020**, *169*, 112100.
22. Ishida, M.; Hara, M.; Fukino, N.; Kakizaki, T.; Morimitsu, Y., Glucosinolate metabolism, functionality and breeding for the improvement of Brassicaceae vegetables. *Breed. Sci.* **2014**, *64*, 48-59.
23. Sønderby, I. E.; Geu-Flores, F.; Halkier, B. A., Biosynthesis of glucosinolates – gene discovery and beyond. *Trends Plant Sci.* **2010**, *15*, 283-290.
24. Halkier, B. A.; Gershenzon, J., Biology and biochemistry of glucosinolates. *Annu. Rev. Plant Biol.* **2006**, *57*, 303-33.
25. Glawischnig, E.; Mikkelsen, M. D.; Halkier, B. A., Glucosinolates: Biosynthesis and Metabolism. In *Sulphur in Plants*, Abrol, Y. P.; Ahmad, A., Eds. Springer Netherlands: Dordrecht, **2003**; pp 145-162.
26. Sánchez-Pujante, P. J.; Borja-Martínez, M.; Pedreño, M. Á.; Almagro, L., Biosynthesis and bioactivity of glucosinolates and their production in plant *in vitro* cultures. *Planta* **2017**, *246*, 19-32.
27. Agerbirk, N.; Olsen, C. E., Glucosinolate structures in evolution. *Phytochemistry* **2012**, *77*, 16-45.
28. Wittstock, U.; Halkier, B. A., Glucosinolate research in the *Arabidopsis* era. *Trends Plant Sci.* **2002**, *7*, 263-70.
29. Agerbirk, N.; Olsen, C. E., Isoferuloyl derivatives of five seed glucosinolates in the crucifer genus *Barbarea*. *Phytochemistry* **2011**, *72*, 610-623.
30. Linscheid, M.; Wendisch, D.; Strack, D., The structures of sinapic acid esters and their metabolism in cotyledons of *Raphanus sativus*. *Z. Naturforsch. C* **1980**, *35*, 907.
31. Reichelt, M.; Brown, P. D.; Schneider, B.; Oldham, N. J.; Stauber, E.; Tokuhisa, J.; Kliebenstein, D. J.; Mitchell-Olds, T.; Gershenzon, J., Benzoic acid glucosinolate esters and other glucosinolates from *Arabidopsis thaliana*. *Phytochemistry* **2002**, *59*, 663-71.
32. Kissen, R.; Rossiter, J. T.; Bones, A. M., The 'mustard oil bomb': not so easy to assemble?! Localization, expression and distribution of the components of the myrosinase enzyme system. *Phytochem. Rev.* **2009**, *8*, 69-86.
33. Agerbirk, N.; De Vos, M.; Kim, J. H.; Jander, G., Indole glucosinolate breakdown and its biological effects. *Phytochem. Rev.* **2008**, *8*, 101-120.
34. Buskov, S.; Hasselstrøm, J.; Olsen, C. E.; Sørensen, H.; Sørensen, J. C.; Sørensen, S., Supercritical fluid chromatography as a method of analysis for the determination of 4-hydroxybenzylglucosinolate degradation products. *J. Biochem. Biophys. Methods* **2000**, *43*, 157-174.
35. Greer, M. A., Isolation from rutabaga seed of progoitrin, the precursor of the naturally occurring antithyroid compound, goitrin (1-5-vinyl-2-thiooxazolidone). *J. Am. Chem. Soc.* **1956**, *78*, 1260-1261.
36. Hauder, J.; Winkler, S.; Bub, A.; Rufer, C. E.; Pignitter, M.; Somoza, V., LC-MS/MS quantification of sulforaphane and indole-3-carbinol metabolites in human plasma and urine after dietary intake of selenium-fortified broccoli. *J. Agric. Food Chem.* **2011**, *59*, 8047-57.
37. McDanell, R.; McLean, A. E. M.; Hanley, A. B.; Heaney, R. K.; Fenwick, G. R., Chemical and biological properties of indole glucosinolates (glucobrassicins): A review. *Food Chem. Toxicol.* **1988**, *26*, 59-70.
38. Agerbirk, N.; Olsen, C. E., Glucosinolate hydrolysis products in the crucifer *Barbarea vulgaris* include a thiazolidine-2-one from a specific phenolic isomer as well as oxazolidine-2-thiones. *Phytochemistry* **2015**, *115*, 143-151.
39. Angelino, D.; Dosz, E. B.; Sun, J.; Hoefflinger, J. L.; Van Tassell, M. L.; Chen, P.; Harnly, J. M.; Miller, M. J.; Jeffery, E. H., Myrosinase-dependent and -independent formation and control of isothiocyanate products of glucosinolate hydrolysis. *Front. Plant Sci.* **2015**, *6* (831).

40. Hanschen, F. S.; Lamy, E.; Schreiner, M.; Rohn, S., Reactivity and stability of glucosinolates and their breakdown products in foods. *Angew. Chem. Int. Ed.* **2014**, *53*, 11430-11450.
41. Matusheski, N. V.; Swarup, R.; Juvik, J. A.; Mithen, R.; Bennett, M.; Jeffery, E. H., Epithiospecifier protein from broccoli (*Brassica oleracea* L. ssp. *italica*) inhibits formation of the anticancer agent sulforaphane. *J. Agric. Food Chem.* **2006**, *54*, 2069-76.
42. Rosa, E. A. S.; Heaney, R. K.; Fenwick, G. R.; Portas, C. A. M., Glucosinolates in crop plants. In *Horticultural Reviews*, **1997**.
43. Pastorczyk, M.; Bednarek, P.; Kopriva, S., Chapter Seven - The function of glucosinolates and related metabolites in plant innate immunity. In *Advances in Botanical Research*, Academic Press: **2016**; Vol. 80, pp 171-198.
44. Tierens, K. F. M.-J.; Thomma, B. P. H. J.; Brouwer, M.; Schmidt, J.; Kistner, K.; Porzel, A.; Mauch-Mani, B.; Cammue, B. P. A.; Broekaert, W. F., Study of the role of antimicrobial glucosinolate-derived isothiocyanates in resistance of *Arabidopsis* to microbial pathogens. *Plant Physiol.* **2001**, *125*, 1688-1699.
45. Buxdorf, K.; Yaffe, H.; Barda, O.; Levy, M., The effects of glucosinolates and their breakdown products on necrotrophic fungi. *PLoS ONE* **2013**, *8*, e70771.
46. Greenhalgh, J. R.; Mitchell, N. D., The involvement of flavour volatiles in the resistance to downy mildew of wild and cultivated forms of *Brassica oleracea*. *New Phytol.* **1976**, *77*, 391.
47. Śmiechowska, A.; Bartoszek, A.; Namieśnik, J., Determination of glucosinolates and their decomposition products—indoles and isothiocyanates in cruciferous vegetables. *Crit. Rev. Anal. Chem.* **2010**, *40*, 202-216.
48. Chen, C.-W.; Ho, C.-T., Thermal degradation of allyl isothiocyanate in aqueous solution. *J. Agric. Food Chem.* **1998**, *46*, 220-223.
49. Chiang, W. C. K.; Pusateri, D. J.; Leitz, R. E. A., Gas chromatography/mass spectrometry method for the determination of sulforaphane and sulforaphane nitrile in broccoli. *J. Agric. Food Chem.* **1998**, *46*, 1018-1021.
50. De Nicola, G. R.; Montaut, S.; Rollin, P.; Nyegue, M.; Menut, C.; Iori, R.; Tatibouët, A., Stability of benzylic-type isothiocyanates in hydrodistillation-mimicking conditions. *J. Agric. Food Chem.* **2013**, *61*, 137-142.
51. Drobnička, L.; Kristian, P.; Augustin, J., The chemistry of the — NCS group. In *Cyanates and Their Thio Derivatives*, Patai, S., Ed. **1977**; pp 1003-1221.
52. Zhang, Y.; Talalay, P., Anticarcinogenic activities of organic isothiocyanates: Chemistry and mechanisms. *Cancer Res.* **1994**, *54*, 1976s-1981s.
53. Lamy, E.; Scholtes, C.; Herz, C.; Mersch-Sundermann, V., Pharmacokinetics and pharmacodynamics of isothiocyanates. *Drug Metab. Rev.* **2011**, *43*, 387-407.
54. Baillie, T. A.; Slatyer, J. G., Glutathione: a vehicle for the transport of chemically reactive metabolites *in vivo*. *Acc. Chem. Res.* **1991**, *24*, 264-270.
55. Budnowski, J.; Hanschen, F. S.; Lehmann, C.; Haack, M.; Brigelius-Flohé, R.; Kroh, L. W.; Blaut, M.; Rohn, S.; Hanske, L., A derivatization method for the simultaneous detection of glucosinolates and isothiocyanates in biological samples. *Anal. Biochem.* **2013**, *441*, 199-207.
56. Pilipczuk, T.; Kusznierevich, B.; Chmiel, T.; Przychodzen, W.; Bartoszek, A., Simultaneous determination of individual isothiocyanates in plant samples by HPLC-DAD-MS following SPE and derivatization with *N*-acetyl-L-cysteine. *Food Chem.* **2017**, *214*, 587-596.
57. Franco, P.; Spinuzzi, S.; Pagnotta, E.; Lazzeri, L.; Ugolini, L.; Camborata, C.; Roda, A., Development of a liquid chromatography-electrospray ionization-tandem mass spectrometry method for the simultaneous analysis of intact glucosinolates and isothiocyanates in Brassicaceae seeds and functional foods. *J. Chromatogr. A* **2016**, *1428*, 154-161.
58. Tsao, R.; Yu, Q.; Potter, J.; Chiba, M., Direct and simultaneous analysis of sinigrin and allyl isothiocyanate in mustard samples by high-performance liquid chromatography. *J. Agric. Food Chem.* **2002**, *50*, 4749-53.

59. Vastenhout, K. J.; Tornberg, R. H.; Johnson, A. L.; Amolins, M. W.; Mays, J. R., High-performance liquid chromatography-based method to evaluate kinetics of glucosinolate hydrolysis by *Sinapis alba* myrosinase. *Anal. Biochem.* **2014**, *465*, 105-113.
60. Possenti, M.; Baima, S.; Raffo, A.; Durazzo, A.; Giusti, A. M.; Natella, F., Glucosinolates in Food. In *Glucosinolates*, Mérillon, J.-M.; Ramawat, K. G., Eds. Springer International Publishing: Cham, **2016**; pp 1-46.
61. Popova, I. E.; Morra, M. J., Simultaneous quantification of sinigrin, sinalbin, and anionic glucosinolate hydrolysis products in *Brassica juncea* and *Sinapis alba* seed extracts using ion chromatography. *J. Agric. Food Chem.* **2014**, *62*, 10687-93.
62. Borgen, B. H.; Thangstad, O. P.; Ahuja, I.; Rossiter, J. T.; Bones, A. M., Removing the mustard oil bomb from seeds: transgenic ablation of myrosin cells in oilseed rape (*Brassica napus*) produces MINELESS seeds. *J. Exp. Bot.* **2010**, *61*, 1683-1697.
63. Sodhi, Y. S.; Mukhopadhyay, A.; Arumugam, N.; Verma, J. K.; Gupta, V.; Pental, D.; Pradhan, A. K., Genetic analysis of total glucosinolate in crosses involving a high glucosinolate Indian variety and a low glucosinolate line of *Brassica juncea*. *Plant Breed.* **2002**, *121*, 508-511.
64. Bellostas, N.; Kachlicki, P.; Sørensen, J. C.; Sørensen, H., Glucosinolate profiling of seeds and sprouts of *B. oleracea* varieties used for food. *Sci. Hortic.* **2007**, *114*, 234-242.
65. Berhow, M. A.; Polat, U.; Glinski, J. A.; Glensk, M.; Vaughn, S. F.; Isbell, T.; Ayala-Diaz, I.; Marek, L.; Gardner, C., Optimized analysis and quantification of glucosinolates from *Camelina sativa* seeds by reverse-phase liquid chromatography. *Ind. Crops Prod.* **2013**, *43*, 119-125.
66. Daxenbichler, M. E.; Spencer, G. F.; Carlson, D. G.; Rose, G. B.; Brinker, A. M.; Powell, R. G., Glucosinolate composition of seeds from 297 species of wild plants. *Phytochemistry* **1991**, *30*, 2623-2638.
67. Ibrahim, N.; Allart-Simon, I.; De Nicola, G. R.; Iori, R.; Renault, J.-H.; Rollin, P.; Nuzillard, J.-M., Advanced NMR-based structural investigation of glucosinolates and desulfoglucosinolates. *J. Nat. Prod.* **2018**, *81*, 323-334.
68. Kuszniereicz, B.; Iori, R.; Piekarska, A.; Namiesnik, J.; Bartoszek, A., Convenient identification of desulfoglucosinolates on the basis of mass spectra obtained during liquid chromatography-diode array-electrospray ionisation mass spectrometry analysis: method verification for sprouts of different Brassicaceae species extracts. *J. Chromatogr. A* **2013**, *1278*, 108-15.
69. Olsen, C. E.; Huang, X.-C.; Hansen, C. I. C.; Cipollini, D.; Ørgaard, M.; Matthes, A.; Geu-Flores, F.; Koch, M. A.; Agerbirk, N., Glucosinolate diversity within a phylogenetic framework of the tribe *Cardamineae* (Brassicaceae) unraveled with HPLC-MS/MS and NMR-based analytical distinction of 70 desulfoglucosinolates. *Phytochemistry* **2016**, *132*, 33-56.
70. Kjær, A.; Jensen, R. B., Isothiocyanates III. The volatile of isothiocyanates in seeds of rape (*Brassica napus* L.). *Acta Chem. Scand.* **1953**, *7*, 1271-1275.
71. Kjær, A. J., R. B., Isothiocyanates XX. 4-Pentenyl isothiocyanate, a new mustard oil occurring as a glucoside (glucobrassicinapin) in nature. *Acta Chem. Scand.* **1956**, *10*, 1356-1371.
72. Millán, S.; Sampedro, M. C.; Gallejones, P.; Castellón, A.; Ibargoitia, M. L.; Goicolea, M. A.; Barrio, R. J., Identification and quantification of glucosinolates in rapeseed using liquid chromatography-ion trap mass spectrometry. *Anal. Bioanal. Chem.* **2009**, *394*, 1661-1669.
73. Kjær, A.; Gmelin, R.; Larsen, I., Isothiocyanates XII. 3-Methylthiopropyl isothiocyanate (ibervirin), a new naturally occurring mustard oil. *Acta Chem. Scand.* **1955**, *9*, 1143-1147.
74. Kjær, A.; Gmelin, R., Isothiocyanates XI. 4-Methylthiobutyl isothiocyanate, a new naturally occurring mustard oil. *Acta Chem. Scand.* **1955**, *9*, 542-544.
75. Leoni, O.; Iori, R.; Palmieri, S.; Esposito, E.; Menegatti, E.; Cortesi, R.; Nastruzzi, C., Myrosinase-generated isothiocyanate from glucosinolates: isolation,

- characterization and *in vitro* antiproliferative studies. *Bioorg. Med. Chem.* **1997**, *5*, 1799-806.
76. Maldini, M.; Foddai, M.; Natella, F.; Petretto, G. L.; Rourke, J. P.; Chessa, M.; Pintore, G., Identification and quantification of glucosinolates in different tissues of *Raphanus raphanistrum* by liquid chromatography tandem-mass spectrometry. *J. Food Compos. Anal.* **2017**, *61*, 20-27.
77. Montaut, S.; Montagut-Romans, A.; Chiari, L.; Benson, H. J., Glucosinolates in *Draba borealis* DC. (Brassicaceae) in a taxonomic perspective. *Biochem. Syst. Ecol.* **2018**, *78*, 31-34.
78. Blažević, I.; Radonić, A.; Mastelić, J.; Zekić, M.; Skočibušić, M.; Maravić, A., Glucosinolates, glycosidically bound volatiles and antimicrobial activity of *Aurinia sinuata* (Brassicaceae). *Food Chem.* **2010**, *121*, 1020-1028.
79. De Nicola, G. R.; Blažević, I.; Montaut, S.; Rollin, P.; Mastelić, J.; Iori, R.; Tatibouët, A., Glucosinolate distribution in aerial parts of *Degenia velebitica*. *Chem. Biodiversity* **2011**, *8*, 2090-2096.
80. Kjær, A.; Larsen, I.; Gmelin, R., Isothiocyanates XIV. 5-Methylthiopentyl isothiocyanate, a new mustard oil present in nature as a glucoside (glucoberteroin). *Acta Chem. Scand.* **1955**, *9*, 1311-1316.
81. Daxenbichler, M.; Van Etten, C.; Wolff, I., Notes-Identification of a new, naturally occurring, steam-volatile isothiocyanate from *Lesquerella lasiocarpa* seed. *J. Org. Chem.* **1961**, *26*, 4168-4169.
82. Ina, K.; Ina, H.; Ueda, M.; Yagi, A.; Kishima, I.,  $\omega$ -Methylthioalkyl isothiocyanates in wasabi. *Agric. Biol. Chem.* **1989**, *53*, 537-538.
83. Vaughn, S. F.; Berhow, M. A., Glucosinolate hydrolysis products from various plant sources: pH effects, isolation, and purification. *Ind. Crops Prod.* **2005**, *21*, 193-202.
84. Bennett, R. N.; Mellon, F. A.; Kroon, P. A., Screening crucifer seeds as sources of specific intact glucosinolates using ion-pair high-performance liquid chromatography negative ion electrospray mass spectrometry. *J. Agric. Food Chem.* **2004**, *52*, 428-38.
85. Hasapis, X.; J. MacLeod, A.; Moreau, M., Glucosinolates of nine Cruciferae and two Capparaceae species. *Phytochemistry* **1981**, *20*, 2355-2358.
86. Ciska, E.; Martyniak-Przybyszewska, B.; Kozłowska, H., Content of glucosinolates in cruciferous vegetables grown at the same site for two years under different climatic conditions. *J. Agric. Food Chem.* **2000**, *48*, 2862-7.
87. Jaki, B.; Sticher, O.; Veit, M.; Fröhlich, R.; Pauli, G. F., Evaluation of glucoiberin reference material from *Iberis amara* by spectroscopic fingerprinting. *J. Nat. Prod.* **2002**, *65*, 517-522.
88. Kore, A. M.; Spencer, G. F.; Wallig, M. A., Purification of the  $\omega$ -(methylsulfinyl)alkyl glucosinolate hydrolysis products: 1-isothiocyanato-3-(methylsulfinyl)propane, 1-isothiocyanato-4-(methylsulfinyl)butane, 4-(methylsulfinyl)butanenitrile, and 5-(methylsulfinyl)pentanenitrile from broccoli and *Lesquerella fendleri*. *J. Agric. Food Chem.* **1993**, *41*, 89-95.
89. Schultz, O.-E.; Gmelin, R., Das Senfölglukosid „Glukoiberin“ und der Bitterstoff „Ibamarin“ von *Iberis amara* L. (Schleifenblume). IX. Mitteilung über Senfölglukoside. *Arch. Pharm.* **1954**, *287*, 404-411.
90. Kiddle, G.; Bennett, R. N.; Botting, N. P.; Davidson, N. E.; Robertson, A. A. B.; Wallsgrove, R. M., High-performance liquid chromatographic separation of natural and synthetic desulphoglucosinolates and their chemical validation by UV, NMR and chemical ionisation-MS methods. *Phytochem. Anal.* **2001**, *12*, 226-242.
91. Procházka, Ž., Isolation of sulforaphane from hoare cress (*Lepidium draba* L.). *Collect. Czech. Chem. Commun.* **1959**, *24*, 2429-2430.
92. Etoh, H.; Nishimura, A.; Takasawa, R.; Yagi, A.; Saito, K.; Sakata, K.; Kishima, I.; Ina, K.,  $\omega$ -Methylsulfinylalkyl isothiocyanates in wasabi, *Wasabia japonica* Matsum. *Agric. Biol. Chem.* **1990**, *54*, 1587-1589.

93. Kjær, A.; Gmelin, R., Isothiocyanates XIX. L(-)-5-Methylsulphinylpentyl isothiocyanate, the aglucone of a new naturally occurring glucoside (glucoalyssin). *Acta Chem. Scand.* **1956**, *10*, 1100-1110.
94. Schultz, O.-E.; Wagner, W., Glucoalyssin, ein neues Senfölglycosid aus *Alyssum*-Arten. *Z. Naturforsch. B* **1956**, *11*, 417.
95. Song, L.; Iori, R.; Thornalley, P. J., Purification of major glucosinolates from Brassicaceae seeds and preparation of isothiocyanate and amine metabolites. *J. Sci. Food Agric.* **2006**, *86*, 1271-1280.
96. Christensen, B. W.; Kjær, A., A mustard oil of *Hesperis matronalis* seed, 6-methylsulphinylohexyl isothiocyanate. *Acta Chem. Scand.* **1963**, 846-847.
97. Montaut, S.; Grandbois, J.; Righetti, L.; Barillari, J.; Iori, R.; Rollin, P., Updated glucosinolate profile of *Dithyrea wislizenii*. *J. Nat. Prod.* **2009**, *72*, 889-893.
98. Kjær, A. C., B., Isothiocyanates XXX. Glucohirsutin, a new naturally occurring glucoside furnishing 8-methylsulphinyloctyl isothiocyanate on enzymic hydrolysis. *Acta Chem. Scand.* **1958**, *12*, 833-838.
99. Yamane, A.; Fujikura, J.; Ogawa, H.; Mizutani, J., Isothiocyanates as alleopathic compounds from *Rorippa indica* Hiern. (Cruciferae) roots. *J. Chem. Ecol.* **1992**, *18*, 1941-1954.
100. Kjær, A.; Gmelin, R., Isothiocyanates XXIII. L(-)-9-Methylsulphinylnonyl isothiocyanate, a new mustard oil present as a glucoside (glucoarabin) in *Arabis* species. *Acta Chem. Scand.* **1956**, *10*, 1358-1359.
101. Kjær, A. G., R.; Jensen, R. B., Isothiocyanates XXI. (-)-10-Methylsulphinyldecyl isothiocyanate, a new mustard oil present as a glucoside (glucocamelinin) in *Camelina* species. *Acta Chem. Scand.* **1956**, *10*, 1614-1619.
102. Kjær, A.; Schuster, A., Glucosinolates in seeds of *Neslia paniculata*. *Phytochemistry* **1972**, *11*, 3045-3048.
103. Iori, R.; Barillari, J.; Gallienne, E.; Bilardo, C.; Tatibouët, A.; Rollin, P., Thiofunctionalised glucosinolates: Unexpected transformation of desulfoglucoraphenin. *Tetrahedron Lett.* **2008**, *49*, 292-295.
104. Kim, K. H.; Moon, E.; Kim, S. Y.; Choi, S. U.; Lee, J. H.; Lee, K. R., 4-Methylthio-butanyl derivatives from the seeds of *Raphanus sativus* and their biological evaluation on anti-inflammatory and antitumor activities. *J. Ethnopharmacol.* **2014**, *151*, 503-508.
105. Schmid, H.; Karrer, P., Über Inhaltsstoffe des Rettichs I. Über Sulforaphen, ein Senföl aus Rettichsamen (*Raphanus sativus* L. var. alba). *Helv. Chim. Acta* **1948**, *31*, 1017-1028.
106. Huang, X.; Renwick, J. A. A.; Sachdev-Gupta, K., A chemical basis for differential acceptance of *Erysimum cheiranthoides* by two *Pieris* species. *J. Chem. Ecol.* **1993**, *19*, 195-210.
107. Emam, S. S.; El-Moaty, H. I. A., Glucosinolates, phenolic acids and anthraquinones of *Isatis microcarpa* Boiss and *Pseuderucaria clavate* (Boiss&Reut.) family: Cruciferae. *J. Appl. Sci. Res.* **2009**, *5*, 2315-2322.
108. Rodman, J. E.; Chew, F. S., Phytochemical correlates of herbivory in a community of native and naturalized Cruciferae. *Biochem. Syst. Ecol.* **1980**, *8*, 43-50.
109. Fabre, N.; Bon, M.; Moulis, C.; Fouraste, I.; Stanislas, E., Three glucosinolates from seeds of *Brassica juncea*. *Phytochemistry* **1997**, *45*, 525-527.
110. Gan, R.-Y.; Lui, W.-Y.; Wu, K.; Chan, C.-L.; Dai, S.-H.; Sui, Z.-Q.; Corke, H., Bioactive compounds and bioactivities of germinated edible seeds and sprouts: An updated review. *Trends Food Sci. Technol.* **2017**, *59*, 1-14.
111. Aisyah, S.; Gruppen, H.; Andini, S.; Bettonvil, M.; Severing, E.; Vincken, J.-P., Variation in accumulation of isoflavonoids in *Phaseoleae* seedlings elicited by *Rhizopus*. *Food Chem.* **2016**, *196*, 694-701.
112. Aisyah, S.; Gruppen, H.; Madzora, B.; Vincken, J. P., Modulation of isoflavonoid composition of *Rhizopus oryzae* elicited soybean (*Glycine max*) seedlings by light and wounding. *J. Agric. Food Chem.* **2013**, *61*, 8657-8667.
113. Aisyah, S.; Gruppen, H.; Slager, M.; Helmink, B.; Vincken, J. P., Modification of prenylated stilbenoids in peanut (*Arachis hypogaea*) seedlings by the same fungi

- that elicited them: The fungus strikes back. *J. Agric. Food Chem.* **2015**, *63*, 9260-8.
114. Aisyah, S.; Vincken, J.-P.; Andini, S.; Mardiah, Z.; Gruppen, H., Compositional changes in (iso)flavonoids and estrogenic activity of three edible *Lupinus* species by germination and *Rhizopus*-elicitation. *Phytochemistry* **2016**, *122*, 65-75.
115. Baenas, N.; García-Viguera, C.; Moreno, D. A., Biotic elicitors effectively increase the glucosinolates content in Brassicaceae sprouts. *J. Agric. Food Chem.* **2014**, *62*, 1881-1889.
116. Baenas, N.; García-Viguera, C.; Moreno, D. A., Elicitation: a tool for enriching the bioactive composition of foods. *Molecules (Basel, Switzerland)* **2014**, *19*, 13541-13563.
117. Baenas, N.; Villano, D.; García-Viguera, C.; Moreno, D. A., Optimizing elicitation and seed priming to enrich broccoli and radish sprouts in glucosinolates. *Food Chem.* **2016**, *204*, 314-319.
118. Graham, T. L.; Graham, M. Y., Signaling in soybean phenylpropanoid responses: Dissection of primary, secondary, and conditioning effects of light, wounding, and elicitor treatments. *Plant Physiol.* **1996**, *110*, 1123-1133.
119. Natella, F.; Maldini, M.; Nardini, M.; Azzini, E.; Foddai, M. S.; Giusti, A. M.; Baima, S.; Morelli, G.; Scaccini, C., Improvement of the nutraceutical quality of broccoli sprouts by elicitation. *Food Chem.* **2016**, *201*, 101-109.
120. Pérez-Balibrea, S.; Moreno, D. A.; García-Viguera, C., Improving the phytochemical composition of broccoli sprouts by elicitation. *Food Chem.* **2011**, *129*, 35-44.
121. Yang, R.; Guo, L.; Jin, X.; Shen, C.; Zhou, Y.; Gu, Z., Enhancement of glucosinolate and sulforaphane formation of broccoli sprouts by zinc sulphate via its stress effect. *J. Funct. Foods* **2015**, *13*, 345-349.
122. Yang, R.; Hui, Q.; Gu, Z.; Zhou, Y.; Guo, L.; Shen, C.; Zhang, W., Effects of  $\text{CaCl}_2$  on the metabolism of glucosinolates and the formation of isothiocyanates as well as the antioxidant capacity of broccoli sprouts. *J. Funct. Foods* **2016**, *24*, 156-163.
123. Ramirez-Estrada, K.; Vidal-Limon, H.; Hidalgo, D.; Moyano, E.; Golenioswki, M.; Cusidó, R. M.; Palazon, J., Elicitation, an effective strategy for the biotechnological production of bioactive high-added value compounds in plant cell factories. *Molecules* **2016**, *21*, 182.
124. Araya-Cloutier, C.; den Besten, H. M. W.; Aisyah, S.; Gruppen, H.; Vincken, J.-P., The position of prenylation of isoflavonoids and stilbenoids from legumes (Fabaceae) modulates the antimicrobial activity against Gram-positive pathogens. *Food Chem.* **2017**, *226*, 193-201.
125. Araya-Cloutier, C.; Vincken, J. P.; van Ederen, R.; den Besten, H. M. W.; Gruppen, H., Rapid membrane permeabilization of *Listeria monocytogenes* and *Escherichia coli* induced by antibacterial prenylated phenolic compounds from legumes. *Food Chem.* **2018**, *240*, 147-155.
126. Park, I. S.; Kim, H. J.; Jeong, Y.-S.; Kim, W.-K.; Kim, J.-S., Differential abilities of Korean soybean varieties to biosynthesize glyceollins by biotic and abiotic elicitors. *Food Sci. Biotechnol.* **2017**, *26*, 255-261.
127. Ludwig-Müller, J.; Schubert, B.; Pieper, K.; Ihmig, S.; Hilgenberg, W., Glucosinolate content in susceptible and resistant chinese cabbage varieties during development of clubroot disease. *Phytochemistry* **1997**, *44*, 407-414.
128. Ahn, E.; Kim, J.; Shin, D., Antimicrobial effects of allyl isothiocyanates on several microorganisms. *Korean J. Food Sci. Technol.* **2001**, *31*, 206-211.
129. Aires, A.; Mota, V. R.; Saavedra, M. J.; Monteiro, A. A.; Simoes, M.; Rosa, E. A.; Bennett, R. N., Initial *in vitro* evaluations of the antibacterial activities of glucosinolate enzymatic hydrolysis products against plant pathogenic bacteria. *J. Appl. Microbiol.* **2009**, *106*, 2096-105.
130. Aires, A.; Mota, V. R.; Saavedra, M. J.; Rosa, E. A.; Bennett, R. N., The antimicrobial effects of glucosinolates and their respective enzymatic hydrolysis



- products on bacteria isolated from the human intestinal tract. *J. Appl. Microbiol.* **2009**, *106*, 2086-95.
131. Jang, M.; Hong, E.; Kim, G. H., Evaluation of antibacterial activity of 3-butenyl, 4-pentenyl, 2-phenylethyl, and benzyl isothiocyanate in *Brassica* vegetables. *J. Food Sci.* **2010**, *75*, M412-6.
  132. Savoia, D., Plant-derived antimicrobial compounds: alternatives to antibiotics. *Future Microbiol.* **2012**, *7*, 979-90.
  133. Stotz, H. U.; Sawada, Y.; Shimada, Y.; Hirai, M. Y.; Sasaki, E.; Krischke, M.; Brown, P. D.; Saito, K.; Kamiya, Y., Role of camalexin, indole glucosinolates, and side chain modification of glucosinolate-derived isothiocyanates in defense of *Arabidopsis* against *Sclerotinia sclerotiorum*. *Plant J.* **2011**, *67*, 81-93.
  134. Sewell, D. L.; Pfaller, M. A.; Barry, A. L., Comparison of broth macrodilution, broth microdilution, and E-test antifungal susceptibility test for fluconazole. *J. Clin. Microbiol.* **1994**, *32*, 2099-2102.
  135. Kar, S.; Roy, K., QSAR of phytochemicals for the design of better drugs. *Expert Opin. Drug Discovery* **2012**, *7*, 877-902.
  136. Dufour, V.; Stahl, M.; Baysse, C., The antibacterial properties of isothiocyanates. *Microbiology (Reading, England)* **2015**, *161*, 229-43.
  137. Poole, L. B., The basics of thiols and cysteines in redox biology and chemistry. *Free Radical Biol. Med.* **2015**, *80*, 148-157.
  138. Brown, L.; Wolf, J. M.; Prados-Rosales, R.; Casadevall, A., Through the wall: extracellular vesicles in Gram-positive bacteria, mycobacteria and fungi. *Nat. Rev. Microbiol.* **2015**, *13*, 620.
  139. Zhang, G.; Meredith, T. C.; Kahne, D., On the essentiality of lipopolysaccharide to Gram-negative bacteria. *Curr. Opin. Microbiol.* **2013**, *16*, 779-85.
  140. Nikaido, H., Molecular basis of bacterial outer membrane permeability revisited. *Microbiol. Mol. Biol. Rev.* **2003**, *67*, 593-656.
  141. Pages, J. M.; Masi, M.; Barbe, J., Inhibitors of efflux pumps in Gram-negative bacteria. *Trends Mol. Med.* **2005**, *11*, 382-9.
  142. De Nobel, J. G.; Barnett, J. A., Passage of molecules through yeast cell walls: A brief essay-review. *Yeast (Chichester, England)* **1991**, *7*, 313-23.
  143. Lambert, P. A., Cellular impermeability and uptake of biocides and antibiotics in Gram-positive bacteria and mycobacteria. *J. Appl. Microbiol.* **2002**, *92*, 46S-54S.
  144. Kollár, R.; Reinhold, B. B.; Petráková, E.; Yeh, H. J. C.; Ashwell, G.; Drgonová, J.; Kapteyn, J. C.; Klis, F. M.; Cabib, E., Architecture of the Yeast Cell Wall:  $\beta(1\rightarrow6)$ -Glucan interconnects mannoprotein,  $\beta(1\rightarrow3)$ -glucan, and chitin. *J. Biol. Chem.* **1997**, *272*, 17762-17775.
  145. Lamping, E.; Baret, P. V.; Holmes, A. R.; Mon, B. C.; Goffeau, A.; Cannon, R. D., Fungal PDR transporters: Phylogeny, topology, motifs and function. *Fungal Genet. Biol.* **2010**, *47*, 127.
  146. Murakami, S., Chapter 1 Structures and transport mechanisms of RND efflux pumps. In *Efflux-mediated antimicrobial resistance in bacteria - Mechanisms, regulation and clinical implications*, Li, Z.-Z.; Elkins, C. A.; Zgurskaya, H. I., Eds. Springer International Publishing: Switzerland, **2016**.
  147. Natalya, B.; Elkins, C. A., Antimicrobial drug efflux pumps in other Gram-positive bacteria. In *Efflux-mediated antimicrobial resistance in bacteria*, Li, X.-Z.; Elkins, C. A.; Zgurskaya, H. I., Eds. Springer International Publishing: Switzerland, **2016**; pp 197-218.
  148. Shiomi, N.; Fukuda, H.; Fukuda, Y.; Murata, K.; Kimura, A., Nucleotide sequence and characterization of a gene conferring resistance to ethionine in yeast *Saccharomyces cerevisiae*. *J. Ferment. Bioeng.* **1991**, *71*, 211-215.
  149. Collet, J. F.; Messens, J., Structure, function, and mechanism of thioredoxin proteins. *Antioxid. Redox Signal.* **2010**, *13*, 1205-16.
  150. Ishihama, Y.; Schmidt, T.; Rappsilber, J.; Mann, M.; Hartl, F. U.; Kerner, M. J.; Frishman, D., Protein abundance profiling of the *Escherichia coli* cytosol. *BMC Genomics* **2008**, *9*, 102.

151. Fahey, J. W.; Stephenson, K. K.; Wade, K. L.; Talalay, P., Urease from *Helicobacter pylori* is inactivated by sulforaphane and other isothiocyanates. *Biochem. Biophys. Res. Commun.* **2013**, 435, 1-7.
152. Nowicki, D.; Maciąg-Dorszyńska, M.; Bogucka, K.; Szalewska-Pałasz, A.; Herman-Antosiewicz, A., Various modes of action of dietary phytochemicals, sulforaphane and phenethyl isothiocyanate, on pathogenic bacteria. *Sci. Rep.* **2019**, 9, 13677.
153. Luciano, F. B.; Hosseini, F. S.; Beta, T.; Holley, R. A., Effect of free-SH containing compounds on allyl isothiocyanate antimicrobial activity against *Escherichia coli* O157:H7. *J. Food Sci.* **2008**, 73, M214-20.

---

## Modulation of glucosinolate composition in Brassicaceae seeds by germination and fungal elicitation

---

Glucosinolates (GSLs) are of interest for potential antimicrobial activity of their degradation products and exclusive presence in Brassicaceae. Compositional changes of aliphatic, benzenic, and indolic GSLs of *Sinapis alba*, *Brassica napus*, and *B. juncea* seeds by germination and fungal elicitation were studied. *Rhizopus oryzae* (non-pathogenic), *Fusarium graminearum* (non-pathogenic), and *F. oxysporum* (pathogenic) were employed. Thirty-one GSLs were detected by RP-UHPLC-PDA-ESI-MS<sup>n</sup>. Aromatic-acylated derivatives of 3-butenyl GSL, *p*-hydroxybenzyl GSL, and indol-3-ylmethyl GSL were for the first time tentatively annotated and confirmed to be not artefacts. For *S. alba*, germination, *Rhizopus*-elicitation, and *F. graminearum*-elicitation increased total GSL content, mainly consisting of *p*-hydroxybenzyl GSL, by 2-3 fold. For *B. napus* and *B. juncea*, total GSL content was unaffected by germination or elicitation. In all treatments, aliphatic GSL content was decreased ( $\geq 50\%$ ) in *B. napus*, and remained unchanged in *B. juncea*. Indolic GSLs were induced in all species by germination and non-pathogenic elicitation.

**Keywords:** Brassicaceae, crucifer, elicitation, *Fusarium*, germination, glucosinolate, LC-MS, plant defense, *Rhizopus*, seeds

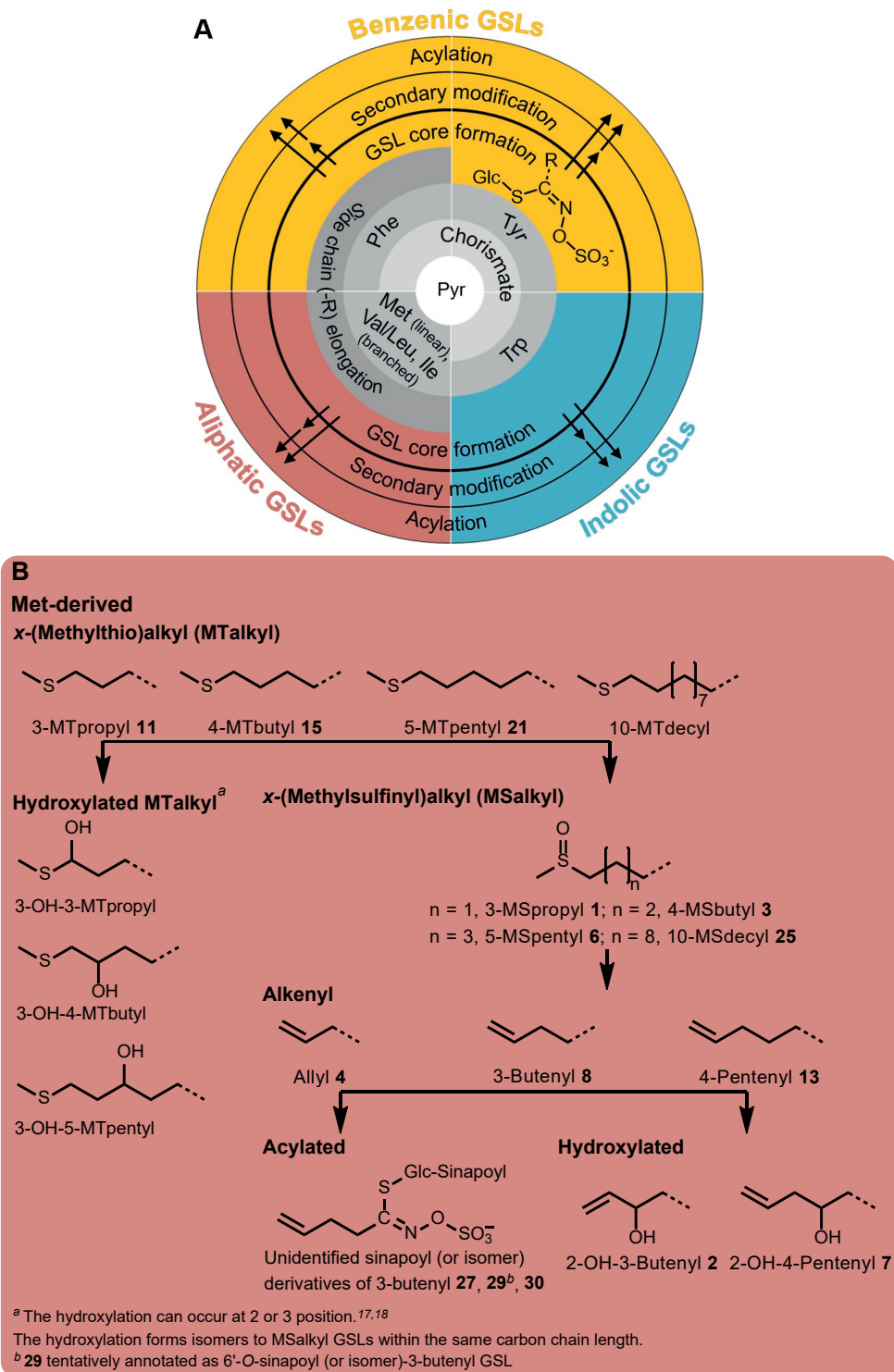
Based on: Andini, S.; Dekker, P.; Gruppen, H.; Araya-Cloutier, C.; Vincken, J.-P., Modulation of glucosinolate composition in Brassicaceae seeds by germination and fungal elicitation. *J. Agric. Food Chem.* **2019**, 67, 12770-12779.

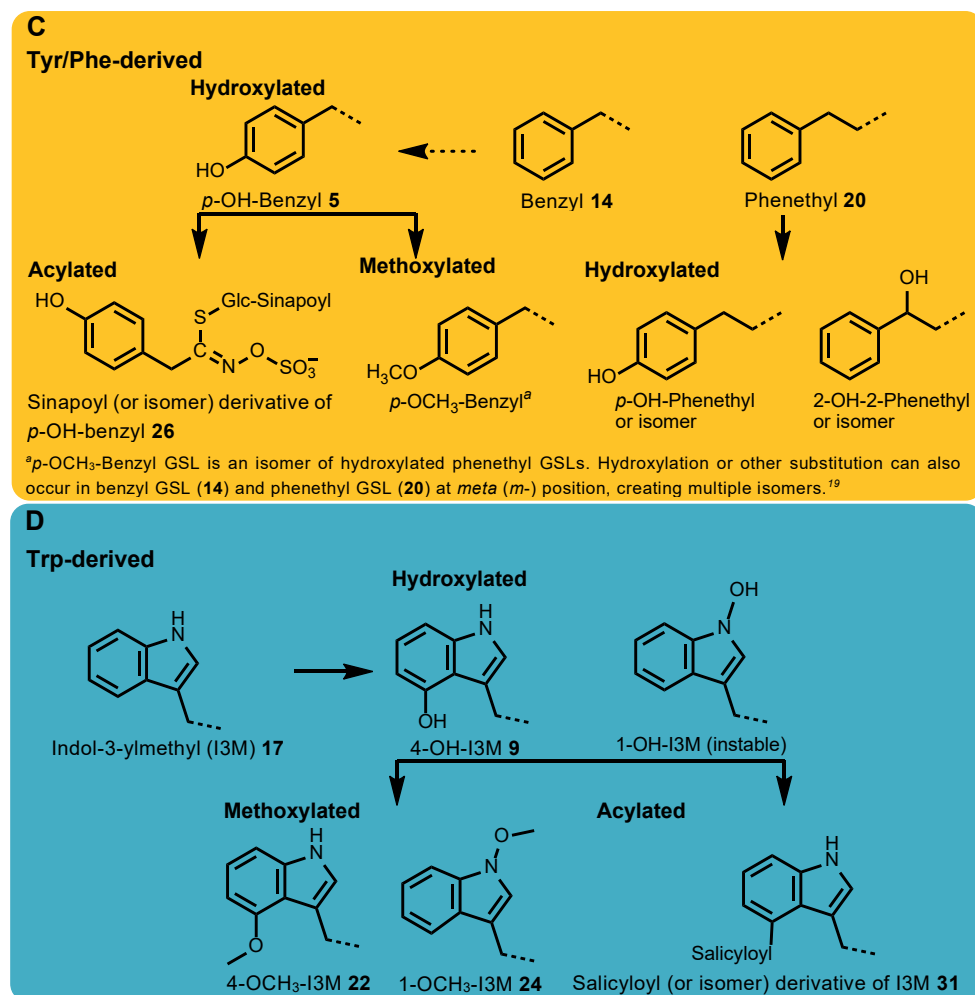
## 2.1. Introduction

Plants from the family of Brassicaceae are of global economic importance. They are consumed throughout the world in many forms, such as leafy vegetables, root vegetables, sprouts, vegetable oil, and condiments. Compounds from Brassicaceae gain more research interest because of their potential antimicrobial activity (both with respect to disease resistance of brassicaceous species and as natural preservatives to enhance the open shelf-life of food products),<sup>1-3</sup> which is often associated with isothiocyanates (ITCs), a class of compounds which are degradation products of GSLs.<sup>4,5</sup>

The biosynthesis of GSLs consists of three stages (**Figure 2.1A**): (i) side chain elongation of the amino acids, especially Met, Val/Leu, Ile, and Phe, (ii) formation of the GSL core, and (iii) secondary modification of the side chain, e.g. oxidation and hydroxylation.<sup>6,7</sup> In addition to step (iii), substitution at the thioglucosyl group, e.g. acylation, might occur, which has been identified by Linscheid *et al.*<sup>8</sup>, Reichelt *et al.*<sup>9</sup>, and Agerbirk and Olsen<sup>10</sup>. GSLs are classified into various classes based on their side chain: aliphatic GSLs (**Figure 2.1B**) derived mostly from Met, benzenic GSLs (**Figure 2.1C**) from Phe or Tyr, and indolic GSLs (**Figure 2.1D**) from Trp.<sup>11</sup>

The content of GSLs in the growing plants can be influenced by applying abiotic and biotic stressors.<sup>20-24</sup> In regards to biotic stressors, fungi are commonly applied on mature Brassicaceae plant tissues, e.g. leaves. Studies have indicated various effects of pathogenic fungi, e.g. *Fusarium oxysporum* and *Alternaria brassicae*, on the content of aliphatic, benzenic, and indolic GSLs in infected leaves of various Brassicaceae species and varieties.<sup>4,12,20</sup> In regards to abiotic stressors, phytohormones and salts are often applied on germinating Brassicaceae seeds.<sup>24-29</sup> Most of studies indicated that total GSL content could be increased, but none reported an improvement on GSL diversity. Research on fungal elicitation of germinating Brassicaceae seeds has been done once in 1996.<sup>30</sup> That study reported the effect of *Plasmodiophora brassicae* on GSL content per class in roots of four varieties of Chinese cabbage (*Brassica campestris* ssp. *pekinensis*), and indicated no clear trend on the compositional changes of GSLs.<sup>30</sup> Studies on the effect of fungal elicitation on the compositional changes of particular major secondary metabolites have been performed on a different plant family, i.e. Leguminosae, and found that fungal elicitation induced the accumulation of isoflavonoids and stilbenoids which had stronger antimicrobial activity.<sup>31</sup> Using a similar approach, i.e. fungal elicitation, we aimed for an induction of GSL production (in terms of content and diversity) in the germinating Brassicaceae seeds, which then can be used to yield high amount of ITCs with potential antimicrobial activity.





**Figure 2.1.** Simplified biosynthesis route of GSL classes, i.e. aliphatic, benzenic, and indolic (A), subclasses of Met-derived aliphatic GSLs (B, red box), benzenic GSLs (C, yellow box), and indolic GSLs (D, blue box) in Brassicaceae, especially *S. alba*, *B. napus*, and *B. juncea*. The biosynthesis route was adapted from Bianco *et al.*, Lee *et al.*, Agerbirk and Olsen, Abdel-Farid *et al.*, Wittstock and Halkier, Yi *et al.*<sup>11-16</sup> The biosynthesis route of aliphatic GSLs starts from pyruvate (Pyr) and continues to the formation of methionine (Met) for the linear ones or of valine (Val)/leucine (Leu) and isoleucine (Ile) for the branched ones (i.e. branched alkyl GSLs, which have been found in the tribe *Cardamineae*).<sup>17</sup> As it is still questioned if alanine (Ala) is a precursor of methyl GSL and linear alkyl GSLs,<sup>11,17</sup> Ala is omitted in **Figure 2.1A**. The biosynthesis route of aromatic GSLs starts from Pyr to the formation of chorismate and continues to the formation of phenylalanine (Phe) or tyrosine (Tyr), or tryptophan (Trp), leading to the formation of benzenic GSLs or indolic GSLs. Dashed arrow in **Figure 2.1C** indicates putative biosynthesis step. The GSL core structure given in **Figure 2.1B-D** is omitted, except for the thioglucose-acylated GSLs, and only the side chain (-R) is shown. Bold face number after the name of GSLs correspond to the number in **Table S2.1**.

The induction of GSLs seems to be dependent on the fungus employed and the plant species and variety. Three different fungi were used as stressors in this study, namely *Rhizopus oryzae*, *F. graminearum*, and *F. oxysporum* to modulate the composition of GSLs in various Brassicaceae seeds. *R. oryzae* is food grade and non-phytopathogenic and has often been used for the elicitation of germinating legume seeds.<sup>31-35</sup> *F. graminearum* is not pathogenic to most Brassicaceae plants, whereas *F. oxysporum* is.<sup>36</sup> To the best of our knowledge, our study is the first to report the changes in GSL composition in seeds of *Sinapis alba*, *B. napus*, and *B. juncea* upon germination and fungal elicitation. The changes of GSL composition were monitored by RP-UHPLC-ESI-MS<sup>n</sup> analysis. It was hypothesized that the pathogenic fungus would induce GSL production extensively, compared to the non-pathogenic fungi.

## 2.2. Materials and methods

### 2.2.1. Standard compounds and other chemicals

Authentic standards of twelve different GSLs (with peak numbers in bold face according to **Table S2.1**): benzyl GSL (**14**), phenethyl GSL (**20**), *p*-hydroxybenzyl GSL (**5**), 4-(methylthio)butyl GSL (**15**), 5-(methylthio)butyl GSL (**21**), 3-(methylsulfinyl)propyl GSL (**1**), 4-(methylsulfinyl)butyl GSL (**3**), allyl GSL (**4**), 3-butenyl GSL (**8**), 4-pentenyl GSL (**13**), (*R*)-2-hydroxy-3-butenyl GSL (**2**), and indol-3-ylmethyl (I3M) GSL (**17**), were purchased from Phytolab GmbH & Co (Vestenbergsgreuth, Germany). Isopropanol, acetonitrile (ACN), MeOH, water with 0.1% (v/v) formic acid (FA) (ULC/MS grade), and ACN with 0.1% (v/v) FA (ULC-MS grade) were purchased from Biosolve BV (Valkenswaard, The Netherlands). Hydrogen peroxide (30% v/v) was purchased from Merck (Darmstadt, Germany) and commercial bleach solution (< 5% v/v hypochlorite) from Van Dam Bodegraven B.V. (Bodegraven, The Netherlands). *Tert*-butanol (99.7%) was obtained from Sigma Aldrich (St. Louis, MO, U.S.A.). Water used during experiments other than UHPLC-MS analysis was obtained with use of a Milli-Q A10 Gradient system (18.2 MΩ.cm, 3 ppb TOC) (Merck Millipore, Darmstadt, Germany). Dimethyl sulfoxide (DMSO) was purchased from Ducheda Biochemie (The Netherlands).

Oatmeal agar (OA) was purchased from Becton, Dickinson and Company (New Jersey, U.S.A.). Malt extract agar (MEA) and agar technical were purchased from Oxoid Limited (Hampshire, U.K.). Peptone physiological salt solution (PPS) was ordered from Triticum Microbiologie (Eindhoven, The Netherlands).

### 2.2.2. Plant materials

Seeds of *Sinapis alba* (yellow mustard 'Emergo', 393810), *Brassica napus* ('Helga', 392600), and *B. juncea* var. *rugosa rugosa* (Chinese mustard/amsoi, 160400) were purchased from Vreeken's Zaden (Dordrecht, The Netherlands, <https://www.vreeken.nl/>). *B. juncea* var. *rugosa rugosa* is mentioned as *B. juncea* in the following text.

### 2.2.3. Fungal cultures

The fungal strains of *Fusarium graminearum* CBS 104.09 and *F. oxysporum* CBS 186.53 were purchased from CBS Fungal Biodiversity Centre (Utrecht, The Netherlands). *Rhizopus oryzae* LU581 was kindly provided by the Laboratory of Food Microbiology, Wageningen University (Wageningen, The Netherlands).

### 2.2.4. Surface sterilization and germination

For each germination experiment, seeds of all three species (15 g) were sterilized by immersion in a 100× diluted commercial bleach solution (500 ppm NaOCl) for 15 min. After this, the seeds were rinsed 3 times with sterilized water and soaked for 8 h in excess of sterilized water in the absence of light.

Seeds were germinated at 25 °C in a modified sprouting machine (Sprouter micro-farm EQMM; Easygreen, San Diego, CA, U.S.A.) in the absence of light. The machine was modified as described by Aisyah *et al.*<sup>33</sup> Prior to placing the seeds, the sprouting machine was cleaned according to the cleaning procedure from the manufacturer. Seeds were evenly distributed in one layer on germination trays (17.8 × 8.9 cm). Before application of the stressor, sterilized water was applied by spraying every 3 h for a period of 15 min (around 17 mL/min). This resulted in a relative humidity (RH) of 90-100%. After application of the stressor, i.e. 48 h after start of the germination, RH was set at 55-85% by replacing spraying for fog distribution over the seedlings for 15 min per 3 h. This fog was generated by a mini fogger (Conrad, Oldenzaal, The Netherlands).

### 2.2.5. Application of stressor

Stressor, in the form of a fungal spore suspension, was applied to the seedlings 48 h after start of germination. Previously, *R. oryzae* was grown on a MEA plate for 7 days at 30 °C, whereas *F. graminearum* and *F. oxysporum* were grown separately on OA plates for 7 days at 25 °C.

The seedlings were inoculated with the fungal suspension, obtained by scraping off the plate fully covered by the mould with 9 mL PPS. The suspension with an average count of  $1.0 \times 10^6$  CFU/mL was evenly distributed over the 2-day-old seedlings (0.2 mL/g seedlings) and gently homogenized.

Seven-day-old seedlings (treated and non-treated) were harvested and freeze-dried. The experiment was repeated independently 3 times.

### 2.2.6. Sample extraction

Lyophilized seeds and seedlings were milled into fine powder by using a high speed rotor mill (Retsch Ultra Centrifugal Mill ZM 200; Haan, Germany) with a 0.5 mm sieve. The sample extraction was performed using a Speed Extractor (E-916; Buchi, Flawil, Switzerland). Ground material (400 mg) was mixed with sand (granulation 0.3-0.9 mm, dried at 750 °C; Buchi) in a 40-mL stainless steel extraction cell. Prior to extraction, samples were defatted using *n*-hexane. Then,



the extraction was carried out with absolute MeOH at 65 °C. As GSLs are completely soluble in absolute MeOH, extraction with absolute MeOH gives the advantage of rapid solvent evaporation and sample preparation. Results with absolute MeOH were comparable to those obtained with MeOH-H<sub>2</sub>O (7:3) (data not shown). The in-plant myrosinase was inactive under the extraction conditions used. The extraction was done in 3 cycles consuming 76 mL solvent. Afterward, the extract was evaporated under reduced pressure (Syncore Polyvap, Buchi), resolubilized in *tert*-butanol, and freeze-dried. The dried extracts were stored at -20 °C and resolubilized in absolute MeOH to a concentration of 5 mg/mL for RP-UHPLC-MS<sup>n</sup> analysis. The hexane fractions contained no GSLs; thus, they were not considered for further analysis.

### 2.2.7. RP-UHPLC-MS<sup>n</sup> analysis

Analysis of GSLs was performed on an Accela ultra high performance liquid chromatography (UHPLC) system (Thermo Scientific, San Jose, CA, U.S.A.) equipped with a pump, autosampler, and photodiode array (PDA) detector. An LTQ Velos electrospray ionization (ESI) ion trap mass spectrometer (MS) (Thermo Scientific) was coupled to the LC system.

Sample (1 µL) was injected onto an Acquity UPLC-BEH shield RP18 column (2.1 mm i.d. × 150 mm, 1.7 µm particle size; Waters, Milford, MA, U.S.A.) with an Acquity UPLC BEH shield RP18 VanGuard precolumn (2.1 mm i.d. × 5 mm, 1.7 µm particle size; Waters). Water acidified with 0.1% (v/v) FA + 1% (v/v) ACN, eluent A, and ACN acidified with 0.1% (v/v) FA, eluent B, were used as solvent at a flow rate of 400 µL/min. The temperature of sample tray was controlled at 15 °C. The column was set at 35 °C. The PDA detector was set to monitor absorption at 200-400 nm. The following elution gradient was used: 0-5.5 min, an isocratic on 0% (v/v) B; 5.5-32.4 min, a linear gradient to 49% B; 32.4-33.5 min, a linear gradient from 49 to 100% B; 33.5-39 min, an isocratic on 100% B; 39-40 min, a linear gradient from 100% to 0% B; 40-45.6 min, an isocratic on 0% B.

Mass spectrometric analysis was performed on an LTQ Velos equipped with a heated ESI-MS probe coupled to RP-UHPLC. The spectra were acquired in an *m/z* (mass to charge ratio) range of 92-1000 Da in both positive (PI) and negative ionization (NI) modes. Data-dependent MS<sup>n</sup> analysis was performed on the most intense ion with a normalized collision energy of 35%. The system was tuned with GSB via automatic tuning using Tune Plus (Xcalibur v.2.2, Thermo Scientific). Nitrogen was used as sheath gas, and helium as auxiliary gas. The ion transfer tube (ITT) temperature was set at 300 °C, and the source voltage was 4.5 kV for both ionization modes.

In each set of analysis, calibration curves of *p*-hydroxybenzyl GSL (for benzenic GSLs), 4-pentenyl GSL (for aliphatic GSLs), and I3M GSL (for indolic GSLs) standards were made in the range of 1-650 µM. Calibration curves ( $R^2 \geq 0.993$ ) were based on the peak area of the full MS signal of the external standards in NI mode. The twelve GSL standards were analyzed at 10 µM and 50 µM to

support peak annotation and quantification by using MS-based relative response factors (RRF). The concentration of GSLs whose standard compounds were not available in the analysis was quantified by using RRF of a GSL with the most similar structure and molecular weight (**Table S2.2**). Peaks **10** and **28** were present in trace amounts and since their subclass was not annotated, no quantification was done for these peaks. Operation of the LC-MS system and data processing were done by using the software packages Xcalibur 2.2 and LTQ Tuneplus 2.7 (both Thermo Scientific, San Jose, U.S.A.).

### 2.2.8. Statistical analysis

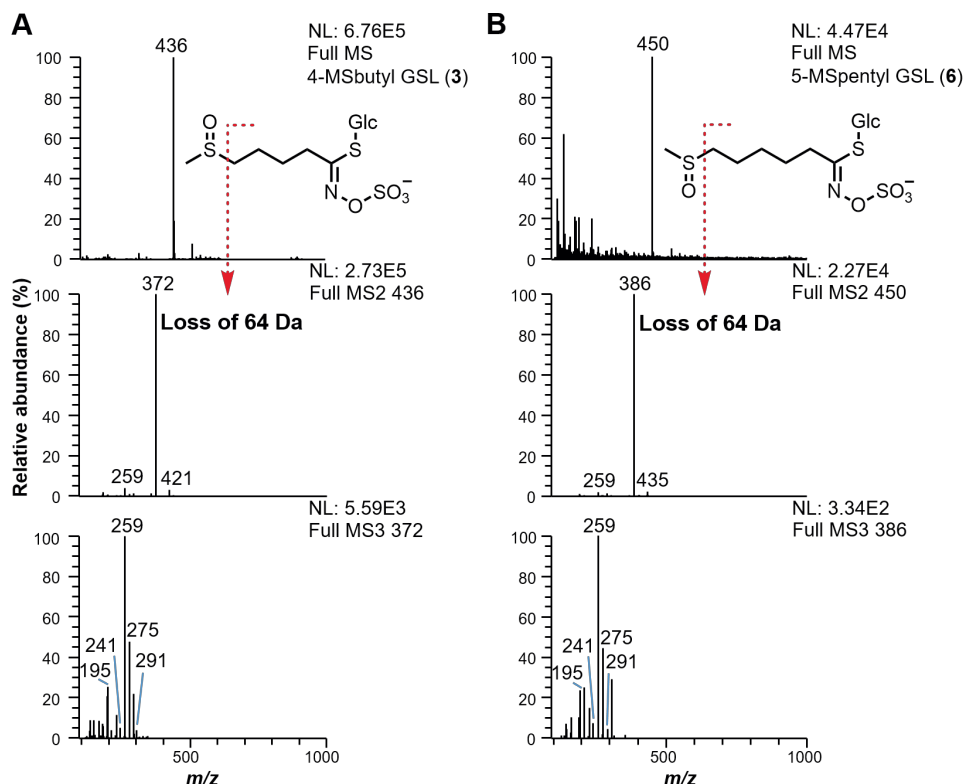
To test for significance between treatments within species, the data was statistically evaluated by analysis of variance (ANOVA), followed by Tukey *post hoc* analysis using IBM SPSS Statistic v.23 software (SPSS Inc., Chicago, IL, U.S.A.).

## 2.3. Results

### 2.3.1. Tentative annotation of GSLs

Based on information extracted from literature, detailed hereafter and in the **Supplementary Information**, 31 GSLs in total were tentatively annotated from *S. alba*, *B. napus*, and *B. juncea* by RP-UHPLC-PDA-MS<sup>n</sup> analysis.

The first criterion to distinguish peaks of GSLs from other types of compounds is the presence of fragment ion at  $m/z$  of 259 in NI mode.<sup>37</sup> The second criterion is to distinguish classes of GSLs: the  $m/z$  of deprotonated molecular ion  $[M-H]^-$  of intact aliphatic and benzenic GSLs is at an even number as they contain one nitrogen atom, whereas that of indolic GSLs is at an odd number as they contain two nitrogen atoms. The third criterion is to confirm the classes of GSLs as well as to notice the presence of substituents having a conjugated system: benzenic GSLs with O-substitution on the phenyl ring, indolic GSLs, and aromatic acyl derivatives of any GSLs, show specific UV<sub>max</sub>. However, for minor trace peaks this criterion is less secure. The three criteria, summarized in **Table S2.3**, are useful for fast screening the class of a GSL. The molecular ions  $[M-H]^-$  ( $m/z$ ) of GSLs, the fragmentation patterns, retention times, and UV absorption spectra allowed the annotation of 31 GSLs from *S. alba*, *B. napus*, and *B. juncea* (**Table S2.1**), where the annotation of twelve GSLs was confirmed by the standards listed in the section **2.2.1** and that of nineteen GSLs was tentative. As many GSLs share similar fragmentation patterns and modifications of the side chain can create many possible isomers with no substantial differences in polarity (e.g. hydroxylated phenethyl GSL and methoxylated benzyl GSL, **Figure 2.1C**), annotation can be difficult. Consequently, several peaks (e.g. **10**, **12**, **18**, **19**, **28**) were tentatively annotated with multiple possible molecular structures and/or formulae (**Table S2.1**).



**Figure 2.2.** MS spectra of standard 4-(methylsulfinyl)butyl GSL (4-MSbutyl, **3**) (**A**) and tentatively annotated 5-(methylsulfinyl)pentyl GSL (5-MSpentyl, **6**) (**B**). Fragmentation occurred for the most abundant ion. The fragment ion with a neutral loss of 64 Da ( $\text{CH}_3\text{SOH}$ ) as the most abundant ion in MS<sup>2</sup> spectra is the characteristics of MS<sup>2</sup> spectra of (methylsulfinyl)alkyl GSLs. The fragment ions with  $m/z$  of 195, 241, 259, 275, and 291 shown in MS<sup>3</sup> spectra are diagnostic fragment ions for GSLs.

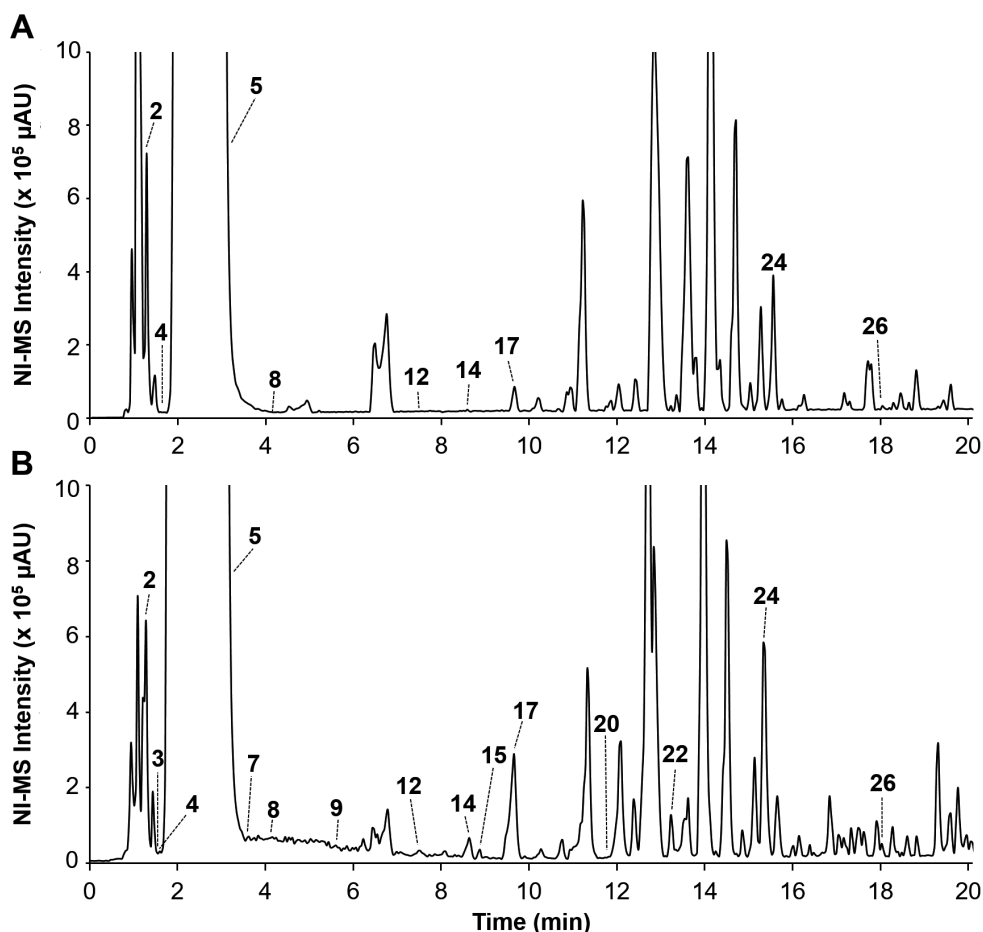
Of nineteen GSLs, four (**11**, **6**, **25**, **7**) were tentatively annotated as 3-(methylthio)propyl GSL, 5-(methylsulfinyl)pentyl GSL, 10-(methylsulfinyl)decyl GSL, and 2-hydroxy-4-pentenyl GSL, respectively, according to fragmentation pattern of the analog within the same subclass whose standards were available in the analysis and the logic of their retention times. The MS spectra of 4-(methylsulfinyl)butyl GSL (**3**) (the standard) and 5-(methylsulfinyl)pentyl GSL (**6**) (present in an extract), as representatives, are displayed in **Figure 2.2**. In addition, fragmentation patterns of **6** and **7** were in line with Cataldi *et al.*<sup>38</sup> who analyzed the reference rapeseed (*B. napus*). According to the molecular weight and retention time, **12** and **19** were tentatively annotated as x-hydroxy-4-(methylthio)butyl GSL and x-hydroxy-5-(methylthio)pentyl GSL, respectively, where the hydroxylation might occur at 2- or 3-position.<sup>17,18</sup> Two indolic GSLs (**9**, **24**) were tentatively annotated as 4-hydroxy-I3M GSL and 1-methoxy-I3M GSL,

respectively, according to fragment ions of those observed in rapeseed in our analysis as well as in the analysis done by Cataldi *et al.*<sup>38</sup> using a reference rapeseed. Another indolic GSL (**22**) was tentatively annotated as 4-methoxy-I3M GSL according to the discriminating fragmentation pattern for 4-methoxy-I3M GSL and 1-methoxy-I3M GSL observed by Pfalz *et al.*<sup>39</sup> in *Arabidopsis thaliana* and Olsen *et al.*<sup>17</sup> According to this discriminating fragmentation pattern for the 4- and 1-substituted indolic GSLs (**Figure S2.2**), one more indolic GSL (**31**) was tentatively annotated as 4-salicyloxy (or isomer)-I3M GSL. Four GSLs (**26, 27, 29, 30**) were tentatively annotated as GSLs acylated at the thioglucosyl group, by comparison the fragmentation patterns to the existing reports on various purified acylated GSLs.<sup>9,13</sup> Peak **18** might represent a benzenic GSL with a side chain formula of  $C_8H_9O$ , with potentially different isomeric structures (**Table S2.1**). Two GSLs (**16, 23**) were tentatively annotated as C5 and C6 alkyl GSLs, respectively, according to the presence of diagnostic fragment ions of GSLs, molecular weight and retention time.

Two detected peaks were left unclassified (**Table S2.1**). Peaks **10** and **28** had a molecular weight 14 Da different from **16** and **23**, respectively. However, **10** and **28** demonstrated a neutral loss of 18 Da in MS<sup>2</sup> fragmentation, which was not observed for the aliphatic GSLs **16** and **23**. Therefore, **10** and **28** were tentatively annotated with potential side chain formulae of  $C_4H_9$  or  $C_3H_5O$  and  $C_7H_{15}$  or  $C_6H_{11}O$ , respectively (**Table S2.1**).

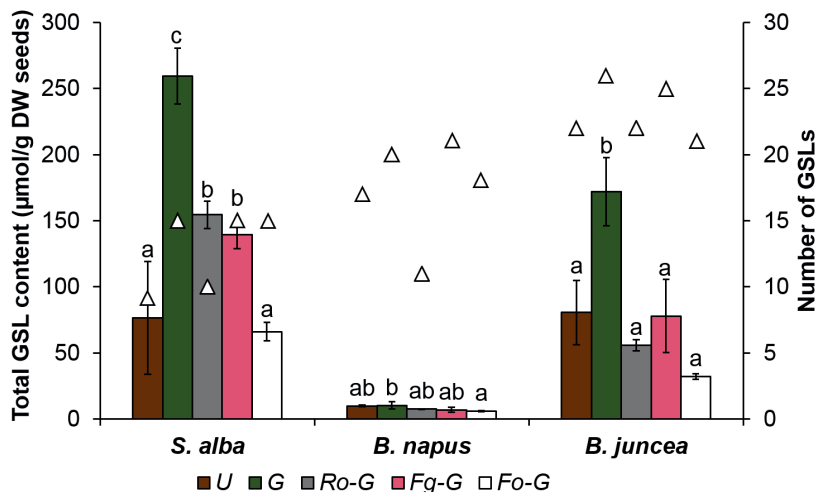
### **2.3.2. Overall compositional changes of GSLs by germination and fungal elicitation**

(*R*)-2-hydroxy-3-butenyl GSL (**2**), I3M GSL (**17**), and 1-methoxy-I3M GSL (**24**) were present throughout all the studied seeds and (elicited) seedlings (**Table S2.1**). GSL profile in the untreated *S. alba* seeds consisted of 9 GSLs and this number was increased upon germination up to 15 GSLs (**Figure 2.3**). This diversity was not improved further by fungal elicitation, but even decreased by *R. oryzae* (**Figure 2.4**), and this trend applied to *B. napus* and *B. juncea*.



**Figure 2.3.** NI-MS chromatograms of *S. alba* seeds (the untreated, Sa\_U) (A) and seedlings (the germinated, Sa\_G) (B). The color codes refer to those in Figure 2.5-2.7.

Furthermore, **Figure 2.4** illustrates the total GSL content in the seeds, untreated seedlings, and treated seedlings. *S. alba* and *B. juncea* seeds were the richest in GSLs, with 76.5 and 80.5  $\mu\text{mol/g}$  DW, respectively, whereas *B. napus* seeds contained only 9.6  $\mu\text{mol/g}$  DW. The total GSL content in *S. alba* was significantly increased by 2.9 fold upon germination, 2.4 fold upon *Rhizopus*-elicitation, and 2.2 fold upon *F. graminearum*-elicitation. In *B. napus* and *B. juncea*, neither germination nor fungal elicitation enhanced the total GSL content significantly. These results were not significantly affected after considering a dry weight loss (commonly reported at around 10%) due to respiration during germination.<sup>40-43</sup>



**Figure 2.4.** Total GSL content ( $\mu\text{mol/g DW}$ , primary y-axis) and GSL diversity indicated by the number of GSLs (triangles) (secondary y-axis) in the untreated (U), germinated (G), *R. oryzae*-germinated (Ro-G), *F. graminearum*-germinated (Fg-G), and *F. oxysporum*-germinated (Fo-G) seeds of *S. alba*, *B. napus*, and *B. juncea*. Data of total GSL content are the mean values from three biologically independent experiments. Error bars show standard deviation of total GSL content. Different letters at the bars show significant difference of the mean of total GSL content between treatments at  $p < 0.05$ .

### 2.3.3. Compositional changes of aliphatic GSLs

The aliphatic GSL content in *S. alba* seeds was  $4.0 \mu\text{mol/g DW}$ , and this content remained similar in the non-elicited seedling and *F. graminearum*-elicited seedling, but was decreased ( $> 50\%$ ) in *R. oryzae*-elicited seedling (**Figure 2.5A**). Furthermore, the total aliphatic content was increased by 60% in *F. oxysporum*-elicited seedlings. Differently, the aliphatic GSL content in *B. napus* seed was  $8.3 \mu\text{mol/g DW}$ , and this content decreased to  $3.6 \mu\text{mol/g DW}$  already upon germination, and that content in the seedlings was statistically similar to that in the fungal elicited ones (**Figure 2.5B**). **Figure 2.5C** shows that the aliphatic GSL content in *B. juncea* seed was  $79.8 \mu\text{mol/g DW}$ , much higher than that in *S. alba* and *B. napus* seeds. Furthermore, this content in *B. juncea* seed was stable upon any treatment, i.e. germination and fungal elicitation, but decreased (50%) in the *F. oxysporum* elicitation (**Figure 2.5C**).

With respect to the chemical diversity, **Figure 2.5A** indicates that there were 3 subclasses of aliphatic GSLs, namely hydroxylated alkenyl, alkenyl, and hydroxylated MTalkyl in *S. alba* seeds. (*R*)-2-Hydroxy-3-butenyl GSL (**2**) represented 80% of total aliphatic GSL content, whereas the rest was composed of 3-butenyl GSL (**8**), allyl GSL (**4**), and *x*-OH-4-(methylthio)butyl GSL (**12**). Upon germination, the content of hydroxylated alkenyl subclass was stable, the alkenyl subclass was reduced significantly, and the OH-MTalkyl subclass was increased.

Upon fungal elicitation the diversity was not improved, but the content of OH-MTalkyl subclass was increased by *Fusarium*-elicitations (**Figure 2.5A**).

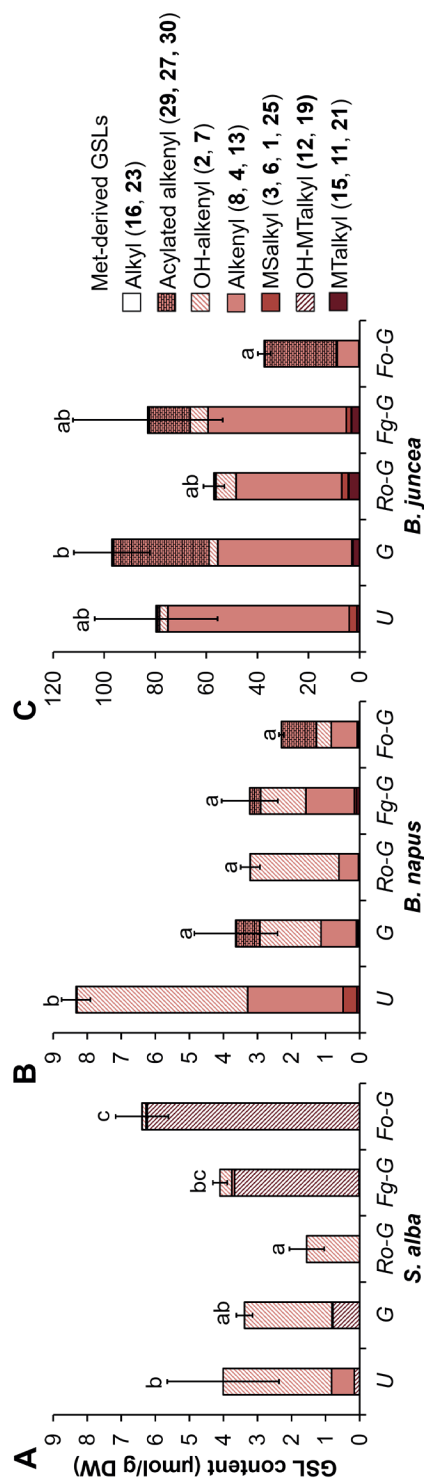
**Figure 2.5B** indicates that *B. napus* untreated seeds consisted of 4 major aliphatic subclasses, namely hydroxylated alkenyl, alkenyl, MSalkyl, and MTalkyl, from the highest to the lowest content. Upon germination, the four subclasses remained present with the same two top major ones. Interestingly, the acylated alkenyl GSL, particularly 6'-*O*-sinapoyl (or isomer)-3-butenyl GSL (**29**), emerged upon germination and *Fusarium*-elicitation. In contrast, MTalkyl GSLs and acylated alkenyl GSLs were absent in *Rhizopus*-elicited seedlings. It is noteworthy to mention that the acylated GSLs were not artefacts; in our anhydrous methanol extraction at 65 °C esterification did not occur, because the chromatograms did not contain peaks corresponding to methyl esters of sinapic acid or other aromatic acids.

**Figure 2.5C**, with the help of **Table S2.6**, indicates that *B. juncea* seed consisted of 6 aliphatic subclasses, namely MTalkyl, MSalkyl, alkenyl, hydroxylated alkenyl, acylated alkenyl, and alkyl. 3-Butenyl GSL (**8**) was the predominant (77% of total aliphatic GSL content). The other 5 subclasses were present at a proportion of less than 4%. Upon germination, there was a significant increased content of acylated alkenyl subclass, i.e. sinapoyl (or isomer) derivatives of 3-butenyl GSL (from 1.0 to 37.3  $\mu\text{mol/g DW}$ ). Both *Fusarium*-elicited seedlings also contained acylated alkenyl GSLs at a comparable level to that in the non-elicited seedling (**Table S2.6**). In contrast, *Rhizopus*-elicited seedlings contained acylated alkenyl subclass in a very low level (0.4  $\mu\text{mol/g DW}$ ).

### 2.3.4. Compositional changes of benzenic GSLs

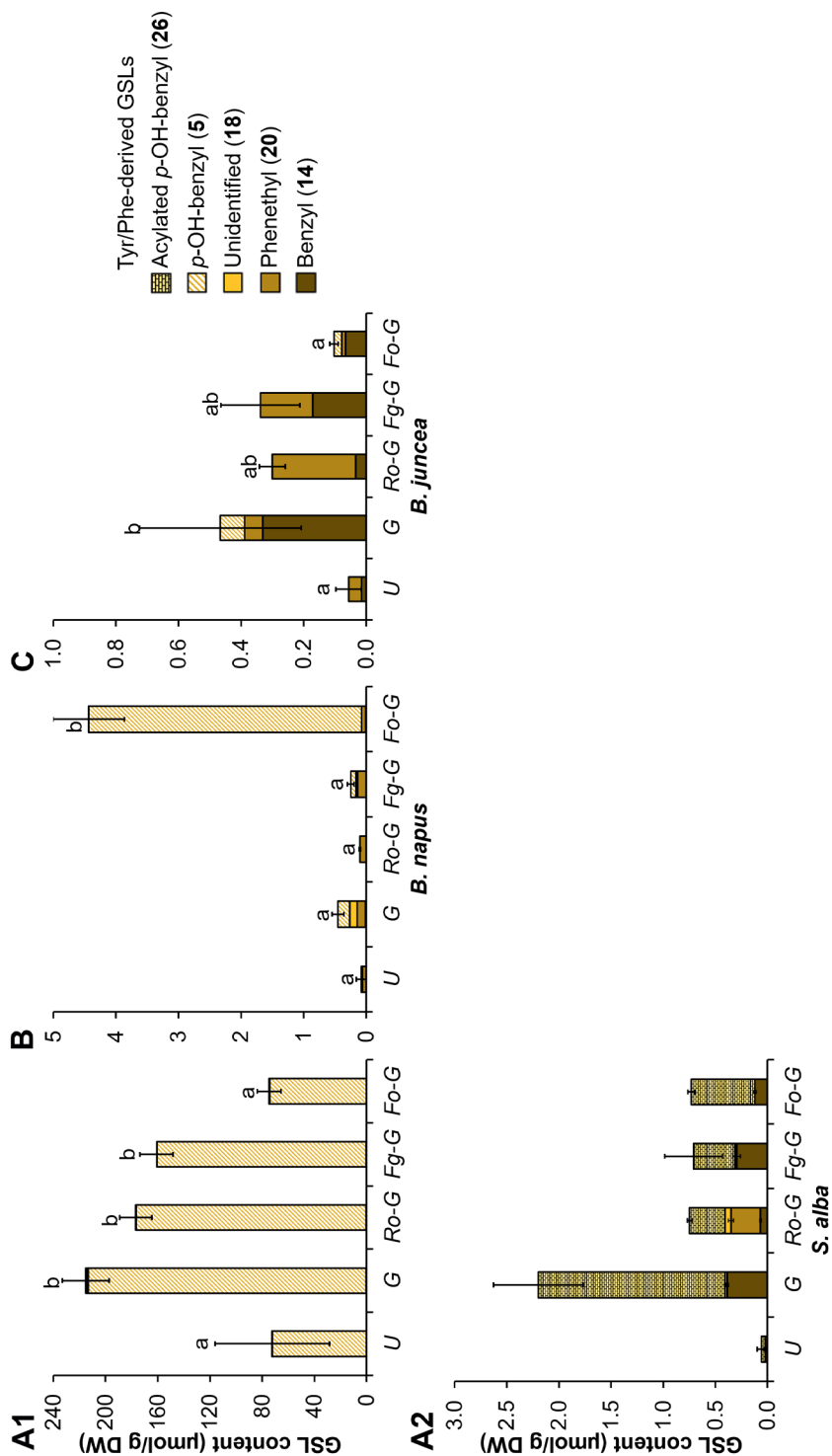
The benzenic GSL content in *S. alba* seed was high, 72.4  $\mu\text{mol/g DW}$ , and this content was increased by two to three fold in the non-elicited seedlings, *Rhizopus*-, and *F. graminearum*-elicited seedlings, but remained the same in *F. oxysporum*-elicited seedling (**Figure 2.6A1**). Differently, the benzenic GSL content in *B. napus* seed was very low, less than 0.1  $\mu\text{mol/g DW}$ , and this content increased up to 4.4  $\mu\text{mol/g DW}$  upon *F. oxysporum* elicitation (**Figure 2.6B**). **Figure 2.6C** shows that benzenic GSL content in *B. juncea* was as low as that in *B. napus*. Total benzenic GSL content in *B. juncea* was increased to 0.5  $\mu\text{mol/g DW}$  by germination, but remained the same by fungal elicitation (**Figure 2.6C**).

With respect to the chemical diversity, **Figure 2.6A1** indicates an abundant amount of *p*-hydroxybenzyl GSL (**5**), which contributed to more than 99% of the total benzenic GSL content, in *S. alba* seed and (elicited) seedlings. The presence of other benzenic GSLs can be seen more clearly in **Figure 2.6A2**. Interestingly, the content of acylated benzenic GSL, i.e. 6'-*O*-sinapoyl (or isomer)-*p*-hydroxybenzyl GSL (**26**) was increased to 1.8  $\mu\text{mol/g DW}$  by germination. But, the content in the fungal-elicited seedlings (0.3-0.6  $\mu\text{mol/g DW}$ ) was significantly less than that in the non-elicited seedling.



**Figure 2.5.** The total content of aliphatic GSLs and their diversity per subclass in the untreated (U), germinated (G), *R. oryzae*-germinated (Ro-G), *F. graminearum*-germinated (Fg-G), and *F. oxysporum*-germinated (Fo-G) seeds of *S. alba* (A), *B. napus* (B), and *B. juncea* (C). The bars from bottom to top correspond to a more downstream in the biosynthesis. Data are the mean values from three biologically independent experiments. Error bars show standard deviation of total content. Different letters at the bars show significant difference of the mean of total content between treatments at  $p < 0.05$ . The first compound mentioned in the brackets in the legend was in general the predominant within the subclass. The content of alkyl subclass (16, 23) was invisible due to its low content ( $< 0.9\%$  of total aliphatic content).





**Figure 2.6.** The total content of benzenic GSLs and their diversity in the untreated (U), germinated (G), *R. oryzae*-germinated (Ro-G), *F. graminearum*-germinated (Fg-G) and *F. oxysporum*-germinated (Fo-G) seeds of *S. alba* (A1), *B. napus* (B), and *B. juncea* (C). The content of minor benzenic GSLs in *S. alba* (A2). Data are the mean values from three biologically independent experiments. Error bars show standard deviation of total content. Different letters at the bars show significant difference of the mean of total content between treatments at  $p < 0.05$ .

**Figure 2.6B**, with the help of **Table S2.5**, indicates only 2 benzenic GSLs found in *B. napus* seeds at very low content ( $< 0.1 \mu\text{mol/g DW}$ ), namely *p*-hydroxybenzyl GSL (**5**) and phenethyl GSL (**20**). The content of GSL **5** was dramatically increased by *F. oxysporum* elicitation. Two more Phe-derived GSLs, namely benzyl GSL (**14**) and hydroxylated or methoxylated Phe-derived GSLs with side chain formula of  $\text{C}_8\text{H}_9\text{O}$  (**18**), were present in the non- and *F. graminearum*-elicited seedlings.

**Figure 2.6C** demonstrates that *B. juncea* seeds contained benzyl GSL (**14**) and phenethyl GSL (**20**). Upon germination and *F. oxysporum* elicitation, the diversity of benzenic GSLs was slightly improved, indicated by the presence of *p*-hydroxybenzyl GSL (**5**).

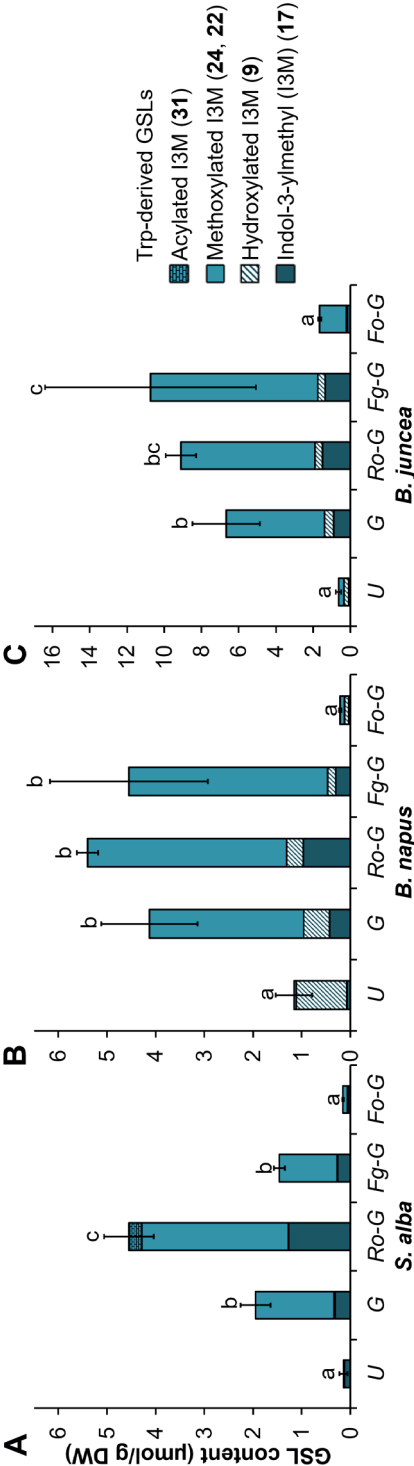
### 2.3.5. Compositional changes of indolic GSLs

**Figure 2.7** indicates that the total content of indolic GSLs in *S. alba*, *B. napus*, and *B. juncea* seeds was generally low, i.e. less than  $1.2 \mu\text{mol/g DW}$ . The content was increased upon germination, *Rhizopus* elicitation, and *F. graminearum* elicitation up to  $10.8 \mu\text{mol/g DW}$ , but remained unchanged upon *F. oxysporum* elicitation. In addition, **Figure 2.7** shows that germination and fungal elicitation resulted in a higher proportion of methoxyl derivatives of I3M GSL (**22**, **24**). The acylated indolic GSL (**31**) was only found in *S. alba* seedlings elicited by *R. oryzae* (**Figure 2.7A**).

## 2.4. Discussion

### 2.4.1. Tentative annotation of GSLs and the predominant GSLs in the studied brassicaceous seeds

LC-MS<sup>n</sup> analysis in the NI mode allows GSL peak tentative annotation due to robust ion MS<sup>n</sup> data that are unique to GSLs as described in the **Supplementary Information**. Of 31 GSLs annotated, 12 were confirmed by comparison with their authentic standards. The predominant GSLs in the three seed species were among the 12 GSLs. *p*-Hydroxybenzyl GSL (**5**) ( $72 \mu\text{mol/g DW}$ ) was the signature GSL in *S. alba* seed, supporting Popova *et al.* (2014) ( $110\text{--}210 \mu\text{mol/g}$  defatted seed meal).<sup>44</sup> (*R*)-2-Hydroxy-3-butenyl GSL (**2**), 3-butenyl GSL (**8**), and 4-hydroxy-I3M GSL (**9**) were the signature GSLs in *B. napus* seed ( $5.0$ ,  $2.5$ , and  $1.0 \mu\text{mol/g DW}$ , respectively), supporting Borgen *et al.* (2010) ( $3.1$ ,  $1.7$ , and  $4.4 \mu\text{mol/g DW}$ , respectively).<sup>45</sup> 3-Butenyl GSL (**8**) and allyl GSL (**4**) were the signature GSLs in *B. juncea* seed ( $61.6$  and  $9.3 \mu\text{mol/g DW}$ , respectively), supporting Sodhi *et al.* (2002) ( $66\text{--}90$  and  $20\text{--}37 \mu\text{mol/g DW}$ , respectively).<sup>46</sup> Most of minor GSLs tentatively annotated in our study were also found or suggested in previous studies. Different GSL contents between studies can be caused by many factors, e.g. origins and varieties of the plants.



**Figure 2.7.** The total content of indolic GSLs and their diversity in the untreated (U), germinated (G), *R. oryzae*-germinated (Ro-G), *F. graminearum*-germinated (Fg-G), and *F. oxysporum*-germinated (Fo-G) seeds of *S. alba* (A), *B. napus* (B), and *B. juncea* (C). The bars from bottom to top corresponds to a more downstream in the biosynthesis. Data are the mean values from three biologically independent experiments. Error bars show standard deviation of total content. Different letters at the bars show significant difference of the mean of total content between treatments at  $p < 0.05$ .

### 2.4.2. Germination without fungus activates biosynthesis of GSLs

Based on total GSL content presented in **Figure 2.4**, there is an evidence that germination, without additional elicitor, activates GSL biosynthesis in *S. alba*, one of the GSL-rich species. Furthermore, based on GSL compositions indicated in **Figure 2.5-2.7** and **Table S2.4-2.6**, germination activates GSL biosynthesis in all the three plant species: indolic GSL in all species, benzenic GSLs in *S. alba* and *B. juncea*, and acylated aliphatic GSLs in *B. napus* and *B. juncea*. In comparison with Leguminosae seeds, where germination induces mainly deglycosylation of isoflavonoids,<sup>31-33,35</sup> germination of Brassicaceae seeds, instead, activates biosynthesis of GSLs leading mainly to a higher accumulation of more downstream GSLs, e.g. acylated aliphatic in *Brassica* species (**Figure 2.5B-C**), acylated benzenic in *S. alba* (**Figure 2.6A2**), and methoxylated indolic in all species (**Figure 2.7**). Given the increase in GSL content and/or diversity upon germination, it is suggested that GSL hydrolysis to ITCs or other turnover is not a quantitatively major process, although this was not further substantiated in this study.

### 2.4.3. Elicitation by fungus does not boost GSL content or diversity beyond that by germination

**Figure 2.4** indicates clearly that the elicitation by non-pathogenic *R. oryzae* and *F. graminearum*, as well as pathogenic *F. oxysporum* do not increase GSL content further than what could be obtained by germination alone, instead GSL content tends to decrease. This could be an indication of GSL degradation. This is related to the possibility that plant cell damage might occur upon fungal elicitation due to the fungal cell expansion on the growing seeds. Consequently, GSLs and myrosinase contact each other, releasing the antimicrobial compounds. Further research is necessary to confirm this. In contrast, in the case of legumes, e.g. lupine beans, elicitation by *R. oryzae* during germination increased the isoflavonoid content further up to 2 fold.<sup>35</sup>

Compared with germination alone, GSL diversity was not enhanced by fungal elicitation (**Figure 2.4**), instead there was a reduction of GSLs, i.e. degradation. Such reduction was observed with sinapoyl (or isomer) derivatives of 3-butenyl GSL (aliphatic class) in *B. napus* and *B. juncea* seedlings due to *Rhizopus* elicitation (**Figure 2.5B-C**, by Ro-G) and with 6'-O-sinapoyl (or isomer)-*p*-hydroxybenzyl GSL (**26**) in *S. alba* due to all three fungal elicitations (**Figure 2.6A2**). Little is known about the degradation of acylated GSLs. In another study,<sup>10</sup> the content of isoferuloylated GSLs decreased upon germination, which was not due to leaching, but probably due to hydrolysis. Our study suggests that the degradation of sinapoyl (or isomer) derivatives is inducible by fungi, but the mechanism by which they are degraded (by in-plant myrosinase and/or fungal enzymes) remains unclear.

Furthermore, fungal elicitation modulated GSL composition in a different manner per GSL class, per plant species, and per fungal species, particularly for aliphatic and benzenic classes (**Figure 2.5** and **Figure 2.6**). There was no clear trend to which direction the composition of aliphatic GSLs and benzenic GSLs was shifted. In some cases more downstream GSLs were induced (e.g. increased content of phenethyl GSL (**20**) by Ro-G in *B. juncea*, **Figure 2.6C**), whereas in other cases, more upstream GSLs were induced (e.g. increased content of MTalkyl subclass by Ro-G in *B. juncea*, **Figure 2.5C**). This inconsistent shift in aliphatic and benzenic biosynthesis suggests that the downstream aliphatic and benzenic GSLs do not necessarily contribute to a better antimicrobial activity than the upstream ones. In contrast, in the case of legumes, the isoflavonoid composition was consistently shifted to more downstream isoflavonoids after germination and fungal elicitation. Isoflavonoids with different skeletons were made along with another modification, i.e. prenylation, known to increase the antimicrobial activity of isoflavonoids.<sup>31-33</sup>

Among GSL degradation products, ITCs are known to be the most potent antimicrobials.<sup>1,47</sup> However, it remains unclear whether ITCs derived from a more downstream GSL are more active than those derived from a more upstream GSL, or whether aliphatic ITCs are more active than benzenic ones.<sup>1,48,49</sup> Further studies to reveal the antimicrobial activity of various ITCs are necessary.

#### **2.4.4. The content of indolic GSL is affected by the pathogenicity of the fungus**

Studies have proven that indolic GSLs in *B. oleracea* and *B. juncea* seedlings were inducible by additional phytohormones, e.g. salicylic acid and methyl jasmonate.<sup>27,50</sup> Our study is the first to report that indolic GSLs are inducible by germination as well as by fungal elicitation. The induction of downstream steps in indolic GSL biosynthesis is consistently observed by the presence of the methoxylated indolic subclass as the main subclass induced (**Figure 2.7**). Methoxylated indolic GSLs, in particular 4-methoxy-I3M GSL (**22**), have been reported to be vital for defense against pathogens and to facilitate innate immunity.<sup>51,52</sup> We hypothesized that the pathogenic fungus would affect GSL profiles more extensively, compared to the non-pathogenic fungi. We observed a consistently lower content of 4-methoxy-I3M GSL (**22**), in particular, and total indolic GSLs, in general, in seedlings infected by pathogenic *F. oxysporum*, compared with the non-pathogenic fungi. Our study potentially suggests that for Brassicaceae germinating seeds, the content of indolic GSLs could be used as a marker to distinguish between elicitation by pathogenic or non-pathogenic fungi. There is no similar study on this matter. Therefore, further research needs to be done to confirm our findings, for instance extending the number of Brassicaceae species and varieties and the attacking fungi based on their pathogenicity level.

This is the first report on the compositional changes of GSLs in Brassicaceae seeds, which have their own unique GSL profiles, upon germination and fungal elicitation. The accumulation of GSLs in germinating Brassicaceae seeds could not be successfully enhanced by fungal elicitation. This indicates that the approach which was successfully employed for increasing the accumulation of isoflavonoids in leguminaceous seedlings could not simply be extrapolated to a different plant family to enhance the accumulation of its respective major phytochemicals. Furthermore, our hypothesis that the pathogenic fungus would induce higher and more diverse GSL production could not be accepted. There was neither a clear trend in the effect of the pathogenicity of the fungus on the total GSL content and diversity. Opposite to our hypothesis, the elicitation with pathogenic fungus (i.e. *F. oxysporum*) consistently caused lower content of indolic GSLs than that with non-pathogenic fungi (*F. graminearum* and *R. oryzae*).

### **2.5. Acknowledgement**

The authors are thankful to Frederike Wiggers for her help in several germination experiments and to the three anonymous reviewers for helpful comments.

### **2.6. Funding source**

The authors are grateful to Indonesia Endowment Fund for Education (LPDP), Ministry of Finance of Republic Indonesia, to financially support PhD study of SA. The authors declare no competing financial interest.

## 2.7. References

1. Aires, A.; Mota, V. R.; Saavedra, M. J.; Rosa, E. A.; Bennett, R. N., The antimicrobial effects of glucosinolates and their respective enzymatic hydrolysis products on bacteria isolated from the human intestinal tract. *J. Appl. Microbiol.* **2009**, *106*, 2086-95.
2. Borges, A.; Abreu, A. C.; Ferreira, C.; Saavedra, M. J.; Simões, L. C.; Simões, M., Antibacterial activity and mode of action of selected glucosinolate hydrolysis products against bacterial pathogens. *J. Food Sci. Technol.* **2015**, *52*, 4737-4748.
3. Tierens, K. F. M.-J.; Thomma, B. P. H. J.; Brouwer, M.; Schmidt, J.; Kistner, K.; Porzel, A.; Mauch-Mani, B.; Cammue, B. P. A.; Broekaert, W. F., Study of the role of antimicrobial glucosinolate-derived isothiocyanates in resistance of *Arabidopsis* to microbial pathogens. *Plant Physiol.* **2001**, *125*, 1688-1699.
4. Abdel-Farid, I. B.; Jahangir, M.; van den Hondel, C. A. M. J. J.; Kim, H. K.; Choi, Y. H.; Verpoorte, R., Fungal infection-induced metabolites in *Brassica rapa*. *Plant Sci.* **2009**, *176*, 608-615.
5. Bones, A. M.; Rossiter, J. T., The enzymic and chemically induced decomposition of glucosinolates. *Phytochemistry* **2006**, *67*, 1053-1067.
6. Sánchez-Pujante, P. J.; Borja-Martínez, M.; Pedreño, M. Á.; Almagro, L., Biosynthesis and bioactivity of glucosinolates and their production in plant in vitro cultures. *Planta* **2017**, *246*, 19-32.
7. Sønderby, I. E.; Geu-Flores, F.; Halkier, B. A., Biosynthesis of glucosinolates – gene discovery and beyond. *Trends Plant Sci.* **2010**, *15*, 283-290.
8. Linscheid, M.; Wendisch, D.; Strack, D., The structures of sinapic acid esters and their metabolism in cotyledons of *Raphanus sativus*. *Z. Naturforsch. C* **1980**, *35*, 907.
9. Reichelt, M.; Brown, P. D.; Schneider, B.; Oldham, N. J.; Stauber, E.; Tokuhisa, J.; Kliebenstein, D. J.; Mitchell-Olds, T.; Gershenzon, J., Benzoic acid glucosinolate esters and other glucosinolates from *Arabidopsis thaliana*. *Phytochemistry* **2002**, *59*, 663-71.
10. Agerbirk, N.; Olsen, C. E., Isoferuloyl derivatives of five seed glucosinolates in the crucifer genus *Barbarea*. *Phytochemistry* **2011**, *72*, 610-623.
11. Agerbirk, N.; Olsen, C. E., Glucosinolate structures in evolution. *Phytochemistry* **2012**, *77*, 16-45.
12. Abdel-Farid, I. B.; Jahangir, M.; Mustafa, N. R.; van Dam, N. M.; van den Hondel, C. A. M. J. J.; Kim, H. K.; Choi, Y. H.; Verpoorte, R., Glucosinolate profiling of *Brassica rapa* cultivars after infection by *Leptosphaeria maculans* and *Fusarium oxysporum*. *Biochem. Syst. Ecol.* **2010**, *38*, 612-620.
13. Bianco, G.; Agerbirk, N.; Losito, I.; Cataldi, T. R., Acylated glucosinolates with diverse acyl groups investigated by high resolution mass spectrometry and infrared multiphoton dissociation. *Phytochemistry* **2014**, *100*, 92-102.
14. Lee, S.; Kaminaga, Y.; Cooper, B.; Pichersky, E.; Dudareva, N.; Chapple, C., Benzoylation and sinapoylation of glucosinolate R-groups in *Arabidopsis*. *Plant J.* **2012**, *72*, 411-422.
15. Wittstock, U.; Halkier, B. A., Cytochrome P450 CYP79A2 from *Arabidopsis thaliana* L. Catalyzes the conversion of L-phenylalanine to phenylacetaldoxime in the biosynthesis of benzylglucosinolate. *J. Biol. Chem.* **2000**, *275*, 14659-66.
16. Yi, G. E.; Robin, A. H.; Yang, K.; Park, J. I.; Kang, J. G.; Yang, T. J.; Nou, I. S., Identification and expression analysis of glucosinolate biosynthetic genes and estimation of glucosinolate contents in edible organs of *Brassica oleracea* subspecies. *Molecules (Basel, Switzerland)* **2015**, *20*, 13089-111.
17. Olsen, C. E.; Huang, X.-C.; Hansen, C. I. C.; Cipollini, D.; Ørgaard, M.; Matthes, A.; Geu-Flores, F.; Koch, M. A.; Agerbirk, N., Glucosinolate diversity within a phylogenetic framework of the tribe *Cardamineae* (Brassicaceae) unraveled with HPLC-MS/MS and NMR-based analytical distinction of 70 desulfoglucosinolates. *Phytochemistry* **2016**, *132*, 33-56.

18. Kjær, A.; Schuster, A., Glucosinolates in *Erysimum hieracifolium* L.; Three new, naturally occurring glucosinolates. *Acta Chem. Scand* **1970**, *24*, 1631-1638.
19. Agerbirk, N.; Olsen, C. E.; Heimes, C.; Christensen, S.; Bak, S.; Hauser, T. P., Multiple hydroxyphenethyl glucosinolate isomers and their tandem mass spectrometric distinction in a geographically structured polymorphism in the crucifer *Barbarea vulgaris*. *Phytochemistry* **2015**, *115*, 130-142.
20. Doughty, K. J.; Porter, A. J. R.; Morton, A. M.; Kiddle, G.; Bock, C. H.; Wallsgrove, R., Variation in the glucosinolate content of oilseed rape (*Brassica napus* L.) leaves. *Ann. Appl. Biol.* **1991**, *118*, 469-477.
21. Guo, L.; Yang, R.; Wang, Z.; Guo, Q.; Gu, Z., Glucoraphanin, sulforaphane and myrosinase activity in germinating broccoli sprouts as affected by growth temperature and plant organs. *J. Funct. Foods* **2014**, *9*, 70-77.
22. Jahangir, M.; Abdel-Farid, I. B.; Choi, Y. H.; Verpoorte, R., Metal ion-inducing metabolite accumulation in *Brassica rapa*. *J. Plant Physiol.* **2008**, *165*, 1429-37.
23. Jahangir, M.; Abdel-Farid, I. B.; Kim, H. K.; Choi, Y. H.; Verpoorte, R., Healthy and unhealthy plants: The effect of stress on the metabolism of Brassicaceae. *Environ. Exp. Bot.* **2009**, *67*, 23-33.
24. Yang, R.; Guo, L.; Jin, X.; Shen, C.; Zhou, Y.; Gu, Z., Enhancement of glucosinolate and sulforaphane formation of broccoli sprouts by zinc sulphate via its stress effect. *J. Funct. Foods* **2015**, *13*, 345-349.
25. Baenas, N.; Villano, D.; García-Viguera, C.; Moreno, D. A., Optimizing elicitation and seed priming to enrich broccoli and radish sprouts in glucosinolates. *Food Chem.* **2016**, *204*, 314-319.
26. Natella, F.; Maldini, M.; Nardini, M.; Azzini, E.; Foddai, M. S.; Giusti, A. M.; Baima, S.; Morelli, G.; Scaccini, C., Improvement of the nutraceutical quality of broccoli sprouts by elicitation. *Food Chem.* **2016**, *201*, 101-109.
27. Pérez-Balibrea, S.; Moreno, D. A.; García-Viguera, C., Improving the phytochemical composition of broccoli sprouts by elicitation. *Food Chem.* **2011**, *129*, 35-44.
28. Tian, Q.; Rosselot, R. A.; Schwartz, S. J., Quantitative determination of intact glucosinolates in broccoli, broccoli sprouts, Brussels sprouts, and cauliflower by high-performance liquid chromatography-electrospray ionization-tandem mass spectrometry. *Anal. Biochem.* **2005**, *343*, 93-9.
29. Yang, R.; Hul, Q.; Gu, Z.; Zhou, Y.; Guo, L.; Shen, C.; Zhang, W., Effects of  $\text{CaCl}_2$  on the metabolism of glucosinolates and the formation of isothiocyanates as well as the antioxidant capacity of broccoli sprouts. *J. Funct. Foods* **2016**, *24*, 156-163.
30. Ludwig-Müller, J.; Schubert, B.; Pieper, K.; Ihmig, S.; Hilgenberg, W., Glucosinolate content in susceptible and resistant chinese cabbage varieties during development of clubroot disease. *Phytochemistry* **1997**, *44*, 407-414.
31. Araya-Cloutier, C.; den Besten, H. M. W.; Aisyah, S.; Gruppen, H.; Vincken, J.-P., The position of prenylation of isoflavonoids and stilbenoids from legumes (Fabaceae) modulates the antimicrobial activity against Gram positive pathogens. *Food Chem.* **2017**, *226*, 193-201.
32. Aisyah, S.; Gruppen, H.; Andini, S.; Bettonvil, M.; Severing, E.; Vincken, J.-P., Variation in accumulation of isoflavonoids in *Phaseoleae* seedlings elicited by *Rhizopus*. *Food Chem.* **2016**, *196*, 694-701.
33. Aisyah, S.; Gruppen, H.; Madzora, B.; Vincken, J. P., Modulation of isoflavonoid composition of *Rhizopus oryzae* elicited soybean (*Glycine max*) seedlings by light and wounding. *J. Agric. Food Chem.* **2013**, *61*, 8657-8667.
34. Aisyah, S.; Gruppen, H.; Slager, M.; Helmink, B.; Vincken, J. P., Modification of prenylated stilbenoids in peanut (*Arachis hypogaea*) seedlings by the same fungi that elicited them: The fungus strikes back. *J. Agric. Food Chem.* **2015**, *63*, 9260-8.
35. Aisyah, S.; Vincken, J.-P.; Andini, S.; Mardiah, Z.; Gruppen, H., Compositional changes in (iso)flavonoids and estrogenic activity of three edible *Lupinus* species by germination and *Rhizopus*-elicitation. *Phytochemistry* **2016**, *122*, 65-75.



36. Gaetán, S. A., Occurrence of Fusarium Wilt on Canola Caused by Fusarium oxysporum f. sp. conglutinans in Argentina. *Plant Dis.* **2005**, *89*, 432-432.
37. Fabre, N.; Poinot, V.; Debrauwer, L.; Vigor, C.; Tulliez, J.; Fourasté, I.; Moulis, C., Characterisation of glucosinolates using electrospray ion trap and electrospray quadrupole time-of-flight mass spectrometry. *Phytochem. Anal.* **2007**, *18*, 306-319.
38. Cataldi, T. R. I.; Rubino, A.; Lelario, F.; Bufo, S. A., Naturally occurring glucosinolates in plant extracts of rocket salad (*Eruca sativa* L.) identified by liquid chromatography coupled with negative ion electrospray ionization and quadrupole ion-trap mass spectrometry. *Rapid Commun. Mass Spectrom.* **2007**, *21*, 2374-2388.
39. Pfalz, M.; Mukhaimar, M.; Perreau, F.; Kirk, J.; Hansen, C. I. C.; Olsen, C. E.; Agerbirk, N.; Kroymann, J., Methyl transfer in glucosinolate biosynthesis mediated by indole glucosinolate O-Methyltransferase 5. *Plant Physiol.* **2016**, *172*, 2190-2203.
40. Bettey, M., Finch-Savage, W. E., Respiratory enzyme activities during germination in *Brassica* seed lots of differing vigour. *Seed Sci. Res.* **1996**, *6*, 165-173.
41. Gu, Y.; Guo, Q.; Zhang, L.; Chen, Z.; Han, Y.; Gu, Z., Physiological and biochemical metabolism of germinating broccoli seeds and sprouts. *J. Agric. Food Chem.* **2012**, *60*, 209-13.
42. Lorenz, K., Cereal sprouts: composition, nutritive value, food applications. *Crit. Rev. Food Sci. Nutr.* **1980**, *13*, 353-85.
43. Simons, R.; Vincken, J. P.; Roidos, N.; Bovee, T. F. H.; Van Iersel, M.; Verbruggen, M. A.; Gruppen, H., Increasing soy isoflavonoid content and diversity by simultaneous malting and challenging by a fungus to modulate estrogenicity. *J. Agric. Food Chem.* **2011**, *59*, 6748-6758.
44. Popova, I. E.; Morra, M. J., Simultaneous quantification of sinigrin, sinalbin, and anionic glucosinolate hydrolysis products in *Brassica juncea* and *Sinapis alba* seed extracts using ion chromatography. *J. Agric. Food Chem.* **2014**, *62*, 10687-93.
45. Borgen, B. H.; Thangstad, O. P.; Ahuja, I.; Rossiter, J. T.; Bones, A. M., Removing the mustard oil bomb from seeds: transgenic ablation of myrosin cells in oilseed rape (*Brassica napus*) produces MINELESS seeds. *J. Exp. Bot.* **2010**, *61*, 1683-1697.
46. Sodhi, Y. S.; Mukhopadhyay, A.; Arumugam, N.; Verma, J. K.; Gupta, V.; Pental, D.; Pradhan, A. K., Genetic analysis of total glucosinolate in crosses involving a high glucosinolate Indian variety and a low glucosinolate line of *Brassica juncea*. *Plant Breed.* **2002**, *121*, 508-511.
47. Buxdorf, K.; Yaffe, H.; Barda, O.; Levy, M., The effects of glucosinolates and their breakdown products on necrotrophic fungi. *PLoS ONE* **2013**, *8*, e70771.
48. Ahn, E.; Kim, J.; Shin, D., Antimicrobial effects of allyl isothiocyanates on several microorganisms. *Korean J. Food Sci. Technol.* **2001**, *31*, 206-211.
49. Dufour, V.; Stahl, M.; Baysse, C., The antibacterial properties of isothiocyanates. *Microbiology (Reading, England)* **2015**, *161*, 229-43.
50. Augustine, R.; Bisht, N. C., Biotic elicitors and mechanical damage modulate glucosinolate accumulation by co-ordinated interplay of glucosinolate biosynthesis regulators in polyploid *Brassica juncea*. *Phytochemistry* **2015**, *117*, 43-50.
51. Bednarek, P.; Pisłowska-Bednarek, M.; Svatos, A.; Schneider, B.; Doubek, J.; Mansurova, M.; Humphry, M.; Consonni, C.; Panstruga, R.; Sanchez-Vallet, A.; Molina, A.; Schulze-Lefert, P., A glucosinolate metabolism pathway in living plant cells mediates broad-spectrum antifungal defense. *Science (New York, N.Y.)* **2009**, *323*, 101-6.
52. Clay, N. K.; Adio, A. M.; Denoux, C.; Jander, G.; Ausubel, F. M., Glucosinolate metabolites required for an Arabidopsis innate immune response. *Science (New York, N.Y.)* **2009**, *323*, 95-101.

## 2.8. Supplementary information

### 2.8.1. Tentative annotation of GSLs in UHPLC-PDA-ESI-MS<sup>n</sup> analysis

#### 2.8.1.1. General criteria for GSL annotation

In the MS<sup>2</sup> fragmentation (**Table S2.3**), the deprotonated molecular ion [M-H]<sup>-</sup> of intact GSLs produces sulfated glucosyl ion at  $m/z$  259, which is the signature fragment ion for GSLs (**Figure S2.1**).<sup>1-3</sup> The relative abundance of this fragment ion depends on the side chain. Frequently, this fragment ion is predominant or at a high abundance. (Methylsulfinyl)alkyl GSLs (**1**, **3**, **6**, **25**) consistently have a predominant fragment ion [M-H-64]<sup>-</sup> due to a neutral loss of CH<sub>3</sub>SOH (**Figure S2.1**).<sup>2,4</sup>

The other fragment ions of GSLs in the MS<sup>2</sup>, shown in **Figure S2.1**, are at  $m/z$  195, 241, 275, and 291 which are assigned as thioglucosyl anion, C<sub>6</sub>H<sub>9</sub>O<sub>8</sub>S<sup>-</sup>, the sulfated thioglucosyl anion, and C<sub>6</sub>H<sub>11</sub>O<sub>9</sub>S<sub>2</sub><sup>-</sup>, respectively.<sup>2,3,5</sup> The losses of glucosyl moiety ([M-H-162]<sup>-</sup>), thioglucosyl moiety ([M-H-196]<sup>-</sup>), and an intense neutral loss of sulfur trioxide and anhydroglucose ([M-H-242]<sup>-</sup>) were also observed. This observation is in accordance with Kokkonen *et al* and Velasco *et al*.<sup>6,7</sup>

Two indolic GSLs which exhibit identical molecular masses, i.e. 4-methoxyindol-3-ylmethyl GSL (**22**) and 1(or *N*)-methoxyindol-3-ylmethyl GSL (**24**), were distinguished by comparison with reported elution order during RP-LC separation.<sup>1,8</sup> In agreement with He<sup>9</sup>, 4-methoxyindol-3-ylmethyl GSL, which has a C-NH group, is more polar than 1-methoxyindol-3-ylmethyl GSL with its C-N-OCH<sub>3</sub>.<sup>9</sup> Additionally, in agreement with Olsen *et al*. and Pfalz *et al*. loss of OCH<sub>3</sub> from *N*-methoxy was observed, but not from *C*-methoxy indolic GSLs (**Figure S2.2**).<sup>10,11</sup>

#### 2.8.1.2. Tentative annotation of GSLs acylated at thioglucosyl group

By extrapolation of MS fragmentation patterns from previous studies on purified acyl derivatives of other GSLs,<sup>12,13</sup> four peaks were tentatively annotated as sinapoyl (or isomer) derivatives of *p*-hydroxybenzyl GSL and 3-butenyl GSL.

In MS<sup>2</sup>, **26** ( $m/z$  630) was fragmented to the predominant ion  $m/z$  424. The fragmentation refers to a loss of 206 Da, which possibly represent a sinapoyl group or another dimethoxy-hydroxycinnamic acid. In addition, a fragment ion at  $m/z$  223, which refers to anion of sinapic acid or isomer, was present at a high abundance. A neutral loss of 206 and a fragment ion of 223 have been attributed to a sinapoyl (or isomer) derivative of (*S*)-2-hydroxy-2-phenethyl GSL (glucobarbarin) where the sinapoyl (or isomer) group was attached at thioglucosyl group.<sup>12</sup> Furthermore, the position of the sinapoyl (or isomer) group at the thioglucosyl group and not at the side chain was confirmed in our study, as fragment ions at  $m/z$  465, 401, 481, and 497 were observed (**Figure S2.4** and **Figure S2.5**). Additionally, Bianco *et al*.<sup>12</sup> observed a fragment ion at  $m/z$  of 235

for the purified 6'-O-isoferuloyl-(S)-2-hydroxy-2-phenethyl GSL, which was proposed to be an ion corresponding to isoferuloyl attached at 6'-position. Likewise, if sinapoyl (or isomer) group replaces isoferuloyl group, the fragment ion will have an  $m/z$  of 265 (**Figure S2.4A**). This fragment ion was observed for **26**. Furthermore, previous studies have indicated that acylation of GSLs at the thioglucosyl group mostly occurred at the 6'-position.<sup>12-14</sup> Taken together, **26** was tentatively annotated as 6'-O-sinapoyl (or isomer)-*p*-hydroxybenzyl GSL (**Figure S2.6**).

Similar to peak **26**, peaks **27**, **29**, and **30** had a neutral loss of 206 Da in MS<sup>2</sup> fragmentation, giving a fragment ion at  $m/z$  372, corresponding to 3-butenyl GSL. Based on this, **27**, **29**, and **30** were annotated as sinapoyl (or isomer) derivatives of 3-butenyl GSL. The annotation was also confirmed by a distinct UV absorption maximum at 300-334 nm indicating the occurrence of an aromatic substituent, in line with Reichelt *et al.*<sup>13</sup> and Lee *et al.*<sup>15</sup> As **29** occurred more frequently and in a higher abundance than **27** and **30** (**Table S2.5** and **Table S2.6**), and **29** yielded a fragment ion at  $m/z$  of 265, it is suggested that **29** corresponds to 6'-O-sinapoyl (or isomer)-3-butenyl GSL (**Figure S2.4**).

#### 2.8.1.3. Tentative annotation of acylated indolic GSL

**31** was tentatively annotated as a salicyloxy (or isomer) derivative of indol-3-ylmethyl GSL. Assuming that only the 1- and 4-positions can be hydroxylated in indolic GSL biosynthesis,<sup>11</sup> the position of salicyloxy group (or isomer) was possibly at the 4-position, instead of at the 1-position. The tentative annotation was based on (i) the presence of predominant signature fragment ions at  $m/z$  291, 275, 259, and 195 in MS<sup>2</sup> (**Figure S2.1**) and  $m/z$  97 in MS<sup>3</sup> (**Table S2.1**), (ii) the  $m/z$  of the parent ion at an odd number (583, nitrogen rule), which refers to the indolic class (**Table S2.3**), (iii) the discriminating fragmentation patterns of 4- and 1-substitution of indol-3-ylmethyl GSL (**Figure S2.2** and **Figure S2.3**), (iv) salicyloxy (or isomer) group fits to the  $m/z$  of the parent ion and fragment ions, and (v) the UV<sub>max</sub> at 275 nm (corresponding to indol-3-ylmethyl GSL) and 315 nm (corresponding to a salicyloxy group or isomer). Therefore, **31** was tentatively annotated as 4-salicyloxy (or isomer)-indol-3-ylmethyl GSL.

#### 2.8.1.4. Tentative annotation of peaks **10**, **12**, **16**, **18**, **19**, **23**, and **28**

According to the molecular weight, **10** (374 Da), **16** (388 Da), **23** (402 Da), and **28** (416 Da) could be hydroxylated alkenyl GSLs, alkyl GSLs, or oxoalkyl GSLs. The four GSLs have sequential masses by 14 Da, which is often associated to a methylene (-CH<sub>2</sub>) group.

**Peak 10** and **28** demonstrated a neutral loss of 18 Da in the MS<sup>2</sup> fragmentation which might associate to H<sub>2</sub>O. This is usually an indication of a presence of a hydroxyl group leading to a suggestion of hydroxylated alkenyl GSLs. However, **10** eluted later than (*R*)-2-hydroxy-3-butenyl GSL (**2**), whereas **28**

eluted much later than 2-hydroxy-4-pentenyl GSL (**7**). This raises the possibility of being oxoalkyl GSLs. 5-Oxoheptyl GSL was discovered by Kjær and Thomsen<sup>16</sup> in another plant family, i.e. Capparidaceae. However, to date there is no fragmentation data reported for oxoalkyl GSL that would support the neutral loss of 18 Da. Therefore, the structures of **10** and **28** could not be tentatively annotated and were grouped as unclassified aliphatic GSLs (**Table S2.1**), with potential side chain formulae of C<sub>4</sub>H<sub>9</sub> or C<sub>3</sub>H<sub>5</sub>O and C<sub>7</sub>H<sub>15</sub> or C<sub>6</sub>H<sub>11</sub>O, respectively.

In contrast, **16** and **23**, whose similar molecular weight to **2** and **7**, respectively, did not demonstrate a neutral loss of 18 Da in the MS<sup>2</sup> fragmentation. Meanwhile, **2** and **7**, tentatively annotated as hydroxylated alkenyl GSLs (confirmed by the authentic standard **2**), demonstrated a neutral loss of 18 Da. Furthermore, retention times of **16** and **23** were substantially later than **2** and **7**. Therefore, **16** and **23** were possibly alkyl GSLs with C<sub>5</sub> and C<sub>6</sub>, respectively (**Table S2.1**). However, our analytical method could not distinguish isomers (straight or branched alkyl chain).

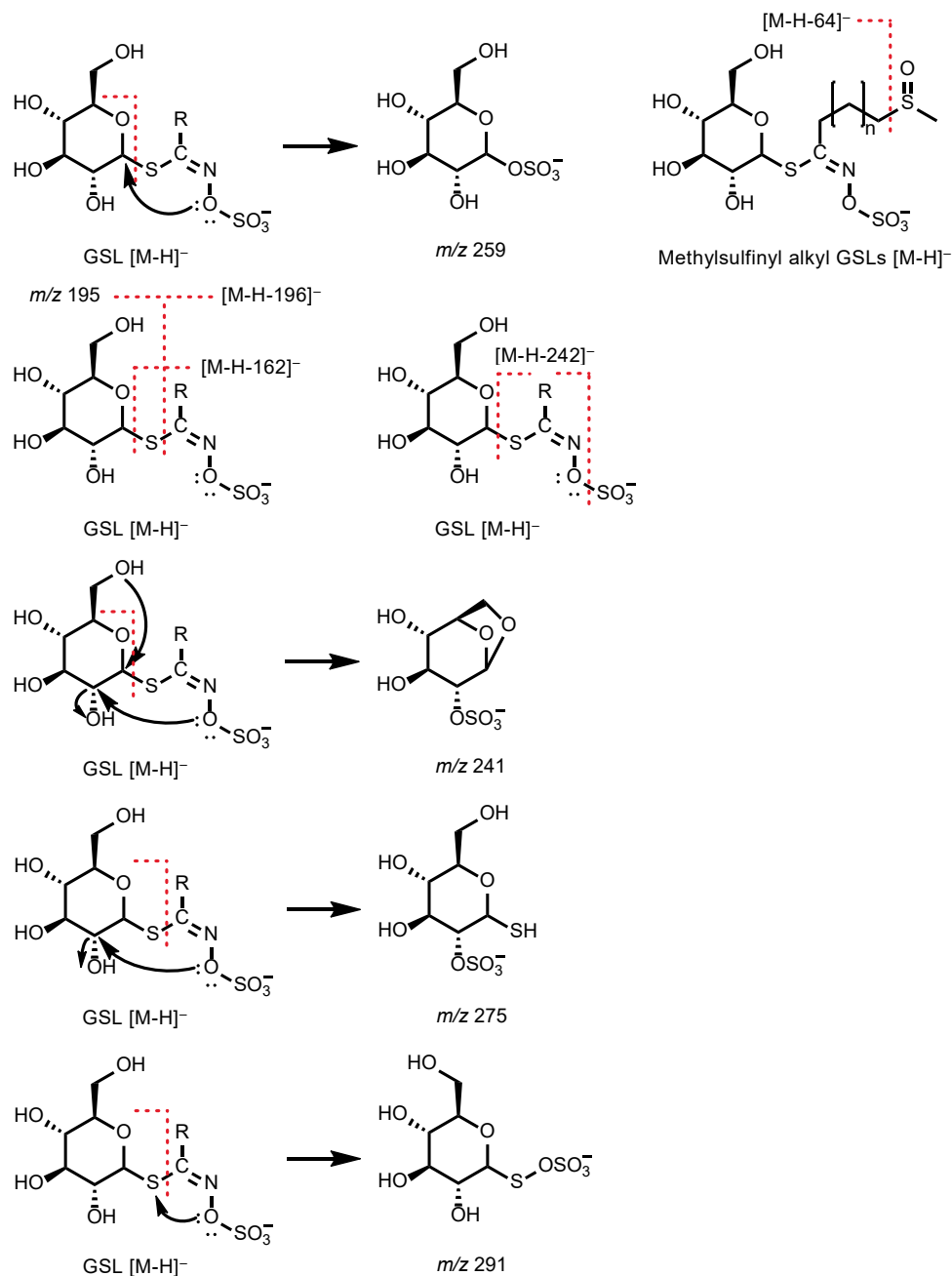
According to the molecular weight, **12** (436 Da), **18** (438 Da), and **19** (450 Da) could be aliphatic or benzenic GSLs, but not indolic GSLs (**Table S2.1** and **Table S2.3**). Because **12**, **18**, and **19** were present as trace peaks, the UV absorption around 260-270 nm shown in **Figure S2.7** could not be used as basis for the tentative annotation. These three peaks showed similar fragmentations, e.g. a neutral loss of 18 Da.

**12** and **19** have similar molecular weight to 4-(methylsulfinyl)butyl GSL (**3**) and 5-(methylsulfinyl)pentyl GSL (**6**), respectively. The possibility of being their isomers is likely (**Figure 2.1B**). If the neutral loss of 18 Da is related to the hydroxyl group substitution, **12** and **19** could be a hydroxylated 4-(methylthio)butyl GSL and a hydroxylated 5-(methylthio)pentyl GSL, respectively. Their retention times were, as expected, earlier than 4-(methylthio)butyl GSL (**15**) and 5-(methylthio)pentyl GSL (**21**). The presence of hydroxylated (methylthio)alkyl GSLs has been reported by Kjær and Schuster<sup>17</sup>, with hydroxylation occurred at 2-position. Olsen *et al.* found the hydroxylation at 3-position.<sup>10</sup>

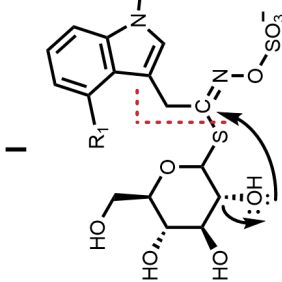
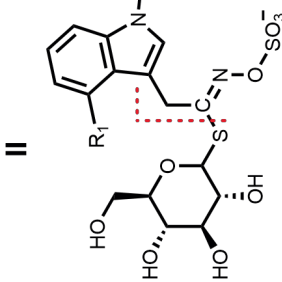
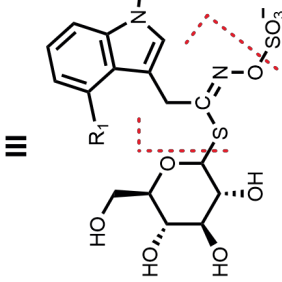
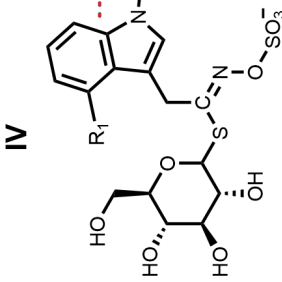
According to the molecular weight and assuming that the possible subclasses of aliphatic GSLs in our samples are as mentioned in **Table S2.1** with possible modifications of hydroxylation, oxidation, and desaturation, **18** (438 Da) could be an aliphatic GSL, e.g. 3-(methylsulfonyl)propyl GSL. However, the retention time of **18** (9.95 min) was most likely in a disagreement as its polarity should not be largely different from 3-(methylsulfinyl)propyl GSL (**1**, 1.44 min). Therefore, **18** would possibly be a benzenic GSL, rather than an aliphatic GSL. The possible side chain formula for **18** would be C<sub>8</sub>H<sub>9</sub>O. The possible structure is a hydroxylated phenethyl GSL or a methoxylated benzyl GSL, where the substitution could be on the phenyl ring or on the alkyl chain. Furthermore, **18** suffered a neutral loss of 18 Da in the MS<sup>2</sup> fragmentation. For the case of benzenic GSLs this loss is often associated to hydroxylation on the alkyl chain, rather than on the aromatic ring.<sup>2,18</sup>

In line with our study, the loss of 18 Da was not observed for the standard *p*-hydroxybenzyl GSL (**5**). Agerbirk *et al.*<sup>18</sup> also found similar observation for *p*- and *m*-hydroxyphenethyl GSLs. Furthermore, based on what has been found in nature,<sup>12,19</sup> 2-hydroxy-2-phenethyl GSL would be more likely for GSL **18** than 1-hydroxy-2-phenethyl GSL. Unfortunately, our analysis did not include the standards of any hydroxylated phenethyl GSLs nor methoxylated benzyl GSLs, and, thus, was not able to distinguish these isomers. Therefore, **18** was suggested to be a benzenic GSL with a possible side chain formula of C<sub>8</sub>H<sub>9</sub>O.

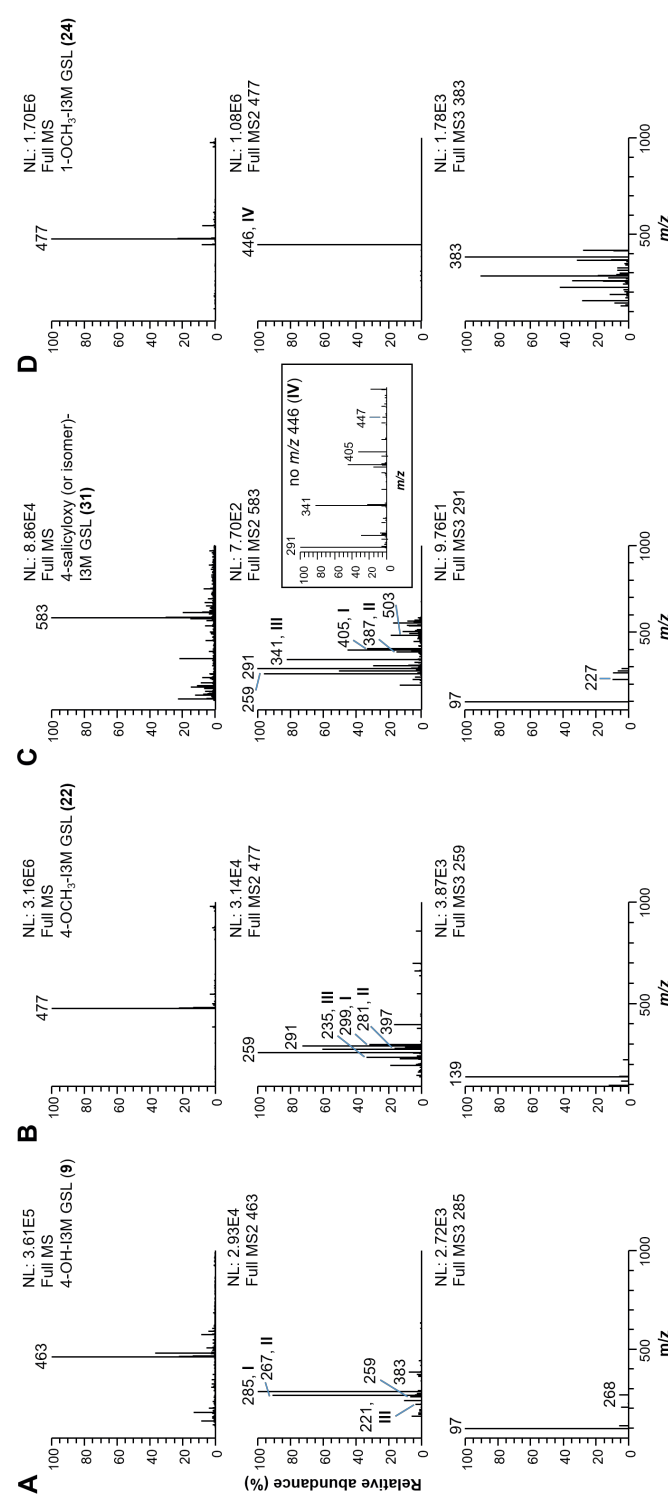
## 2.8.2. Supplementary figures



**Figure S2.1.** Characteristic MS<sup>2</sup> fragmentation of GSL anions.<sup>1,4,5</sup> The dashed red lines indicate the fragmentation sites. Fragment ion at  $m/z$  259 was frequently predominant for most GSLs, except for (methylsulfinyl)alkyl GSLs:  $m/z$  corresponding to [M-H-64]<sup>-</sup>.

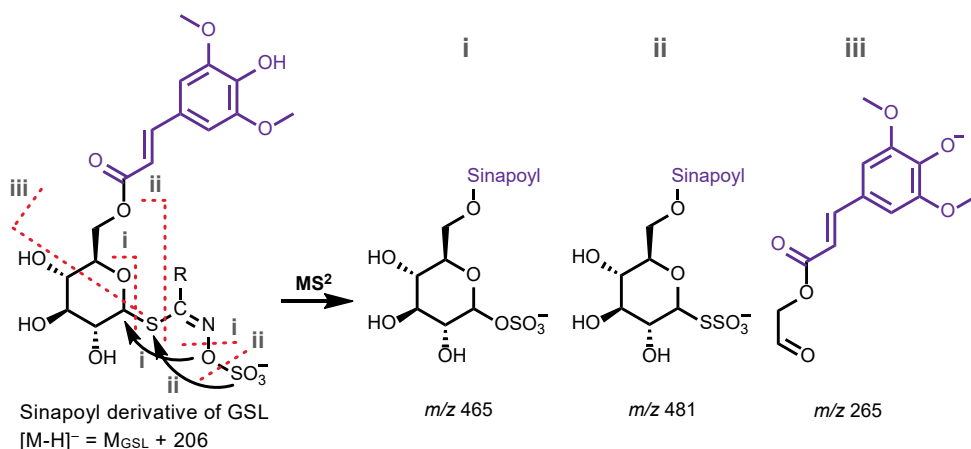
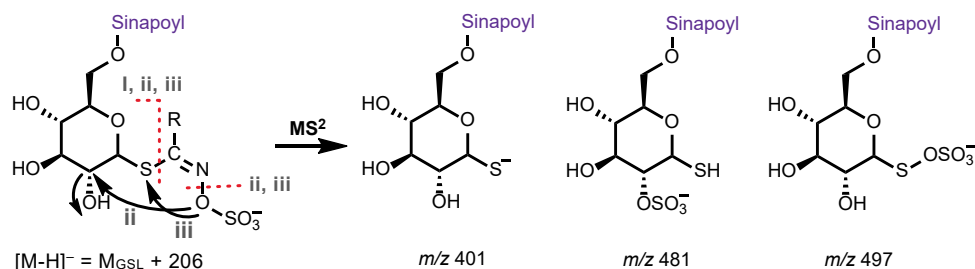
<b>I</b>	<b>II</b>	<b>III</b>	<b>IV</b>												
															
[M-H-178] <sup>+</sup>				[M-H-196] <sup>+</sup>				[M-H-242] <sup>+</sup>				[M-H-R <sub>2</sub> ] <sup>+</sup>			
indolic GSL side chain <sup>a</sup>				R <sub>1</sub>	R <sub>2</sub>	I	II	III	IV	Ref.	Observed in this study?				
4-OH-I3M				OH	H	yes	yes	yes	no	Pfalz <sup>11</sup>	yes				
1-OH-I3M <sup>b</sup>				H	OH	no	no	no	yes	Pfalz <sup>11</sup>	no				
4-OCH <sub>3</sub> -I3M				OCH <sub>3</sub>	H	yes	yes	yes	no	Pfalz <sup>11</sup> ; Olsen <sup>10</sup>	yes				
1-OCH <sub>3</sub> -I3M				H	OCH <sub>3</sub>	no	no	no	yes	Pfalz <sup>11</sup> ; Olsen <sup>10</sup>	yes				
1-hexose-I3M				H	C <sub>6</sub> H <sub>10</sub> O <sub>6</sub> (hexose)	no	no	no	yes	Pfalz <sup>11</sup>	no				
4-salicyloxy (or isomer)-I3M				C <sub>7</sub> H <sub>5</sub> O <sub>3</sub> (salicyloxy or isomer)	H	yes	yes	yes	no		yes				

**Figure S2.2.** Fragmentation patterns of 4- and 1-substituted indolic GSLs. <sup>a</sup>I3M stands for indol-3-ylmethyl. <sup>b</sup>1-OH-I3M GSL is often not detectable due to its high instability.<sup>20</sup>

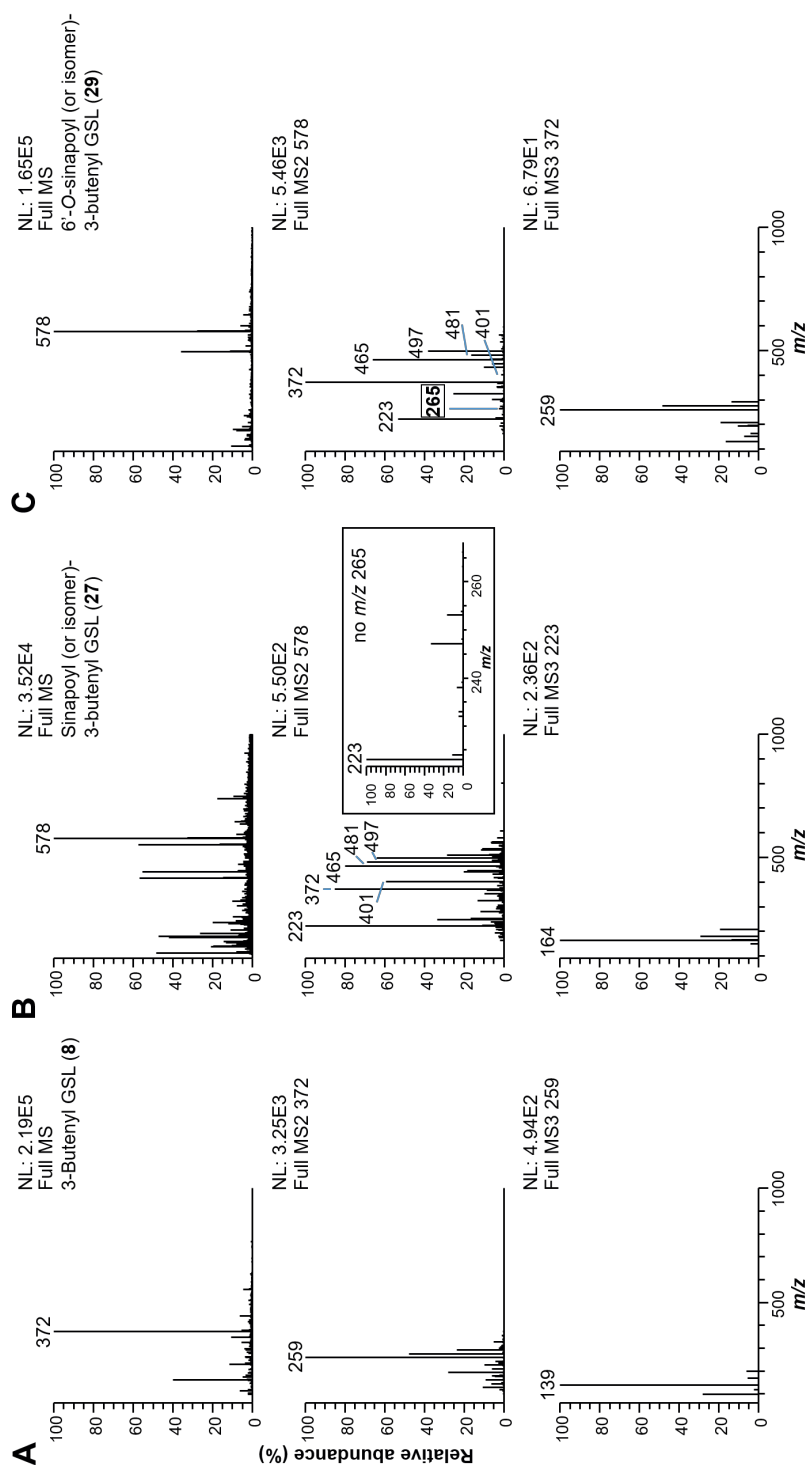


**Figure S2.3.** MS spectra of tentatively annotated 4-hydroxy-I3M GSL (9) (A), 4-methoxy-I3M GSL (22) (B), 4-salicyloxy-I3M GSL (31) (C), and 1-methoxy-I3M GSL (24) (D), where I3M stands for indol-3-ylmethyl. The Roman numerals following the  $m/z$  values refer to those in **Figure S2.2**, where the fragmentation patterns are explained.

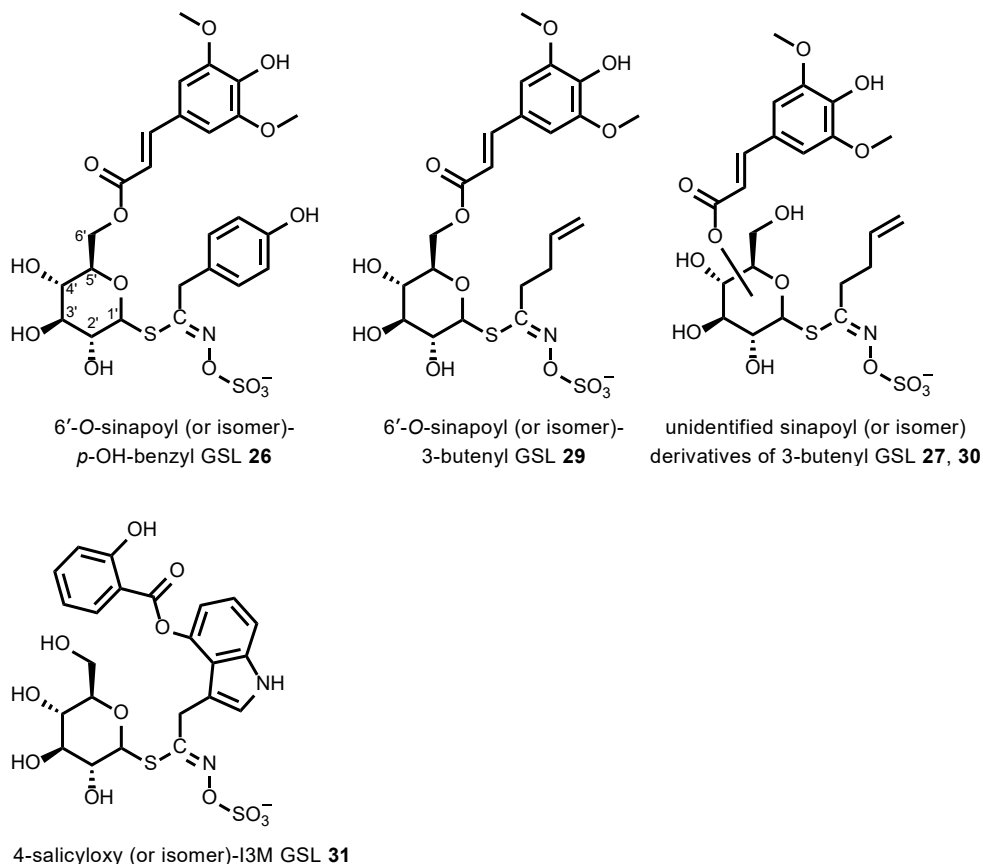


**A**

**B**


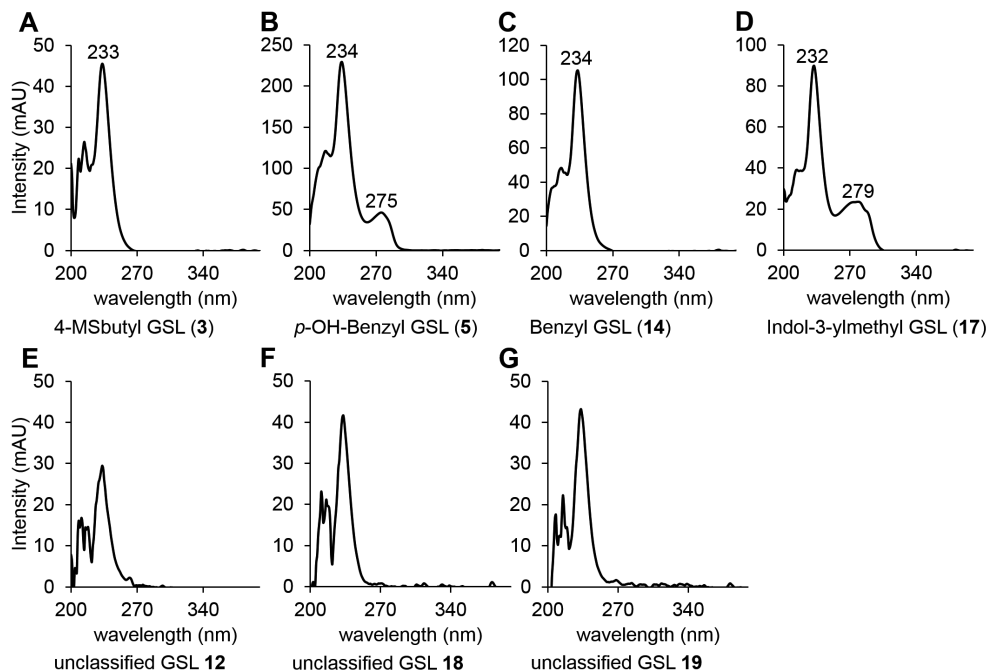
**Figure S2.4.** MS<sup>2</sup> fragmentation of 6'-O-sinapoyl (or isomer) derivative of GSLs: proposed fragment ions extrapolated from those by Bianco *et al.*<sup>12</sup> who analyzed pure 6'-O-isoferuloyl-(S)-2-OH-2-phenethyl GSL (**A**) and proposed fragment ions following the diagnostic fragmentation patterns of non-acylated GSLs (**B**). For the sake of clarity, the acyl group is drawn as sinapoyl. According to Bianco *et al.*<sup>12</sup>, the fragment ion at  $m/z$  235 was only observed for 6'-substitution for isoferuloyl, where the analog fragment ion for sinapoyl (or isomer) has  $m/z$  of 265. This fragment ion was observed for **26** and **29**. Therefore, **26** and **29** were tentatively annotated as 6'-O-sinapoyl (or isomer) derivative of *p*-OH-benzyl GSL and 6'-O-sinapoyl (or isomer) derivative of 3-butenyl GSL, respectively. Fragment ions, except  $m/z$  of 265, were observed for **27** and **30** too, where the position of sinapoyl (or isomer) substitution cannot be distinguished.



**Figure S2.5.** MS spectra of standard 3-butenyl GSL (8) (A), tentatively annotated unidentified sinapoyl (or isomer) derivative of 3-butenyl GSL (27) (B), and tentatively annotated 6'-O-sinapoyl (or isomer) derivative of 3-butenyl GSL (29) (C), which illustrate the different fragmentation patterns of sinapoyl (or isomer) derivatives of a GSL where the sinapoyl (or isomer) group is in different positions (6'-O vs others).



**Figure S2.6.** Sinapoyl (or isomer) derivatives of *p*-OH-benzyl GSL and 3-butenyl GSL, and 4-salicyloxy (or isomer)-indol-3-ylmethyl GSL. Bold face numbers refer to those in **Table S2.1**. For the sake of clarity, the acyl group is drawn as sinapoyl or salicyloxy.



**Figure S2.7.** UV absorption spectra of authentic standards of 4-(methylsulfinyl)butyl GSL (3) (A), *p*-OH-benzyl GSL (5) (B), benzyl GSL (14) (C), and indol-3-ylmethyl GSL (17) (D), and of tentatively annotated *x*-hydroxy-4-(methylthio)butyl GSL 12 (E), a benzenic GSL 18 (F), and *x*-hydroxy-5-(methylthio)pentyl GSL 19 (G).

## 2.8.3. Supplementary tables

**Table S2.1.** (Tentative) annotation of 31 GSLs found in the untreated (U), germinated (G), *R. oryzae*-germinated (Ro-G), *F. graminearum*-germinated (Fg-G), and *F. oxysporum*-germinated (Fo-G) *S. alba* (Sa), *B. napus* (Bn), and *B. juncea* var. *rugosa rugosa* (Bj) seeds.

No.	$t_g$ (min)	$\lambda_{max}$ (nm)	[M-H] <sup>+</sup>	MS <sup>2</sup>	MS <sup>3</sup>	Potential molecular formulae	(Semi)systematic name (trivial name) <sup>a</sup>	Occurrence
<b>Met-derived GSLs</b>								
<b>(Methylthio)alkyl GSLs</b>								
11	6.35	- <sup>b</sup>	406 <sup>c</sup>	259 <sup>d</sup> , 326 (27), 291 (6), 275 (41), 228 (23), 227 (13), 210 (8), 195 (15), 164 (8)	139, 241 (7), 199 (5), 181 (3), 97 (31), 81 (3)	C <sub>11</sub> H <sub>20</sub> NO <sub>9</sub> S <sub>3</sub> <sup>-</sup>	3-(Methylthio)propyl GSL (Glucobervirin)	Bj
15	8.80	-	420	259, 340 (24), 291 (9), 275 (38), 242 (24), 241 (3), 227 (22), 224 (8), 195 (17), 178 (15)	139, 241 (7), 199 (6), 181 (2), 97 (37), 81 (6)	C <sub>12</sub> H <sub>22</sub> NO <sub>9</sub> S <sub>3</sub> <sup>-</sup>	4-(Methylthio)butyl GSL (Glucocerucin) <sup>*</sup>	Sa_G, Sa_Fg-G, Bn (except Bn_Ro-G), Bj
21	12.22	-	434	259, 354 (23), 291 (12), 275 (43), 256 (20), 241 (21), 238 (13), 227 (10), 195 (22), 192 (20)	139, 241 (5), 199 (11), 97 (36)	C <sub>13</sub> H <sub>24</sub> NO <sub>9</sub> S <sub>3</sub> <sup>-</sup>	5-(Methylthio)pentyl GSL (Glucoberteroin) <sup>*</sup>	Bn (except Bn_Ro-G), Bj
<b>Hydroxy-(methylthio)alkyl GSLs</b>								
12	7.57	-	436	259, 418 (16), 390 (12), 368 (15), 356 (22), 346 (6), 291 (16), 275 (21), 274 (2), 258 (24), 240 (2), 195 (7), 194 (12), 129 (4)	139, 244 (2), 199 (9), 179 (5), 169 (2), 97 (30), 81 (5)	C <sub>12</sub> H <sub>22</sub> NO <sub>10</sub> S <sub>3</sub> <sup>-</sup>	Possible x-hydroxy-4- (methylthio)butyl GSL <sup>e</sup>	Sa (except Sa_Ro-G), Bj_G, Bj_Ro-G, Bj_Fg-G
19	10.23	-	450	259, 432 (16), 404 (18), 383 (10), 370 (23), 361 (64), 305 (22), 291 (21), 288 (2), 275 (26), 272 (19), 254 (2), 208 (16)	139, 199 (6), 169 (7), 97 (23)	C <sub>13</sub> H <sub>24</sub> NO <sub>10</sub> S <sub>3</sub> <sup>-</sup>	Possible x-hydroxy-5- (methylthio)pentyl GSL	Bn_G, Bn_Fg-G
<b>(Methylsulfinyl)alkyl GSLs</b>								
1	1.44	-	422	358, 407 (4), 291 (2), 275 (2), 259 (6), 195 (1)	259, 291 (2), 278 (16), 275 (38), 227 (11), 196 (11), 195 (21), 180 (21), 162 (59), 145 (6), 135 (6), 116 (9)	C <sub>11</sub> H <sub>20</sub> NO <sub>10</sub> S <sub>3</sub> <sup>-</sup>	3-(Methylsulfinyl)propyl GSL (Glucoberein) <sup>*</sup>	Bj (except Bj_Fo-G)
3	1.70	-	436	372, 421 (3), 291 (1), 275 (1), 259 (4)	259, 292 (23), 291 (3), 275 (49), 241 (6), 227 (13), 210 (7), 195 (31), 194 (21), 176 (4), 145 (6), 130 (9)	C <sub>12</sub> H <sub>22</sub> NO <sub>10</sub> S <sub>3</sub> <sup>-</sup>	4-(Methylsulfinyl)butyl GSL (Glucoraphanin) <sup>*</sup>	Sa_G, Sa_Fg-G, Bn_U, Bn_Fg-G, Bn_Fo-G, Bj (except Bj_Fo-G)
6	3.12	-	450	386, 435 (2), 291 (1), 259 (2)	259, 354 (3), 306 (23), 291 (3), 275 (53), 241 (5), 227 (17), 224 (4), 208 (16), 195 (24), 190 (7), 145 (10), 144 (15)	C <sub>13</sub> H <sub>24</sub> NO <sub>10</sub> S <sub>3</sub> <sup>-</sup>	5-(Methylsulfinyl)pentyl GSL (Glucocallysin)	Bn, Bj (except Bj_Fo-G)
25	16.13	-	520	456, 505 (3), 291 (2), 259 (1)	259, 376 (33), 291 (11), 278 (38), 275 (52), 263 (23), 227 (11), 214 (28), 195 (19)	C <sub>18</sub> H <sub>34</sub> NO <sub>10</sub> S <sub>3</sub> <sup>-</sup>	10-(Methylsulfinyl)decyl GSL (Glucocamelinin)	Bn_U, Bn_G, Bn_Fg-G

No.	$t_g$ (min)	$\lambda_{max}$ (nm)	[M-H] <sup>+</sup> MS <sup>2</sup>	MS <sup>3</sup>	Potential molecular formulae	(Semi)systematic name (trivial name) <sup>a</sup>	Occurrence
<b>Alkenyl GSLs</b>							
<b>4</b>	1.94	-	358	259, 291 (1), 278 (19), 275 (48), 241 (5), 227 (11), 195 (24), 180 (21), 165 (2), 162 (63), 145 (7), 135 (5), 116 (8)	C <sub>10</sub> H <sub>18</sub> NO <sub>9</sub> S <sub>2</sub> <sup>-</sup>	Allyl GSL (Sinigrin)*	Sa (except Sa_Ro-G), Bn, B <sub>j</sub>
<b>8</b>	4.00	-	372	259, 292 (21), 291 (3), 275 (44), 241 (4), 236 (15), 227 (8), 210 (4), 195 (26), 194 (23), 179 (3), 176 (7), 149 (3), 145 (6), 130 (9)	C <sub>11</sub> H <sub>18</sub> NO <sub>9</sub> S <sub>2</sub> <sup>-</sup>	3-Butenyl GSL (Gluconaph)*	Sa_U, Sa_Fg-G, Sa_Fo-G, Bn, B <sub>j</sub>
<b>13</b>	7.94	-	386	259, 306 (22), 291 (2), 275 (47), 241 (3), 227 (11), 224 (4), 208 (18), 195 (24), 193 (6), 190 (9), 163 (19), 145 (6), 144 (12), 139 (2)	C <sub>12</sub> H <sub>20</sub> NO <sub>9</sub> S <sub>2</sub> <sup>-</sup>	4-Pentenyl GSL (Glucobrassicinapin)*	Bn, B <sub>j</sub>
<b>Hydroxy-alkenyl GSLs</b>							
<b>2</b>	1.66	-	388	332, 370 (3), 308 (24), 275 (45), 259 (85), 210 (43), 195 (30), 192 (10), 146 (11), 136 (40)	C <sub>11</sub> H <sub>18</sub> NO <sub>10</sub> S <sub>2</sub> <sup>-</sup>	(R)-2-Hydroxy-3-butenyl GSL (Progoitrin)*	Sa, Bn, B <sub>j</sub>
<b>7</b>	3.13	-	402	259, 384 (3), 332 (48), 322 (30), 291 (10), 275 (48), 241 (4), 227 (6), 224 (57), 206 (10), 195 (27), 160 (14), 139 (4), 136 (15)	C <sub>12</sub> H <sub>20</sub> NO <sub>10</sub> S <sub>2</sub> <sup>-</sup>	2-Hydroxy-4-pentenyl GSL (Gluconapoleiferin)	Sa_G, Sa_Fg-G, Sa_Fo-G, Bn, B <sub>j</sub> _G, B <sub>j</sub> _Fg-G, B <sub>j</sub> _Fo-G
<b>Sinapoyl (or isomer) alkenyl GSLs</b>							
<b>27</b>	18.41	300	578	223, 532 (7), 510 (13), 497 (46), 481 (70), 465 (69), 447 (69), 432 (9), 401 (33), 372 (60), 325 (10), 281 (10), 253 (13), 247 (24)	C <sub>22</sub> H <sub>28</sub> NO <sub>13</sub> S <sub>2</sub> <sup>-</sup>	Possible unidentified sinapoyl (or isomer) derivative of 3-butenyl GSL	B <sub>j</sub> (except B <sub>j</sub> _Ro-G)
<b>29</b>	20.02	334	578	372, 497 (12), 481 (15), 465 (33), 447 (9), 401 (6), 368 (21), 367 (69), 354 (4), 325 (17), 265 (4), 223 (44), 176 (5), 145 (9)	C <sub>22</sub> H <sub>28</sub> NO <sub>13</sub> S <sub>2</sub> <sup>-</sup>	Possible 6'-O-sinapoyl (or isomer)-3-butenyl GSL	Bn_U, Bn_G, Bn_Fo-G, B <sub>j</sub>
<b>30</b>	20.35	328	578	223, 532 (17), 510 (12), 497 (34), 481 (36), 465 (60), 447 (11), 372 (9), 401 (1), 259 (1), 247 (44), 223 (77)	C <sub>22</sub> H <sub>28</sub> NO <sub>13</sub> S <sub>2</sub> <sup>-</sup>	Possible unidentified sinapoyl (or isomer) derivative of 3-butenyl GSL	B <sub>j</sub> (except B <sub>j</sub> _Ro-G)
<b>Alkyl GSLs</b>							
<b>16</b>	9.63	-	388	343, 344 (27), 342 (47), 308 (12), 301 (39), 291 (2), 275 (36), 259 (71), 227 (10), 210 (9), 192 (4), 195 (19), 165 (6), 163 (6), 145 (6), 139 (3)	C <sub>12</sub> H <sub>22</sub> NO <sub>9</sub> S <sub>2</sub> <sup>-</sup>	Pentenyl GSL or isomer	B <sub>j</sub>

No.	$t_R$ (min)	$\lambda_{max}$ (nm)	[M-H] <sup>+</sup> MS <sup>2</sup>	MS <sup>3</sup>	Potential molecular formulae	(Semi)systematic name (trivial name) <sup>a</sup>	Occurrence
<b>23</b>	14.24	-	402	259, 357 (22), 322 (20), 315 (11), 291 (4), 275 (47), 241 (6), 227 (12), 224 (26), 211 (3), 209 (11), 206 (12), 195 (23), 179 (5), 163 (6), 160 (10), 145 (8), 139 (3)	$C_{13}H_{24}NO_9S_2^-$	Hexyl GSL or isomer	Bj (except Bj_Fo-G)
<b>Unclassified aliphatic GSLs<sup>f</sup></b>							
<b>10</b>	5.99	-	374	259, 356 (33), 330 (38), 328 (78), 306 (28), 302 (23), 294 (13), 291 (6), 286 (18), 275 (45), 228 (8), 196 (19), 195 (23), 181 (7), 178 (7), 163 (8), 145 (8), 132 (7)	$C_{11}H_{20}NO_9S_2^-$ or $C_{10}H_{18}NO_{10}S_2^-$	Possible $C_{14}H_{16}$ GSL or $C_3H_5O$ GSL	Bj (except Bj_Fo-G)
<b>28</b>	18.45	-	416	259, 398 (9), 372 (34), 370 (22), 349 (27), 348 (13), 343 (22), 336 (15), 291 (6), 275 (34), 238 (26), 227 (12), 223 (9), 220 (8), 195 (14), 174 (12), 163 (6)	$C_{14}H_{26}NO_9S_2^-$ or $C_{13}H_{22}NO_{10}S_2^-$	Possible $C_{17}H_{15}$ GSL or $C_6H_{11}O$ GSL	Bn_G, Bn_Fg-G, Bn_Fo-G, Bj_G, Bj_Ro-G, Bj_Fg-G
<b>Tyr/Phe-derived GSLs</b>							
<b>14</b>	8.51	-	408	259, 328 (27), 291 (2), 275 (38), 246 (1), 241 (3), 230 (18), 227 (6), 217 (2), 215 (11), 212 (36), 195 (16), 166 (22), 163 (3), 145 (3), 139 (1), 129 (2)	$C_{14}H_{18}NO_9S_2^-$	Benzyl GSL (Glucotropaeolin)*	Sa, Bn_G, Bn_Fg-G, Bn_Fo-G, Bj (except Bj_U)
<b>18</b>	9.95	-	438	259, 420 (12), 392 (11), 371 (10), 358 (31), 291 (8), 276 (3), 275 (19), 260 (32), 242 (1), 196 (14), 195 (9), 129 (7)	$C_{15}H_{20}NO_{10}S_2^-$	Possible $C_8H_9O$ GSL <sup>g</sup>	Sa_Ro-G, Bn_G, Bn_Fg-G
<b>20</b>	11.95	-	422	259, 342 (25), 291 (5), 275 (41), 260 (6), 244 (21), 241 (5), 231 (2), 229 (12), 226 (8), 199 (2), 195 (18), 180 (21), 163 (2), 145 (4), 139 (2), 129 (2)	$C_{15}H_{20}NO_9S_2^-$	Phenethyl GSL (Glucanasturtin)*	Sa (except Sa_U), Bn, Bj
<b>5</b>	2.93	276	424	259, 344 (29), 291 (12), 275 (48), 246 (19), 241 (4), 231 (11), 228 (13), 195 (12), 182 (30), 163 (2), 145 (4), 139 (3)	$C_{14}H_{18}NO_{10}S_2^-$	p-Hydroxybenzyl GSL (Glucosinalbin)*	Sa, Bn (except Bn_Ro-G), Bj_G, Bj_Fo-G
<b>26</b>	18.25	278, 316	630	424, 550 (4), 497 (35), 481 (22), 465 (68), 447 (5), 401 (1) 351 (4), 303 (5), 265 (3), 231 (2), 228 (3), 223 (38)	$C_{25}H_{28}NO_{14}S_2^-$	Possible 6'-O-sinapoyl (or isomer)-p-hydroxybenzyl GSL	Sa

No.	$t_R$ (min)	$\lambda_{max}$ (nm)	[M-H] <sup>-</sup> MS <sup>2</sup>	MS <sup>3</sup>	Potential molecular formulae	(Semi)systematic name (trivial name) <sup>a</sup>	Occurrence
<b>Trp-derived GSLs</b>							
<b>17</b>	9.67	279	447	259, 367 (24), 291 (32), 275 (42), 269 (18), 256 (4), 254 (12), 251 (10), 241 (3), 227 (9), 205 (29), 195 (14), 163 (3), 139 (3)	139, 241 (5), 199 (13), 169 (4), 97 (39), 81 (5)	C <sub>16</sub> H <sub>13</sub> N <sub>2</sub> O <sub>6</sub> S <sub>2</sub> <sup>-</sup> (Glucobrassicin) <sup>*</sup>	Indol-3-ylmethyl (13M) GSL Sa, Bn, Bj
<b>9</b>	5.42	265	463	285, 383 (7), 291 (1), 275 (3), 267 (83), 259 (7), 240 (13), 221 (4), 205 (2), 195 (1), 160 (8)	97, 268 (2), 205 (1), 187 (1), 112 (3)	C <sub>16</sub> H <sub>13</sub> N <sub>2</sub> O <sub>10</sub> S <sub>2</sub> <sup>-</sup>	4-Hydroxy-13M GSL Sa_G, Sa_Fg-G, Sa_Fo-G, Bn, Bj
<b>22</b>	13.15	266	477	259, 397 (17), 299 (25), 291 (58), 284 (8), 281 (16), 275 (70), 254 (3), 241 (7), 235 (19), 227 (17), 204 (3), 195 (14), 163 (4)	139, 241 (5), 223 (2), 199 (16), 131 (2), 97 (30)	C <sub>17</sub> H <sub>17</sub> N <sub>2</sub> O <sub>10</sub> S <sub>2</sub> <sup>-</sup>	4-Methoxy-13M GSL Sa (except Sa_U), Bn, Bj
<b>24</b>	15.89	280	477	446, 285 (1), 259 (1)	383, 416 (36), 413 (11), 365 (22), 348 (5), 341 (14), 313 (4), 291 (9), 284 (97), 275 (6), 259 (49), 224 (43), 205 (6), 188 (6), 160 (4), 154 (19), 144 (10)	C <sub>17</sub> H <sub>17</sub> N <sub>2</sub> O <sub>10</sub> S <sub>2</sub> <sup>-</sup>	1-Methoxy-13M GSL Sa, Bn, Bj
<b>31</b>	20.58	275, 316	583	291, 565 (8), 553 (7), 539 (6), 503 (27), 405 (26), 390 (26), 387 (16), 341 (80), 308 (10), 305 (24), 275 (42), 259 (76), 227 (6), 195 (8)	97, 275 (4), 263 (7), 262 (7)	C <sub>23</sub> H <sub>23</sub> NO <sub>12</sub> S <sub>2</sub> <sup>-</sup>	Possible 4-salicyloxy (or isomer)-13M GSL Sa_Ro-G

<sup>a</sup> The annotation of 12 GSLs marked with (\*) was confirmed by the authentic standards. The word "possible" indicates that the suggested GSLs have never been identified in Brassicaceae plants by conclusive methods.

<sup>b</sup> The apparent  $\lambda_{max}$  was only ~233 nm.

<sup>c</sup> The  $m/z$  of the molecular anion of a GSL, [M-H]<sup>-</sup>, is the same as its molecular weight. Mostly 5 isotopes were detected in MS spectra for [M-H]<sup>-</sup>: M, M+1, M+2, M+3, M+4 with relative abundance of 100%, 15-23%, 11-17%, 2-4%, and 1-2%, respectively.

<sup>d</sup> The most abundant fragment ion is mentioned at first without any brackets following afterwards. The most abundant ion in MS<sup>2</sup> fragmentation was further fragmented in MS<sup>3</sup>.

<sup>e</sup> The position of hydroxylation (x) could be at 2 or 3.<sup>10,17</sup>

<sup>f</sup> The side chain formula of C<sub>6</sub>H<sub>5</sub> and C<sub>7</sub>H<sub>15</sub> can refer to alkyl GSLs, whereas C<sub>3</sub>H<sub>5</sub>O and C<sub>6</sub>H<sub>11</sub>O can refer to  $\alpha$ -oxoalkyl GSLs or hydroxylated alkenyl GSLs. However, the tentative annotation for peaks **10** and **28** remains as unclassified GSLs (further explanation can be found in sections 2.3.1 and 2.8.1).

<sup>g</sup> Because peak **18** was present in trace amounts, its UV spectrum (**Figure S2.7F**) could not be used for tentative peak annotation. Multiple isomers for **18** could be possible, i.e. a non-phenolic or phenolic hydroxylated phenethyl GSL or a methoxylated benzyl GSL.



**Table S2.2.** NI-MS-based relative response factors (RRFs) of the twelve GSL standards.

No.	GSL	RRF <sup>a</sup>	Applied for GSL
<b>Aliphatic</b>			
15 <sup>b</sup>	4-(Methylthio)butyl	0.92	15, 11, 12
21	5-(Methylthio)pentyl	1.22	21, 19
1	3-(Methylsulfinyl)propyl	0.50	1
3	4-(Methylsulfinyl)butyl	0.56	3, 6, 25
4	Allyl	0.62	4
8	3-Butenyl	0.68	8, 27, 29, 30
13	4-Pentenyl	1.00	13, 16, 23
2	(R)-2-OH-3-Butenyl	0.56	2, 7
<b>Benzenic</b>			
14	Benzyl	1.71	14
20	Phenethyl	2.18	20, 18
5	<i>p</i> -OH-Benzyl	1.00	5, 26
<b>Indolic</b>			
17	Indol-3-ylmethyl	1.00	17, 9, 22, 24, 31

<sup>a</sup> The response factors of aliphatic GSLs, aromatic GSLs, and indolic GSL were set relatively to 4-pentenyl GSL, *p*-OH-benzyl GSL, and indol-3-ylmethyl GSL, respectively. The values were an average of three independent repetitions with a relative standard deviation less than 11%. The relative response factors of *p*-OH-benzyl GSL and indol-3-ylmethyl GSL to 4-pentenyl GSL were 0.53 and 0.74, respectively.

<sup>b</sup> Bold face numbers correspond to the numbers in **Table S2.1**.

**Table S2.3.** Fast screening to identify the class of GSLs in the PDA-UHPLC-MS analysis.

Class	$\lambda_{\max}$ <sup>a</sup>	[M-H] <sup>-</sup>	Fragment ion at <i>m/z</i> 259?
<i>Non-acylated</i>			
<b>Aliphatic</b>	~233	Even number	Yes
<b>Benzenic</b>			
with O on phenyl	~233, 263-275 nm	Even number	Yes
without O on phenyl	~233	Even number	Yes
<b>Indolic</b>	~233, 265-301 nm	Odd number	Yes
<i>Aromatic-acylated</i>	300-334 nm	Even/odd number <sup>b</sup>	Yes

<sup>a</sup> UV absorption spectra of representatives of each class are illustrated in **Figure S2.7**. GSLs have a characteristic UV spectrum, typically a maximum near 225-235 nm from the thiohydroxymate group. There is no  $\lambda_{\max}$  at 280 nm for benzenic GSLs, which is characteristic of indolic GSLs. The  $\lambda_{\max}$  of indolic GSLs can vary from 265-301 nm depending on the substituents. Additional  $\lambda_{\max}$  around 300-334 nm corresponds to aromatic acyl moiety. In the text, the aromatic acyl moiety is frequently mentioned without the word "aromatic".

<sup>b</sup> Even or odd number depends on the class.

**Table S2.4.** Content of GSLs in the untreated (U), germinated (G), *R. oryzae*-germinated (Ro-G), *F. graminearum*-germinated (Fg-G), and *F. oxysporum*-germinated (Fo-G) *S. alba* (Sa) seed.

No.	GSL <sup>a</sup>	Content (μmol/g DW)				
		Sa U	Sa G	Sa Ro-G	Sa Fg-G	Sa Fo-G
11	3-(Methylthio)propyl	n.d. <sup>b</sup>	n.d.	n.d.	n.d.	n.d.
15	4-(Methylthio)butyl	n.d.	0.00±0.00	n.d.	0.01±0.00	0.00±0.00
21	5-(Methylthio)pentyl	n.d.	n.d.	n.d.	n.d.	n.d.
<b>Sub-total MTalkyl</b>		<b>n.d.</b>	<b>0.00±0.00</b>	<b>n.d.</b>	<b>0.01±0.00</b>	<b>0.00±0.00</b>
12	Possible x-OH-4-MTbutyl	0.16±0.04	0.78±0.15	n.d.	3.66±0.22	6.23±0.78
19	Possible x-OH-5-MTpentyl	n.d.	n.d.	n.d.	n.d.	n.d.
<b>Sub-total OH-MTalkyl</b>		<b>0.16±0.04</b>	<b>0.78±0.15</b>	<b>n.d.</b>	<b>3.66±0.22</b>	<b>6.23±0.78</b>
1	3-(Methylsulfinyl)propyl	n.d.	n.d.	n.d.	n.d.	n.d.
3	4-(Methylsulfinyl)butyl	n.d.	0.00±0.00	n.d.	0.00±0.00	0.00±0.00
6	5-(Methylsulfinyl)pentyl	n.d.	n.d.	n.d.	n.d.	n.d.
25	10-(Methylsulfinyl)decyl	n.d.	n.d.	n.d.	n.d.	n.d.
<b>Sub-total MSalkyl</b>		<b>n.d.</b>	<b>0.00±0.00</b>	<b>n.d.</b>	<b>0.00±0.00</b>	<b>0.00±0.00</b>
4	Allyl	0.07±0.07	0.02±0.00	n.d.	0.03±0.00	0.01±0.00
8	3-Butenyl	0.60±0.60	0.00±0.00	n.d.	0.05±0.00	0.02±0.00
13	4-Pentenyl	n.d.	n.d.	n.d.	n.d.	n.d.
<b>Sub-total alkenyl</b>		<b>0.66±0.66</b>	<b>0.02±0.00</b>	<b>n.d.</b>	<b>0.08±0.01</b>	<b>0.03±0.00</b>
2	(R)-2-OH-3-Butenyl	3.19±0.99	2.55±0.30	1.55±0.51	0.34±0.01	0.12±0.01
7	2-OH-4-Pentenyl	n.d.	0.02±0.00	n.d.	0.01±0.00	0.00±0.00
<b>Sub-total OH-alkenyl</b>		<b>3.19±0.99</b>	<b>2.57±0.30</b>	<b>1.55±0.51</b>	<b>0.35±0.01</b>	<b>0.13±0.01</b>
27	Sinapoyl-3-butenyl or isomer	n.d.	n.d.	n.d.	n.d.	n.d.
29	Sinapoyl-3-butenyl or isomer	n.d.	n.d.	n.d.	n.d.	n.d.
30	Sinapoyl-3-butenyl or isomer	n.d.	n.d.	n.d.	n.d.	n.d.
<b>Sub-total sinapoyl alkenyl or isomer</b>		<b>n.d.</b>	<b>n.d.</b>	<b>n.d.</b>	<b>n.d.</b>	<b>n.d.</b>
16	Pentyl or isomer	n.d.	n.d.	n.d.	n.d.	n.d.
23	Hexyl or isomer	n.d.	n.d.	n.d.	n.d.	n.d.
<b>Sub-total alkyl</b>		<b>n.d.</b>	<b>n.d.</b>	<b>n.d.</b>	<b>n.d.</b>	<b>n.d.</b>
<b>Total aliphatic</b>		<b>4.01±1.64</b>	<b>3.39±0.24</b>	<b>1.55±0.51</b>	<b>4.10±0.22</b>	<b>6.39±0.78</b>
14	Benzyl	0.02±0.01	0.39±0.01	0.07±0.01	0.30±0.04	0.12±0.01
20	Phenethyl	n.d.	0.02±0.01	0.28±0.02	0.02±0.00	0.00±0.00
5	<i>p</i> -OH-Benzyl	72.29±43.83	212.92±18.10	176.17±12.32	160.18±12.48	74.04±9.07
26	Sinapoyl- <i>p</i> -OH-benzyl or isomer	0.04±0.04	1.79±0.43	0.34±0.02	0.40±0.27	0.61±0.03
18	Possible C <sub>8</sub> H <sub>9</sub> O	n.d.	n.d.	0.06±0.00	n.d.	n.d.
<b>Total benzenic</b>		<b>72.35±43.88</b>	<b>215.12±17.90</b>	<b>176.91±12.29</b>	<b>160.89±12.66</b>	<b>74.77±9.04</b>
17	Indol-3-ylmethyl (I3M)	0.12±0.07	0.31±0.06	1.27±0.22	0.26±0.02	0.05±0.00
9	4-OH-I3M	n.d.	0.02±0.00	n.d.	0.01±0.00	0.00±0.00
24	1-OCH <sub>3</sub> -I3M	0.02±0.02	0.95±0.18	2.64±0.36	0.47±0.04	0.03±0.00
22	4-OCH <sub>3</sub> -I3M	n.d.	0.66±0.09	0.37±0.08	0.72±0.06	0.06±0.01
31	Salicyloxy (or isomer)-I3M	n.d.	n.d.	0.27±0.01	n.d.	n.d.
<b>Total indolic</b>		<b>0.14±0.08</b>	<b>1.95±0.31</b>	<b>4.55±0.51</b>	<b>1.46±0.11</b>	<b>0.15±0.01</b>
<b>Total GSLs</b>		<b>76.50±42.70</b>	<b>220.45±17.93</b>	<b>183.01±12.28</b>	<b>166.44±12.76</b>	<b>81.31±8.65</b>

<sup>a</sup> Details of the tentative annotation of the peaks follow Table S2.1.<sup>b</sup> n.d. peak not detected.

**Table S2.5.** Content of GSLs in the untreated (U), germinated (G), *R. oryzae*-germinated (Ro-G), *F. graminearum*-germinated (Fg-G), and *F. oxysporum*-germinated (Fo-G) *B. napus* (Bn) seed.

No.	GSL <sup>a</sup>	Content (μmol/g DW)				
		Bn U	Bn G	Bn Ro-G	Bn Fg-G	Bn Fo-G
11	3-(Methylthio)propyl	n.d. <sup>b</sup>	n.d.	n.d.	n.d.	n.d.
15	4-(Methylthio)butyl	0.07±0.05	0.01±0.02	n.d.	0.03±0.01	0.02±0.00
21	5-(Methylthio)pentyl	0.01±0.01	0.03±0.04	n.d.	0.05±0.05	0.03±0.01
<b>Sub-total MTalkyl</b>		<b>0.08±0.05</b>	<b>0.04±0.06</b>	<b>n.d.</b>	<b>0.08±0.06</b>	<b>0.04±0.01</b>
12	Possible x-OH-4-MTbutyl	n.d.	n.d.	n.d.	n.d.	n.d.
19	Possible x-OH-5-MTpentyl	n.d.	0.01±0.01	n.d.	0.01±0.02	n.d.
<b>Sub-total OH-MTAlkyl</b>		<b>n.d.</b>	<b>0.01±0.01</b>	<b>n.d.</b>	<b>0.01±0.02</b>	<b>n.d.</b>
1	3-(Methylsulfinyl)propyl	n.d.	n.d.	n.d.	n.d.	n.d.
3	4-(Methylsulfinyl)butyl	0.21±0.22	n.d.	n.d.	0.00±0.00	0.00±0.00
6	5-(Methylsulfinyl)pentyl	0.18±0.13	0.03±0.02	0.03±0.03	0.02±0.02	0.02±0.00
25	10-(Methylsulfinyl)decyl	0.02±0.03	0.02±0.03	n.d.	0.04±0.07	n.d.
<b>Sub-total MSalkyl</b>		<b>0.41±0.27</b>	<b>0.05±0.01</b>	<b>0.03±0.03</b>	<b>0.06±0.05</b>	<b>0.03±0.00</b>
4	Allyl	0.07±0.14	0.04±0.03	0.23±0.01	0.08±0.05	0.02±0.00
8	3-Butenyl	2.51±0.27	0.77±0.11	0.27±0.04	1.12±0.58	0.63±0.05
13	4-Pentenyl	0.21±0.02	0.24±0.03	0.09±0.01	0.22±0.02	0.12±0.01
<b>Sub-total alkenyl</b>		<b>2.79±0.38</b>	<b>1.04±0.13</b>	<b>0.59±0.03</b>	<b>1.42±0.65</b>	<b>0.77±0.07</b>
2	(R)-2-OH-3-Butenyl	4.97±0.41	1.70±1.56	2.53±0.30	1.25±1.22	0.40±0.03
7	2-OH-4-Pentenyl	0.06±0.02	0.08±0.08	0.06±0.03	0.08±0.06	0.03±0.00
<b>Sub-total OH-alkenyl</b>		<b>5.02±0.39</b>	<b>1.79±1.64</b>	<b>2.60±0.29</b>	<b>1.33±1.28</b>	<b>0.43±0.04</b>
27	Sinapoyl-3-butenyl or isomer	n.d.	n.d.	n.d.	n.d.	n.d.
29	Sinapoyl-3-butenyl or isomer	0.02±0.03	0.71±0.45	n.d.	0.32±0.64	1.03±0.13
30	Sinapoyl-3-butenyl or isomer	n.d.	n.d.	n.d.	n.d.	n.d.
<b>Sub-total sinapoyl alkenyl or isomer</b>		<b>0.02±0.03</b>	<b>0.71±0.45</b>	<b>n.d.</b>	<b>0.32±0.64</b>	<b>1.03±0.13</b>
16	Pentyl or isomer	n.d.	n.d.	n.d.	n.d.	n.d.
23	Hexyl or isomer	n.d.	n.d.	n.d.	n.d.	n.d.
<b>Sub-total alkyl</b>		<b>n.d.</b>	<b>n.d.</b>	<b>n.d.</b>	<b>n.d.</b>	<b>n.d.</b>
<b>Total aliphatic</b>		<b>8.33±0.42</b>	<b>3.63±1.21</b>	<b>3.21±0.28</b>	<b>3.22±0.82</b>	<b>2.30±0.07</b>
14	Benzyl	n.d.	0.01±0.01	n.d.	0.00±0.00	0.01±0.01
20	Phenethyl	0.06±0.04	0.13±0.03	0.10±0.01	0.13±0.02	0.06±0.01
5	<i>p</i> -OH-Benzyl	0.02±0.04	0.19±0.12	n.d.	0.09±0.06	4.36±0.56
26	Sinapoyl- <i>p</i> -OH-benzyl or isomer	n.d.	n.d.	n.d.	n.d.	n.d.
18	Possible C <sub>8</sub> H <sub>9</sub> O	n.d.	0.12±0.06	n.d.	0.03±0.04	n.d.
<b>Total benzenic</b>		<b>0.08±0.08</b>	<b>0.45±0.10</b>	<b>0.10±0.01</b>	<b>0.25±0.05</b>	<b>4.43±0.57</b>
17	Indol-3-ylmethyl (I3M)	0.07±0.02	0.43±0.16	0.97±0.12	0.30±0.01	0.04±0.00
9	4-OH-I3M	1.04±0.38	0.53±0.60	0.34±0.00	0.17±0.14	0.08±0.01
24	1-OCH <sub>3</sub> -I3M	0.02±0.00	2.04±0.43	2.84±0.26	2.49±0.86	0.04±0.00
22	4-OCH <sub>3</sub> -I3M	0.02±0.02	1.13±0.22	1.26±0.09	1.60±0.61	0.05±0.01
31	Salicyloxy (or isomer)-I3M	n.d.	n.d.	n.d.	n.d.	n.d.
<b>Total indolic</b>		<b>1.16±0.37</b>	<b>4.13±0.99</b>	<b>5.41±0.22</b>	<b>4.56±1.62</b>	<b>0.21±0.02</b>
<b>Total GSLs</b>		<b>9.56±0.67</b>	<b>8.22±2.10</b>	<b>8.72±0.23</b>	<b>8.03±2.26</b>	<b>6.94±0.58</b>

<sup>a</sup> Details of the tentative annotation of the peaks follow Table S2.1.<sup>b</sup> n.d. peak not detected.

**Table S2.6.** Content of GSLs in the untreated (U), germinated (G), *R. oryzae*-germinated (Ro-G), *F. graminearum*-germinated (Fg-G), and *F. oxysporum*-germinated (Fo-G) *B. juncea* var. *rugosa* (*Bj*) seed.

No.	GSL <sup>a</sup>	Content (μmol/g DW)				
		<i>Bj</i> U	<i>Bj</i> G	<i>Bj</i> Ro-G	<i>Bj</i> Fg-G	<i>Bj</i> Fo-G
11	3-(Methylthio)propyl	0.05±0.02	0.58±0.87	0.64±0.04	0.86±1.09	0.03±0.00
15	4-(Methylthio)butyl	1.00±1.55	1.89±2.27	3.57±0.05	2.21±2.36	0.20±0.03
21	5-(Methylthio)pentyl	0.03±0.01	0.10±0.06	0.08±0.00	0.10±0.07	0.02±0.00
<b>Sub-total MTalkyl</b>		<b>1.08±1.26</b>	<b>2.57±3.20</b>	<b>4.29±0.02</b>	<b>3.17±3.51</b>	<b>0.25±0.04</b>
12	Possible x-OH-4-MTbutyl	n.d.	0.03±0.07	0.07±0.01	0.07±0.09	n.d.
19	Possible x-OH-5-MTpentyl	n.d.	n.d.	n.d.	n.d.	n.d.
<b>Sub-total OH-MTalkyl</b>		<b>n.d.</b>	<b>0.03±0.07</b>	<b>0.07±0.01</b>	<b>0.07±0.09</b>	<b>n.d.</b>
1	3-(Methylsulfinyl)propyl	0.75±0.05	0.16±0.32	0.24±0.03	0.31±0.43	n.d.
3	4-(Methylsulfinyl)butyl	2.13±1.23	0.21±0.33	2.35±0.28	1.54±1.98	0.00±0.00
6	5-(Methylsulfinyl)pentyl	0.15±0.06	0.08±0.06	0.07±0.00	0.09±0.07	0.01±0.00
25	10-(Methylsulfinyl)decyl	n.d. <sup>b</sup>	n.d.	n.d.	n.d.	n.d.
<b>Sub-total MSalkyl</b>		<b>3.03±1.01</b>	<b>0.45±0.70</b>	<b>2.67±0.20</b>	<b>1.93±2.46</b>	<b>0.01±0.00</b>
4	Allyl	9.26±0.82	5.55±4.55	8.18±0.56	7.17±6.04	0.53±0.02
8	3-Butenyl	61.60±26.64	46.83±13.98	33.04±3.10	46.84±25.18	8.03±0.54
13	4-Pentenyl	0.05±0.01	0.10±0.02	0.05±0.00	0.08±0.04	0.01±0.00
<b>Sub-total alkenyl</b>		<b>70.91±22.44</b>	<b>52.47±18.48</b>	<b>41.27±2.99</b>	<b>54.09±31.13</b>	<b>8.57±0.45</b>
2	( <i>R</i> )-2-OH-3-Butenyl	3.20±3.64	2.81±3.94	7.81±0.66	6.78±7.68	0.04±0.00
7	2-OH-4-Pentenyl	n.d.	0.62±0.42	n.d.	0.27±0.30	0.15±0.01
<b>Sub-total OH-alkenyl</b>		<b>3.20±2.97</b>	<b>3.43±3.54</b>	<b>7.81±0.54</b>	<b>7.06±7.41</b>	<b>0.19±0.01</b>
27	Sinapoyl-3-butenyl or isomer	0.05±0.04	1.93±1.42	n.d.	0.94±0.88	1.79±0.23
29	Sinapoyl-3-butenyl or isomer	0.95±0.40	34.06±24.43	0.41±0.04	14.12±13.60	24.95±2.44
30	Sinapoyl-3-butenyl or isomer	0.07±0.06	1.26±0.88	n.d.	0.79±1.01	1.52±0.34
<b>Sub-total sinapoyl alkenyl or isomer</b>		<b>1.06±0.41</b>	<b>37.26±26.73</b>	<b>0.41±0.03</b>	<b>15.85±15.42</b>	<b>28.26±1.90</b>
16	Pentyl or isomer	0.14±0.01	0.44±0.21	0.03±0.01	0.20±0.09	0.08±0.00
23	Hexyl or isomer	0.27±0.04	0.29±0.57	0.41±0.02	0.50±0.58	n.d.
<b>Sub-total alkyl</b>		<b>0.41±0.03</b>	<b>0.72±0.40</b>	<b>0.44±0.01</b>	<b>0.70±0.54</b>	<b>0.08±0.00</b>
<b>Total aliphatic</b>		<b>79.77±24.05</b>	<b>96.99±14.87</b>	<b>56.96±4.06</b>	<b>82.90±29.31</b>	<b>37.38±2.49</b>
14	Benzyl	0.01±0.00	0.33±0.19	0.03±0.01	0.17±0.14	0.07±0.01
20	Phenethyl	0.04±0.04	0.06±0.02	0.27±0.05	0.17±0.17	0.01±0.00
5	<i>p</i> -OH-Benzyl	n.d.	0.08±0.05	n.d.	n.d.	0.02±0.01
26	Sinapoyl- <i>p</i> -OH-benzyl or isomer	n.d.	n.d.	n.d.	n.d.	n.d.
18	Possible C <sub>8</sub> H <sub>9</sub> O	n.d.	n.d.	n.d.	n.d.	n.d.
<b>Total benzenic</b>		<b>0.06±0.04</b>	<b>0.47±0.26</b>	<b>0.30±0.04</b>	<b>0.34±0.13</b>	<b>0.10±0.01</b>
17	Indol-3-ylmethyl (I3M)	0.09±0.02	0.90±0.33	1.50±0.14	1.34±1.59	0.17±0.01
9	4-OH-I3M	0.25±0.13	0.48±0.67	0.40±0.06	0.40±0.55	0.04±0.01
24	1-OCH <sub>3</sub> -I3M	0.17±0.10	2.51±0.46	3.57±0.41	4.09±1.90	0.25±0.02
22	4-OCH <sub>3</sub> -I3M	0.13±0.06	2.78±1.10	3.63±0.51	4.90±2.43	1.19±0.09
31	Salicyloxy (or isomer)-I3M	n.d.	n.d.	n.d.	n.d.	n.d.
<b>Total indolic</b>		<b>0.64±0.18</b>	<b>6.68±1.81</b>	<b>9.11±0.99</b>	<b>10.75±5.67</b>	<b>1.65±0.11</b>
<b>Total GSLs</b>		<b>80.47±24.19</b>	<b>104.18±15.64</b>	<b>66.45±5.00</b>	<b>94.06±33.20</b>	<b>39.13±2.54</b>

<sup>a</sup> Details of the tentative annotation of the peaks follow Table S2.1.

<sup>b</sup> n.d. peak not detected.

#### 2.8.4. Supplementary references

1. Baenas, N.; Moreno, D. A.; Garcia-Viguera, C., Selecting sprouts of Brassicaceae for optimum phytochemical composition. *J. Agric. Food Chem.* **2012**, *60*, 11409-20.
2. Fabre, N.; Poinot, V.; Debrauwer, L.; Vigor, C.; Tulliez, J.; Fourasté, I.; Moulis, C., Characterisation of glucosinolates using electrospray ion trap and electrospray quadrupole time-of-flight mass spectrometry. *Phytochem. Anal.* **2007**, *18*, 306-319.
3. Maldini, M.; Foddai, M.; Natella, F.; Petretto, G. L.; Rourke, J. P.; Chessa, M.; Pintore, G., Identification and quantification of glucosinolates in different tissues of *Raphanus raphanistrum* by liquid chromatography tandem-mass spectrometry. *J. Food Compos. Anal.* **2017**, *61*, 20-27.
4. Agerbirk, N.; Olsen, C. E.; Cipollini, D.; Ørgaard, M.; Linde-Laursen, I.; Chew, F. S., Specific glucosinolate analysis reveals variable levels of epimeric glucobarbarins, dietary precursors of 5-phenyloxazolidine-2-thiones, in watercress types with contrasting chromosome numbers. *J. Agric. Food Chem.* **2014**, *62*, 9586-9596.
5. Rochfort, S. J.; Trenerry, V. C.; Imsic, M.; Panozzo, J.; Jones, R., Class targeted metabolomics: ESI ion trap screening methods for glucosinolates based on MSn fragmentation. *Phytochemistry* **2008**, *69*, 1671-9.
6. Kokkonen, P. S.; van der Greef, J.; Niessen, W. M. A.; Tjaden, U. R.; ten Hove, G. J.; van de Werken, G., Identification of intact glucosinolates using direct coupling of high-performance liquid chromatography with continuous-flow frit fast atom bombardment tandem mass spectrometry. *Biol. Mass Spectrom.* **1991**, *20*, 259-267.
7. Velasco, P.; Francisco, M.; Moreno, D. A.; Ferreres, F.; Garcia-Viguera, C.; Cartea, M. E., Phytochemical fingerprinting of vegetable *Brassica oleracea* and *Brassica napus* by simultaneous identification of glucosinolates and phenolics. *Phytochem. Anal.* **2011**, *22*, 144-52.
8. Kushad, M. M.; Brown, A. F.; Kurilich, A. C.; Juvik, J. A.; Klein, B. P.; Wallig, M. A.; Jeffery, E. H., Variation of glucosinolates in vegetable crops of *Brassica oleracea*. *J. Agric. Food Chem.* **1999**, *47*, 1541-8.
9. He, H., *Studies for Growth Adaptation and Identification of Glucosinolates on Chinese Brassicas*. Herbert Utz Verlag GmbH: München, **1999**.
10. Olsen, C. E.; Huang, X.-C.; Hansen, C. I. C.; Cipollini, D.; Ørgaard, M.; Matthes, A.; Geu-Flores, F.; Koch, M. A.; Agerbirk, N., Glucosinolate diversity within a phylogenetic framework of the tribe *Cardamineae* (Brassicaceae) unraveled with HPLC-MS/MS and NMR-based analytical distinction of 70 desulfoglucosinolates. *Phytochemistry* **2016**, *132*, 33-56.
11. Pfalz, M.; Mukhaimar, M.; Perreau, F.; Kirk, J.; Hansen, C. I. C.; Olsen, C. E.; Agerbirk, N.; Kroymann, J., Methyl transfer in glucosinolate biosynthesis mediated by indole glucosinolate O-methyltransferase 5. *Plant Physiol.* **2016**, *172*, 2190-2203.
12. Bianco, G.; Agerbirk, N.; Losito, I.; Cataldi, T. R., Acylated glucosinolates with diverse acyl groups investigated by high resolution mass spectrometry and infrared multiphoton dissociation. *Phytochemistry* **2014**, *100*, 92-102.
13. Reichelt, M.; Brown, P. D.; Schneider, B.; Oldham, N. J.; Stauber, E.; Tokuhisa, J.; Kliebenstein, D. J.; Mitchell-Olds, T.; Gershenzon, J., Benzoic acid glucosinolate esters and other glucosinolates from *Arabidopsis thaliana*. *Phytochemistry* **2002**, *59*, 663-71.
14. Linscheid, M.; Wendisch, D.; Strack, D., The structures of sinapic acid esters and their metabolism in cotyledons of *Raphanus sativus*. *Z. Naturforsch. C* **1980**, *35*, 907.
15. Lee, S.; Kaminaga, Y.; Cooper, B.; Pichersky, E.; Dudareva, N.; Chapple, C., Benzoylation and sinapoylation of glucosinolate R-groups in *Arabidopsis*. *Plant J* **2012**, *72*, 411-422.

16. Kjær, A., Thomsen, H., Gluconorcappasalin, a thioglucoside producing 5-oxoheptyl isothiocyanate on enzymatic hydrolysis. *Acta Chem. Scand.* **1963**, *17*, 561-562.
17. Kjær, A.; Schuster, A., Glucosinolates in *Erysimum hieracifolium* L.; There new, naturally occurring glucosinolates. *Acta Chem. Scand.* **1970**, *24*, 1631-1638.
18. Agerbirk, N.; Olsen, C. E.; Heimes, C.; Christensen, S.; Bak, S.; Hauser, T. P., Multiple hydroxyphenethyl glucosinolate isomers and their tandem mass spectrometric distinction in a geographically structured polymorphism in the crucifer *Barbarea vulgaris*. *Phytochemistry* **2015**, *115*, 130-142.
19. Agerbirk, N.; Olsen, C. E.; Nielsen, J. K., Seasonal variation in leaf glucosinolates and insect resistance in two types of *Barbarea vulgaris* ssp. *arcuata*. *Phytochemistry* **2001**, *58*, 91-100.
20. Pfalz, M.; Mikkelsen, M. D.; Bednarek, P.; Olsen, C. E.; Halkier, B. A.; Kroymann, J., Metabolic engineering in *Nicotiana benthamiana* reveals key enzyme functions in *Arabidopsis* indole glucosinolate modification. *Plant Cell* **2011**, *23*, 716-29.

---

## Simultaneous analysis of glucosinolates and isothiocyanates by RP-UHPLC-ESI-MS<sup>n</sup>

---

A new method to simultaneously analyze various glucosinolates (GSLs) and isothiocyanates (ITCs) by RP-UHPLC-ESI-MS<sup>n</sup> has been developed and validated for 14 GSLs and 15 ITCs. It involved derivatization of ITCs with *N*-acetyl-L-cysteine (NAC). The limits of detection were 0.4–1.6  $\mu\text{M}$  for GSLs and 0.9–2.6  $\mu\text{M}$  for NAC-ITCs. The analysis of *Sinapis alba*, *Brassica napus*, and *B. juncea* extracts spiked with 14 GSLs and 15 ITCs indicated that the method generally had good intra- ( $\leq 10\%$  *RSD*) and inter-day precisions ( $\leq 16\%$  *RSD*). Recovery of the method was unaffected by the extracts and within 71–110% for GSLs and 66–122% for NAC-ITCs. The method was able to monitor the enzymatic hydrolysis of standard GSLs to ITCs in mixtures. Furthermore, GSLs and ITCs were simultaneously determined in Brassicaceae plant extracts before and after myrosinase treatment. This method can be applied to further investigate the enzymatic conversion of GSLs to ITCs in complex mixtures.

**Keywords:** breakdown product, dithiocarbamate, glucosinolate, LC-MS analysis, mustard, thioglucosidase, validation

### 3.1. Introduction

Glucosinolates (GSLs) are widely distributed in all plant tissues within the Brassicaceae family. They play an important role to defend the plants against pathogen and insect attacks.<sup>1</sup> This defense system is assisted by myrosinase. Just like GSLs, myrosinase is found in all tissues of Brassicaceae plants, but it is located in different cells.<sup>2</sup> Myrosinase gets in contact with GSLs when the plant tissues are damaged.<sup>3</sup> In an environment of pH 5-7, this interaction mostly yields the conversion of GSLs into microbiologically active isothiocyanates (ITCs) (**Figure 3.1A**).<sup>4-6</sup> Previous studies reported that depending on the structure, ITCs could inhibit the growth of fungi and bacteria pathogenic to plants<sup>7,8</sup> and humans<sup>9-11</sup>. This underlines the potential of ITCs as a new class of plant-derived antimicrobial compounds.

The chemical diversity of GSLs, imparted by various side chains (R-group), determines which ITCs can be formed.<sup>12</sup> In general, the R-group can be an aliphatic, benzenic, or indolic group. Based on the type of R-group, GSLs and ITCs can be classified at least into 8 and 7 subclasses, respectively (**Table 3.1**). ITCs have one subclass less, because those with an indole R-group are unstable.<sup>13</sup> Although ITCs share the R-group of GSLs, ITCs have a completely different core structure than GSLs (**Figure 3.1A**). Consequently, ITCs and GSLs have different volatility and ionization ability, making simultaneous analysis difficult. Therefore, GSLs and ITCs have frequently been analyzed separately by mainly liquid chromatography (LC) and gas chromatography (GC).<sup>14</sup>

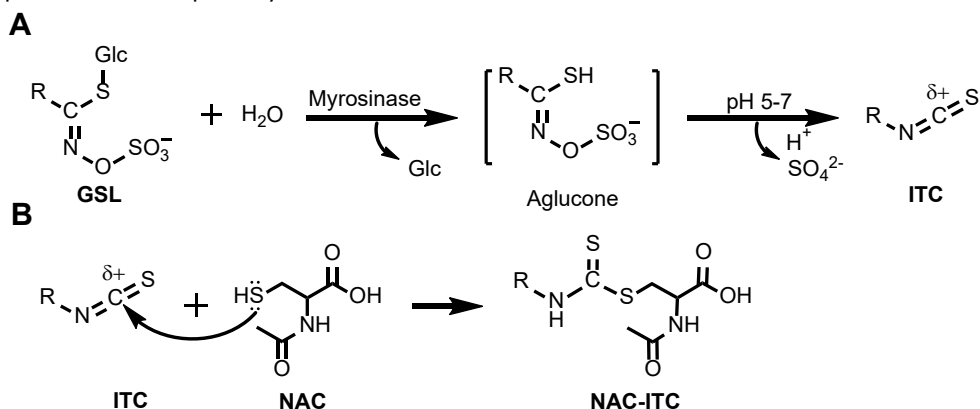
GSLs are highly polar because of a thioglucosyl group (–SGlc) and a strong acid residue (SO<sub>4</sub><sup>2-</sup>). The latter causes GSLs to be spontaneously ionized as an anion. Removal of the strong acid residue, i.e. desulfation, is often required in various LC-MS methods.<sup>15-19</sup> However, this step could result in incomplete desulfation, self-dimerisation, and self-degradation.<sup>20-22</sup> LC-MS methods for direct quantitative analysis of individual intact GSLs without desulfation were developed.<sup>23-26</sup> However, efficient LC-MS analysis of intact GSLs was historically challenging<sup>27</sup> and most methods included only few GSLs and do not cover the analysis of ITCs.

The volatility of ITCs makes GC a convenient technique for ITC analysis. However, several ITCs were thermally unstable. Allyl ITC (AITC) and 4-(methylsulfinyl)butyl ITC (4-MSITC) were transformed into allyl thiocyanate and 3-butenyl ITC (BuITC), respectively, in the GC injection port.<sup>28,29</sup> LC analysis of ITCs was developed previously employing derivatization with thiol compounds, which can overcome the limitation of GC analysis.<sup>30-32</sup> In particular, Pilipczuk *et al.*<sup>31</sup> successfully developed an LC-MS method to quantify various individual ITCs derivatized with *N*-acetyl-L-cysteine (NAC), a safe derivatization reagent. This derivatization allowed the ionization of ITCs, while keeping their R-groups intact (**Figure 3.1B**). However, this LC-MS method did not cover the analysis of GSLs.



Tsao *et al.*<sup>33</sup> developed a method to simultaneously analyze allyl GSL (AGSL) and AITC by using HPLC with UV detection at 228 nm for AGSL and 242 nm for AITC. This method is, however, not suitable for analyzing GSLs in a mixture because many compounds absorb at 228 nm. Franco *et al.*<sup>34</sup> developed a simultaneous method for specific pairs of GSLs/ITCs, without pre-column derivatization, by using RP-HPLC-ESI-MS/MS. This method was applicable to analyze the compounds in complex matrices, however, it was only evaluated for 4-(methylsulfinyl)butyl GSL/ITC and 4-(methylthio)butyl GSL/ITC. Another HPLC-based method developed to simultaneously analyze GSLs and ITCs was also evaluated only for few pairs, e.g. allyl GSL/ITC, phenyl GSL/ITC, and benzyl GSL/ITC.<sup>35</sup> Moreover, one study described simultaneous analysis of only few pairs of GSLs/ITCs by another separation technique, namely capillary electrophoresis micellar electrokinetic chromatography (CE-MEKC).<sup>36</sup> Altogether, to date there is no method which has been evaluated to analyze many more GSLs and ITCs in complex mixtures in a single analytical run.

In this study, we aimed at developing and validating an LC-MS method which can simultaneously analyze various GSLs and ITCs in complex mixtures. Derivatization of ITCs with NAC was included in the method to enhance the ionization ability of ITCs.<sup>31</sup> The method would enable to monitor the *in vitro* enzymatic hydrolysis of GSLs and the formation of ITCs in standard mixtures and plant extracts upon myrosinase treatment.



**Figure 3.1.** Conversion of GSL to ITC by myrosinase at pH 5-7 (**A**) and derivatization reaction of ITC with NAC (**B**). Carbon atom in the ITC functional group is electrophilic.

## 3.2. Materials and methods

### 3.2.1. Standard compounds and other chemicals

Authentic standards of 14 GSLs listed in **Table 3.1** were purchased from Phytolab GmbH & Co (Vestenbergsgreuth, Germany). Authentic standards of 9 ITCs (with peak numbers in boldface according to **Table 3.1**): 3-(methylsulfinyl)propyl ITC (3-MSITC, **11**), 4-(methylsulfinyl)butyl ITC (4-MSITC, **12**), 6-(methylsulfinyl)hexyl

ITC (6-MSITC, **13**), 9-(methylsulfinyl)nonyl ITC (9-MSITC, **14**), 4-(methylsulfinyl)-3-butenyl ITC (4-MS-3-en-ITC, **15**), 3-(methylsulfonyl)propyl ITC (3-MSOITC, **16**), 3-(methylthio)propyl ITC (3-MTITC, **17**), 4-(methylthio)butyl ITC (4-MTITC, **18**), and 5-(methylthio)pentyl ITC (5-MTITC, **19**) were purchased from Abcam (Cambridge, UK). Authentic standards of the other 6 ITCs: propyl ITC (PITC, **110**), allyl ITC (AITC, **111**), 3-butenyl ITC (BuITC, **112**), 4-pentenyl ITC (PeITC, **114**), benzyl ITC (BITC, **115**), and phenethyl ITC (PhEITC, **117**) were purchased from Sigma-Aldrich (St. Louis, MO, U.S.A.) or Merck (Darmstadt, Germany). Authentic standard of NAC-4-MSITC was purchased from Cayman Chemical (Ann Arbor, MI, U.S.A.). Authentic standards of NAC-BITC and NAC-PhEITC were purchased from Abcam (Cambridge, UK).

NAC, NaOH, KH<sub>2</sub>PO<sub>4</sub>, myrosinase, *n*-hexane, and *tert*-butanol were purchased from Sigma-Aldrich (St. Louis, MO, U.S.A.) or Merck (Darmstadt, Germany). DMSO was purchased from Duchefa Biochemie (Haarlem, The Netherlands). Isopropanol (IPA) (ULC/MS grade), acetonitrile (ACN) acidified with 0.1% (v/v) formic acid (FA) (ULC/MS grade), water acidified with 0.1% (v/v) FA (ULC/MS grade), and methanol (MeOH) (ULC/MS grade) were purchased from Biosolve BV (Valkenswaard, The Netherlands). High purity water was produced in-house using a Milli-Q A10 Gradient system (18.2 MΩ.cm, 3 ppb TOC) (Merck Millipore, Darmstadt, Germany).

### **3.2.2. Plant materials**

Seeds of *Sinapis alba* (yellow mustard 'Emergo', 393810), *Brassica napus* ('Helga', 392600), and *B. juncea* var. *rugosa rugosa* (Chinese mustard/amsol, 160400) were purchased from Vreeken's Zaden (Dordrecht, The Netherlands, <https://www.vreeken.nl/>). *B. juncea* var. *rugosa rugosa* is referred to as *B. juncea* in the following text.

### **3.2.3. Preparation of stock solutions of GSLs, ITCs, and NAC**

Stock solutions (5 mM) of GSLs and ITCs were prepared in phosphate buffer pH 7 (0.1 M) and in IPA, respectively. All standard GSLs and ITCs were weighed on a Mettler XP6 microbalance (Mettler-Toledo International Inc., U.S.A.). Stock solutions were kept at -20 °C before use. A stock solution of NAC (100 mM) was freshly prepared in phosphate buffer pH 7.0 (0.1 M).

### **3.2.4. Extraction of GSLs from Brassicaceae seeds**

Ground seeds of *S. alba*, *B. napus*, and *B. juncea* were extracted in a SpeedExtractor E-916 (Büchi, Flawil, Switzerland) by using absolute methanol at 65 °C as described in previous study.<sup>37</sup> Afterwards, the extract was evaporated under reduced pressure (Syncore Polyvap, Büchi), resolubilized in *tert*-butanol, and freeze-dried. The dried extracts were stored at -20 °C.

**Table 3.1.** GSLs and ITCs in the study.

Subclass	Structure of R-group	(Semi)systematic name of R-group	Abbreviation of GSL or ITC	Trivial name of GSL or ITC	Code <sup>a</sup>	Retention time (tR, min)
Aliphatic (Methylsulfinyl)alkyl		3-(Methylsulfinyl)propyl	3-MSGSL 3-MSITC	Glucoliberin Iberin	<b>G1*</b> <b>I1*</b>	1.99 17.53
		4-(Methylsulfinyl)butyl	4-MSGSL 4-MSITC	Glucoraphanin Sulforaphane	<b>G2*</b> <b>I2*</b>	3.11 19.88
		5-(Methylsulfinyl)pentyl	5-MSGSL 5-MSITC	Glucosylsin Alysin	<b>G19</b> <b>I19</b>	4.37 23.44
		6-(Methylsulfinyl)hexyl	n.a. <sup>b</sup> 6-MSITC	n.a. Hesperin	- <b>I3*</b>	- 27.51
		9-(Methylsulfinyl)nonyl	n.a. 9-MSITC	n.a. 9-(Methylsulfinyl)nonyl ITC	n.a. <b>I4*</b>	- 36.53
		4-(Methylsulfinyl)-3-butenyl	4-MS-3-en-GSL 4-MS-3-en-ITC	Glucoraphenin Sulforaphene	<b>G5*</b> <b>I5*</b>	3.36 20.44
		3-(Methylsulfonyl)propyl	3-MSoGSL 3-MSoITC	Glucoscheiroin Cheiroin	<b>G6*</b> <b>I6*</b>	2.33 19.60
		3-(Methylthio)propyl	3-MTGSL 3-MTITC	Glucoliberin Iberin	<b>G7</b> <b>I7*</b>	12.60 32.49
		4-(Methylthio)butyl	4-MTGSL 4-MTITC	Glucoscheiroin Erucin	<b>G8*</b> <b>I8*</b>	15.08 35.78
		5-(Methylthio)pentyl	5-MTGSL 5-MTITC	Glucoscheiroin Berteroin	<b>G9*</b> <b>I9*</b>	18.73 39.15
		Propyl	n.e. <sup>c</sup> PITC	n.e. Propyl ITC	- <b>I10*</b>	- 29.04
		2-Propenyl (Allyl)	AGSL AITC	Sinigrin Allyl ITC	<b>G11*</b> <b>I11*</b>	2.90 25.87
		3-Butenyl	BuGSL BuITC	Glucoscheiroin 3-Butenyl ITC	<b>G12*</b> <b>I12*</b>	7.82 31.66
Alkyl						
Alkenyl						

Subclass	Structure of R-group	(Semi)systematic name of R-group	Abbreviation of GSL or ITC	Trivial name of GSL or ITC	Code <sup>a</sup>	Retention time (t <sub>R</sub> , min)
Hydroxy-alkenyl		4-Pentenyl	PeGSL PeITC	Glucobrassicinapin 4-Pentenyl ITC	<b>G14*</b> <b>I14*</b>	14.05 36.04
		2-Hydroxy-3-butenyl	2-OH-BuGSL n.e.	Progoitrin n.e.	<b>G13*</b> -	2.67 -
		2-Hydroxy-4-pentenyl	2-OH-PeGSL n.e.	Gluconapoleiferin n.e.	<b>G20</b> -	9.30 -
Benzenic		Benzyl	BGSL BITC	Glucotropaeolin Benzyl ITC	<b>G15*</b> <b>I15*</b>	14.72 36.53
		Phenethyl	PhEGSL PhEITC	Gluconasturtiin Phenethyl ITC	<b>G17*</b> <b>I17*</b>	18.54 39.38
		<i>p</i> -Hydroxybenzyl	<i>p</i> -OH-BGSL <i>p</i> -OH-BITC	Glucosinalbin <i>p</i> -Hydroxy-benzyl ITC	<b>G16*</b> <b>I16</b>	3.83 30.15
Indolic		Indole-3-ylmethyl	I3MGSL n.e.	Glucobrassicin n.e.	<b>G18*</b> -	16.59 -

<sup>a</sup> Codes in the chromatograms for GSLs start with **G** and for ITCs (analyzed as NAC-ITCs) start with **I**. Asterisk (\*) is to indicate that the authentic standard was available in the study.

<sup>b</sup> n.a. refers to GSLs or ITCs which were not available in this study.

<sup>c</sup> n.e. refers to GSLs or ITCs which have never been reported.

### 3.2.5. Derivatization of ITCs with NAC

Four different experiments were carried out in which NAC was combined with (i) standard mixtures of 14 GSLs and 15 ITCs, (ii) plant extracts spiked with mixtures of 14 GSLs and 15 ITCs, (iii) a mixture of standard GSLs and myrosinase, and (iv) mixtures of plant extracts and myrosinase.

(i) Derivatization experiments of the mixtures of standard ITCs and GSLs were performed for making calibration curves of each ITC and GSL, to evaluate the linearity range, to determine *LOD* and *LOQ*, and to quantify GSLs and ITCs in the samples. NAC was added into the mixtures of 14 GSLs and 15 ITCs. The final molar concentration of NAC was 5 times higher than that of total ITCs. IPA was added to the mixtures to a concentration of 25% (v/v), in which both GSLs and ITCs were soluble (**Figure S3.1**). During preparation, all solutions were kept in an ice bath. All reaction mixtures were incubated at 50 °C for 2 h with constant mixing at 900 rpm. Then, the samples were chilled and analyzed by RP-UHPLC-MS. The completeness of the derivatization after 2 h incubation was established for 4-MSITC, BITC, and PhEITC by comparing the amount of NAC derivatives, which were formed, to that of their respective standards (NAC-4-MSITC, NAC-BITC, and NAC-PhEITC) (**Figure S3.2**). Based on this, it was assumed that the derivatization of the 12 other ITCs was also completed in 2 h.

(ii) Derivatization experiments of extracts spiked with mixtures of 14 GSLs and 15 ITCs were performed for evaluating the applicability of the method for analyzing GSLs and NAC-ITCs in extracts, in terms of precision and recovery. The approach described earlier was applied in which a mixture of 14 GSLs and 15 ITCs was added to *S. alba*, *B. napus*, and *B. juncea* seed extracts. Two final concentrations at the mid-levels of calibration range for each GSL and ITC were applied, i.e. 10 µM and 30 µM. Therefore, the final concentrations of NAC were 0.75 mM ( $5 \times 10 \mu\text{M} \times 15 \text{ ITCs}$ ) and 2.25 mM ( $5 \times 30 \mu\text{M} \times 15 \text{ ITCs}$ ), respectively. The final concentration of the extracts was 5 mg/mL prepared from the dried extracts solubilized in DMSO (final concentration of 5%) in phosphate buffer pH 7.0. The mixtures were conditioned in phosphate buffer pH 7.0 and incubated for 2 h at 50 °C with a constant mixing at 900 rpm. Dilution of extracts in phosphate buffer pH 7.0 was made for analyzing GSLs and ITCs present at a higher concentration than 60 µM (the upper limit of the calibration range).

(iii) Derivatization experiments of a mixture of standard GSLs and myrosinase, i.e. simultaneous enzymatic hydrolysis of GSLs and derivatization of ITCs, were performed for testing the applicability of the method to monitor the hydrolysis of GSLs and the formation of ITCs. The mixture of 14 standard GSLs (30 µM each) and myrosinase (0.01 U/mL, 1 unit of enzymatic activity was defined as the amount of enzyme that releases 1 µmol glucose per min with allyl GSL as the substrate, at pH 6.0 and 25 °C) were incubated in phosphate buffer pH 7.0 (0.1 M) at 50 °C in the presence of NAC (2.1 mM). GSLs and ITCs were monitored over time until all GSL peaks disappeared, and the intensity of all NAC-ITC peaks did not increase

anymore, i.e. up to 4 h. After incubation, IPA was added to a concentration of 25% (v/v), the samples were chilled and analyzed by RP-UHPLC-ESI-MS.

The GSL hydrolysis rates ( $\mu\text{M/h}$ ) were defined as the decrease of GSL concentration over the time and determined as the slope of the plot of GSL concentration ( $\mu\text{M}$ ) vs time (h). The NAC-ITC formation rates ( $\mu\text{M/h}$ ) were defined as the increase of NAC-ITC concentration over the time and determined as the slope of the plot of NAC-ITC concentration ( $\mu\text{M}$ ) vs time (h).

(iv) Derivatization experiments of mixtures of Brassicaceae seed extracts and myrosinase were performed with the same incubation as before to test the applicability of the method to analyze GSLs and ITCs in plant extracts upon myrosinase treatment and NAC derivatization. Shortly, the dried extracts were dissolved in DMSO and then 10 times diluted in phosphate buffer pH 7.0 (0.1 M). Plant extracts 5 mg/mL, myrosinase 0.05 U/mL, and NAC at 5  $\times$  estimated concentration of ITCs were incubated at 50 °C for 4 h, with a final concentration of DMSO of 5%. Under this condition all GSL peaks disappeared within 4 h (data not shown). The concentration of ITCs in *B. napus*, *B. juncea*, and *S. alba* seed extracts was estimated from the original GSL concentration analyzed previously<sup>37</sup>. Afterwards, IPA was added to a concentration of 25% (v/v). The samples were chilled and analyzed by RP-UHPLC-ESI-MS. When the concentration of GSLs and ITCs exceeded 60  $\mu\text{M}$  (the upper limit of the calibration range), they were diluted in phosphate buffer pH 7.0.

### **3.2.6. Simultaneous RP-UHPLC-MS<sup>n</sup> analysis of GSLs and NAC-ITCs**

Analysis of GSLs and NAC-ITCs was performed on an Accela ultra high performance liquid chromatography (UHPLC) system (Thermo Scientific, San Jose, CA, U.S.A.) equipped with a pump, autosampler, and photodiode array (PDA) detector. An LTQ Velos electron spray ionization (ESI) ion trap mass spectrometer (MS) (Thermo Scientific) was coupled to the LC system.

Sample (1  $\mu\text{L}$ ) was injected onto an Acquity UPLC-BEH shield RP18 column (2.1 mm i.d.  $\times$  150 mm, 1.7  $\mu\text{m}$  particle size; Waters, Milford, MA, U.S.A.) with an Acquity UPLC BEH shield RP18 VanGuard precolumn (2.1 mm i.d.  $\times$  5 mm, 1.7  $\mu\text{m}$  particle size; Waters). Water acidified with 0.1% (v/v) FA, eluent A, and ACN acidified with 0.1% (v/v) FA, eluent B, were used as solvent at a flow rate of 300  $\mu\text{L/min}$ . The temperature of the sample tray was controlled at 4 °C to prevent further reaction. Different column oven temperatures were tested: 25 °C, 35 °C, and 45 °C. The PDA detector was set to monitor absorption at 200-400 nm. The elution gradient used was: 0-6.7 min, isocratic on 0% (v/v) B; 6.7-12.5 min, linear gradient to 8% B; 12.5-24.2 min, linear gradient from 8 to 16% B; 24.2-41.8 min, linear gradient from 16 to 40% B; 41.8-43.5 min, linear gradient from 40 to 100% B; 43.5-50.5 min, isocratic on 100% B; 50.5-52 min, linear gradient from 100% to 0% B; 52-59 min, isocratic on 0% B.

Mass spectrometric analysis was performed on an LTQ Velos equipped with a heated ESI-MS probe coupled to RP-UHPLC. The spectra were acquired in an  $m/z$  (mass to charge ratio) range of 92-1,000 Da in both positive (PI) and negative ionization (NI) modes. The PI mode was used only for identification of NAC-ITCs to complement the data from NI mode. Data-dependent MS<sup>n</sup> analysis was performed on the most intense (product) ion with normalized collision energy of 35%. Nitrogen was used as sheath and auxiliary gas. The ion transfer tube temperature was 300 °C, and the source voltage was 4.0 kV (PI) or 4.5 kV (NI).

The identification and quantification of peaks were performed in Xcalibur (v.2.2, Thermo Scientific). The identification was based on UV and MS spectra. GSLs were detected in NI and their fragmentation pattern referred to Andini *et al.*<sup>37</sup> NAC-ITCs have UV<sub>max</sub> at 268 nm and were detected in NI and PI modes. The diagnostic fragment ion for NAC-ITCs was [NAC-H]<sup>-</sup> ( $m/z$  162, the most abundant) in NI mode and [NAC+H]<sup>+</sup> ( $m/z$  164, >15% abundance) in PI mode. The quantification of GSLs and NAC-ITCs was based on the response in NI mode. The quantification of 3-(methylthio)propyl GSL (3-MTGSL), 5-(methylsulfinyl)pentyl GSL (5-MSGSL), 2-hydroxy-4-pentenyl GSL (2-OH-PeGSL), 5-(methylsulfinyl)pentyl ITC (5-MSITC), and *p*-hydroxybenzyl ITC (*p*-OH-BITC) (i.e. the compounds without standards) was performed by using the calibration equation of the standard GSL or ITC from the same subclass with the closest structural resemblance and molecular weight (**Table S3.1**).

### 3.2.7. Linearity of the Calibration Curves

Calibration series of 14 GSLs and 15 ITCs (i.e. NAC-ITCs) were prepared at concentrations 2 μM (for GSLs) or 3 μM (for ITCs) to 60 μM. The calibration curves, consisting of 8 data points, were obtained by plotting concentration versus NI-MS chromatographic peak area of the analyte at  $m/z$  of its molecular ion. The linearity of the calibration curves was indicated by the coefficient of determination ( $R^2$ ).

### 3.2.8. Limits of Detection and Quantification

The limit of detection ( $LOD$ ) were determined from the calibration curves.<sup>38</sup> The  $LOD$  is the smallest concentration of analyte in the test sample that can be reliably distinguished from zero.<sup>39</sup> Root mean square error (RMSE) approach was applied to calculate  $LOD$ . According to Bernal & Guo<sup>38</sup> this approach uses both the variability of the blank and of the measurement values. The following formulas were used to calculate the  $LOD$ ,

$$LOD = \frac{3.3 RMSE}{a} \quad (3.1)$$

$$RMSE = \left( \frac{\sum_{i=1}^n (y - y(x))^2}{n - 2} \right)^{0.5} \quad (3.2)$$

where  $RMSE$  is the residual standard deviation of the calibration curve,  $a$  is the slope of the calibration curve,  $y$  is the measured peak area,  $y(x)$  is the theoretical peak area calculated from the calibration equation, and  $n$  is the number of

regression points. The  $LOD$  should meet the following two requirements: (i)  $LOD < C_{min}$ , and (ii)  $10 \times LOD > C_{min}$ . The limit of quantification ( $LOQ$ ) was calculated according to Pilipczuk *et al.* and FDA.<sup>31,40</sup>

$$LOQ = 3 \times LOD \quad (3.3)$$

### 3.2.9. Precision

For the standard mixtures of 14 GSLs and 15 ITCs, the intra-day precision was determined by replicate analysis ( $n = 3$ ) at five concentrations ranging from 5 to 50  $\mu\text{M}$  in one day. The inter-day precision was determined by replicate analysis in three separate days ( $n = 3$ ). The standard mixtures were subjected to the NAC-derivatization. The intra- and inter-day precisions for the standard mixtures were expressed as percentage of overall relative standard deviation (%  $RSD$ ) of the NI-MS chromatographic peak areas of the analytes. The overall precisions (%  $RSD$ ) were calculated using **Eq. 3.4**, where  $RSD_i$  (%) is  $RSD$  (i.e. coefficient of variation, CV) for the  $i$ -th concentration point, and  $n$  is the number of calibration points.<sup>31</sup>

For the spiked extracts of *S. alba*, *B. napus*, and *B. juncea*, the intra- and inter-day precisions were determined simultaneously: 2 replicates in day 1 and another 2 replicates in day 2. The extracts were spiked with a mixture of 14 GSLs and 15 ITCs (each analyte at 30  $\mu\text{M}$ ). The spiked extracts were subjected to the NAC-derivatization. The intra- and inter-day precisions for the spiked extracts were expressed as percentage of overall relative standard deviation (%  $RSD$ ) of the concentrations of the spiked analytes and evaluated simultaneously by one-way ANOVA.<sup>40, 41</sup>

$$RSD = \sqrt{\frac{1}{n} \sum_{i=1}^n RSD_i^2} \quad (3.4)$$

### 3.2.10. Recovery

To further evaluate the applicability of the method for analyzing extracts, recovery was determined by analyzing the three different Brassicaceae seed extracts (i.e. *S. alba*, *B. napus*, and *B. juncea*), spiked with 14 GSL and 15 ITC standards (each at two levels: 10  $\mu\text{M}$  and 30  $\mu\text{M}$ ), derivatized with NAC. Recovery (%) was calculated as

$$R (\%) = \frac{x_{spiked} - x_{unspiked}}{x_{ref}} \times 100 \quad (3.5)$$

where  $x_{spiked}$  was the measured concentration of the analyte in the spiked experiment,  $x_{unspiked}$  was the measured concentration of the analyte in the unspiked experiment, and  $x_{ref}$  was the true concentration which was spiked to the extract. Four repetitions were performed.

According to FDA<sup>40</sup>, a good recovery for the working analyte concentrations in this study should be between 80-110%. To test whether the recovery was within the range, the recovery whose average outside the range was statistically



evaluated by analysis of variance (ANOVA) one-sample t-test using IBM SPSS Statistic v.23 software (SPSS Inc., Chicago, IL, U.S.A.).

### 3.3. Results and discussion

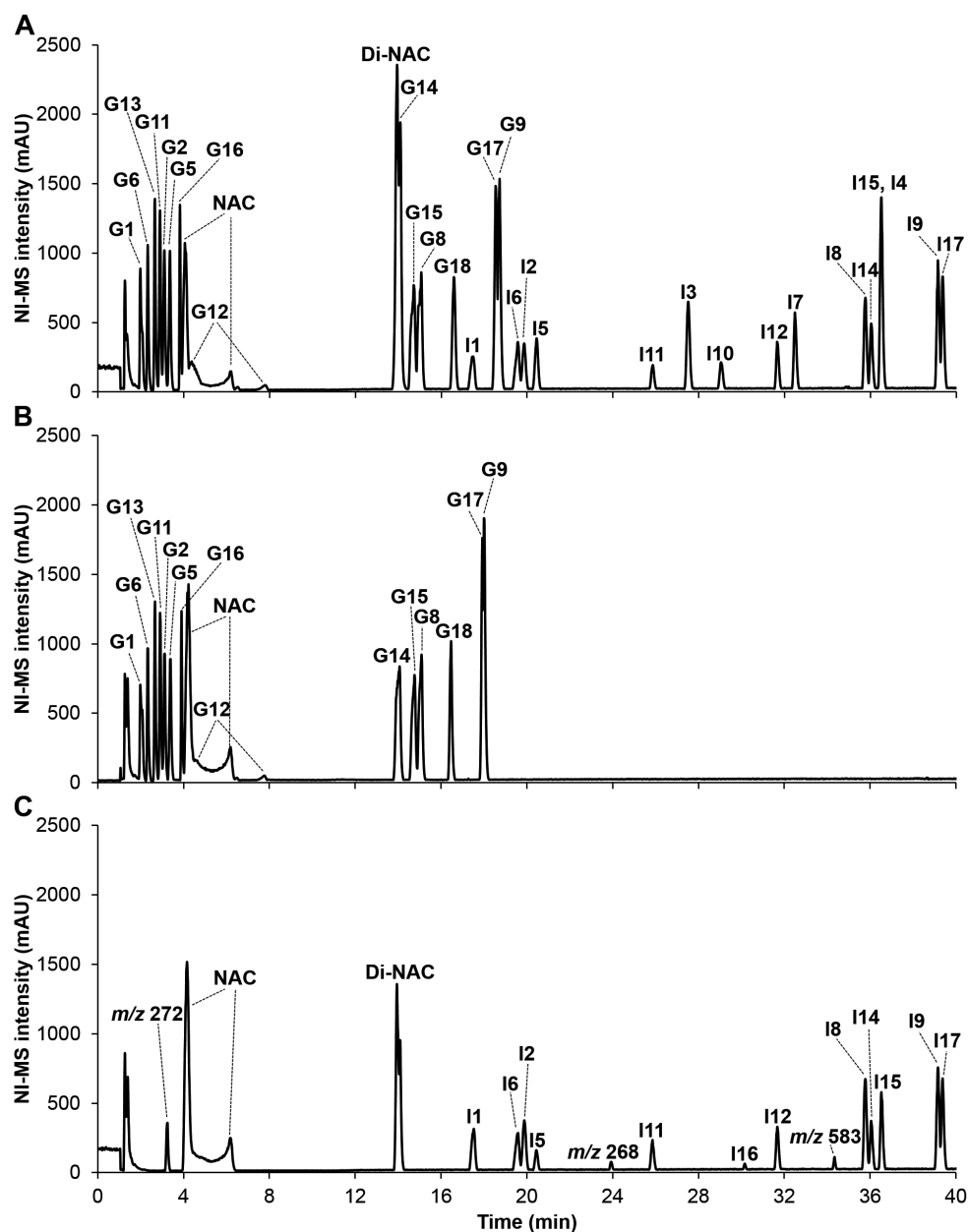
#### 3.3.1. Development of RP-UHPLC-PDA-ESI-MS<sup>n</sup> method for GSL and ITC analysis

Simultaneous quantitative analysis of different GSLs and ITCs was performed using RP-UHPLC-PDA-ESI-MS<sup>n</sup>. The method included derivatization of ITCs with NAC, which was based on the method developed by Pilipczuk *et al.*,<sup>31</sup> enabling detection of ITCs in MS. The method of Pilipczuk *et al.*<sup>31</sup> was modified to also enable analysis of very polar GSLs.

To ensure a good separation of the very polar GSLs, two important parameters were optimized. First was the column oven temperature as it influences the elution; the lower the temperature, the more delay in elution, which benefits the separation of polar compounds. Three different column oven temperatures, i.e. 25 °C, 35 °C, and 45 °C, were tested. At column oven temperature of 25 °C sharp peaks were obtained and the seven most polar GSLs (**G1**, **G6**, **G13**, **G11**, **G2**, **G5**, and **G16**), which were eluted within 5 min, were separated (**Figure 3.2A**). Column oven temperature of 25 °C was also applied in previous research analyzing intact GSLs by LC-ESI-MS.<sup>24</sup> In contrast, higher column oven temperatures, i.e. 35 °C and 45 °C, resulted in poor separation for these seven most polar GSLs (data not shown). Column oven temperatures lower than 25 °C might improve the separation, but as this would extend the analysis time and cause high backpressure, this was not further elaborated.

Secondly, the polarity of the solvent is important for analyzing both GSLs and NAC-ITCs. All GSLs are soluble in water, but not all NAC-ITCs are soluble in water. IPA has been found to be better than methanol and ethanol to dissolve ITCs.<sup>31</sup> Furthermore, to dissolve both GSLs and ITCs in one mixture, 25% (v/v) aqueous IPA was found to be a better solvent than IPA 50%. This was indicated by the elution profiles of representative GSLs and ITCs in both solvents shown in **Figure S3.1 (B, D vs C, E)**.

**Figure 3.2A** shows a good baseline separation of 15 NAC-ITC peaks (retention time, t<sub>R</sub>, of 17-40 min) in IPA 25%. Because quantification was based on the MS signal, co-elution (e.g. **I4** and **I15**) and partial peak overlap (e.g. **G15** and **G8**) did not affect the quantification, as the compounds have different *m/z*.



**Figure 3.2.** UHPLC-MS negative ion chromatograms of a mixture of 14 GSLs (each 30  $\mu$ M) and 15 ITCs (each 30  $\mu$ M) derivatized with NAC (2.25 mM) in 25% (v/v) aqueous IPA at 50  $^{\circ}$ C for 2 h (A); a mixture of 14 GSLs (each at 30  $\mu$ M), myrosinase, and NAC upon incubation at 50  $^{\circ}$ C at 0 h (B) and 4 h (C). The chromatograms refers to base peak chromatograms. The analyses were performed at a column oven temperature of 25  $^{\circ}$ C. G12 and NAC each appeared in two peaks, but the identification and quantification of the GSL were still feasible. The elution was depending on the solvent; in the absence of organic solvent, they were eluted as one peak (Figure S3.3).

### 3.3.2. Linearity of the calibration curves

The results of the regression analysis of 14 GSLs and 15 ITCs are listed in **Table 3.2**. Statistical analysis of the calibration data of GSL (2-60  $\mu\text{M}$ ) and ITC (3-60  $\mu\text{M}$ ) showed a high linearity ( $R^2 \geq 0.994$ ).

### 3.3.3. Limits of detection and quantification

All *LOD* and *LOQ* values are presented in **Table 3.2**. The *LOD* values for GSLs and ITCs were within a range of 0.4-2.6  $\mu\text{M}$ . With regard to GSL analysis, our LC-MS method has higher sensitivity than the method with CE-MEKC-UV (*LOD* up to 30  $\mu\text{M}$ )<sup>36</sup>, and this is in line with previous study using LC-MS method.<sup>34</sup> With regard to NAC-ITCs, our analytical protocol generated lower *LOD* values than those obtained by Pilipczuk *et al.*<sup>31</sup> (1.7-4.9  $\mu\text{M}$ ). The *LOQ* values of our method for GSLs and ITCs were within a range of 1.2-7.8  $\mu\text{M}$ . Overall, our new analytical method can be applied for quantification of GSLs and NAC-ITCs at low concentrations.

### 3.3.4. Precision

The intra-day and inter-day precisions of the developed method are displayed in **Table 3.2**. For the analyte concentration applied in our study, good intra-day and inter-day precisions should be  $\leq 10\%$  *RSD* and  $16\%$  *RSD*, respectively.<sup>40</sup>

For GSL analysis in the standard mixtures, the intra- and inter-day precisions of the method for all GSLs ( $\leq 8.9\%$  *RSD* and  $\leq 14.8\%$  *RSD*, respectively) complied with the FDA requirement.

For GSL analysis in the spiked extracts, the intra-day and inter-day precisions of most GSLs (0.6-10.0% *RSD* and 2.0-16.0% *RSD*, respectively) were within the permitted FDA range. PeGSL (**G14**) and *p*-OH-BGSL (**G16**) had lower intra- and inter-day precisions than the other GSLs in the three spiked extracts.

For NAC-ITC analysis in the standard mixtures, the intra- and inter-day precisions of the method (7.2-10.0% *RSD* and 10.8-16.0% *RSD*, respectively) complied with the FDA requirement for most ITCs. Only two ITCs had a slightly lower intra- and inter-day precision (up to 11.9% *RSD* and 17.9% *RSD*, respectively). The intra-day precision of 9 NAC-ITCs in a previous study was higher (1.8-5.0% *RSD*).<sup>31</sup> In our study the calibration series of NAC-ITCs was made from the NAC-derivatization of the authentic standards of ITCs, and not from the purified or authentic standard NAC-ITCs as in Pilipczuk *et al.*<sup>31</sup> Therefore, the intra-day precision obtained in our study reflected the variation not only of the actual LC-MS analysis, but also of the NAC-derivatization process.

For NAC-ITC analysis in the spiked extracts, the intra-day precisions of the method tended to vary among extracts rather than among analytes. NAC-ITC analysis in the spiked *S. alba* and *B. juncea* extracts had intra- (2.8-10.0% *RSD*) and inter-day precisions (3.3-14.7% *RSD*) within the FDA requirement, except for the intra-day precision of **I10** and **I12** in *S. alba* extract (up to 13.6% *RSD*). However, the analysis of 9 of 15 NAC-ITCs in the spiked *B. napus* extract had lower

intra-day precision (11.4-18.4% *RSD*) than the FDA requirement. This might be due to the presence of other low molecular weight thiol compounds (such as glutathione (GSH), the dominant thiol compound in most plant cells<sup>42,43</sup>) in the extract, which might compete with NAC in reacting with ITCs. Nevertheless, this competition was not expected in our study, because GSL extraction was done in absolute methanol where GSH is insoluble.<sup>44</sup> When the extraction is done in aqueous solvent, co-extracting GSH, the level of this thiol compound in the extract should be considered. Despite this relatively low intra-day precision of NAC-ITCs in the spiked *B. napus* extract, the inter-day precision of the majority (10 NAC-ITCs) complied with the FDA.

### 3.3.5. Recovery

The recovery of 14 GSLs and 15 NAC-ITCs spiked in *S. alba*, *B. napus*, and *B. juncea* extracts was evaluated. Two concentration levels were applied, i.e. 10  $\mu$ M and 30  $\mu$ M. The chromatograms of *B. napus* extracts, as a representative, are shown in **Figure S3.4**. All GSLs and ITCs added to the extract were distinguishable, and their intensity increased upon increasing concentration, except for **G12** and **G13** as they were constitutively present in high abundance ( $> 80 \mu$ M, outside the range of concentrations used for calibration).

The recovery is the closeness of agreement between the true value of the analyte concentration and the experimental result.<sup>40, 41</sup> According to FDA<sup>40</sup>, a good recovery for our working analyte concentrations should be between 80-110%.

The recoveries for GSLs ranged from  $71 \pm 18\%$  to  $110 \pm 6\%$  (**Table 3.2**), complying with the FDA requirement ( $p > 0.05$ ). PeGSL (**G14**) had a tendency to have a lower recovery than the other 13 GSLs in all the three spiked extracts.

The recoveries of NAC-ITCs ranged from  $66 \pm 8\%$  to  $122 \pm 15\%$  (**Table 3.2**). NAC-PITC (**I10**) had a tendency to have a lower recovery, whereas NAC-3-MSoITC (**I6**) had a tendency to have a higher recovery than the other 14 NAC-ITCs in all three spiked extracts. Only NAC-PITC (**I10**) in *S. alba* extract had a recovery lower than the minimum FDA requirement (80%,  $p < 0.05$ ). Pilipczuk *et al.*<sup>31</sup> found satisfactory recoveries (83-104%) for 9 NAC-ITCs, including NAC-methyl ITC and NAC-ethyl ITC (shorter-chained analogues of PITC). Considering ITC's physicochemical properties, e.g. boiling point and reactivity, we found no plausible explanation for the low recovery of PITC.

Overall, our method is well suited to quantify various GSLs and ITCs (as NAC-ITCs) in complex mixtures, such as plant extracts, with a high precision and recovery for most analytes. The method also offers an alternative way of making calibration series of NAC-ITCs, which is from the fresh NAC-derivatization of standard ITCs.

Table 3.2. Validation data of 14 different GSLs and 15 different ITCs analyzed by RP-UHPLC-MS<sup>a</sup> with pre-column NAC-derivatization.

Code	Analyte	R <sup>2</sup>	LOD (μM)	LOQ (μM) <sup>a</sup>	Intra-day precision (% RSD) <sup>b</sup>			Inter-day precision (% RSD)			Recovery (%) (mean ± SD) <sup>c</sup>				
					SM	Sa	Bn	SM	Sa	Bn	Sa	Bn	Bj		
GSL															
G1	3-MSGSL	0.9989	1.3	3.9	5.9	3.9	8.8	10.3	8.0	4.2	9.1	10.6	93.3 ± 3.2	99.1 ± 8.7	84.9 ± 8.4
G2	4-MSGSL	0.9985	1.6	4.7	6.4	2.4	5.4	8.4	12.5	5.0	7.1	9.2	100.2 ± 5.7	108.6 ± 8.2	101.2 ± 10.0
G5	4-MS-3-en-GSL	0.9992	1.2	3.5	7.4	3.1	4.3	5.8	12.5	4.0	5.3	7.3	99.7 ± 4.3	110.1 ± 6.1	100.9 ± 7.9
G6	3-MSoGSL	0.9988	1.3	4.0	7.7	2.2	7.8	4.0	9.1	3.6	8.3	4.4	93.8 ± 3.7	106.2 ± 7.5	99.9 ± 10.1
G8	4-MTGSL	0.9989	1.3	3.8	7.4	3.2	4.6	7.7	14.8	3.5	5.6	10.0	93.3 ± 3.4	104.7 ± 6.2	94.9 ± 10.1
G9	5-MTGSL	0.9999	0.4	1.2	8.9	2.4	5.3	2.5	12.2	2.6	6.3	4.6	87.5 ± 2.3	102.8 ± 6.8	98.0 ± 5.0
G11	AGSL	0.9989	1.3	3.9	8.3	4.0	3.5	3.9	12.3	5.5	4.2	4.2	94.4 ± 5.6	101.8 ± 4.4	99.5 ± 8.6
G12	BuGSL	0.9983	1.6	4.9	4.9	7.6	8.9	9.0	13.2	8.4	9.3	9.4	107.2 ± 9.2	99.1 ± 4.3	96.9 ± 3.8
G13	2-OH-BuGSL	0.9998	0.7	2.0	8.0	3.2	4.5	9.6	10.4	3.6	5.8	10.8	93.4 ± 3.4	98.8 ± 3.6	97.5 ± 8.9
G14	PeGSL	0.9994	1.0	2.9	8.0	8.8	24.2	13.1	11.8	9.8	27.0	14.1	76.9 ± 5.6	71.0 ± 18.3	80.6 ± 9.4
G15	BGSL	0.9991	1.2	3.6	7.2	1.8	5.7	2.2	11.0	2.0	5.9	3.1	97.3 ± 2.0	107.3 ± 5.9	101.2 ± 3.3
G16	p-OH-BGSL	0.9999	0.6	1.9	7.7	9.8	10.5	19.8	13.7	10.9	11.6	22.1	94.8 ± 7.9	100.6 ± 8.9	89.1 ± 14.5
G17	PhEGSL	0.9992	1.1	3.4	7.4	0.6	8.5	3.4	11.5	2.1	8.8	4.5	96.4 ± 2.3	99.9 ± 8.0	99.5 ± 4.7
G18	13MGSL	0.9999	0.6	1.8	7.3	2.7	7.4	3.9	10.2	9.7	8.2	5.3	108.9 ± 12.1	101.1 ± 6.3	95.6 ± 5.4
ITC															
I1	3-MSITC	0.9978	1.4	4.2	8.2	4.0	7.8	5.7	12.1	5.3	14.3	6.3	99.6 ± 5.6	105.6 ± 16.7	111.6 ± 5.2
I2	4-MSITC	0.9982	1.7	5.2	10.0	3.8	9.3	5.2	14.6	11.5	13.7	5.6	99.8 ± 13.1	101.7 ± 15.1	110.9 ± 5.0
I3	6-MSITC	0.9952	1.3	3.8	9.2	3.0	13.8	6.1	17.9	3.3	15.3	6.8	96.1 ± 3.3	102.3 ± 16.1	108.6 ± 5.5
I4	9-MSITC	0.9996	0.9	2.8	9.0	3.6	18.4	5.0	12.9	3.8	18.5	5.1	99.1 ± 3.4	96.1 ± 17.6	105.3 ± 5.4
I5	4-MS-3-en-ITC	0.9981	1.4	4.2	8.2	2.8	8.7	6.2	15.6	5.5	12.9	6.9	101.0 ± 6.3	103.9 ± 14.5	110.1 ± 5.7
I6	3-MSoITC	0.9961	2.0	5.8	8.6	6.9	11.6	7.7	11.8	7.1	12.0	8.3	112.7 ± 7.4	121.9 ± 14.8	117.9 ± 8.0
I7	3-MTITC	0.9953	1.9	5.6	8.2	3.9	9.7	6.6	15.0	7.7	13.8	7.4	92.9 ± 8.0	95.6 ± 14.3	103.1 ± 5.7
I8	4-MTITC	0.9981	1.5	4.5	9.7	4.1	6.9	4.8	12.2	6.1	13.3	5.0	92.0 ± 6.1	92.0 ± 13.6	102.0 ± 4.6
I9	5-MTITC	0.9995	0.9	2.7	7.9	10.0	14.0	4.4	11.4	10.5	16.1	4.9	88.0 ± 8.2	86.0 ± 14.4	94.1 ± 4.7
I10	PITC	0.9947	1.9	5.5	11.9	13.6	16.4	9.3	16.5	14.7	20.7	10.3	66.0 ± 7.8*	74.9 ± 18.4	75.0 ± 5.8
I11	AITC	0.9970	1.9	5.8	9.2	6.8	13.6	6.0	12.3	7.6	15.9	6.5	95.7 ± 5.4	95.2 ± 15.7	97.0 ± 5.1
I12	BuITC	0.9991	1.3	3.8	9.5	10.7	11.4	6.1	11.8	10.8	16.4	6.8	80.3 ± 8.5	81.9 ± 13.0	85.1 ± 4.3
I14	PeITC	0.9936	2.6	7.8	10.5	8.3	11.4	4.5	12.3	9.2	16.2	5.0	72.5 ± 5.0	79.0 ± 8.1	78.1 ± 2.9
I15	BITC	0.9983	1.6	4.8	7.2	3.3	7.1	4.2	12.1	4.7	7.4	4.7	101.5 ± 5.2	102.6 ± 6.7	101.2 ± 3.6
I17	PhEITC	0.9978	2.1	6.2	8.9	8.7	12.3	4.6	10.8	9.0	15.8	5.2	110.0 ± 7.5	109.9 ± 15.0	105.6 ± 3.6

<sup>a</sup> R<sup>2</sup>, LOD, and LOQ were obtained from a series of standard GSL and ITC mixtures in 8 different concentrations within a range of 2–60 μM and 3–60 μM.<sup>b</sup> The intra- and inter-day precisions for standard mixtures (SM) was expressed as % RSD of the chromatographic peak areas of the analytes, whereas that for spiked extracts (*Sinapis alba* (Sa), *Brassica napus* (Bn), and *B. juncea* (Bj) seeds) was expressed as % RSD of the concentration of the analytes.<sup>c</sup> ANOVA one-sample t-test were performed for comparing means of % recovery of the lowest and the highest to the standard guideline (the min. 80% or the max. 110%) (FDA, 2015). \*The recovery of NAC-PITC (I10) in *S. alba* seed extract was significantly lower than the minimum guideline (80%,  $p < 0.05$ ). The rest of GSLs and ITCs in the three extracts had recovery within the range of the standard guideline.

### 3.3.6. Detection of various enzymatic hydrolysis products of GSLs

At neutral conditions, most GSLs are degraded to form ITCs upon myrosinase treatment.<sup>4-6</sup> Our new analytical method was applied to monitor simultaneously the decrease of the concentration of 14 different standard GSLs and the increase of the concentration of their corresponding ITCs, in the form of NAC derivatives, during enzymatic hydrolysis. In our study, ITCs were the default rearrangement products of the aglucones (**Figure 3.1**) in the GSL extracts treated with the commercial myrosinase, supporting previous studies.<sup>45,46</sup> **Figure 3.2B** shows the presence of 14 GSLs before hydrolysis with myrosinase. **Figure 3.2C** indicates that after incubation with myrosinase and NAC at 50 °C for 4 h, all 14 GSLs were hydrolyzed, peaks corresponding to 12 NAC-ITCs and 3 unknown peaks appeared.

Upon myrosinase treatment 2-hydroxylated alkenyl GSLs and indolic GSLs form unstable ITCs which further form other types of products.<sup>13, 47</sup> (R)-2-OH-BuGSL or progoitrin (**G13**) is known to form unstable 2-OH-3-butenyl ITC which spontaneously cyclizes forming 5-ethenyl-1,3-oxazolidine-2-thione (i.e. goitrin)<sup>47</sup> (**Figure S3.5A**). However, the reaction product of a mixture of **G13**, myrosinase, and NAC is unknown in literature. Therefore, it remains unclear whether goitrin or the unstable 2-OH-3-butenyl ITC had reacted with NAC (**Figure S3.5B-C**) which might depend on the rates of cyclization of the ITC and of reaction between the ITC and NAC. In addition, the reaction product between goitrin and NAC has never been described in literature. A peak at a tR of 34.3 min and *m/z* of 583 (**Figure 3.2C**) might correspond to a dimer of reaction product between NAC and the hydrolysis product of **G13** with a molecular formula of C<sub>20</sub>H<sub>32</sub>N<sub>4</sub>O<sub>8</sub>S<sub>4</sub> (584 Da) (**Figure S3.5D**). The fragmentation gave an ion at *m/z* of 291 (possibly the monomer) at the most abundant, and this was fragmented to an ion at *m/z* of 162 (possibly the NAC). Meanwhile, indol-3-ylmethyl (I3M) GSL (**G18**) forms various hydrolysis products, e.g. indole-3-acetonitrile and I3M ITC which further reacts with water to form indole-3-carbinol.<sup>13, 48, 49</sup> However, these compounds and their possible reaction products with NAC were not detected in our LC-MS analysis.

Furthermore, **Figure 3.2C** indicates two other peaks at 3.25 min (*m/z* 272) and 23.94 min (*m/z* 268), which were related to **G5** and **G16**, i.e. GSLs partially converted to their corresponding ITCs (**I5** and **I16**) (**Table 3.3**). The presence of the first peak was never indicated previously, and the annotation requires structural elucidation by NMR spectroscopy. A previous study found that **G5** was hydrolyzed to form **I5** which was unstable and rapidly converted to a water-soluble degradation product, namely 6-[(methylsulfinyl)methyl]-1,3-thiazinan-2-thione, at 25 °C, pH 7.<sup>50</sup> However, this compound was not detected in our LC-MS analysis. The second peak was tentatively annotated as C<sub>12</sub>H<sub>15</sub>NO<sub>4</sub>S (269 Da) which was possibly an ester from *p*-OH-benzyl alcohol and NAC (**Figure S3.6**), and observed after 3-h incubation. **G16** formed not only **I16** (13% conversion, **Table 3.3**), but

also *p*-OH-benzyl alcohol which is in line with the finding of Buskov *et al.* confirming the structure by NMR spectroscopy.<sup>51</sup>

Overall, our results underlines that the amount of ITCs formed upon hydrolysis of GSLs does not necessarily equal that of hydrolyzed GSLs, and this is influenced by the side chain. Therefore, the amount of ITCs formed upon hydrolysis of GSLs should be determined appropriately.

**Table 3.3.** Rates ( $\mu\text{M/h}$ ) of enzymatic hydrolysis of GSLs and formation of NAC-ITCs from ITCs released upon hydrolysis and simultaneous NAC-derivatization, and conversion of GSLs to ITCs.

GSL or ITC	R-group <sup>a</sup>	Hydrolysis of GSL		Formation of NAC-ITC		
		Rate	R <sup>2</sup>	Rate	R <sup>2</sup>	Conversion (%)
Subclass x-(Methylsulfinyl)alkyl (MS)						
G1, I1	3-MS	13.6	0.981	11.7	0.968	100
G2, I2	4-MS	11.2	0.987	10.7	0.922	100
Subclass x-(Methylsulfinyl)alkenyl (MS-en)						
G5, I5	4-MS-3-en	11.9	0.986	7.4	0.945	63
Subclass x-(Methylsulfonyl)alkyl (MSo)						
G6, I6	3-MSo	17.3	0.966	10.4	0.965	100
Subclass x-(Methylthio)alkyl (MT)						
G8, I8	4-MT	18.4	0.982	10.1	0.952	100
G9, I9	5-MT	19.7	0.991	9.7	0.968	100
Subclass Alkenyl						
G11, I11	A	20.6	0.990	11.1	0.959	100
G12, I12	Bu	25.4	0.994	9.0	0.866	100
G13, n.a.	2-OH-Bu	28.4	0.999	n.a. <sup>b</sup>	n.a.	n.a.
G14, I14	Pe	20.3	0.966	9.3	0.870	100
Subclass Benzenic						
G15, I15	B	26.9	0.989	9.1	0.809	100
G16, I16	<i>p</i> -OH-B	29.7	0.959	n.d. <sup>c</sup>	n.d.	13
G17, I17	PhE	20.8	0.985	11.0	0.919	100
Subclass Indolic						
G18, n.a.	I3M	25.7	0.983	n.a.	n.a.	n.a.

<sup>a</sup> R-groups are presented in the abbreviations, referring to **Table 3.1**.

<sup>b</sup> n.a. stands for not available, due to the degradation products were not ITCs.

<sup>c</sup> n.d. indicates that the concentration of the compound cannot be determined due to lack of standard. Therefore, the conversion (13%) was calculated by taking the concentration BITC equivalent for this *p*-OH-BITC.

### 3.3.7. Quantitative monitoring the enzymatic conversion of standard GSLs to NAC-ITCs

**Figures 3.3A** (no organic solvent) and **3.3B** (25% IPA) demonstrate the progress of hydrolysis of an aliphatic GSL (**G1**) and an aromatic GSL (**G15**), as representatives, and the progress of NAC-derivatization of the corresponding ITCs (**I1** and **I15**). The graphs for the other GSLs and NAC-ITCs are displayed in **Figure S3.7**. In general, the hydrolysis of all GSLs at 50 °C, pH 7.0 occurred to completion at 1.5-2.5 h, whereas the complete conversion to their respective NAC-ITCs lasted longer (2.5-3.5 h). **Table 3.3** shows the rates of GSL hydrolysis and NAC-ITC

formation for all tested compounds. The hydrolysis rates of the 14 GSLs were within 11.2-29.7  $\mu\text{M}/\text{h}$ . A previous study using the same commercial *S. alba* myrosinase, but different incubation temperature (37 °C), found much higher hydrolysis rates (369-800  $\mu\text{M}/\text{h}$ ).<sup>35</sup> The lower hydrolysis rates found in our study in comparison with this previous study<sup>35</sup> were probably because we used a lower concentration of myrosinase (0.05 U/mL vs 1.10-14.52 U/mL). The formation rates of NAC-ITCs were within 7.4-11.7  $\mu\text{M}/\text{h}$ . The slower rate of NAC-ITCs formation compared to GSL hydrolysis might be explained by the effect of solvent as the solubility of ITCs are favored in organic solvent. **Figure 3.3B** indicates that when the hydrolysis of GSLs and the formation of NAC-ITCs co-occurred in IPA 25%, the rates were comparable. However, the hydrolysis of 3-MSGSL in IPA 25% was not fully accomplished in 4 h (**Figure 3.3B**). Therefore, the rest of experiments on the simultaneous enzymatic hydrolysis of GSLs and NAC-ITC formation occurred in absence of IPA.

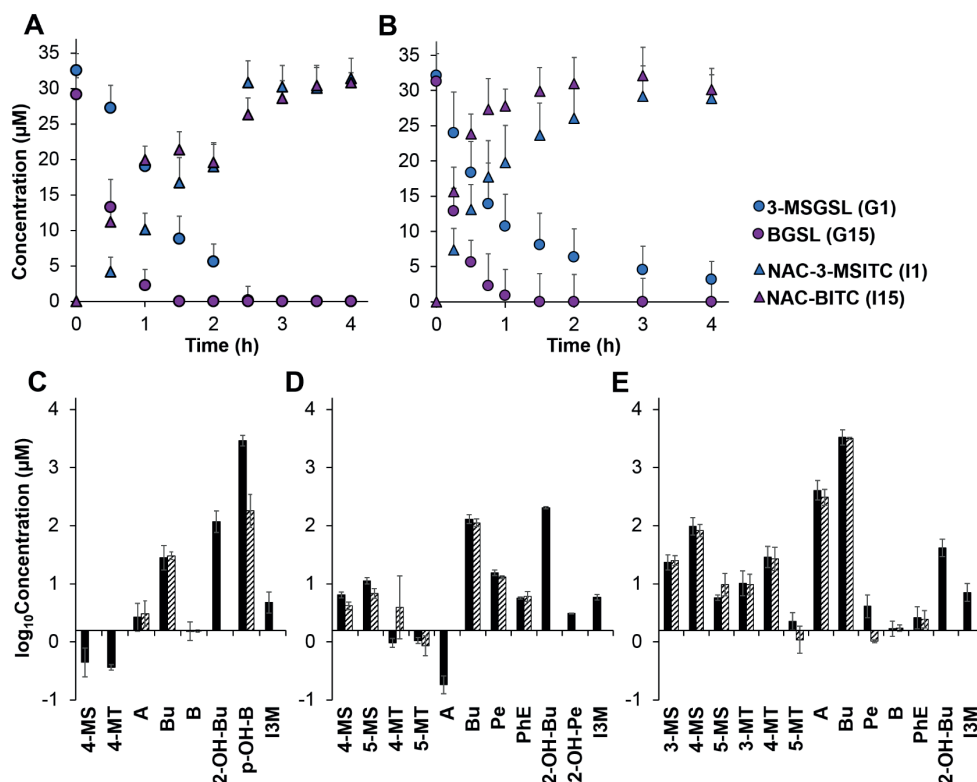
Based on the hydrolysis rates (**Table 3.3**), the alkenyl, benzenic, and indolic GSLs were the most preferred substrates of myrosinase (hydrolysis rate of 20.3-29.7  $\mu\text{M}/\text{h}$ ), followed by (methylthio)alkyl and (methylsulfonyl)alkyl GSLs (17.3-19.7  $\mu\text{M}/\text{h}$ ). The least preferred substrates were (methylsulfinyl)alkyl and (methylsulfinyl)alkenyl GSLs (11.2-13.6  $\mu\text{M}/\text{h}$ ). In our study, the myrosinase used was originally isolated from *S. alba* seed. *p*-OH-BGSL (**G16**), is the most abundant GSL in this seed and had the highest hydrolysis rate (29.7  $\mu\text{M}/\text{h}$ ). Our finding supports previous studies<sup>36, 52</sup> indicating that myrosinase acts more efficiently on the most abundant GSL present in the plant, to which both myrosinase and GSL belong to.

### 3.3.8. The enzymatic conversion of constitutive GSLs to ITCs in plant extracts

To further test the applicability of our method, simultaneous enzymatic hydrolysis of GSLs and NAC-derivatization of ITCs was also performed in the three Brassicaceae seed extracts. The condition of this hydrolysis was similar to that of the hydrolysis of standard GSLs in our study (50 °C, buffer pH 7.0), except for the presence of DMSO 5% to assist the solubilization of the extracts. Under this condition, all GSLs were hydrolyzed completely within 4 h (similar to the experiments without DMSO; data not shown).

**Figure 3.3C-E** indicates the concentration (in logarithmic scale) of GSLs in extracts of each species before hydrolysis and of NAC-ITCs after 4 h hydrolysis. The predominant GSLs in *S. alba*, *B. napus*, and *B. juncea* seed extracts at 5 mg/mL were *p*-OH-BGSL (**G16**) 1857  $\mu\text{M}$ , 2-OH-BuGSL (**G13**) 128  $\mu\text{M}$ , and BuGSL (**G12**) 2012  $\mu\text{M}$ , respectively, which equaled to 61, 4, and 66  $\mu\text{mol}/\text{g}$  DW seed, respectively. The result was in agreement with previous study.<sup>37</sup>





**Figure 3.3.** Simultaneous enzymatic hydrolysis of GSLs and NAC-derivatization of ITCs that were released: the decrease in concentration of GSLs (circles) and the increase in concentration of NAC-ITCs (triangles) during enzymatic hydrolysis of standard GSLs in the absence of organic solvent (**A**), in IPA 25% (**B**); concentration (in logarithmic scale) of constitutive GSLs (filled bars) before hydrolysis and their corresponding ITCs (hatched bars) in *S. alba* (**C**), *B. napus* (**D**), and *B. juncea* (**E**) seed extracts (5 mg/mL) after 4 h hydrolysis at 50 °C. Hydroxylated aliphatic GSLs (2-OH-BuGSL and 2-OH-PeGSL) and indole GSL (13MGSL) did not form ITCs upon myrosinase treatment. *p*-OH-BITC was not the only hydrolysis product of *p*-OH-BGSL (**G16**). The error bars are the standard deviations for the means, taken from three independent experiments.

For GSLs which form only ITCs upon myrosinase treatment in neutral pH solution, e.g. 3-MSGSL (**G1**), 4-MTGSL (**G8**), AGSL (**G11**), and BuGSL (**G12**), the concentration of ITCs formed was comparable to that of the corresponding GSLs (**Figure 3.3C-E**), consistent with our results from the hydrolysis of standard GSLs (**Figure 3.3A**, **Figure S3.7**). *p*-OH-BGSL (**G16**) partially formed ITC (**Figure 3.3C**), two hydroxylated alkenyl GSLs (i.e. 2-OH-BuGSL **G13**, 2-OH-PeGSL **G20**) and 13M GSL (**G18**) formed no ITC (**Figure 3.3C-E**), in accordance with the findings obtained in the hydrolysis of standard GSLs (section 3.3.6).

Our method enabled analysis of plant extracts with different GSL and ITC compositions. If the plant extract would contain excessive amounts of ITC, then

the amount of NAC for derivatization might become limiting. In such case, several dilutions of the plant extract should be prepared, while keeping the concentration of NAC constant, e.g. 2.25 mM (as applied in the spike experiments), to confirm that the amount of NAC is sufficient to react with all ITCs.

Several methods to analyze GSLs and ITCs simultaneously were developed previously,<sup>33-36</sup> some of which with high sensitivity and precision.<sup>34, 36</sup> In our study, we have developed an RP-UHPLC-ESI-MS<sup>n</sup> method able to analyze: (i) a more extensive set of GSLs and ITCs simultaneously comprising 8 different subclasses, most of which with representatives of different chain length; (ii) complex mixtures, e.g. plant extracts, by MS detection (more specific than UV detection); (iii) GSLs and ITCs directly after hydrolysis and NAC-derivatization, i.e. simultaneous hydrolysis and analysis. Overall, this method is valuable for understanding the *in vitro* enzymatic conversion of GSLs to ITCs under various conditions.

### **3.4. Acknowledgement**

The authors are thankful to Sjoera Tjin A-Lim for her help in the preliminary experiments of the enzymatic hydrolysis of GSLs, and to Roelant Hilgers for discussion on the organic chemistry reactions between goitrin and NAC.

### **3.5. Funding source**

The authors are grateful to Indonesia Endowment Fund for Education (LPDP), Ministry of Finance of Republic Indonesia, for the financial support for S.A. during her PhD study.

### 3.6. References

1. Ahuja, I.; Rohloff, J.; Bones, A. M., Defence mechanisms of Brassicaceae: implications for plant-insect interactions and potential for integrated pest management. A review. *Agron. Sustainable Dev.* **2010**, *30*, 311-348.
2. Bones, A. M.; Rossiter, J. T., The myrosinase-glucosinolate system, its organisation and biochemistry. *Physiol. Plant.* **1996**, *97*, 194-208.
3. Wittstock, U.; Kurzbach, E.; Herfurth, A. M.; Stauber, E. J.; Kopriva, S., Chapter Six - Glucosinolate breakdown. In *Advances in Botanical Research*, Academic Press: **2016**; Vol. 80, pp 125-169.
4. Halkier, B. A.; Gershenzon, J., Biology and biochemistry of glucosinolates. *Annu. Rev. Plant Biol.* **2006**, *57*, 303-33.
5. Matusheski, N. V.; Wallig, M. A.; Juvik, J. A.; Klein, B. P.; Kushad, M. M.; Jeffery, E. H., Preparative HPLC method for the purification of sulforaphane and sulforaphane nitrile from *Brassica oleracea*. *J. Agric. Food Chem.* **2001**, *49*, 1867-72.
6. Rosa, E. A. S.; Heaney, R. K.; Fenwick, G. R.; Portas, C. A. M., Glucosinolates in crop plants. In *Horticultural Reviews*, John Wiley & Sons, Inc: **1997**; Vol. 19, pp 99-215.
7. Calmes, B.; N'Guyen, G.; Dumur, J.; Brisach, C. A.; Campion, C.; Iacomì, B.; Pigne, S.; Dias, E.; Macherel, D.; Guillemette, T.; Simoneau, P., Glucosinolate-derived isothiocyanates impact mitochondrial function in fungal cells and elicit an oxidative stress response necessary for growth recovery. *Front. Plant Sci.* **2015**, *6*, 414.
8. Aires, A.; Mota, V. R.; Saavedra, M. J.; Monteiro, A. A.; Simoes, M.; Rosa, E. A.; Bennett, R. N., Initial *in vitro* evaluations of the antibacterial activities of glucosinolate enzymatic hydrolysis products against plant pathogenic bacteria. *J. Appl. Microbiol.* **2009**, *106*, 2096-105.
9. Dias, C.; Aires, A.; Saavedra, M. J., Antimicrobial activity of isothiocyanates from cruciferous plants against methicillin-resistant *Staphylococcus aureus* (MRSA). *Int. J. Mol. Sci.* **2014**, *15*, 19552-19561.
10. Turgis, M.; Han, J.; Caillet, S.; Lacroix, M., Antimicrobial activity of mustard essential oil against *Escherichia coli* O157:H7 and *Salmonella typhi*. *Food Control* **2009**, *20*, 1073-1079.
11. Aires, A.; Mota, V. R.; Saavedra, M. J.; Rosa, E. A.; Bennett, R. N., The antimicrobial effects of glucosinolates and their respective enzymatic hydrolysis products on bacteria isolated from the human intestinal tract. *J. Appl. Microbiol.* **2009**, *106*, 2086-95.
12. Bones, A. M.; Rossiter, J. T., The enzymic and chemically induced decomposition of glucosinolates. *Phytochemistry* **2006**, *67*, 1053-1067.
13. Agerbirk, N.; De Vos, M.; Kim, J. H.; Jander, G., Indole glucosinolate breakdown and its biological effects. *Phytochem. Rev.* **2008**, *8*, 101-120.
14. Śmiechowska, A.; Bartoszek, A.; Namieśnik, J., Determination of glucosinolates and their decomposition products—indoles and isothiocyanates in cruciferous vegetables. *Crit. Rev. Anal. Chem.* **2010**, *40*, 202-216.
15. Bennett, R. N.; Carvalho, R.; Mellon, F. A.; Eagles, J.; Rosa, E. A. S., Identification and quantification of glucosinolates in sprouts derived from seeds of wild *Eruca sativa* L. (salad rocket) and *Diplotaxis tenuifolia* L. (wild rocket) from diverse geographical locations. *J. Agric. Food Chem.* **2007**, *55*, 67-74.
16. Bhandari, S. R.; Jo, J. S.; Lee, J. G., Comparison of glucosinolate profiles in different tissues of nine *Brassica* crops. *Molecules* **2015**, *20*, 15827-41.
17. Kim, H. J.; Lee, M. J.; Jeong, M. H.; Kim, J. E., Identification and quantification of glucosinolates in kimchi by liquid chromatography-electrospray tandem mass spectrometry. *Int. J. Anal. Chem.* **2017**, *2017*, 6753481.
18. Lee, M.-K.; Chun, J.-H.; Byeon, D. H.; Chung, S.-O.; Park, S. U.; Park, S.; Arasu, M. V.; Al-Dhabi, N. A.; Lim, Y.-P.; Kim, S.-J., Variation of glucosinolates in 62

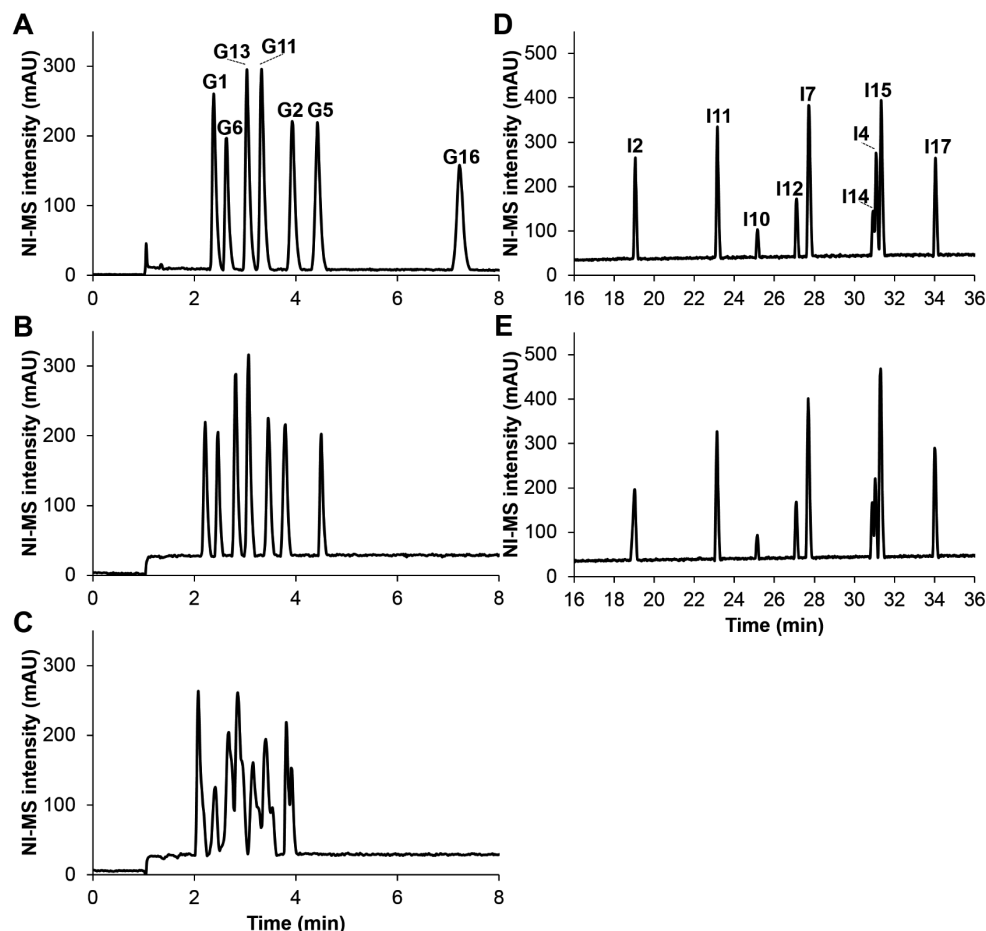
- varieties of Chinese cabbage (*Brassica rapa* L. ssp. *pekinensis*) and their antioxidant activity. *LWT - Food Sci. Technol.* **2014**, *58*, 93-101.
19. Matthaues, B.; Luftmann, H., Glucosinolates in members of the family Brassicaceae: separation and identification by LC/ESI-MS-MS. *J. Agric. Food Chem.* **2000**, *48*, 2234-9.
  20. Bennett, R. N.; Mellon, F. A.; Botting, N. P.; Eagles, J.; Rosa, E. A.; Williamson, G., Identification of the major glucosinolate (4-mercaptobutyl glucosinolate) in leaves of *Eruca sativa* L. (salad rocket). *Phytochemistry* **2002**, *61*, 25-30.
  21. Förster, N.; Ulrichs, C.; Schreiner, M.; Muller, C. T.; Mewis, I., Development of a reliable extraction and quantification method for glucosinolates in *Moringa oleifera*. *Food Chem.* **2015**, *166*, 456-64.
  22. Wathelet, J. P.; Iori, R.; Leoni, O.; Rollin, P.; Quinsac, A.; Palmieri, S., Guidelines for glucosinolate analysis in green tissues used for biofumigation. *Agroindustria* **2004**, *3*, 257-266.
  23. Mellon, F. A.; Bennett, R. N.; Holst, B.; Williamson, G., Intact glucosinolate analysis in plant extracts by programmed cone voltage electrospray LC/MS: Performance and comparison with LC/MS/MS methods. *Anal. Biochem.* **2002**, *306*, 83-91.
  24. Millán, S.; Sampedro, M. C.; Gallejones, P.; Castellón, A.; Ibargoitia, M. L.; Goicolea, M. A.; Barrio, R. J., Identification and quantification of glucosinolates in rapeseed using liquid chromatography-ion trap mass spectrometry. *Anal. Bioanal. Chem.* **2009**, *394*, 1661-1669.
  25. Song, L.; Morrison, J. J.; Botting, N. P.; Thornalley, P. J., Analysis of glucosinolates, isothiocyanates, and amine degradation products in vegetable extracts and blood plasma by LC-MS/MS. *Anal. Biochem.* **2005**, *347*, 234-243.
  26. Tian, Q.; Rosselot, R. A.; Schwartz, S. J., Quantitative determination of intact glucosinolates in broccoli, broccoli sprouts, Brussels sprouts, and cauliflower by high-performance liquid chromatography-electrospray ionization-tandem mass spectrometry. *Anal. Biochem.* **2005**, *343*, 93-9.
  27. Blažević, I.; Montaut, S.; Burčul, F.; Olsen, C. E.; Burow, M.; Rollin, P.; Agerbirk, N., Glucosinolate structural diversity, identification, chemical synthesis and metabolism in plants. *Phytochemistry* **2020**, *169*, 112100.
  28. Chen, C.-W.; Ho, C.-T., Thermal degradation of allyl isothiocyanate in aqueous solution. *J. Agric. Food Chem.* **1998**, *46*, 220-223.
  29. Chiang, W. C. K.; Pusateri, D. J.; Leitz, R. E. A., Gas chromatography/mass spectrometry method for the determination of sulforaphane and sulforaphane nitrile in broccoli. *J. Agric. Food Chem.* **1998**, *46*, 1018-1021.
  30. Budnowski, J.; Hanschen, F. S.; Lehmann, C.; Haack, M.; Brigelius-Flohé, R.; Kroh, L. W.; Blaut, M.; Rohn, S.; Hanske, L., A derivatization method for the simultaneous detection of glucosinolates and isothiocyanates in biological samples. *Anal. Biochem.* **2013**, *441*, 199-207.
  31. Pilipczuk, T.; Kusznierevicz, B.; Chmiel, T.; Przychodzen, W.; Bartoszek, A., Simultaneous determination of individual isothiocyanates in plant samples by HPLC-DAD-MS following SPE and derivatization with *N*-acetyl-L-cysteine. *Food Chem.* **2017**, *214*, 587-596.
  32. Wilson, E. A.; Ennahar, S.; Zhao, M.; Bergaentzle, M.; Marchioni, E.; Bindler, F., Simultaneous determination of various isothiocyanates by RP-LC following precolumn derivatization with mercaptoethanol. *Chromatographia* **2011**, *73*, 137-142.
  33. Tsao, R.; Yu, Q.; Potter, J.; Chiba, M., Direct and simultaneous analysis of sinigrin and allyl isothiocyanate in mustard samples by high-performance liquid chromatography. *J. Agric. Food Chem.* **2002**, *50*, 4749-53.
  34. Franco, P.; Spinozzi, S.; Pagnotta, E.; Lazzeri, L.; Ugolini, L.; Camborata, C.; Roda, A., Development of a liquid chromatography-electrospray ionization-tandem mass spectrometry method for the simultaneous analysis of intact

- glucosinolates and isothiocyanates in Brassicaceae seeds and functional foods. *J. Chromatogr. A* **2016**, 1428, 154-161.
35. Vastenhout, K. J.; Tornberg, R. H.; Johnson, A. L.; Amolins, M. W.; Mays, J. R., High-performance liquid chromatography-based method to evaluate kinetics of glucosinolate hydrolysis by *Sinapis alba* myrosinase. *Anal. Biochem.* **2014**, 465, 105-113.
  36. Gonda, S.; Kiss-Szikszai, A.; Szűcs, Z.; Nguyen, N. M.; Vasas, G., Myrosinase compatible simultaneous determination of glucosinolates and allyl isothiocyanate by capillary electrophoresis micellar electrokinetic chromatography (CE-MEKC). *Phytochem. Anal.* **2016**, 27, 191-198.
  37. Andini, S.; Dekker, P.; Gruppen, H.; Araya-Cloutier, C.; Vincken, J.-P., Modulation of glucosinolate composition in Brassicaceae seeds by germination and fungal elicitation. *J. Agric. Food Chem.* **2019**, 67, 12770-12779.
  38. Bernal, E.; Guo, X., Limit of detection and limit of quantification determination in gas chromatography. In *Advances in Gas Chromatography*, InTech: Rijeka, **2014**; pp 57-81.
  39. Currie, L. A., Nomenclature in evaluation of analytical methods including detection and quantification capabilities (IUPAC Recommendations 1995). In *Pure and Applied Chemistry*, **1995**; Vol. 67, p 1699.
  40. FDA, Guidance for Industry: Studies to Evaluate the Metabolism and Residue Kinetics of Veterinary Drugs in Food-Producing Animals: Validation of Analytical Methods Used in Residue Depletion Studies. In *VICH GL49(R)*, Food and Drug Administration (FDA), Center for Veterinary Medicine, Department of Health and Human Services: Rockville, United States, **2015**; p 23.
  41. Magnusson, B.; Örnemark, U., *Eurachem guide: The fitness for purpose of analytical methods – A laboratory guide to method validation and related topics*. 2nd ed.; www.eurachem.org: **2014**; p 70.
  42. Anjum, N. A.; Umar, S.; Iqbal, M.; Ahmad, I.; Pereira, M. E.; Khan, N. A., Protection of growth and photosynthesis of *Brassica juncea* genotype with dual type sulfur transport system against sulfur deprivation by coordinate changes in the activities of sulfur metabolism enzymes and cysteine and glutathione production. *Russ. J. Plant Physiol.* **2011**, 58, 892.
  43. Ruiz, J. M.; Blumwald, E., Salinity-induced glutathione synthesis in *Brassica napus*. *Planta* **2002**, 214, 965-9.
  44. Haynes, W. M.; Lide, D. R.; Bruno, T. J., *Handbook of Chemistry and Physics 97th Edition*. CRC Press Taylor and Francis Group: Boca Raton, 2016.
  45. Matusheski, N. V.; Juvik, J. A.; Jeffery, E. H., Heating decreases epithiospecifier protein activity and increases sulforaphane formation in broccoli. *Phytochemistry* **2004**, 65, 1273-81.
  46. Matusheski, N. V.; Swarup, R.; Juvik, J. A.; Mithen, R.; Bennett, M.; Jeffery, E. H., Epithiospecifier protein from broccoli (*Brassica oleracea* L. ssp. *italica*) inhibits formation of the anticancer agent sulforaphane. *J. Agric. Food Chem.* **2006**, 54, 2069-76.
  47. Greer, M. A., Isolation from rutabaga seed of progoitrin, the precursor of the naturally occurring antithyroid compound, goitrin (1-5-vinyl-2-thiooxazolidone). *J. Am. Chem. Soc.* **1956**, 78, 1260-1261.
  48. Hauder, J.; Winkler, S.; Bub, A.; Rufer, C. E.; Pignitter, M.; Somoza, V., LC-MS/MS quantification of sulforaphane and indole-3-carbinol metabolites in human plasma and urine after dietary intake of selenium-fortified broccoli. *J. Agric. Food Chem.* **2011**, 59, 8047-57.
  49. McDanell, R.; McLean, A. E. M.; Hanley, A. B.; Heaney, R. K.; Fenwick, G. R., Chemical and biological properties of indole glucosinolates (glucobrassicins): A review. *Food Chem. Toxicol.* **1988**, 26, 59-70.
  50. Song, D.; Liang, H.; Kuang, P.; Tang, P.; Hu, G.; Yuan, Q., Instability and structural change of 4-methylsulfinyl-3-butenyl isothiocyanate in the hydrolytic process. *J. Agric. Food Chem.* **2013**, 61, 5097-5102.

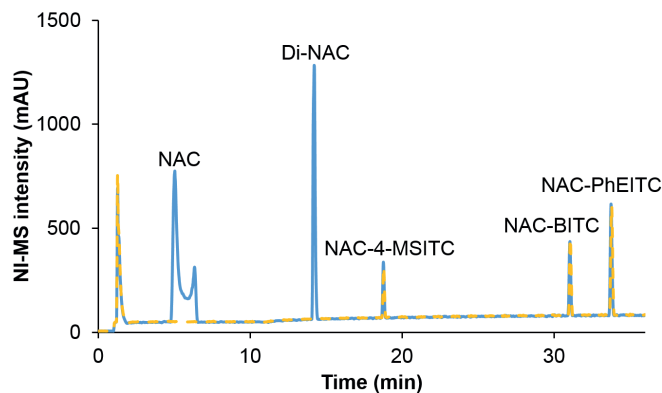
51. Buskov, S.; Hasselstrøm, J.; Olsen, C. E.; Sørensen, H.; Sørensen, J. C.; Sørensen, S., Supercritical fluid chromatography as a method of analysis for the determination of 4-hydroxybenzylglucosinolate degradation products. *J. Biochem. Biophys. Methods* **2000**, *43*, 157-174.
52. Román, J.; Castillo, A.; Cottet, L.; Mahn, A., Kinetic and structural study of broccoli myrosinase and its interaction with different glucosinolates. *Food Chem.* **2018**, *254*, 87-94.

## 3.7. Supplementary information

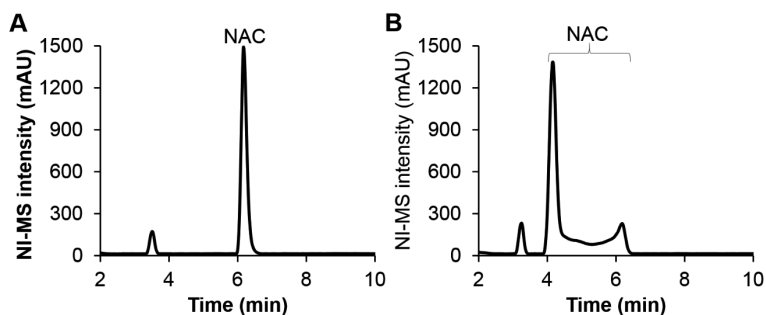
### 3.7.1. Supplementary figures



**Figure S3.1.** Base peak negative ion UHPLC-MS chromatograms of representative GSLs and ITCs in different solvents: GSLs in 0% (v/v) (A), 25% (B), and 50% (C) IPA, ITCs in 25% (D) and 50% (E) IPA. The order of elution remained, with a gradient of 0–6.7 min, isocratic on 0% (v/v) B; 6.7–35.9 min, linear gradient to 40% B; 35.9–37.4 min, linear gradient from 40% to 100% B; 37.4–44.7 min, isocratic on 100% B; 44.7–46.2 min, linear gradient from 100% to 0% B; 46.2–53.5 min, isocratic on 0% B. Concentration of GSLs and ITCs was consistently applied in the different solvents. Oven column temperature was set at 25 °C.

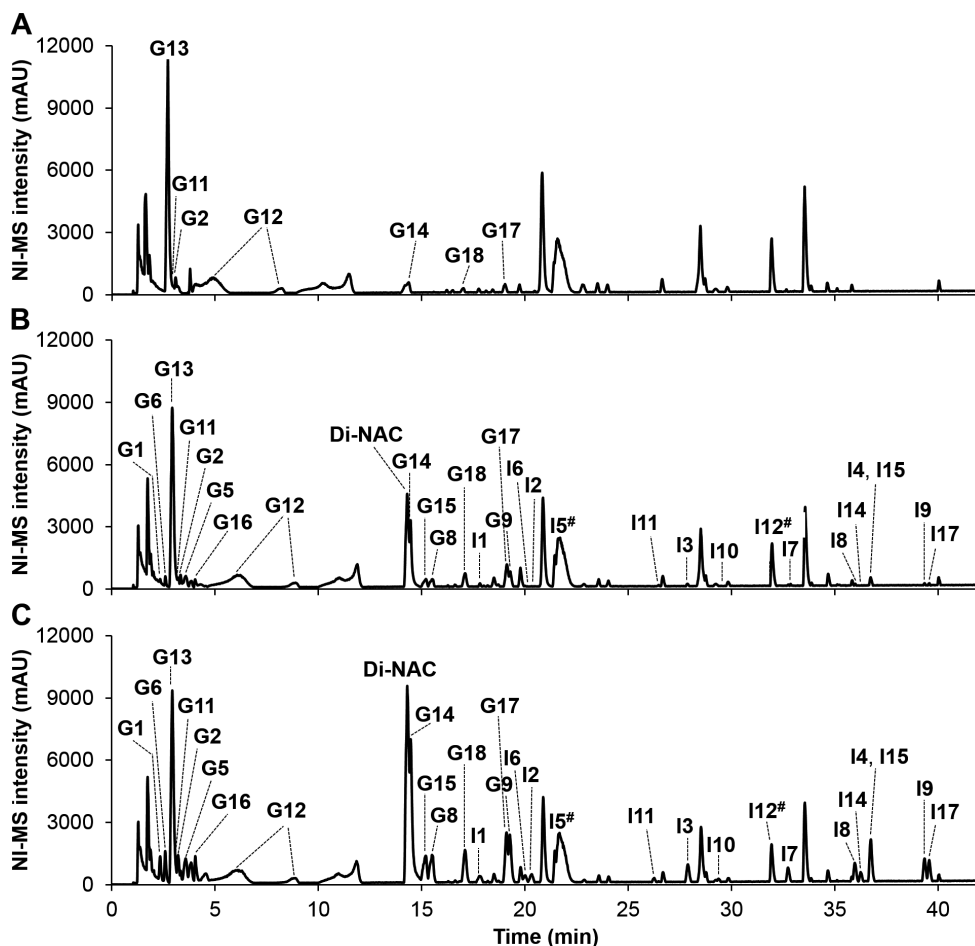


**Figure S3.2.** Base peak negative ion UHPLC-MS chromatograms of NAC-ITCs: obtained from derivatization of ITCs with NAC at 50 °C for 2 h (blue line) and authentic NAC-ITC standards (dashed yellow line). The concentration of ITCs and the NAC-ITC standards was 30  $\mu$ M.

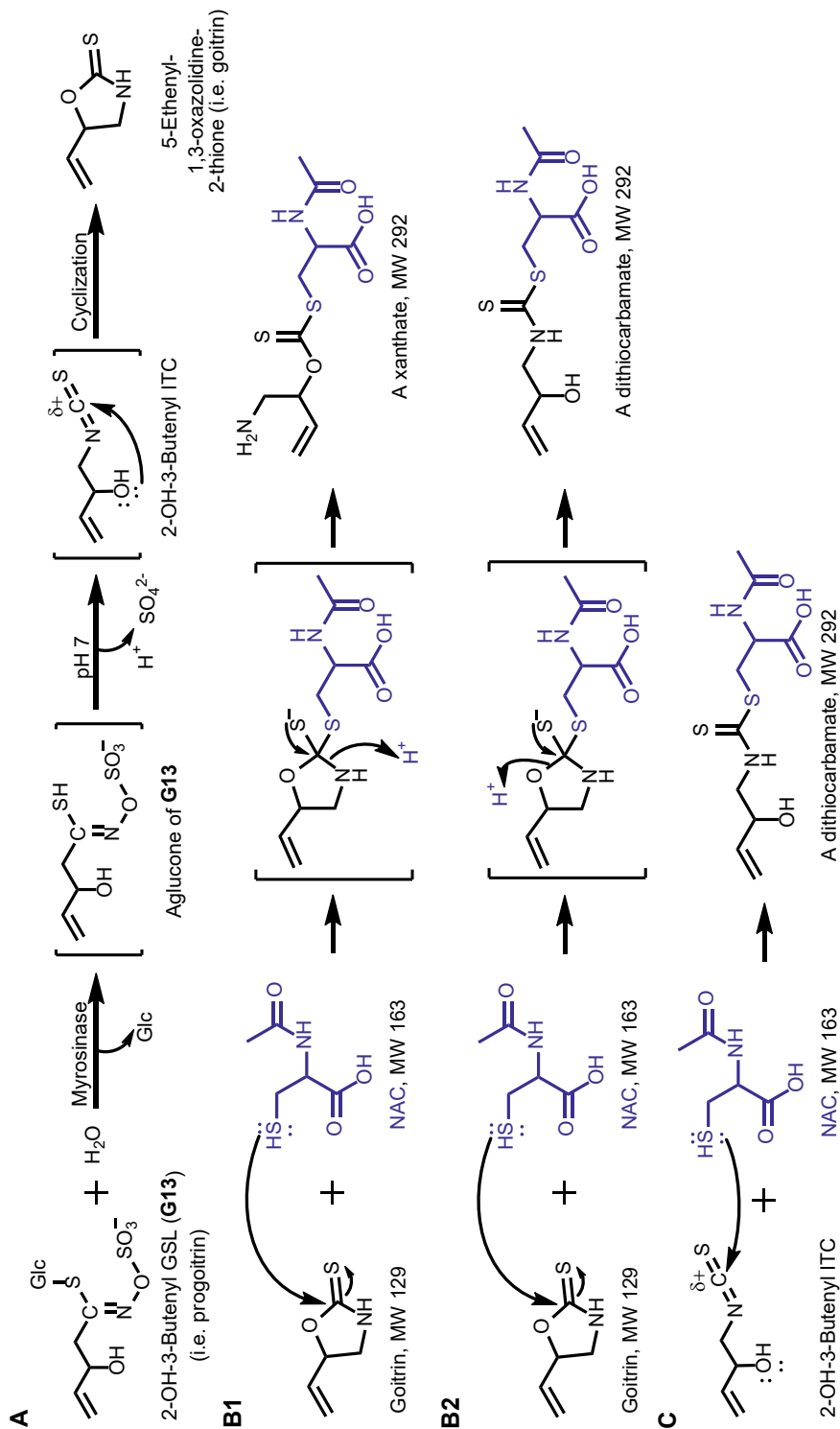


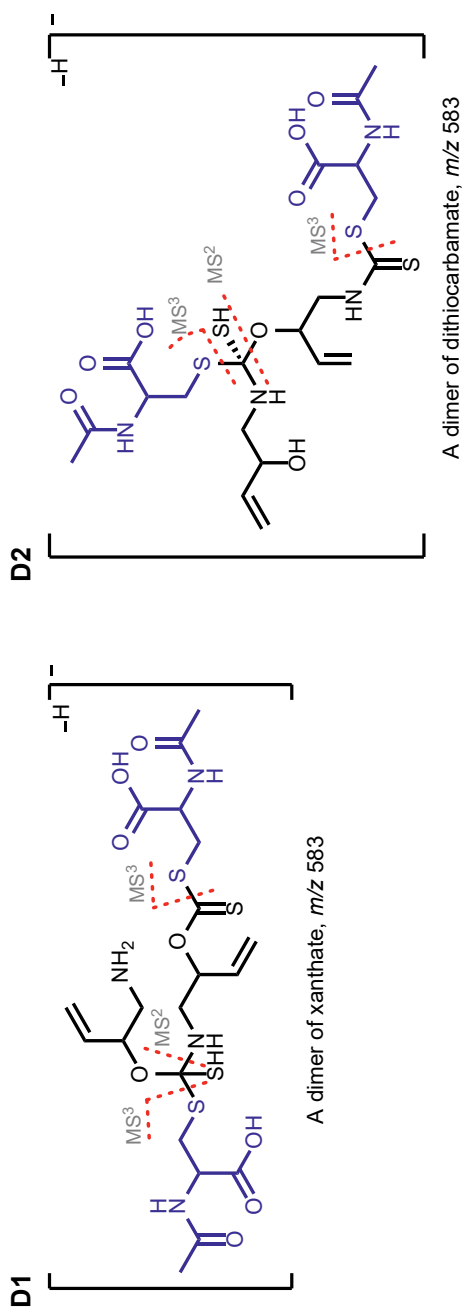
**Figure S3.3.** Base peak negative ion UHPLC-MS chromatograms of NAC in the absence of organic solvent (0% IPA) (**A**) and in 25% IPA (**B**). This is also the case for 3-butenyl GSL (**G12**) (data not shown). The peak eluted before 4 min is out of interest.



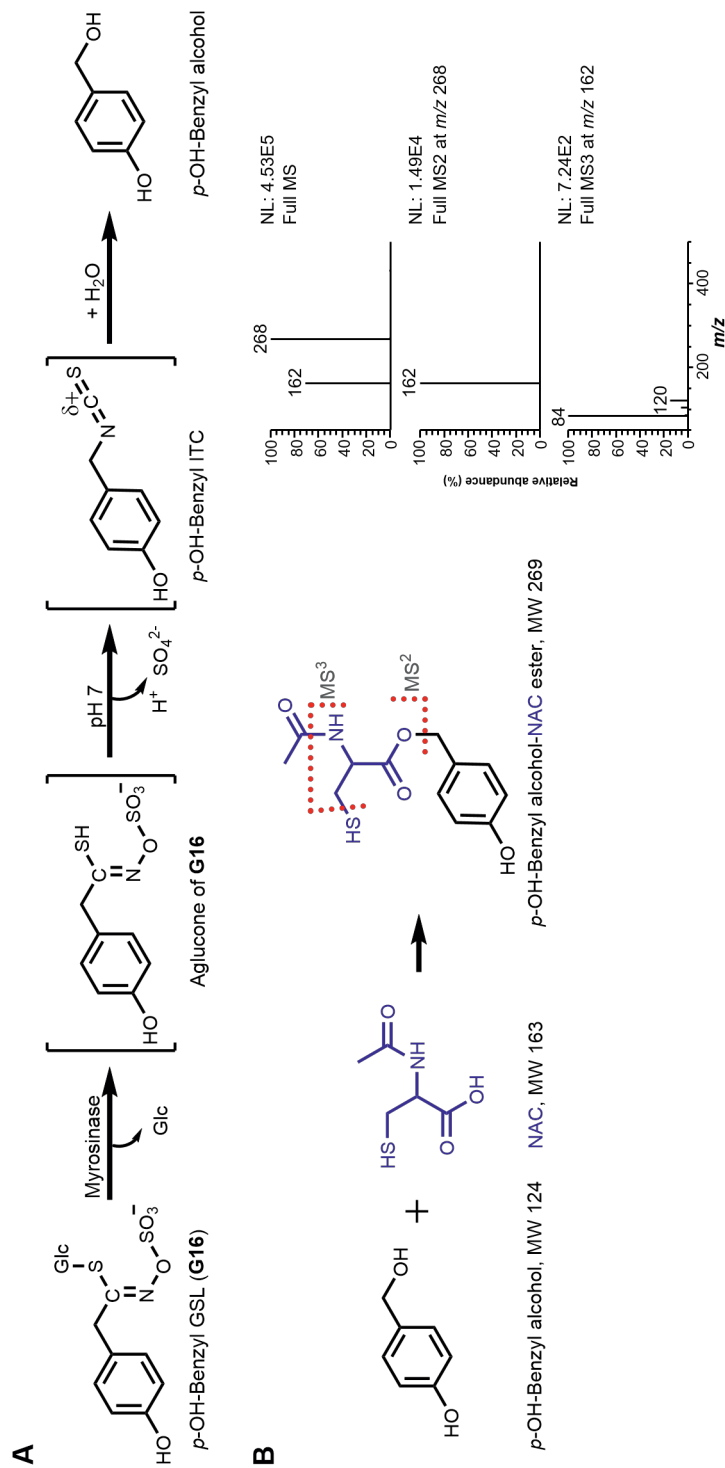


**Figure S3.4.** Base peak negative ion UHPLC-MS chromatograms of extracts of *B. napus* seed, non-spiked (A), spiked with standards of 14 GSLs and 15 ITCs at 10  $\mu$ M (B) and 30  $\mu$ M (C). ITCs were in a form of NAC derivatives. #I5 (NAC-4-MS-3-en-ITC) and I12 (NAC-BuITC) were co-eluted with constitutive compounds (out of our interest) having different molecular weight.

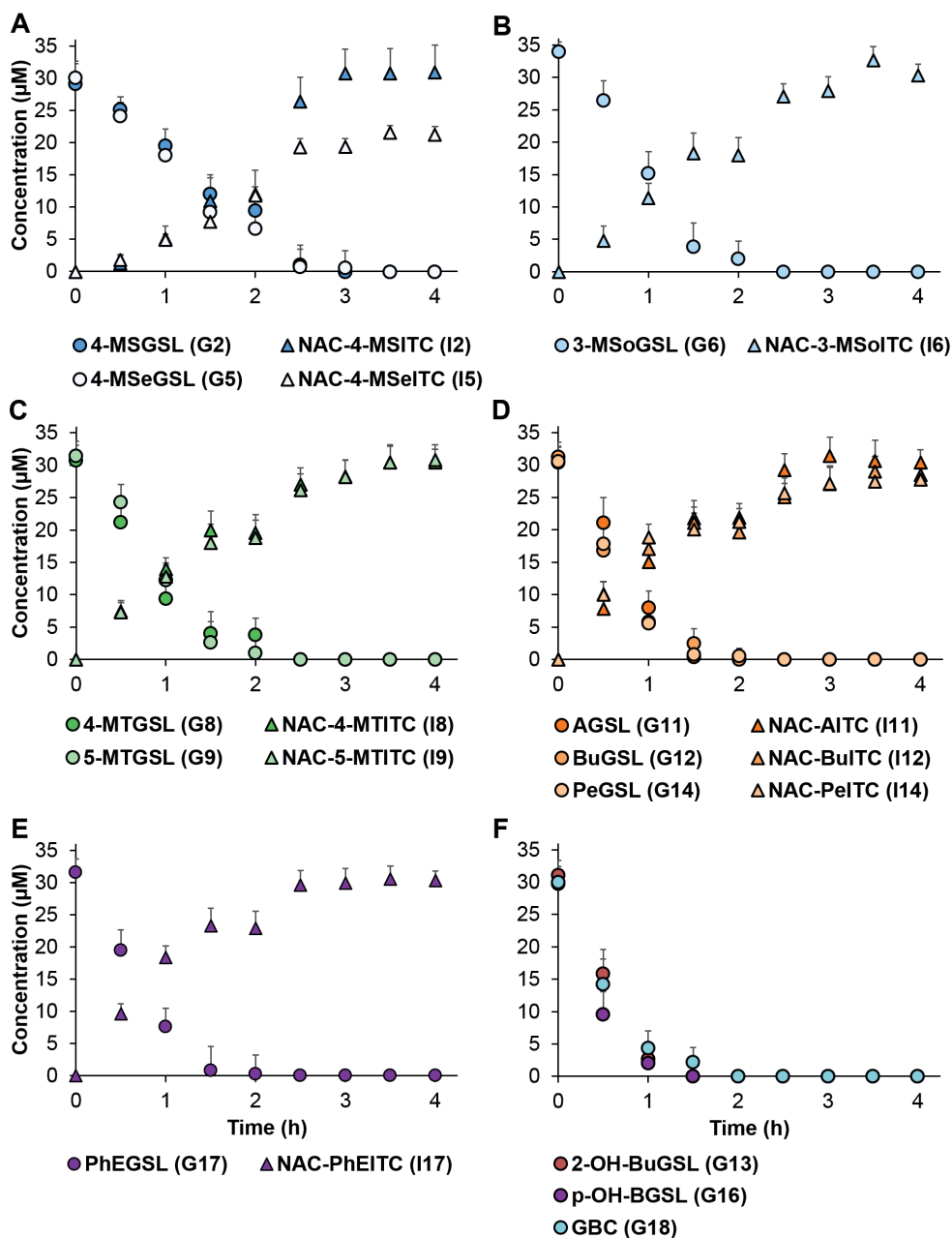




**Figure S3.5.** Hydrolysis scheme of (*R*)-2-OH-3-butenyl GSL (i.e. progointrin) by myrosinase forming unstable 2-OH-3-butenyl ITC which spontaneously undergoes cyclization forming 5-ethenyl-1,3-oxazolidine-2-thione (i.e. goitrin)<sup>1</sup> (**A**); plausible reaction between goitrin and NAC forming a xanthate (**B1**) or a dithiocarbamate (**B2**); reaction between unstable 2-OH-3-butenyl ITC and NAC forming a dithiocarbamate (**C**); a possible dimer of xanthate (**D1**) and dithiocarbamate (**D2**) having a similar fragmentation pattern.



**Figure S3.6.** Hydrolysis scheme of *p*-OH-benzyl GSL by myrosinase forming unstable *p*-OH-benzyl ITC which reacts with water forming *p*-OH-benzyl alcohol <sup>2</sup> (**A**); plausible reaction between *p*-OH-benzyl alcohol and NAC forming an ester and NAC forming an ester and its plausible fragmentation in NI-MS with the MS<sup>n</sup> spectra of the peak (**B**). The peak at *m/z* of 268 was appeared after 3-h incubation.



**Figure S3.7.** The decrease in concentration of GSLs (circles) and the increase in concentration of ITCs (triangles), analysed in a form of NAC derivatives, during enzymatic conversion by commercial myrosinase. The abbreviations and codes of GSLs and ITCs follow **Table 3.1**.

### 3.7.2. Supplementary table

**Table S3.1.** GSLs and NAC-ITCs whose calibration curves were employed to quantify analytes, whose calibration curves could not be made due to lack of standards.

Analyte	Calibration curve of
<b>GSL</b>	
2-OH-4-Pentenyl	( <i>R</i> )-2-OH-3-Butenyl ( <b>G13</b> )
3-(Methylthio)propyl	4-(Methylthio)butyl ( <b>G8</b> )
5-(Methylsulfinyl)pentyl	4-(Methylsulfinyl)butyl ( <b>G2</b> )
<b>ITC</b>	
5-(Methylsulfinyl)pentyl	4-(Methylsulfinyl)butyl ( <b>I2</b> )
<i>p</i> -OH-Benzyl	Benzyl ( <b>I15</b> )

### 3.7.3. Supplementary references

- Greer, M. A., Isolation from rutabaga seed of progoitrin, the precursor of the naturally occurring antithyroid compound, goitrin (1-5-vinyl-2-thioöxazolidone). *J. Am. Chem. Soc.* **1956**, *78*, 1260-1261.
- Buskov, S.; Hasselström, J.; Olsen, C. E.; Sørensen, H.; Sørensen, J. C.; Sørensen, S., Supercritical fluid chromatography as a method of analysis for the determination of 4-hydroxybenzylglucosinolate degradation products. *J. Biochem. Biophys. Methods* **2000**, *43*, 157-174.
- Andini, S.; Dekker, P.; Gruppen, H.; Araya-Cloutier, C.; Vincken, J.-P., Modulation of glucosinolate composition in Brassicaceae seeds by germination and fungal elicitation. *J. Agric. Food Chem.* **2019**, *67*, 12770-12779.
- Liang, X.; Lee, H. W.; Li, Z.; Lu, Y.; Zou, L.; Ong, C. N., Simultaneous quantification of 22 glucosinolates in 12 Brassicaceae vegetables by hydrophilic interaction chromatography–tandem mass spectrometry. *ACS Omega* **2018**, *3*, 15546-15553.
- Agerbirk, N.; Olsen, C. E.; Cipollini, D.; Ørgaard, M.; Linde-Laursen, I.; Chew, F. S., Specific glucosinolate analysis reveals variable levels of epimeric glucobarbarins, dietary precursors of 5-phenyloxazolidine-2-thiones, in watercress types with contrasting chromosome numbers. *J. Agric. Food Chem.* **2014**, *62*, 9586-9596.
- Fabre, N.; Poinso, V.; Debrauwer, L.; Vigor, C.; Tulliez, J.; Fourasté, I.; Moulis, C., Characterisation of glucosinolates using electrospray ion trap and electrospray quadrupole time-of-flight mass spectrometry. *Phytochem. Anal.* **2007**, *18*, 306-319.

---

## The interplay between antimicrobial activity and reactivity of isothiocyanates

---

This study aimed to determine antimicrobial activity (minimum inhibitory concentration, MIC; minimum bactericidal/fungicidal concentration, MBC/MFC) of novel ITCs against food spoilage and pathogenic Gram<sup>-</sup> bacteria, Gram<sup>+</sup> bacteria, and fungi. The activity of the long-chain (C9) 9-(methylthio)nonyl ITC (9-MTITC), 9-(methylsulfinyl)nonyl ITC (9-MSITC), and 9-(methylsulfonyl)nonyl ITC (9-MSoITC) was determined for the first time. Due to the electrophilicity of ITCs, the activity of ITCs was evaluated in nucleophile-rich and nucleophile-poor growth media. ITCs reacted via conjugation with components in a nucleophile-rich growth medium at a rate of 39-141  $\mu\text{mol L}^{-1} \text{h}^{-1}$ , depending on their side chain configuration and temperature. The reaction rates were lowered by a factor of 2-21 when using nucleophile-poor growth media. Consequently, the activity of ITCs was generally improved, with MSITC and MSoITC being the most positively affected (activity increased by a factor of > 4). 9-MSITC and 9-MSoITC had good activity (MIC  $\leq$  25  $\mu\text{g/mL}$ ) against Gram<sup>+</sup> bacteria and fungi. The short-chained (C3) analogues had good activity against Gram<sup>+</sup> bacteria and Gram<sup>-</sup> bacteria. The highest bactericidal/fungicidal activity was obtained for 9-MSITC and 9-MSoITC (MBC/MFC 17.5-25  $\mu\text{g/mL}$ ). Overall, MSITC and MSoITC might be potential new natural food preservatives, but their reactivity with food matrix components should be considered.

**Keywords:** antibacterial, Brassicaceae, electrophilic, food preservative, glucosinolate

Based on: Andini, S.; Araya-Cloutier, C.; Waardenburg, L.; den Besten, H. M. W.; Vincken, J.-P., The interplay between antimicrobial activity and reactivity of isothiocyanates. *LWT*. **2020**, 109843.

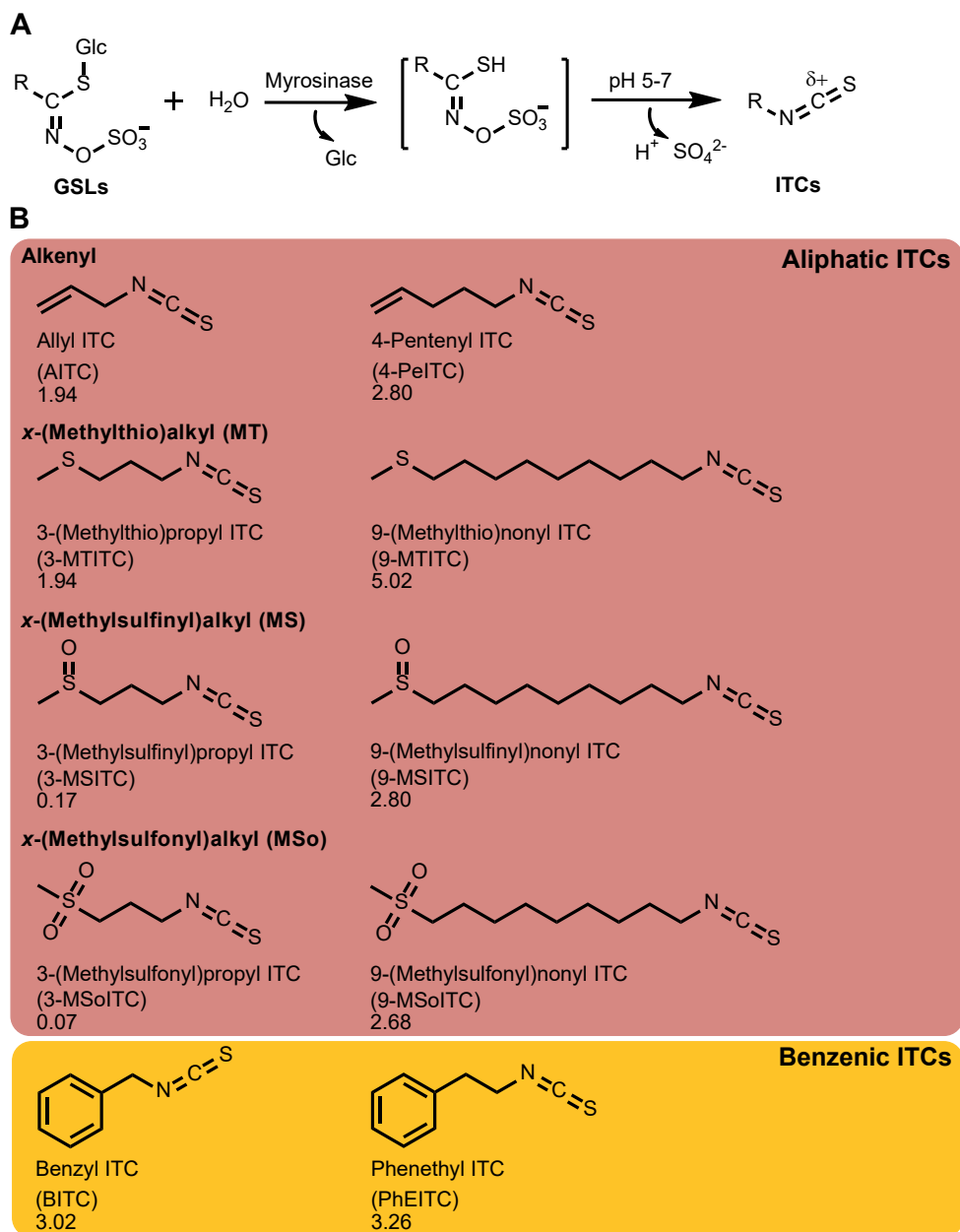
## 4.1. Introduction

Controlling growth of pathogenic and spoilage microorganisms is an ongoing challenge to food industries, especially with the increasing consumer demand for natural preservation methods. Spices, essential oils, and condiments belonging to the plant family of Brassicaceae are known to contain antimicrobial compounds.<sup>1,2</sup> Mustard and wasabi are well-known condiments. Allyl isothiocyanate (AITC) is the major active component in these condiments and has extensively been reported to possess antimicrobial activity against various microorganisms.<sup>3-5</sup> The use of natural AITC as a food preservative is allowed in Japan<sup>6</sup> and has gained Generally Recognized as Safe (GRAS) notice by the U.S. Food and Drug Administration.<sup>7</sup>

ITCs are structurally diverse and naturally obtained from glucosinolates (GSLs), due to the activity of myrosinase (**Figure 4.1A**).<sup>8</sup> ITCs are divided into two classes: aliphatic and benzenic, and the aliphatic consists of various subclasses, e.g. alkenyl, *x*-(methylthio)alkyl (MTITC), *x*-(methylsulfinyl)alkyl (MSITC), and *x*-(methylsulfonyl)alkyl (MSoITC) (**Figure 4.1B**).<sup>9</sup> Some studies reported that benzenic ITCs showed stronger activity against Gram<sup>+</sup> and Gram<sup>-</sup> bacteria than aliphatic ITCs, including AITC.<sup>10-13</sup> This indicates that AITC, which has been the traditional ITC considered for improving shelf life of foods, is not the most potent. Furthermore, other subclasses of aliphatic ITCs, i.e. MTITC, MSITC, and MSoITC, were found to have activity equal or higher than benzenic ITCs.<sup>14,15</sup> However, previous studies have only tested the short-chained (up to C5) ITCs and C8 MSITC. To date, the long-chained (C9) MTITC, MSITC, and MSoITC have never been studied for their antimicrobial activity.

Growth media can significantly influence the antimicrobial activity of ITCs. The electrophilic carbon of ITCs ( $-N=C=S$ ) makes them reactive towards nucleophiles, e.g. thiol ( $-SH$ ), amine ( $-NH-$ ,  $-NH_2$ ), carboxyl ( $-COOH$ ), and hydroxyl ( $-OH$ ) groups.<sup>16</sup> Growth media, composed of protein hydrolysates and/or pure amino acids, contain such nucleophiles. Consequently, ITCs can react with components in growth media leading to a reduced antimicrobial activity. A previous study demonstrated that an ITC lost its antimicrobial activity due to pre-incubation in a rich undefined growth medium.<sup>17</sup> Other studies showed decreased antimicrobial activity of ITCs upon incubation with glutathione and Cys, as well as with other amino acids in excess amount (20 mmol/L,  $\geq 1.5$  mg/mL).<sup>12,18</sup> To date, the antimicrobial activity of different ITCs in relation to the nucleophilic richness of growth media has not been addressed.





**Figure 4.1.** Conversion of GSLs to ITCs by myrosinase at pH 5-7 (**A**) and 10 ITCs used in this study comprising of aliphatic (red box) and benzenic (yellow box) classes (**B**). The electrophilic carbon atom in the ITCs is indicated as C $\delta^+$ . ITCs vary in the type (i.e. subclass) and the alkyl chain length. In **B**, the number underneath the name of the ITC is its  $\log_{10}P$  (at pH 7.2), i.e. a  $\log_{10}$  of partition coefficient of a molecule between the lipid phase (octanol) and aqueous phase (water), calculated by the software ChemDraw Professional (version 18.0.0.231 (4029), PerkinElmer Informatics, Inc., Waltham, MA, U.S.A).

Given the above, this study aimed to determine systematically the antimicrobial activity of 10 ITCs from 5 subclasses and different chain length, including 9-(methylthio)nonyl ITC (9-MTITC), 9-(methylsulfinyl)nonyl ITC (9-MSITC), and 9-(methylsulfonyl)nonyl ITC (9-MSoITC) for the first time, against food spoilage and pathogenic Gram<sup>-</sup> bacteria, Gram<sup>+</sup> bacteria, and fungi. GSL precursors of these 10 ITCs can be naturally obtained.<sup>19,20</sup> The activity of ITCs was evaluated in both nucleophile-rich and nucleophile-poor growth media to assess the effect of the assay conditions on the antimicrobial properties of ITCs. Besides, the concentration of ITCs upon incubation with growth media was monitored to determine the reaction rate of ITCs with nucleophiles present in the growth media.

## 4.2. Materials and methods

### 4.2.1. Standard ITCs, other chemicals, and growth media

Standards of AITC, 4-pentenyl ITC (PeITC), 3-(methylthio)propyl ITC (3-MTITC), benzyl ITC (BITC), and phenethyl ITC (PhEITC), phenylalanine-arginine  $\beta$ -naphthylamide (PABN), and NaCl were from Sigma-Aldrich (St. Louis, MO, USA). Standards of 9-MTITC, 3-(methylsulfinyl)propyl ITC (3-MSITC), 9-MSITC, 3-(methylsulfonyl)propyl ITC (3-MSoITC), and 9-MSoITC were from Abcam (Cambridge, U.K.). Dimethyl sulfoxide (DMSO) was from Ducheda Biochemie (Haarlem, The Netherlands). Ultra-high performance liquid chromatography (UHPLC) grade isopropanol (IPA), formic acid (FA) 0.1% (v/v) in water, and FA 0.1% (v/v) in acetonitrile (ACN) were from Biosolve B.V. (Valkenswaard, The Netherlands).

Growth media: tryptone soya agar (TSA), tryptone soya broth (TSB), malt extract broth (MEB), and malt extract agar (MEA) were from Oxoid Limited (Hampshire, U.K.); bacteriological agar from VWR International B.V. (Valkenswaard, The Netherlands); bacto brain heart infusion (BHI) from Becton, Dickinson and Company (Franklin Lakes, NJ, U.S.A.); and RPMI 1640 from Thermo Fisher Scientific Inc. (Waltham, MA, U.S.A.). Peptone physiological salt solution (PPS) was from Tritium Microbiologie (Eindhoven, The Netherlands). High purity water was produced using a Milli-Q A10 Gradient system (18.2 M $\Omega$ .cm, 3  $\mu$ g/kg total organic carbon (TOC)) (Merck Millipore, Darmstadt, Germany).

### 4.2.2. Microbial cultures

A collection of microorganisms (**Table 4.1**), including the various strains of *B. cereus* isolated from food sources,<sup>21</sup> were kindly provided by the laboratory of Food Microbiology, Wageningen University, The Netherlands.

**Table 4.1.** Microbial strains tested in the study, their type and growth conditions. The inoculum size that was applied in the assays was  $4.0 \pm 0.4 \log_{10}$ (CFU/mL).

Microbial strains	Type of microorganism	Liquid growth media <sup>a</sup>	Growth temperature (°C)	Incubation length (h)
<i>Listeria monocytogenes</i> EGD-e	Gram <sup>+</sup> bacterium	TSB 5× diluted TSB	37	24
<i>Staphylococcus aureus</i> ATCC 25923	Gram <sup>+</sup> bacterium	TSB 5× diluted TSB	37	24
<i>Bacillus cereus</i> ATCC 14579, ATCC 10987, B4078, B4080, B4082, B4084, B4085, B4086, B4087, B4088, B4116, B4117, B4118, B4147, B4153, B4155, B4158	Gram <sup>+</sup> bacterium	TSB 10× diluted TSB	30	24
<i>Escherichia coli</i> K12	Gram <sup>-</sup> bacterium	TSB 10× diluted TSB	37	24
<i>Salmonella enterica</i> Typhimurium S2 505	Gram <sup>-</sup> bacterium	TSB 10× diluted TSB	37	24
<i>Pseudomonas aeruginosa</i> ATCC 27853 (DSM 1117)	Gram <sup>-</sup> bacterium	TSB 10× diluted TSB	37	24
<i>Candida holmii</i> CBS 135	Yeast	MEB	30	48
<i>Saccharomyces cerevisiae</i> S288C	Yeast	MEB	30	48
<i>Aspergillus niger</i> LU1500 spores	Mold	RPMI 1640	30	48

<sup>a</sup> Dilution was not applied for MEB and RPMI 1640 in the antifungal assay since MEB and RPMI 1640 were considered as nucleophile-poor growth media just like 5× and 10× diluted TSB.

#### 4.2.3. Analysis of amino acid composition

Free and total amino acid compositions of TSB, MEB, and RPMI 1640 were determined in duplicate by using the ISO13903:2005 method,<sup>22</sup> adjusted for microscale. Asn and Gln were measured together with Asp and Glu. Trp was determined on the basis of AOAC 988.15.

#### 4.2.4. Antimicrobial assays

Antimicrobial activity of ITCs was determined by following the broth microdilution assay with growth temperature, media, and incubation length specified in **Table 4.1** for each microbial species. The inoculum was prepared by streaking a –80 °C glycerol stock onto BHI agar plates (bacteria) or MEA plates (yeasts). The plates were incubated at 30 or 37 °C for 24 h (bacteria) or 48 h (yeasts). Then, one colony was transferred to 10 mL BHI (bacteria) or MEB (yeasts) and further incubated for 18 h (bacteria) or 24 h (yeasts) at the same temperature as was in the previous step. Afterwards, the culture was diluted in the growth medium to

reach an inoculum size of  $4.0 \pm 0.4 \log_{10}(\text{CFU/mL})$ . A spore suspension of *A. niger* was prepared according to Aisyah *et al.*<sup>23</sup> The spore suspension was collected in a sterile tube and diluted in RPMI 1640 to reach the inoculum size.

Stock solutions of ITCs were prepared at 10 mg/mL in DMSO. A series of concentrations was prepared fresh in growth media. Equal volumes (100  $\mu\text{L}$ ) of compound solution and microbial inoculum were mixed into wells in a 96-well plate. The final concentrations of ITCs varied from 12.5  $\mu\text{g/mL}$  to 200.0  $\mu\text{g/mL}$ . The final concentration of DMSO was max. 2% (v/v), which did not affect the microbial growth (data not shown). Several ITCs were also tested with PA $\beta$ N 25  $\mu\text{g/mL}$ .<sup>24</sup> To evaluate the variation of activity of ITCs among strains within a species, 15 food isolates and 2 reference strains of *B. cereus* were tested against the most active ITC.

Positive control (ampicillin 1.5-15.0  $\mu\text{g/mL}$  for bacteria, except *P. aeruginosa* - ciprofloxacin 1.5  $\mu\text{g/mL}$ , and amphotericin B 4.0  $\mu\text{g/mL}$  for fungi), negative control (the inoculum in the growth media with DMSO 2%), and blank (the growth media) were included in every assay. The cells were incubated with a constant periodic shaking at a certain temperature (**Table 4.1**). The microbial growth was monitored spectrophotometrically (SpectraMax M2e/iD3, Molecular Devices, USA) at OD<sub>600</sub> (OD<sub>540</sub> for assays with RPMI 1640), every 10 min for 24 h (bacteria) or 48 h (fungi). Antimicrobial activity of ITCs was evaluated in three independent biological repetitions, each performed in triplicate.

Time-to-detection (TTD) of growth was defined as the time to have an increase in OD of 0.05 units.<sup>25</sup> When this change in OD was not observed after 24 h or 48 h, cell viability was checked by plate counting to determine MIC and MBC/MFC.<sup>26</sup> MIC was the lowest concentration of compounds that resulted in an inoculum size after incubation equal or less than the initial inoculum size. MBC or MFC was the lowest concentration that resulted in no growth (>99% bacterial or fungal inactivation from the initial inoculum).<sup>24,27</sup>

#### 4.2.5. Liquid chromatography-mass spectrometry (LC-MS) analysis of ITCs in growth media

Reactivity of ITCs in growth media was investigated by using 3-MSITC and 9-MSITC, as representatives. ITCs at 200.0  $\mu\text{g/mL}$  were incubated for 24 h in growth media listed in **Table 4.1**. Samples were analyzed at 0, 2, 4, 6, 8, and 24 h. Prior to the analysis, samples were diluted 4 times and conditioned in IPA 25% (v/v). Concentrations of ITCs were plotted against incubation time. The slopes ( $\mu\text{mol L}^{-1} \text{h}^{-1}$ ) of the graphs for the first 8 h (minimum 3 data points) were considered and referred to as reaction rates of ITCs with nucleophiles present in growth media.

LC-MS analysis was performed on an Accela UHPLC system (Thermo Scientific, San Jose, CA, U.S.A.) coupled to an LTQ Velos electrospray ionization (ESI) ion trap MS (Thermo Scientific). Sample (1  $\mu\text{L}$ ) was injected onto an Acquity UPLC-BEH shield RP18 column (2.1 mm i.d.  $\times$  150 mm, 1.7  $\mu\text{m}$  particle size; Waters,

Milford, MA, USA) with an Acquity UPLC BEH shield RP18 VanGuard precolumn (2.1 mm i.d. × 5 mm, 1.7 µm particle size; Waters). The sample tray and the column oven were controlled at 4 °C and 25 °C, respectively. FA 0.1% in water (eluent A) and FA 0.1% in ACN (eluent B) were used at a flow rate of 300 µL/min. The elution gradient used was 0-6.7 min, isocratic on 0% (v/v) B; 6.7-35.9 min, linear gradient to 40% B; 35.9-37.4 min, linear gradient to 100% B; 37.4-44.7 min, isocratic on 100% B; 44.7-46.2 min, linear gradient to 0% B; 46.2-53.0 min, isocratic on 0% B. The spectra were acquired in positive ionization (PI) mode with a source voltage of 3.5 kV. The identification and quantification of ITCs were performed in Xcalibur (v.2.2, Thermo Scientific). Calibration curves of ITCs were within 0.5-50 µg/mL.

#### 4.2.6. Statistical analysis

To test for significant differences between amino acid compositions among TSB, MEB, and RPMI 1640, data were statistically evaluated by one-way analysis of variance (ANOVA), followed by Tukey *post hoc* test using IBM SPSS Statistic v.23 software (SPSS Inc., Chicago, IL, USA).

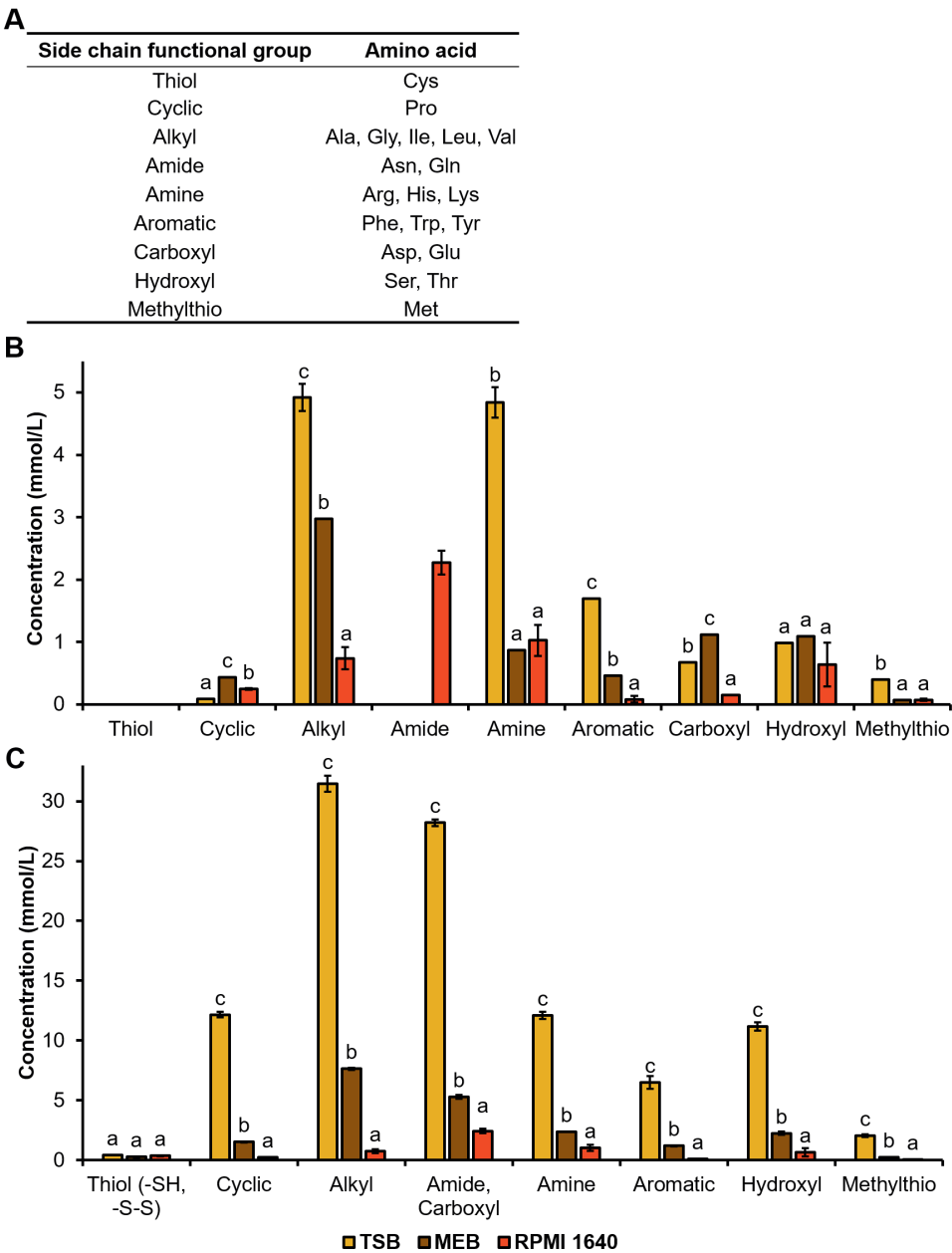
### 4.3. Results

#### 4.3.1. Amino acid compositions of growth media

The nucleophile profiles of growth media used in this study were based on the amino acid compositions. TSB and MEB are undefined media composed of enzymatic digest of plant and animal protein sources, whereas RPMI 1640 is a defined medium composed of free amino acids and other components (e.g. glutathione and cystine). According to the manufacturers, the content of the enzymatic digest of protein sources in TSB, MEB, and RPMI 1640 was 20 g/L, 3 g/L, and 0 g/L respectively.

Twenty amino acids are classified according to the side chain functional groups (**Figure 4.2A**) in 9 groups. Brotzel & Mayr demonstrated a nucleophilicity parameter (*N*) of 15 free amino acids and found that thiol-containing amino acid (Cys, *N* = 23.4) was the most nucleophilic,<sup>28</sup> in line with Hermanson.<sup>16</sup> The second most nucleophilic was the cyclic amino acid (Pro, *N* = 18.1). The other 13 amino acids had *N* in the same range (12.7-14.1) regardless of the side chain functional groups (alkyl, amide, amine, aromatic, carboxyl, hydroxyl). Hermanson described the nucleophilicity order of side chains of amino acids as follows: thiol > amine > carboxyl = hydroxyl.<sup>16</sup>

**Figure 4.2B** shows the free amino acid compositions of TSB, MEB, and RPMI 1640, according to the side chain classification. Free Cys was absent, and free Pro was present in low amount in TSB (0.1 mmol/L, 0.01 mg/mL), MEB (0.4 mmol/L, 0.05 mg/mL), and RPMI 1640 (0.3 mmol/L, 0.03 mg/mL). Furthermore, the sum of other free amino acids was 13.5 mmol/L (1.90 mg/mL) in TSB, 6.6 mmol/L (0.83 mg/mL) in MEB, and 5.0 mmol/L (0.71 mg/mL) in RPMI 1640.



**Figure 4.2.** Amino acid compositions of TSB (golden), MEB (brown), and RPMI 1640 (red): classification of amino acids (A), free amino acid content (B), and total amino acid content (C). The error bars represent the standard deviation from two repetitions. Some error bars are absent due to identical numbers. Different letters within amino acid classes denote significant differences ( $p < 0.05$ ) among growth media.

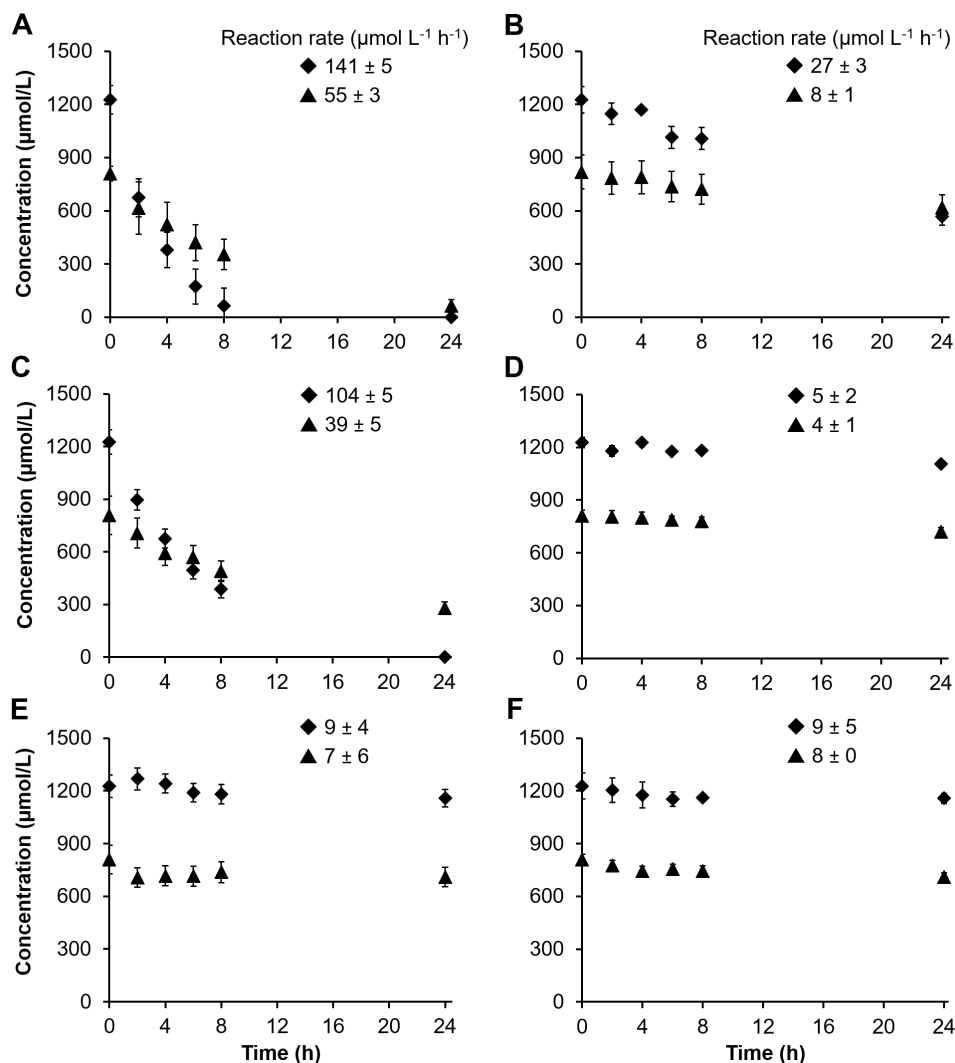
**Figure 4.2C** shows total amino acid compositions of TSB, MEB, and RPMI 1640. It is worth to note that in the analysis of total amino acid composition, all peptide (i.e. amide) bonds and disulfide bonds were broken down. Consequently, concentrations of the total bound thiol-containing amino acid (Cys) residues originated from both free thiol ( $-SH$ ) groups and disulfide ( $-S-S-$ ) bonds. Furthermore, concentrations of the total carboxyl-containing amino acids included amide-containing amino acids (section 4.2.3). Concentrations of total Cys residues were low (0.3-0.4 mmol/L, 0.03-0.05 mg/mL) in TSB, MEB, and RPMI 1640. For TSB and MEB as undefined growth media, it is unknown whether the bound Cys was present with free thiol groups or with disulfide bonds. Meanwhile, for RPMI 1640 as a defined growth medium, it is known from the manufacturer that the bound Cys consisted of 0.2 mmol/L (0.05 mg/mL) cystine (disulfide bond) and 0.003 mmol/L (0.0009 mg/mL) glutathione (free thiol group). Furthermore, Pro was present in high amount in TSB (12.2 mmol/L, 1.40 mg/mL) and low amounts in MEB (1.5 mmol/L, 0.18 mg/mL) and RPMI 1640 (0.3 mmol/L, 0.03 mg/mL). The total content of other amino acid residues in TSB (91.5 mmol/L, 12.14 mg/mL) was 5 and 18 $\times$  higher than that in MEB (19.0 mmol/L, 2.41 mg/mL) and RPMI 1640 (5.0 mmol/L, 0.71 mg/mL), respectively.

Based on the total amino acid contents, TSB is considered and referred to as a nucleophile-rich growth medium, whereas MEB, RPMI 1640, 5 $\times$  diluted TSB, and 10 $\times$  diluted TSB are considered and referred to as nucleophile-poor growth media.

#### 4.3.2. Reactivity of ITCs towards nucleophile-rich and nucleophile-poor growth media

The nucleophiles present in growth media can reduce the concentration of ITCs before they exert their antimicrobial activity. Our previous study indicated that among 15 ITCs, 3-MSITC was one of the most reactive ITCs towards a nucleophile *N*-acetyl-L-cysteine.<sup>29</sup> Therefore, we measured the reaction rates of 3-MSITC and 9-MSITC (as the long-chain analogue) in the different nucleophile-rich and nucleophile-poor growth media, without inoculum, at different temperatures (**Figure 4.3**) according to the conditions applied in the antimicrobial assays (**Table 4.1**).

At 37 °C in nucleophile-rich TSB, the concentrations of 3-MSITC and 9-MSITC were rapidly decreased at a rate of 141 and 55  $\mu\text{mol L}^{-1} \text{h}^{-1}$ , respectively (**Figure 4.3A**). After 24-h incubation, the concentrations of 3-MSITC and 9-MSITC were below the detection limit ( $< 6 \mu\text{mol/L}$ ) and 60  $\mu\text{mol/L}$ , respectively. Meanwhile, at 37 °C in the nucleophile-poor 10 $\times$  diluted TSB, the concentrations of 3-MSITC and 9-MSITC were decreased at a rate of 27 and 8  $\mu\text{mol L}^{-1} \text{h}^{-1}$ , respectively (**Figure 4.3B**), i.e. 5-7 $\times$  less rapidly than in the nucleophile-rich TSB. Additionally, the reaction rates of 3-MSITC and 9-MSITC in the nucleophile-poor 5 $\times$  diluted TSB at 37 °C were measured since this condition was applied in the antimicrobial assay (**Table 4.1**); the rates were 58 and 16  $\mu\text{mol L}^{-1} \text{h}^{-1}$ , respectively, which were 2-3 $\times$  lower than those in the nucleophile-rich TSB (**Figure S4.1**).



**Figure 4.3.** The decrease of concentration of 3-MSITC (diamonds) and 9-MSITC (triangles) during incubation at 37 °C in TSB (A), 37 °C in 10× diluted TSB (B), 30 °C in TSB (C), 30 °C in 10× diluted TSB (D), 30 °C in MEB (E), and 30 °C in RPMI 1640 (F). The initial concentration of ITCs in all experiments was 200 μg/mL (i.e. 3-MSITC 1227 μM and 9-MSITC 810 μM). The concentrations of 3-MSITC at 24 h in A and C were below detection limit (< 6 μmol/L). The detection limit of 9-MSITC was below 2 μmol/L. The error bars represent the standard deviation from three independent repetitions. The reaction rate explains the decrease in concentration of ITCs during the first 8 h with a minimum of 3 data points.

At 30 °C in nucleophile-rich TSB, the concentrations of 3-MSITC and 9-MSITC were also rapidly decreased at a rate of 104 and 39 μmol L<sup>-1</sup> h<sup>-1</sup>, respectively (Figure



**4.3C).** Meanwhile, at 30 °C in the nucleophile-poor 10× diluted TSB, the concentrations of ITCs were relatively stable over time (a reaction rate of 4-5  $\mu\text{mol L}^{-1} \text{h}^{-1}$ , **Figure 4.3D**). Decreasing the amount of nucleophiles by 10× increased ITC stability by 10× or more. Furthermore, the reaction rates of ITCs in nucleophile-poor MEB and RPMI 1640 (**Figures 4.3E-F**) were comparable to those in the nucleophile-poor TSB. It is noteworthy to clarify that MEB was at pH 5.4, whereas TSB and RPMI 1640 were at pH 7.4, and that low pH is known to decrease the reaction rate of ITCs and nucleophiles.<sup>30</sup>

### 4.3.3. Antimicrobial activity of ITCs

**Table 4.2** displays the antibacterial activity (MIC and MBC) of 10 ITCs against 6 species in the nucleophile-rich growth medium (TSB). The long-chained 9-MSoITC had a good activity (MIC 25  $\mu\text{g/mL}$ ) against *B. cereus*, and a moderate activity (MIC 50-100  $\mu\text{g/mL}$ ) against *L. monocytogenes* and *S. aureus*. The lack of activity (MIC > 200  $\mu\text{g/mL}$ ) of ITCs against the Gram<sup>-</sup> bacteria was not improved in the presence of Pa $\beta$ N (broad spectrum efflux pump inhibitor) (data not shown), indicating that the lack of activity was not related to the efflux pump systems. MBC  $\leq$  200  $\mu\text{g/mL}$  was observed only for few ITCs against *B. cereus* and *L. monocytogenes*, with the lowest MBC of 50  $\mu\text{g/mL}$  obtained for 9-MSoITC against *B. cereus*. In general, the activity of most ITCs in the nucleophile-rich medium was low.

**Table 4.2.** Minimum inhibitory concentrations (MIC) and minimum bactericidal concentrations (MBC) of ITCs against various microbes in nucleophile-rich media.

ITC	MIC (MBC), $\mu\text{g/mL}$ <sup>a</sup>					
	Gram <sup>-</sup> bacteria <sup>b</sup>			Gram <sup>+</sup> bacteria		
	<i>Ec</i>	<i>ST</i>	<i>Pa</i>	<i>Bc</i> <sup>c</sup>	<i>Lm</i>	<i>Sa</i>
AITC	>200 <sup>d</sup>	>200	>200	>200	>200	>200
PeITC	>200	>200	>200	>200	>200	>200
3-MTITC	>200	200 (>200)	>200	>200	>200	>200
9-MTITC	>200	>200	>200	>200	>200	>200
3-MSITC	>200	>200	>200	>200	>200	>200
9-MSITC	>200	>200	>200	50 (100)	100-200 (>200) <sup>e</sup>	>200
3-MSoITC	>200	>200	>200	>200	>200	>200
9-MSoITC	>200	>200	>200	25 (50)	50-100 (100)	50-100 (>200)
BITC	>200	200 (>200)	>200	100 (200)	>200	>200
PhEITC	>200	>200	>200	100-200 (200)	>200	>200

<sup>a</sup> Data were obtained from three independent biological repetitions.

<sup>b</sup> *Ec* = *E. coli*, *ST* = *S. Typhimurium*, *Pa* = *P. aeruginosa*, *Bc* = *B. cereus*, *Lm* = *L. monocytogenes*, *Sa* = *S. aureus*.

<sup>c</sup> Data is for *B. cereus* ATCC 14579.

<sup>d</sup> The highest tested concentration was 200  $\mu\text{g/mL}$ .

<sup>e</sup> Two values separated by a dash indicated that the definite MIC was not obtained because a concentration in between (e.g. 150  $\mu\text{g/mL}$ ) was not tested. Some cases, e.g. 100-200 (200), mean that at the lower concentration (e.g. 100  $\mu\text{g/mL}$ ) the cell count in the cell viability test was above the initial inoculum size, but at the higher concentration (e.g. 200  $\mu\text{g/mL}$ ) the cell count equalled >99% cell inactivation of the initial inoculum.

**Table 4.3** displays the antimicrobial activity (MIC and MBC, MFC) of the same 10 ITCs against 9 bacterial and fungal species in the nucleophile-poor growth media (**Table 4.1**). The antibacterial activity of ITCs improved; 16 new MIC values and 13 new MBC values (MIC/MBC < 200 µg/mL) were obtained (**Table 4.3**) in comparison with the results in nucleophile-rich TSB (**Table 4.2**). The only exception was against *P. aeruginosa*. The most remarkably improved antibacterial activity in the nucleophile-poor TSB was observed for 3-MSITC and 3-MSoITC (from MIC > 200 µg/mL to MIC 12.5-25 µg/mL) against *E. coli* and *B. cereus*. The decrease in nucleophile richness of growth media changed the antibacterial activity profile of most ITCs from having low activity (MIC > 200) to having a good activity (MIC ≤ 25 µg/mL). It is worth to note that the effect of growth media dilution on the growth of the tested bacteria and on the susceptibility towards traditional antibiotics was checked. The growth of the tested bacteria (indicated by their TTD) in control experiments without antimicrobials in the nucleophile-poor TSB had less than 1.5 h delay in comparison to that in nucleophile-rich TSB (**Table S4.1**). Also, MIC values of the control antibiotics were the same in nucleophile-rich and nucleophile-poor TSB (**Table S4.2**). These results indicate that the level of TSB dilution made in this study did not influence the growth and susceptibility of the bacteria, and that the improved activity of ITCs in the nucleophile-poor TSB was mainly due to the reduced reaction of ITCs with the media components. Antimicrobial activity of ITCs was affected negatively by nucleophile richness in growth media. Decreasing the nucleophile richness of the growth media 5-10× improved the antimicrobial activity of ITCs by at least 4× to 16×.

ITCs with a good activity came from subclasses MSITC and MSoITC (**Table 4.3**). From all bacterial species, *B. cereus* was found to be the most susceptible. The short-chained (C3) and long-chained (C9) MSITCs and MSoITCs were the most effective against *B. cereus* (having a good activity, MIC 12.5-25 µg/mL). The activity of 9-MSoITC, as a representative, was tested against 15 food isolates and 2 reference strains of *B. cereus*. Variation of its activity among these strains was remarkably low (MIC 12.5-25 µg/mL, MBC 17.5-37.5 µg/mL) (**Table 4.3**). It should be noted that the variation of antimicrobial activity of ITCs among various strains of other microbial species could be larger than that of the tested food isolates of *B. cereus*, as shown by a previous study working with 17 strains of methicillin-resistant *Staphylococcus aureus* (MRSA) (MIC<sub>AITC</sub> 28-220 µg/mL, MIC<sub>BITC</sub> 2.9-110 µg/mL, and MIC<sub>PhEITC</sub> < 7-183 µg/mL).<sup>10</sup> These results suggest that variability can be species-dependent and ITC-dependent, and that it is of relevance to investigate in future studies.

ITCs showed antimicrobial activity (MIC 12.5-200 µg/mL) against the fungal species tested. 9-MSITC and 9-MSoITC showed a good activity (MIC ≤ 25 µg/mL) against yeast *S. cerevisiae* and mold *A. niger* spores. The lowest MFC was 25 µg/mL obtained for 9-MSITC and 9-MSoITC against *S. cerevisiae*.

The results on antibacterial and antifungal activity of ITCs prove that ITCs from MSITC and MSoITC subclasses are more potent than the traditional AITC.

**Table 4.3.** Minimum inhibitory concentrations (MIC) and minimum bactericidal/fungicidal concentrations (MBC/MFC) of ITCs against various microbes in nucleophile-poor media.

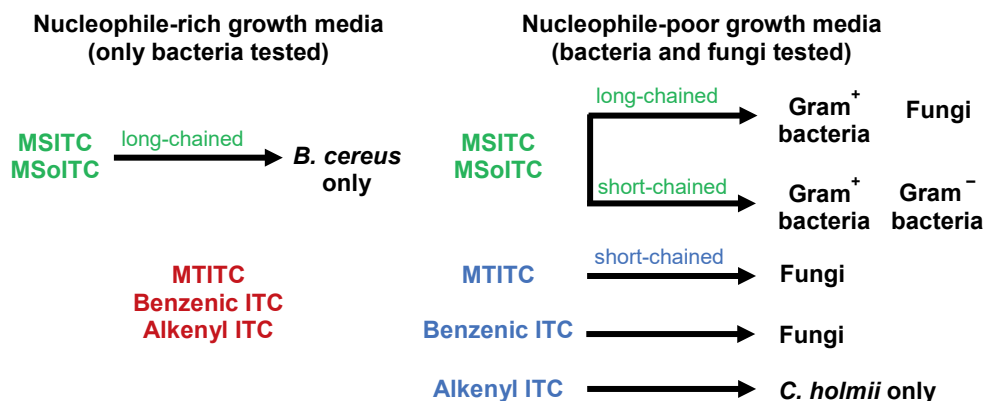
ITC	MIC (MBC or MFC), µg/mL <sup>a</sup>									
	Gram <sup>-</sup> bacteria <sup>b</sup>					Gram <sup>+</sup> bacteria				
	<i>Ec</i>	ST	<i>Pa</i>	<i>Bc</i>	<i>Lm</i>	<i>Sa</i>	<i>Ch</i>	<i>Sc</i>	An spores	
AITC	>200 <sup>c</sup>	>200	>200	>200	>200	>200	50 (100)	>200	100-200 (200) <sup>d</sup>	>200
PeITC	>200	>200	>200	>200	>200	>200	>200	>200	>200	>200
3-MTITC	150-200 (200)	100-200 (>200)	>200	100 (200)	>200	100-200 (>200)	50 (100)	50 (75)	100-200 (200)	>200
9-MTITC	>200	>200	>200	>200	>200	50-100 (>200)	>200	>200	>200	>200
3-MSITC	25 (50)	50 (200)	>200	25 (75)	200 (>200)	100 (>200)	>200	200 (>200)	>200	>200
9-MSITC	200 (>200)	>200	>200	12.5 (25)	25 (50)	50 (200)	50 (100)	12.5-25 (25)	25 (50)	>200
3-MSolITC	25 (50)	50 (200)	>200	12.5-25 (25-50)	50-100 (100)	50 (>200)	100-200 (200)	75 (100)	100-200 (200)	>200
9-MSolITC	>200	>200	>200	12.5-17.5 (17.5)	25 (50)	50-100 (200)	100 (>200)	12.5-25 (25)	25 (50)	>200
BITC	100-200 (200)	200 (>200)	>200	100 (150)	>200	100-200 (>200)	50 (100)	100 (150)	>200	>200
PhEITC	>200	>200	>200	150 (200)	>200	>200	50 (100)	150 (200)	200 (>200)	>200

<sup>a</sup> Data were obtained from three independent biological repetitions.<sup>b</sup> *Ec* = *E. coli*, *ST* = *S. Typhimurium*, *Pa* = *P. aeruginosa*, *Bc* = *B. cereus*, *Lm* = *L. monocytogenes*, *Sa* = *S. aureus*.<sup>c</sup> The highest tested concentration was 200 µg/mL.<sup>d</sup> Two values separated by a dash indicated that the definite MIC was not obtained because the concentrations in between (e.g. 175 µg/mL) were not tested. Some cases, e.g. 150-200 (200), mean that at the lower concentration (e.g. 150 µg/mL) the cell count in the cell viability check was above the initial inoculum size, but at the higher concentration (e.g. 200 µg/mL) the cell count equalled >99% cell inactivation from the initial inoculum.<sup>e</sup> Data is for the 15 food isolates and reference strain *B. cereus* ATCC 10987. The other data in the column is for the reference strain ATCC 14579.

## 4.4. Discussion

### 4.4.1. Reactivity of ITCs to growth media components affects significantly the antimicrobial activity of ITCs

**Figure 4.4** summarizes the specificity of antimicrobial activity of ITCs in the nucleophile-rich and nucleophile-poor growth media. In the nucleophile-rich medium (TSB), only long-chained MSITC and MSoITC showed good antibacterial activity against *B. cereus*. In nucleophile-poor media (5-10× diluted TSB), both short-chained and long-chained MSITC and MSoITC showed good antibacterial activity. The short-chained ones were good against both Gram<sup>+</sup> and Gram<sup>-</sup> bacteria, whereas the long-chained ones were good against Gram<sup>+</sup> bacteria. The long-chained MSITC and MSoITC also showed good antifungal activity in nucleophile-poor growth media (MEB and RPMI 1640). Furthermore, at least one representative of MTITC, benzenic ITC, and alkenyl ITC had moderate antifungal activity. Our results imply that most antibacterial activity of ITCs reported in literature might have been underestimated because TSB or other nucleophile-rich growth media, e.g. brain heart infusion (BHI), lysogeny broth (LB), were used.<sup>12,31-32</sup> Considering the application of ITCs as food preservatives, the reported activity obtained from the assays using nucleophile-rich growth media is valuable to give an estimation of the activity of ITCs in foods rich in nucleophiles.



**Figure 4.4.** The specificity of activity of ITCs in nucleophile-rich and nucleophile-poor growth media. ITCs are presented as subclasses (see **Figure 4.1**). Subclasses displayed in green, blue, and red represent subclasses with MIC ≤ 25 µg/mL (good antimicrobial activity), MIC 50-100 µg/mL (moderate antimicrobial activity), and MIC ≥ 200 µg/mL (low antimicrobial activity), respectively.

Considering the absence of free Cys, the low concentrations of bound Cys residues, and the fast reaction of ITCs in the nucleophile-rich TSB, the nucleophilicity of this growth media seems to be related to amino acids other than

Cys. A couple of studies showed the negative effect of Cys residues on the antimicrobial activity of ITCs,<sup>17,18</sup> whereas only one study indicated the negative effect of Cys and the other nucleophilic amino acids (Arg, Asp, Gln, Glu, Gly, Lys, Phe, Thr, Trp) on the antibacterial activity of ITCs against *E. coli*.<sup>12</sup> Reactivity of ITCs with individual amino acids in model systems and food application is worth study in future.

#### 4.4.2. Sulfinyl and sulfonyl groups improve the antimicrobial activity of ITCs

Within the aliphatic class, MSITC and MSoITC are the oxidized forms of MTITC. Within the same alkyl chain length, these oxidized forms exert higher antimicrobial activity than their non-oxidized forms. This might be due to an increased polarity (lower  $\log_{10}P$ , **Figure 4.1B**) imparted by the sulfinyl and sulfonyl groups. The hydrophilic sulfinyl or sulfonyl group at one side and hydrophobic alkyl group at the other side create an amphiphilic property within an MSITC or MSoITC moiety. This property is necessary for partitioning of compounds through cell membranes.<sup>33,34</sup> Long-chained MSITC and MSoITC generally had higher antimicrobial activity against Gram<sup>+</sup> bacteria and fungi which have a single phospholipid membrane. In contrast, short-chained MSITC and MSoITC showed a potent activity against Gram<sup>-</sup> bacteria. In Gram<sup>-</sup> bacteria, the influx of polar and small (< 600 Da) molecules, including antibiotics, is favored and assisted by water-filled porin channels.<sup>35,36</sup> This is the first study indicating the different specificity of antimicrobial activity of the short-chained and the long-chained MSITC and MSoITC, and that 9-MSITC and 9-MSoITC are potential antimicrobials.

### 4.5. Conclusion

This study proves that: (i) the decreasing concentration of nucleophiles by 5-10× in growth media improved significantly the antimicrobial activity of ITCs by at least 4-16×, (ii) the oxidized MSITC and MSoITC had higher antimicrobial activity than the non-oxidized MTITC, (iii) MSITC and MSoITC were more potent antibacterials than the well-studied AITC, BITC, and PhEITC, (iv) the long-chained 9-MSITC and 9-MSoITC had good activity ( $MIC \leq 25 \mu\text{g/mL}$ ) against Gram<sup>+</sup> bacteria and fungi, whereas the short-chained 3-MSITC and 3-MSoITC had good activity against Gram<sup>+</sup> bacteria and Gram<sup>-</sup> bacteria. Further studies need to explore the potential application of various MSITC and MSoITC, naturally obtained from Brassicaceae plants, as natural food preservatives considering the richness of nucleophiles in the matrix and to investigate their toxicity, as well as studies with a more extended collection of ITCs to unravel the quantitative structure-activity relationship (QSAR).

## **4.6. Acknowledgement**

The authors are grateful to Prof. Dr. Tjakko Abee, the laboratory of Food Microbiology, Wageningen University, for his valuable feedback during discussions; to Shilu Chen, MSc for her contribution on performing antimicrobial assays of several ITCs against *L. monocytogenes*, *E. coli*, *C. holmii*, and *A. niger*; to Aldo Mendoza Santiago, MSc for his contribution on performing antimicrobial assays against 17 *B. cereus* strains; and to Dr. Leon de Jonge, the Animal Nutrition group, Wageningen University, for performing the amino acid analysis.

## **4.7. Funding source**

The authors are grateful to Indonesia Endowment Fund for Education (LPDP), Ministry of Finance of Republic Indonesia, to financially support PhD study of SA. The authors declare no conflict of interest.

## 4.8. References

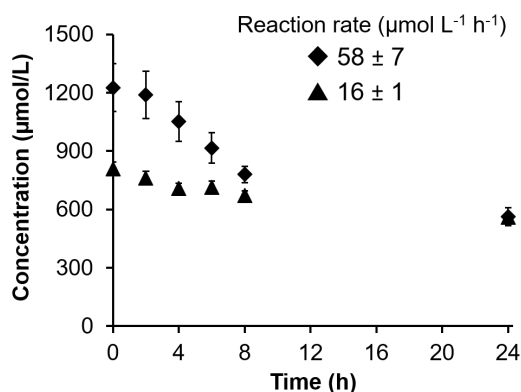
1. Clemente, I.; Aznar, M.; Silva, F.; Nerín, C., Antimicrobial properties and mode of action of mustard and cinnamon essential oils and their combination against foodborne bacteria. *Innovative Food Sci. Emerging Technol.* **2016**, *36*, 26-33.
2. Tajkarimi, M. M.; Ibrahim, S. A.; Cliver, D. O., Antimicrobial herb and spice compounds in food. *Food Control* **2010**, *21*, 1199-1218.
3. Lu, Z.; Dockery, C. R.; Crosby, M.; Chavarria, K.; Patterson, B.; Giedd, M., Antibacterial activities of wasabi against *Escherichia coli* O157:H7 and *Staphylococcus aureus*. *Front. Microbiol.* **2016**, *7*, 1403.
4. Quiles, J. M.; Manyes, L.; Luciano, F. B.; Manes, J.; Meca, G., Effect of the oriental and yellow mustard flours as natural preservative against aflatoxins B<sub>1</sub>, B<sub>2</sub>, G<sub>1</sub>, and G<sub>2</sub> production in wheat tortillas. *J. Food Sci. Technol.* **2015**, *52* (12), 8315-8321.
5. Turgis, M.; Han, J.; Caillet, S.; Lacroix, M., Antimicrobial activity of mustard essential oil against *Escherichia coli* O157:H7 and *Salmonella typhi*. *Food Control* **2009**, *20*, 1073-1079.
6. Isshiki, K.; Tokuoka, K.; Mori, R.; Chiba, S., Preliminary examination of allyl isothiocyanate vapor for food preservation. *Biosci., Biotechnol., Biochem.* **1992**, *56*, 1476-1477.
7. FDA, GRN No. 180: GRAS Notice allyl isothiocyanate in a food shelf life extension and anti-spoilage system. **2005**, <https://www.accessdata.fda.gov/scripts/fdcc/?set=GRASNotices&id=180> (accessed on 20/11/2019).
8. Bones, A. M.; Rossiter, J. T., The enzymic and chemically induced decomposition of glucosinolates. *Phytochemistry* **2006**, *67*, 1053-1067.
9. Agerbirk, N.; Olsen, C. E., Glucosinolate structures in evolution. *Phytochemistry* **2012**, *77*, 16-45.
10. Dias, C.; Aires, A.; Saavedra, M. J., Antimicrobial activity of isothiocyanates from cruciferous plants against methicillin-resistant *Staphylococcus aureus* (MRSA). *Int. J. Mol. Sci.* **2014**, *15*, 19552-19561.
11. Dufour, V.; Alazzam, B.; Ermel, G.; Thepaut, M.; Rossero, A.; Tresse, O.; Baysse, C., Antimicrobial activities of isothiocyanates against *Campylobacter jejuni* isolates. *Front. Cell. Infect. Microbiol.* **2012**, *2*, 53.
12. Nowicki, D.; Rodzik, O.; Herman-Antosiewicz, A.; Szalewska-Palasz, A., Isothiocyanates as effective agents against enterohemorrhagic *Escherichia coli*: Insight to the mode of action. *Sci. Rep.* **2016**, *6*, 22263.
13. Yang, C.-X.; Wu, H.-T.; Li, X.-X.; Wu, H.-Y.; Niu, T.-X.; Wang, X.-N.; Lian, R.; Zhang, G.-L.; Hou, H.-M., Comparison of the inhibitory potential of benzyl isothiocyanate and phenethyl isothiocyanate on Shiga toxin-producing and enterotoxigenic *Escherichia coli*. *LWT* **2020**, *118*, 108806.
14. Haristoy, X.; Fahey, J. W.; Scholtus, I.; Lozniewski, A., Evaluation of the antimicrobial effects of several isothiocyanates on *Helicobacter pylori*. *Planta Med.* **2005**, *71*, 326-330.
15. Wilson, A. E.; Bergaentzlé, M.; Bindler, F.; Marchioni, E.; Lintz, A.; Ennahar, S., In vitro efficacies of various isothiocyanates from cruciferous vegetables as antimicrobial agents against foodborne pathogens and spoilage bacteria. *Food Control* **2013**, *30*, 318-324.
16. Hermanson, G. T., Chapter 1 - Functional Targets. In *Bioconjugate Techniques (2nd Edition)*, Hermanson, G. T., Ed. Academic Press: New York, **2008**; pp 1-168.
17. Kurepina, N.; Kreiswirth, B. N.; Mustaev, A., Growth-inhibitory activity of natural and synthetic isothiocyanates against representative human microbial pathogens. *J. Appl. Microbiol.* **2013**, *115*, 943-954.
18. Luciano, F. B.; Hosseini, F. S.; Beta, T.; Holley, R. A., Effect of free-SH containing compounds on allyl isothiocyanate antimicrobial activity against *Escherichia coli* O157:H7. *J. Food Sci.* **2008**, *73*, M214-20.

19. Andini, S.; Dekker, P.; Gruppen, H.; Araya-Cloutier, C.; Vincken, J.-P., Modulation of glucosinolate composition in Brassicaceae seeds by germination and fungal elicitation. *J. Agric. Food Chem.* **2019**, *67* (46), 12770-12779.
20. Blažević, I.; Montaut, S.; Burčul, F.; Olsen, C. E.; Burow, M.; Rollin, P.; Agerbirk, N., Glucosinolate structural diversity, identification, chemical synthesis and metabolism in plants. *Phytochemistry* **2020**, *169*, 112100.
21. Warda, A. K.; Xiao, Y.; Boekhorst, J.; Wells-Bennik, M. H. J.; Nierop Groot, M. N.; Abee, T., Analysis of germination capacity and germinant receptor (sub)clusters of genome-sequenced *Bacillus cereus* environmental isolates and model strains. *Appl. Environ. Microbiol.* **2017**, *83*, e02490-16.
22. ISO, ISO 13903:2005 Animal feeding stuff - Determination of amino acids content; International Organization for Standardization. Geneva, Switzerland, **2005**.
23. Aisyah, S.; Gruppen, H.; Slager, M.; Helmink, B.; Vincken, J.-P., Modification of prenylated stilbenoids in peanut (*Arachis hypogaea*) seedlings by the same fungi that elicited them: The fungus strikes back. *J. Agric. Food Chem.* **2015**, *63*, 9260-8.
24. Araya-Cloutier, C.; Vincken, J. P.; van Ederen, R.; den Besten, H. M. W.; Gruppen, H., Rapid membrane permeabilization of *Listeria monocytogenes* and *Escherichia coli* induced by antibacterial prenylated phenolic compounds from legumes. *Food Chem.* **2018**, *240*, 147-155.
25. Aryani, D. C.; den Besten, H. M. W.; Hazeleger, W. C.; Zwietering, M. H., Quantifying strain variability in modeling growth of *Listeria monocytogenes*. *Int. J. Food Microbiol.* **2015**, *208*, 19-29.
26. Araya-Cloutier, C.; den Besten, H. M. W.; Aisyah, S.; Gruppen, H.; Vincken, J.-P., The position of prenylation of isoflavonoids and stilbenoids from legumes (Fabaceae) modulates the antimicrobial activity against Gram positive pathogens. *Food Chem.* **2017**, *226*, 193-201.
27. Hayrapetyan, H.; Hazeleger, W. C.; Beumer, R. R., Inhibition of *Listeria monocytogenes* by pomegranate (*Punica granatum*) peel extract in meat paté at different temperatures. *Food Control* **2012**, *23*, 66-72.
28. Brotzel, F.; Mayr, H., Nucleophilicities of amino acids and peptides. *Org. Biomol. Chem.* **2007**, *5* (23), 3814-20.
29. Andini, S.; Araya-Cloutier, C.; Sanders, M.; Vincken, J.-P., Simultaneous analysis of glucosinolates and isothiocyanates by RP-UHPLC-ESI-MS<sup>n</sup>. *J. Agric. Food Chem.* **2020**, *68*, 3121-3131.
30. Hanschen, F. S.; Brüggemann, N.; Brodehl, A.; Mewis, I.; Schreiner, M.; Rohn, S.; Kroh, L. W., Characterization of products from the reaction of glucosinolate-derived isothiocyanates with cysteine and lysine derivatives formed in either model systems or broccoli sprouts. *J. Agric. Food Chem.* **2012**, *60*, 7735-7745.
31. Ko, M. O.; Kim, M. B.; Lim, S. B., Relationship between chemical structure and antimicrobial activities of isothiocyanates from cruciferous vegetables against oral pathogens. *J. Microbiol. Biotechnol.* **2016**, *26*, 2036-2042.
32. Lim, S.; Han, S.-W.; Kim, J., Sulfuraphene identified from radish (*Raphanus sativus* L.) seeds possesses antimicrobial properties against multidrug-resistant bacteria and methicillin-resistant *Staphylococcus aureus*. *J. Funct. Foods* **2016**, *24*, 131-141.
33. Araya-Cloutier, C.; Vincken, J.-P.; van de Schans, M. G. M.; Hageman, J.; Schaftenaar, G.; den Besten, H. M. W.; Gruppen, H., QSAR-based molecular signatures of prenylated (iso)flavonoids underlying antimicrobial potency against and membrane-disruption in Gram positive and Gram negative bacteria. *Sci. Rep.* **2018**, *8*, 9267.
34. Lambert, P. A., Cellular impermeability and uptake of biocides and antibiotics in Gram-positive bacteria and mycobacteria. *J. Appl. Microbiol.* **2002**, *92*, 46S-54S.
35. Nikaido, H., Molecular basis of bacterial outer membrane permeability revisited. *Microbiol. Mol. Biol. Rev.* **2003**, *67*, 593-656.
36. Richter, M. F.; Drown, B. S.; Riley, A. P.; Garcia, A.; Shirai, T.; Svec, R. L.; Hergenrother, P. J., Predictive compound accumulation rules yield a broad-spectrum antibiotic. *Nature* **2017**, *545*, 299-304.



## 4.9. Supplementary information

### 4.9.1. Supplementary figure



**Figure S4.1.** The decrease of concentration of 3-MSITC (diamonds) and 9-MSITC (triangles) during incubation at 37 °C in 5× diluted TSB. The initial concentration of ITCs in all experiments was 200 μg/mL (i.e. 3-MSITC 1227 μM and 9-MSITC 810 μM). The error bars represent the standard deviation from three independent repetitions. The reaction rate explains the decrease of ITCs concentration during the first 8 h with a minimum of 3 data points.

### 4.9.2. Supplementary tables

**Table S4.1.** Time to detection (TTD, h) of the negative controls of *Listeria monocytogenes* (*Lm*), *Staphylococcus aureus* (*Sa*), *Bacillus cereus* (*Bc*), *Escherichia coli* (*Ec*), *Salmonella* Typhimurium (*ST*), and *Pseudomonas aeruginosa* (*Pa*) in TSB and in the diluted TSB

Medium	<i>Lm</i>	<i>Sa</i>	<i>Bc</i>	<i>Ec</i>	<i>ST</i>	<i>Pa</i>
Undiluted TSB	8.3±0.2	6.0±0.1	6.3±0.6	5.9±0.3	5.9±0.1	6.5±0.2
5× Diluted TSB	8.6±0.2	7.6±0.2*	n.a. <sup>a</sup>	n.a.	n.a.	n.a.
10× Diluted TSB	n.a.	n.a.	6.6±0.6	6.7±0.3*	6.2±0.2	6.8±0.2

<sup>a</sup> n.a. stands for not applicable. Such conditions were not applied for those particular bacterial species in the antimicrobial assays.

\* Significant different from the mean of the undiluted TSB. Independent-samples t-test was performed to compare mean of TTD for the undiluted TSB and mean of TTD for the diluted TSB.

**Table S4.2.** Minimum inhibitory concentration (MIC, μg/mL) of the commercial antibiotics (ampicillin or ciprofloxacin) against *Listeria monocytogenes* (*Lm*), *Staphylococcus aureus* (*Sa*), *Bacillus cereus* (*Bc*), *Escherichia coli* (*Ec*), *Salmonella* Typhimurium (*ST*), and *Pseudomonas aeruginosa* (*Pa*)<sup>a</sup>

	<i>Lm</i>	<i>Sa</i>	<i>Bc</i>	<i>Ec</i>	<i>ST</i>	<i>Pa</i>
Ampicillin or ciprofloxacin <sup>b</sup>	0.75-1.50	1.50	15.00	0.75-1.50	0.75-1.50	1.50

<sup>a</sup> The same results were obtained in the antimicrobial assays in the undiluted and 5-10× diluted TSB.

<sup>b</sup> Ciprofloxacin was only for *P. aeruginosa* (*Pa*).



---

## QSAR-based physicochemical properties of isothiocyanate antimicrobials against Gram-negative and Gram-positive bacteria

---

Isothiocyanates (ITCs) exhibit antimicrobial activity, depending on their structures. We aimed at determining QSAR-based physicochemical properties of ITCs important for the antimicrobial activity and developing QSAR models to predict the activity of ITCs as individual and as mixtures. Twenty-six ITCs covering 9 subclasses were tested against *Escherichia coli* and *Bacillus cereus*. Minimum inhibitory concentration (MIC, mM) and growth inhibitory response (GIR, h/mM) were determined and used to develop QSAR models. MIC of the most active ITC was 9.4 µg/mL against *E. coli* and 6.3 µg/mL against *B. cereus*. Multiple linear regression (MLR) models were proposed with a good fit ( $R^2_{adj}$  0.86–0.93) and high internal predictive power ( $Q^2_{adj}$  0.80–0.89). Partial charge, polarity, reactivity, and shape were key physicochemical properties for antibacterial activity of ITCs. Furthermore, ITC compositions and antibacterial activity of Brassicaceae ITC-rich extracts were determined. *Brassica oleracea* ITC-rich extract had MIC 750–1000 µg/mL against both bacteria, and *Camelina sativa* ITC-rich extract had MIC 188 µg/mL against *B. cereus*. Moreover, based on the ITC compositional analysis, the models successfully predicted the antibacterial activity of the extracts. ITCs are promising natural antimicrobial candidates. The models are useful to predict the activity of new ITCs and ITC-rich mixtures.

**Keywords:** antibacterial, crucifer, glucosinolate, isothiocyanate natural preservative, quantitative structure-activity relationship

Based on: Andini, S.; Araya-Cloutier, C.; Lay, B.; Vreeke, G.; Hageman, J.; Vincken, J.-P., QSAR-based physicochemical properties of isothiocyanate antimicrobials against Gram-negative and Gram-positive bacteria. **Submitted for publication.**

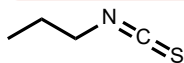
## 5.1. Introduction

Numerous studies were and are carried out to find new safe natural compounds to prevent microbial growth in food products. This is along with consumers' concern about health-related risks caused by synthetic preservatives, as well as with the increased antimicrobial persistence and resistance.<sup>1-3</sup>

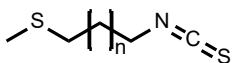
The structural diversity of plant-derived antimicrobial compounds is enormous. Among them, ITCs have been recognized as potential candidates for new antimicrobial compounds with broad spectrum of activity.<sup>4-7</sup> They are naturally obtained from hydrolysis of glucosinolates (GSLs) by myrosinase in the plant family of Brassicaceae.<sup>8</sup> Minimum inhibitory concentrations (MICs) as low as 12.5-25.0 µg/mL were obtained for the most active ITCs against Gram<sup>-</sup> bacteria, Gram<sup>+</sup> bacteria, and fungi.<sup>5</sup> Furthermore, their activity against Gram<sup>-</sup> bacteria is independent of efflux pump inhibitors,<sup>4,5,9</sup> in contrast to the activity of some other antibacterial phytochemicals, such as prenylated isoflavonoids.<sup>10</sup>

Some structure-activity relationships (SAR) of ITCs with regard to their antimicrobial activity were recognized.<sup>9,11-14</sup> However, there are inconsistent results in literature. Some studies reported that benzenic ITCs had higher antimicrobial activity against Gram<sup>-</sup> and Gram<sup>+</sup> bacteria than aliphatic ITCs,<sup>9,11,12</sup> whereas other studies reported differently.<sup>14-16</sup> Previously,<sup>5</sup> we showed some general trends on the SAR of ITCs from both aliphatic and benzenic classes with a more diverse set of compounds (different side chain motifs and lengths) than other studies. Nevertheless, our previous study comprised a relatively small dataset of ITCs ( $n = 10$ ) to establish good quantitative SAR (QSAR).<sup>17</sup> Up to date there is no QSAR study on ITCs as antimicrobials.

In the current study, 26 ITCs, belonging to 9 subclasses (**Figure 5.1**), were studied to reveal the key physicochemical properties of ITCs for their antimicrobial activity against Gram<sup>-</sup> and Gram<sup>+</sup> bacteria. *E. coli* and *B. cereus* have been chosen as a representative of Gram<sup>-</sup> and Gram<sup>+</sup> bacteria, respectively, because among the other tested bacterial species they were the most susceptible towards ITCs.<sup>5</sup> The majority of these 26 ITCs has never been tested before against the two bacterial species. Furthermore, ITC-rich extracts obtained from hydrolysis of GSL-rich extracts from Brassicaceae seeds, namely *Sinapis alba*, *Brassica napus*, *B. juncea*, *B. oleracea*, and *Camelina sativa*, were tested for their antimicrobial activity and used for confirming the prediction ability of the developed QSAR models.

**Alkyl ITC**


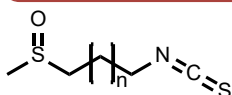
Propyl ITC (PITC)

**x-(Methylthio)alkyl ITC (MTITC)**

 3-(Methylthio)propyl ITC (3-MTITC),  $n = 1$ 

 4-(Methylthio)butyl ITC (4-MTITC),  $n = 2$ 

 5-(Methylthio)pentyl ITC (5-MTITC),  $n = 3$ 

 6-(Methylthio)hexyl ITC (6-MTITC),  $n = 4$ 

 9-(Methylthio)nonyl ITC (9-MTITC),  $n = 7$ 
**x-(Methylsulfinyl)alkyl ITC (MSITC)**

 3-(Methylsulfinyl)propyl ITC (3-MSITC),  $n = 1$ 

 4-(Methylsulfinyl)butyl ITC (4-MSITC),  $n = 2$ 

 5-(Methylsulfinyl)pentyl ITC (5-MSITC),  $n = 3$ 

 6-(Methylsulfinyl)hexyl ITC (6-MSITC),  $n = 4$ 

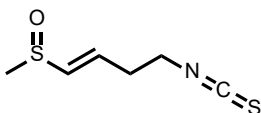
 8-(Methylsulfinyl)octyl ITC (8-MSITC),  $n = 6$ 

 9-(Methylsulfinyl)nonyl ITC (9-MSITC),  $n = 7$ 

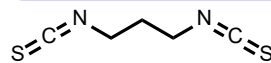
 10-(Methylsulfinyl)decyl ITC (10-MSITC),  $n = 8^a$ 

 11-(Methylsulfinyl)undecyl ITC (11-MSITC),  $n = 9^b$ 

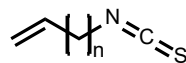
<sup>a, b</sup> The authentic standards were not available, but present in high abundance in hydrolyzed *C. sativa* seed extracts.

**x-(Methylsulfinyl)alkenyl ITC (MS-en-ITC)**


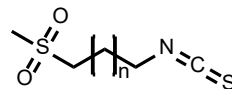
4-(Methylsulfinyl)-3-butenyl ITC (4-MS-3-en-ITC)

**Alkyl DiITC**


1,3-Propylene diITC (P-DiITC)

**Alkenyl ITC**

 Allyl ITC (AITC),  $n = 1$ 

 3-Butenyl ITC (BuITC),  $n = 2$ 

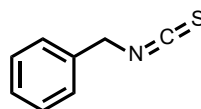
 4-Pentenyl ITC (PeITC),  $n = 3$ 
**x-(Methylsulfonyl)alkyl ITC (MSolTC)**

 3-(Methylsulfonyl)propyl ITC (3-MSolTC),  $n = 1$ 

 4-(Methylsulfonyl)butyl ITC (4-MSolTC),  $n = 2$ 

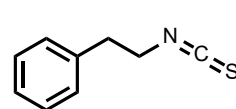
 5-(Methylsulfonyl)pentyl ITC (5-MSolTC),  $n = 3$ 

 6-(Methylsulfonyl)hexyl ITC (6-MSolTC),  $n = 4$ 

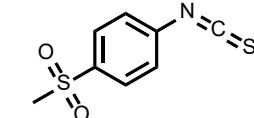
 8-(Methylsulfonyl)octyl ITC (8-MSolTC),  $n = 6$ 

 9-(Methylsulfonyl)nonyl ITC (9-MSolTC),  $n = 7$ 
**Benzenic ITC**


Benzyl ITC (BITC)



Phenethyl ITC (PhEITC)

**x-(Methylsulfonyl)benzenic ITC**


*p*-(Methylsulfonyl)phenyl ITC (*p*-MSoPhITC)

**Figure 5.1.** ITCs used in this study. Subclasses are differentiated by colors.

## 5.2. Materials and methods

### 5.2.1. Standard ITCs and GSLs, other chemicals, and growth media

Structures of 28 ITCs involved in this study are displayed in **Figure 5.1**. Standards were available for 26 ITCs, where 23 of them can be naturally found in Brassicaceae plants.<sup>18</sup> Allyl ITC (AITC), 3-butenyl ITC (BuITC), 4-pentenyl ITC (PeITC), propyl ITC (PITC), 3-(methylthio)propyl ITC (3-MTITC), benzyl ITC (BITC), and phenethyl

ITC (PhEITC) were from Sigma-Aldrich Chemie B.V. (St. Louis, Missouri, U.S.A.). 3-(Methylsulfinyl)propyl ITC (3-MSITC), 4-(methylsulfinyl)butyl ITC (4-MSITC), 5-(methylsulfinyl)pentyl ITC (5-MSITC), 6-(methylsulfinyl)hexyl ITC (6-MSITC), 8-(methylsulfinyl)octyl ITC (8-MSITC), 9-(methylsulfinyl)nonyl ITC (9-MSITC), 4-(methylsulfinyl)-3-butenyl ITC (4-MS-3-en-ITC), 3-(methylsulfonyl)propyl ITC (3-MSoITC), 4-(methylsulfonyl)butyl ITC (4-MSoITC), 5-(methylsulfonyl)pentyl ITC (5-MSoITC), 6-(methylsulfonyl)hexyl ITC (6-MSoITC), 8-(methylsulfonyl)octyl ITC (8-MSoITC), 9-(methylsulfonyl)nonyl ITC (9-MSoITC), 4-(methylthio)butyl ITC (4-MTITC), 5-(methylthio)pentyl ITC (5-MTITC), 6-(methylthio)hexyl isothiocyanate (6-MTITC), and 9-(methylthio)nonyl ITC (9-MTITC) were from Abcam (Cambridge, UK). 1,3-Propylene diisothiocyanate (P-DiITC) and *p*-(methylsulfonyl)phenyl ITC (*p*-MSoPhITC) were from ABCR GmbH (Karlsruhe, Germany).

GSLs (the names of the side chains are abbreviated according to ITCs', unless otherwise stated): 3-MSGSL, 4-MSGSL, 4-MTGSL, 5-MTGSL, AGSL, BGSL, BuGSL, indol-3-ylmethyl GSL (I3MGSL), PeGSL, PhEGSL, *p*-hydroxy-benzyl GSL (*p*-OH-BGSL), and (*R*)-2-hydroxy-3-butenyl GSL ((*R*)-2-OH-BuGSL) were from Phytolab GmbH & Co (Vestenbergsgreuth, Germany).

Ampicillin sodium, NaOH, KH<sub>2</sub>PO<sub>4</sub>, NaCl, and myrosinase were from Sigma-Aldrich Chemie B.V. (St. Louis, Missouri, U.S.A.). Dimethyl sulfoxide (DMSO) was from Ducheda Biochemie (Haarlem, the Netherlands). *N*-acetyl-L-cysteine (NAC) was from Cayman Chemicals (Michigan, USA). UHPLC grade isopropanol (IPA), formic acid (FA) 0.1% in water, and FA 0.1% in acetonitrile (ACN) were from Biosolve B.V. (Valkenswaard, The Netherlands). High purity water was produced in-house using a Milli-Q A10 Gradient system (18.2 MΩ.cm, 3 ppb TOC) (Merck Millipore, Darmstadt, Germany).

Growth media: tryptone soya agar (TSA) and tryptone soya broth (TSB) were from Oxoid Limited (Hampshire, U.K.); bacteriological agar from VWR International B.V. (Valkenswaard, The Netherlands); bacto brain heart infusion (BHI) from Becton, Dickinson and Company (Franklin Lakes, NJ, U.S.A.). Peptone physiological salt solution (PPS) was from Tritium Microbiologie (Eindhoven, The Netherlands).

### 5.2.2. Microbial cultures

Cultures of *E. coli* K12 and *B. cereus* ATCC 14579 were kindly provided by the laboratory of Food Microbiology, Wageningen University, The Netherlands.

### 5.2.3. Plant materials

Seeds of *S. alba* (yellow mustard 'Emergo', 393810), *B. napus* ('Helga', 392600), *B. juncea* var. *rugosa rugosa* (Chinese mustard/amsoi, 160400), *B. oleracea* var. *botrytis* subvar. *Cymosa* (broccoli, 145100), and *C. sativa* (German sesame, 390900) were from Vreeken's Zaden (Dordrecht, The Netherlands, <https://www.vreeken.nl/>). *B. juncea* var. *rugosa rugosa* and *B. oleracea* var.

botrytis subvar. *Cymosa* are mentioned as *B. juncea* and *B. oleracea*, respectively, in the following text.

#### 5.2.4. Extraction of Brassicaceae seeds

Five seed extracts were obtained through methanol extraction, performed in a Speed Extractor (E-916; Büchi, Flawil, Switzerland) as described by Andini *et al.*<sup>19</sup> The obtained extract was evaporated under reduced pressure (Syncore Polyvap, Büchi), resolubilized in *tert*-butanol, and freeze-dried. The dried extracts were stored at -20 °C. Stock extracts (10 mg/mL) were resolubilized in 10% (v/v) DMSO in phosphate buffer pH 7.0.

#### 5.2.5. Enzymatic hydrolysis of the extracts

Seed extracts (2 mg/mL) were mixed with commercial myrosinase (0.05 U/mL, 1 unit of enzymatic activity was defined as the amount of enzyme that releases 1 µmol glucose per min with AGSL as the substrate, at 25 °C, pH 6.0). Hydrolysis was performed at 50 °C, pH 7.0 for 4 h, in two ways: (i) in the presence of NAC for the LC-MS analysis of ITCs,<sup>20</sup> (ii) in the absence of NAC for the antibacterial assay. As a control, the non-hydrolyzed extracts were prepared in the same way, only that the myrosinase solution was replaced by buffer pH 7.0. Prior to the LC-MS analysis, samples were centrifuged for 5 min at 5,000 rpm.

#### 5.2.6. RP-UHPLC-ESI-MS<sup>n</sup> analysis of (hydrolyzed) extracts of Brassicaceae seeds

Analysis of GSLs and ITCs was performed according to Andini *et al.*<sup>20</sup> In short, an Accela ultra high performance liquid chromatography (UHPLC) system (Thermo Scientific, San Jose, CA, USA) coupled to an LTQ Velos electrospray ionization (ESI) ion trap mass spectrometer (MS) (Thermo Scientific) was used. The column oven temperature was set at 25 °C. Eluent A: water acidified with 0.1% (v/v) FA, and eluent B: ACN acidified with 0.1% (v/v) FA, were used at a flow rate of 300 µL/min. The elution gradient was: 0-6.7 min, isocratic on 0% (v/v) B; 6.7-12.5 min, linear gradient to 8% B; 12.5-24.2 min, a linear gradient to 16% B; 24.2-41.8 min, a linear gradient to 40% B; 41.8-43.5 min, a linear gradient to 100% B; 43.5-50.5 min, an isocratic on 100% B; 50.5-52 min, a linear gradient to 0% B; 52-59 min, isocratic on 0% B. (Tentative) annotation and quantification of GSLs and ITCs (as NAC-ITCs) were based on UV and MS spectra, performed in Xcalibur (v.2.2, Thermo Scientific).<sup>19,20</sup> Calibration curves of GSLs and ITCs were made with 7 data points in a range of 2.5-50 µM. Quantification of GSLs and ITCs without authentic standards was based on calibration curves of GSLs and ITCs with the most similar structure and molecular weight (MW). Quantification of long-chained MSGSLs was based on the response factor of standard 4-MSGSL corrected by MW.

### 5.2.7. Antibacterial assay

Antibacterial activity of ITCs was tested by following the broth-microdilution procedure.<sup>5</sup> In short, the inoculum at  $3.7 \pm 0.3 \log_{10}$ CFU/mL was prepared in TSB (specifically 10× diluted TSB). Stock solutions of standard ITCs were prepared at 10 mg/mL in DMSO. Equal volumes (100 µL) of ITC solution and inoculum were mixed into wells in a 96-well plate. Final concentrations of ITCs varied from 3.0 to 200.0 µg/mL (DMSO 2% (v/v) max.). Positive control (ampicillin at final concentration of 1.5 µg/mL for *E. coli*, 15 µg/mL for *B. cereus*), negative control (the inoculum and liquid medium with DMSO 2%), and blank (the liquid medium without any inoculum and antibacterial agent) were included in every assay. The 96-well plate was incubated in a SpectraMax iD3 (Molecular Devices, U.S.A.) at 30 °C for *B. cereus* or 37 °C for *E. coli*, with a constant periodic double orbital shaking. The optical density at 600 nm (OD<sub>600</sub>) was measured every 10 minutes for 24 h. The antibacterial activity of ITCs was evaluated in minimum 3 independent biological repetitions, each performed in duplicate.

Time to detection (TTD) of growth was defined as the time to have an increase in OD of 0.05 units.<sup>21</sup> When there was no change in OD after 24 h, cell viability was checked by plate counting to determine MIC and minimum bactericidal concentration (MBC).<sup>10</sup> MIC is the lowest concentration of compounds that resulted in bacterial count equal or lower than that of the initial inoculum. MBC is the lowest concentration that resulted in no growth after plating, i.e. >99% bacterial inactivation from the initial inoculum. Growth inhibitory response (GIR, h/mM) was defined as the growth inhibitory effect (h) caused by an ITC per its molar-based concentration (mM) (**Figure S5.1**).

All the procedures were also applied for testing the antibacterial activity of (hydrolyzed) extracts of Brassicaceae seeds. (Hydrolyzed) extracts were tested up to 1000 µg/mL. Furthermore, to demonstrate that the antibacterial activity of the hydrolyzed extract was mainly due to ITCs and that there was no interaction between ITCs in the extract, a mixture with similar ITC composition as was in the extract was prepared. This mixture is called as the model extract. The antibacterial activity of the (hydrolyzed) extracts and the model extract was evaluated in 3 independent biological repetitions, each performed in duplicate. GIR of the hydrolyzed extracts and the model extract was calculated based on total concentration (mM) of ITCs in the mixture.

### 5.2.8. Time-kill kinetic assay

Time-kill kinetic curves were made of the most active ITCs against *E. coli* and *B. cereus*. ITCs at their MBC were prepared in 10× diluted TSB in Eppendorf tubes.<sup>22-24</sup> Likewise, hydrolyzed *C. sativa* seed extract was also prepared. The bacterial inoculum was prepared in a similar way as described in the section **5.2.7**. Equal amounts of ITC solution and bacterial inoculum were mixed and incubated for 24 h at 30 °C or 37 °C in a shaking incubator at 800 rpm. At time points 1, 2, 3, 4,



6, and 24 h the aliquots were inoculated aseptically onto TSA plates to check the cell viability. Likewise in the antibacterial susceptibility test, positive control, negative control, and blank were included. The assay was performed in 2 independent biological repetitions, each performed in duplicate.

### 5.2.9. QSAR modeling

Molecular Operating Environment (MOE) software (version 2018.0101, Chemical Computing Group, Montreal, QC, Canada) was used for *in silico* modeling of the antibacterial activity of 26 ITCs against *E. coli* and *B. cereus*. Molecular structures of ITCs were inserted into a database by use of the canonical Simplified Molecular Input Line Entry System (SMILES) obtained from PubChem database.<sup>25</sup> When the SMILES for an ITC was not available in PubChem, the particular ITC was drawn in ChemDraw 18.0 (PerkinElmer Informatics, Inc., Waltham, MA, U.S.A.) and then inserted into MOE.

Energy minimization and conformational search were performed, and the conformer with the lowest energy was chosen. The molecules were energy minimized by using the molecular orbital package (MOPAC) PM3 at a root mean square (RMS) gradient of 0.01 kcal/mol/Å<sup>2</sup>. Furthermore, a conformational search was performed by using the method LowModeMD with a rejection limit of 50, an iteration limit of 10,000, an RMS gradient of 0.1 kcal/mol/Å<sup>2</sup>, an MM iteration limit of 500, an RMSD limit of 0.25, and a conformation limit of 5.

Afterwards, 2D and 3D molecular descriptors were calculated. In addition to the descriptors available at MOE (full list of used descriptors is in **Table S5.1**), the partial charges on the carbon atom and the nitrogen atom of the -N=C=S group were calculated using MOE, as well as the global electrophilicity ( $\omega^o$ ). Global electrophilicity, or electrophilicity from this point onwards, was calculated with the following formulae.<sup>26,27</sup> The descriptor database was curated by eliminating highly inter-correlated descriptors ( $R^2 \geq 0.95$ ) and constant descriptors.

$$\text{hardness}, \eta = \frac{E_{LUMO} - E_{HOMO}}{2} \quad (5.1)$$

$$\text{chemical potential}, \mu = \frac{E_{HOMO} + E_{LUMO}}{2} \quad (5.2)$$

$$\text{global electrophilicity}, \omega^o = \frac{\mu^2}{2\eta} \quad (5.3)$$

MIC, on a molar basis as pMIC (i.e.  $-\log_{10}\text{MIC}$ , mM), was used in previous QSAR studies of other antimicrobial compounds.<sup>10,28,29</sup> However, not all tested ITCs had a defined MIC up to the highest tested concentration.<sup>5</sup> Meanwhile, delayed bacterial growth was observed in the presence of ITCs. Therefore, in this QSAR study, antimicrobial activity of ITCs was also quantified as GIR. GIR as p'GIR (i.e.  $\log_{10}\text{GIR}$ , h/mM) allows us to input the activity of every ITC transparently (i.e. without imputation) to the QSAR modeling. In this current QSAR study, the antibacterial activity of ITCs against *E. coli* and *B. cereus* was separately modeled

using pMIC and p'GIR. ITCs with MIC > 200.0 µg/mL were included in the models by imputing a MIC 400 µg/mL.<sup>10</sup> GIR and MIC values were transformed to a logarithmic scale to (i) improve the normality of data distribution and (ii) to have the same trend of the values and the interpretation of the antibacterial activity (i.e. higher pMIC or p'GIR for higher antibacterial activity and vice versa). The dataset size was relatively low (26 ITCs) and, thus, splitting the dataset into training and test sets was not recommended because the models may not contain all the relevant structural information of the whole dataset.<sup>30</sup>

Next, a genetic algorithm (GA) was used to select a small subset of descriptors (i.e. predictors) best able to predict the antibacterial activities (pMIC or p'GIR) using multiple linear regression. The GA approach has been adapted from Araya-Cloutier *et al.* and de Bruijn *et al.*<sup>10,31</sup> During the GA, a leave-one-out cross validation (LOO-CV) procedure was used to determine the fitness of selected descriptors. The fitness was expressed as a  $Q^2$  value<sup>32</sup> and maximized by the GA. To exclude lucky or unlucky GA runs, every run was repeated 12 times with different starting seeds. Combinations of descriptors with a variance inflation factor (VIF) > 5, indicating a strong inter-correlation, were effectively removed from the GA population by penalizing the fitness during the GA run. GA parameters were optimized using a full factorial experimental design and were found to be: population size = 150, cross-over rate = 0.8, mutation rate = 0.3. The maximum number of iterations was set to 300 and elitism set to 8. The number of descriptors to be selected during a GA run was varied between 2 and 5.

After the GA optimization, the applicability domain (AD) was determined with the Williams plot.<sup>33</sup> In this plot ITCs with large standardized residuals and/or large leverages can be tracked down, indicating ill-fitting or highly influential compounds in the model, and were considered as outliers. Lastly, a permutation test was performed by repeating 100 times the exact procedure but with a permuted pMIC or p'GIR response variable, effectively modeling random data. Using the 100 permuted  $Q^2$  values, a  $p$ -value for the true GA run can be calculated, indicating if this result could have occurred by chance.

To visualize the internal prediction ability of the final chosen model,  $Q^2$  should be > 0.5. Furthermore, observed values of 26 ITCs were plotted against predicted values. If the values were along the trend line having an  $R^2$  > 0.7, the model had a good prediction ability. Furthermore, the difference between  $R^2$  and  $R_o^2$  (i.e.  $R^2$  of the intercept) aimed to be as low as possible (< 0.1).<sup>34</sup> The modified  $R^2$  metric (i.e.  $\overline{R_m^2}$ ) was calculated to fortify the statistical internal predictivity of the model (Figure S5.2).<sup>35</sup>

### 5.3. Results

**Table 5.1** shows the antimicrobial activity expressed as MIC, MBC, and GIR of each ITC against each bacterium. A good antimicrobial in this study was defined as ITCs having a MIC ≤ 25 µg/mL and a GIR ≥ 114 h/mM (the minimum GIR

associated with a MIC of 25 µg/mL was  $114.7 \pm 23.5$  h/mM). P-DiITC, an alkyl ITC with two  $-N=C=S$  functional groups, had the highest antimicrobial activity against *E. coli* (MIC 9.4 µg/mL, GIR 237.8 h/mM) and against *B. cereus* (MIC 6.3 µg/mL, GIR 541.7 h/mM). MBC of P-DiITC was 12.5 µg/mL for each bacterium. In contrast, PITC, the monofunctional analogue, had poor activity (MIC > 200.0 µg/mL, GIR  $\leq 3.0$  h/mM).

All good antibacterial ITCs showed bactericidal effects in the range of 12.5–100.0 µg/mL against *E. coli* and 12.5–50.0 µg/mL against *B. cereus*. Killing kinetic studies (**Figure S5.3**) showed that antibacterial ITCs mainly inhibited bacterial growth during the first 6 h and that after 24 h more than 99.9% of cells were inactivated.

### 5.3.1. Structure-activity relationship

#### 5.3.1.1. Effect of ITC class

Good antibacterial ITCs belonged only to the aliphatic class. Subclasses alkyl bifunctional (P-DiITC), *x*-(methylsulfinyl)alkyl (MSITC), and *x*-(methylsulfonyl)alkyl (MSoITC) were the most active ones. In contrast, the benzenic class showed moderate to low antibacterial activity (MICs  $\geq 100$  µg/mL and GIRs  $\leq 27$  h/mM).

#### 5.3.1.2. Effect of oxidation of sulfur substituent

ITCs from subclasses *x*-(methylthio)alkyl ITC (MTITC), MSITC, and MSoITC share similar structure but have an increasing order in the oxidation state of the sulfur substituent. The lowest MIC obtained for MTITC, MSITC, and MSoITC subclasses was 150.0 µg/mL (each bacterium), 25.0/15.0 µg/mL (*E. coli*/*B. cereus*), and 25.0/9.4 µg/mL (*E. coli*/*B. cereus*), respectively. In line with a previous study,<sup>5</sup> an increased oxidation state of the sulfur substituent in the side chain of ITCs improved the antimicrobial activity of ITCs.

#### 5.3.1.3. Effect of chain length

3-MTITC (MIC 150.0 µg/mL) had higher antimicrobial activity against each bacterium than the other MTITCs with longer chain length (C4 to C9). Meanwhile, MSITCs and MSoITCs exerted different trend of activity per bacterium. Against *E. coli*, the antimicrobial activity of MSITCs increased with decreasing chain length from C9 to C3 (MIC from  $\geq 200.0$  µg/mL to 25.0 µg/mL). Against *B. cereus*, the antimicrobial activity of MSITCs tended to increase with increasing chain length from C5/C6 to C9 (MIC from 50.0 µg/mL to 15.0 µg/mL). The trends of MSoITCs were comparable to those of MSITCs against *E. coli* (i.e. antimicrobial activity increase with decreasing chain length). Against *B. cereus* MSoITCs C3–C9 were considered to have good antimicrobial activity (MIC  $\leq 25$  µg/mL, GIR > 114 h/mM) whereas the C6 analogue had moderate activity (MIC 37.5 µg/mL).

**Table 5.1.** Antibacterial activity of ITCs, ITC-rich Brassicaceae extracts, and the model *B. oleracea* ITC-rich extract.<sup>a</sup>

No.	ITC <sup>b</sup>	<i>E. coli</i>			<i>B. cereus</i>		
		MIC	MBC	GIR	MIC	MBC	GIR
Pure ITCs							
1	PITC	>200.0	>200.0	2.9±2.7 <sup>c</sup>	>200.0	>200.0	0.5±0.2
2	P-DiITC	9.4	12.5	237.8±6.9	6.3	12.5	541.7±192.6
3	AITC	>200	>200.0	3.2±0.3	>200.0	>200.0	3.0±2.0
4	BuITC	>200	>200.0	4.4±2.6	>200.0	>200.0	1.3±1.4
5	PeITC	>200	>200.0	1.6±1.2	>200.0	>200.0	0.9±0.2
6	3-MTITC	150.0	200.0	19.6±4.5	150.0	200.0	24.5±5.5
7	4-MTITC	>200.0	>200.0	10.1±3.4	200.0	>200.0	14.8±0.5
8	5-MTITC	>200.0	>200.0	5.2±2.4	200.0	>200.0	15.9±1.1
9	6-MTITC	>200.0	>200.0	2.1±0.9	>200.0	>200.0	19.1±5.9
10	9-MTITC	>200.0	>200.0	1.3±0.5	>200.0	>200.0	9.5±8.5
11	3-MSITC	25.0	50.0	140.7±37.1	25.0	50.0	114.7±23.5
12	4-MSITC	50.0	200.0	84.2±28.2	25.0	50.0	115.9±11.2
13	5-MSITC	50.0	200.0	68.7±3.4	50.0	100.0	73.1±2.7
14	6-MSITC	100.0	200.0	35.1±11.5	50.0	75.0	96.9±26.9
15	8-MSITC	>200.0	>200.0	16.1±0.6	25.0	50.0	177.9±0.3
16	9-MSITC	200.0	>200.0	12.2±7.9	15.0	25.0	356.7±9.3
17	4-MS-3-en-ITC	25.0	100.0	208.5±65.1	25.0	50.0	121.6±13.6
18	3-MSoITC	25.0	50.0	247.1±31.0	25.0	50.0	196.2±73.1
19	4-MSoITC	25.0	100.0	144.0±6.0	25.0	50.0	184.2±64.1
20	5-MSoITC	75.0	150.0	79.7±0.3	25.0	50.0	157.0±0.7
21	6-MSoITC	100.0	150.0	46.6±24.7	37.5	50.0	124.9±33.9
22	8-MSoITC	>200.0	>200.0	19.0±2.8	12.5	25.0	212.8±0.2
23	9-MSoITC	>200.0	>200.0	2.2±1.5	9.4	12.5	624.1±154.8
24	BITC	150.0	200.0	18.2±5.4	100.0	150.0	27.1±0.8
25	PhEITC	>200.0	>200.0	7.8±2.7	150.0	200.0	20.5±1.4
26	<i>p</i> -MSOPhITC	>200.0	>200.0	7.7±2.2	>200.0	>200.0	16.7±3.8
ITC-rich Brassicaceae seed extracts							
<i>Camelina sativa</i> (Cs)		>1000.0 <sup>d</sup>	>1000.0	3.1±1.7 <sup>e</sup>	188.0	375.0	155.4±8.8
<i>Brassica oleracea</i> (Bo)		1000.0	>1000.0	106.9±19.9	750.0	1000.0	76.2±27.1
<i>Brassica juncea</i> (Bj)		>1000.0	>1000.0	1.5±1.3	>1000.0	>1000.0	0.3±0.4
<i>Brassica napus</i> (Bn)		>1000.0	>1000.0	3.3±2.0	>1000.0	>1000.0	2.2±2.1
<i>Sinapis alba</i> (Sa)		>1000.0	>1000.0	3.0±3.6	>1000.0	>1000.0	3.7±2.6
Model Bo extract <sup>f</sup>		1000.0	>1000.0	109.0±2.2	1000.0	>1000.0	56.2±3.5

<sup>a</sup> The antibacterial activity is expressed as minimum inhibitory concentration (MIC, µg/mL), minimum bactericidal concentration (MBC, µg/mL), and growth inhibitory response (GIR, h/mM).

<sup>b</sup> PITC, P-DiITC, and *p*-MSoPhITC are non-plant derived ITCs. The GSL precursor of 5-MSoITC can be biosynthetically formed in plants, but its presence has never been identified unambiguously.<sup>18</sup>

<sup>c</sup> GIR is displayed as the average and standard deviation from three to seven independent biological repetitions.

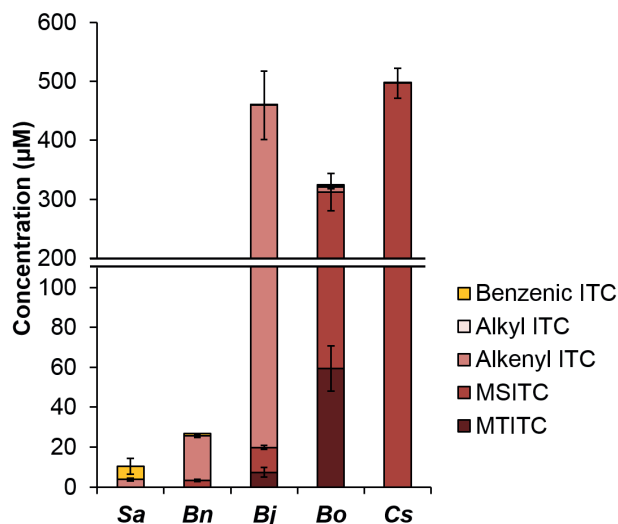
<sup>d</sup> MIC and MBC of the ITC-rich extracts and the model extract refer to the concentrations of extracts, and not to the concentration of ITCs. The highest concentration of the ITC-rich extracts in the assays was 1000.0 µg/mL.

<sup>e</sup> GIR of the ITC-rich extracts is expressed in h/mM based on the concentration of the 5 major ITCs in the extracts.

<sup>f</sup> The model *C. sativa* ITC-rich extract could not be made due to lack of authentic standards of 10-MSITC and 11-MSITC.

### 5.3.2. Antibacterial activity of ITC-rich extracts and their ITC compositions

ITC-rich extracts were obtained from Brassicaceae seed extracts, rich in GSLs, treated with commercial myrosinase. The detailed information on the compositions of GSLs and ITCs in the extracts before and after hydrolysis are available in **Supplementary Information**, including **Figure S5.4** and **Tables S5.2-4**. The overview of ITC compositions of the myrosinase-treated seed extracts at 1.0 mg/mL is presented in **Figure 5.2**.



**Figure 5.2.** Compositions of ITCs in 1 mg/mL myrosinase-treated seed extracts. *Sa*: *S. alba*, *Bn*: *B. napus*, *Bj*: *B. juncea*, *Bo*: *B. oleracea*, and *Cs*: *C. sativa*.

*B. oleracea* ITC-rich extract had antibacterial activity against *E. coli* (MIC 1000.0  $\mu\text{g/mL}$ , corresponding to an ITC concentration of 53.5  $\mu\text{g/mL}$  or 324.1  $\mu\text{M}$ , GIR 106.9 h/mM) and *B. cereus* (MIC 750.0  $\mu\text{g/mL}$  corresponding to an ITC concentration of 40.1  $\mu\text{g/mL}$  or 243.1  $\mu\text{M}$ , GIR 76.2 h/mM) (**Table 5.1**). This extract was rich in short-chained (*C3* and *C4*) MSITCs (252.0  $\mu\text{M}$ ) and MTITCs (59.2  $\mu\text{M}$ ) (**Figure 5.2**, **Table S5.4**). In contrast, the *C. sativa* ITC-rich extract had good antibacterial activity only against *B. cereus* (MIC 188.0  $\mu\text{g/mL}$ , corresponding to an ITC concentration of 24.3  $\mu\text{g/mL}$  or 93.5  $\mu\text{M}$ , GIR 155.4 h/mM) but not against *E. coli* (MIC > 1000.0  $\mu\text{g/mL}$ , GIR 3.1 h/mM). *C. sativa* ITC-rich extract was rich in the long-chained (*C9-C11*) MSITCs (496.3  $\mu\text{M}$ ) (**Table S5.4**). *B. juncea* ITC-rich extract was mainly composed of alkenyl ITCs (439.7  $\mu\text{M}$ ) and had poor antibacterial activity against each bacterium (MIC > 1000.0  $\mu\text{g/mL}$ , GIR  $\leq 1.5$  h/mM). This was consistent with the results found for the pure alkenyl ITCs. These findings emphasize that ITC composition is more important than just ITC content for the antimicrobial activity of Brassicaceae extracts treated with myrosinase. The other two extracts from *S. alba* and *B. napus* contained less than

30  $\mu\text{M}$  ITCs (mainly composed of benzenic ITC and alkenyl ITC, respectively) and had poor antibacterial activity against *E. coli* and *B. cereus* ( $\text{MIC} > 1000.0 \mu\text{g/mL}$ ,  $\text{GIR} \leq 3.7 \text{ h/mM}$ ).

### 5.3.3. QSAR modeling

In this study, 26 ITCs were used as training set to build QSAR models using pMIC ( $-\log_{10}\text{MIC}$ , mM) and p'GIR ( $\log_{10}\text{GIR}$ , h/mM) as activity response variables. QSAR models were developed with up to 5 molecular descriptors ( $k = 2, 3, 4, 5$ ) to prevent overfitting<sup>36</sup> or having too complex models, i.e. preference goes to models with lower number of descriptors. For this, the selection of the number of descriptors was firstly based on the internal predictive power ( $Q^2$ ) upon increased number of descriptors.<sup>31</sup> Models with  $k = 3, 4, 5$  generally had equally high internal predictive power, higher than that with  $k = 2$  (**Figure S5.5**). Therefore, the optimal number of descriptors in the models was based on other criteria specified in **Table 5.2**. All developed QSAR models had a good fit ( $R^2 \geq 0.75$ ,  $R^2_{adj} \geq 0.73$ , and  $\overline{R^2_m} \geq 0.71$ ) and a good internal predictive power ( $Q^2 \geq 0.68$ ,  $Q^2_{adj} \geq 0.66$ ). Based on the number of descriptors, statistical performance, and outliers, the models with 4 descriptors ( $k = 4$ ) were chosen as best for both bacteria (highlighted in bold in **Table 5.2**). **Figure 5.3** illustrates the good fit of the predicted values calculated by the chosen models to the observed values ( $R^2 \geq 0.88$ ) and high internal predictive ability ( $Q^2 \geq 0.83$ ). The permutation tests indicated that all the chosen models were significant ( $p\text{-value} < 0.000$ ) (**Figure S5.6**). One structural outlier (high leverage value), i.e. *p*-MSoPhITC, was found for pMIC model for *B. cereus* (**Table 5.2**, **Figure S5.7**). **Table 5.3** shows the chosen models with their associated molecular descriptors and coefficients (definition of all descriptors is in **Table S5.1**).

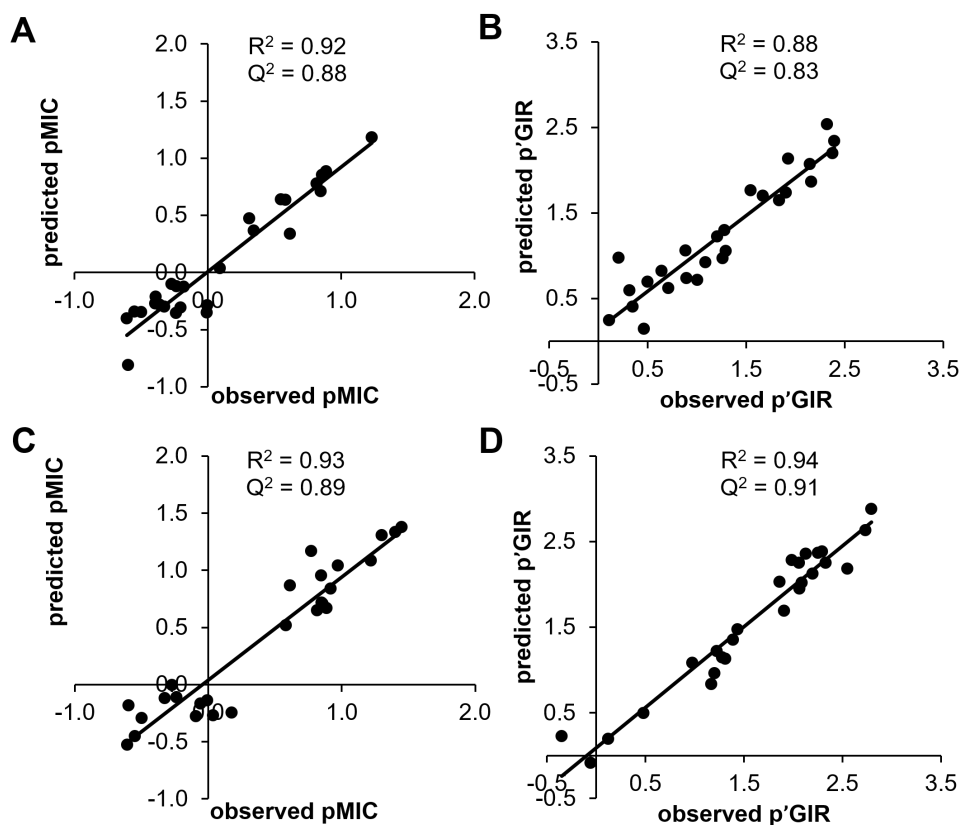
#### 5.3.3.1. QSAR models for *E. coli*

The pMIC model for *E. coli* (**Table 5.3**) indicated that the antibacterial activity of ITCs was positively correlated to topological polar surface area (*TPSA*), fractional charge-weighted negative surface area (*FCASA-*), and hydrophilic volume (*vsurf\_W1*), but negatively correlated to fractional charge-weighted positive surface area (*FCASA+*). As one might expect that *FCASA-* and *FCASA+* can be strongly inter-correlated, it is worth to note that the variance inflation factor (VIF) values of *FCASA-* and *FCASA+* were low ( $< 5$ ), meaning no strong inter-correlation, and that their contribution to the prediction was significant ( $p\text{-values} < 0.05$ ). The p'GIR model for *E. coli* indicated that the antibacterial activity of ITCs was positively correlated to electronic energy (*PM3\_Eele*) and hydrophobic integrity moment (*vsurf\_ID6*), but negatively correlated to relative positive partial charge (*PEOE\_RPC+*) and molecular shape specified by ratio of principal moment of inertia *PMI2/PMI3* (*npr2*).

**Table 5.2.** Statistical performance of the multiple linear regression (MLR) models obtained using GA-selection of variables.<sup>a</sup>

Bacteria	k	RMSE	p-value	R <sup>2</sup>	R <sup>2</sup> <sub>adj</sub>	$\overline{R_m^2}$	Q <sup>2</sup>	Q <sup>2</sup> <sub>adj</sub>	VIF <sub>max</sub>	$\sigma_{min}$	$\sigma_{max}$	Outlier
<i>E. coli</i>												
pMIC	2	0.265	2.0E-08	0.79	0.77	0.71	0.73	0.71	1.04	-1.77	2.24	PITC
	3	0.184	3.4E-11	0.90	0.89	0.88	0.87	0.86	3.47	-1.75	1.84	P-DiITC
	4	<b>0.171</b>	<b>3.9E-11</b>	<b>0.92</b>	<b>0.90</b>	<b>0.81</b>	<b>0.88</b>	<b>0.86</b>	<b>4.26</b>	<b>-1.21</b>	<b>2.01</b>	No
	5	0.153	2.1E-11	0.94	0.92	0.94	0.90	0.87	4.27	-1.39	2.94	No
pGIR	2	0.378	1.2E-07	0.75	0.73	0.71	0.68	0.66	1.35	-1.93	1.82	No
	3	0.285	1.1E-09	0.86	0.85	0.83	0.81	0.79	3.05	-3.04	1.48	PeITC
	4	<b>0.268</b>	<b>1.4E-09</b>	<b>0.88</b>	<b>0.86</b>	<b>0.88</b>	<b>0.83</b>	<b>0.80</b>	<b>4.45</b>	<b>-2.86</b>	<b>1.20</b>	No
	5	0.249	1.1E-09	0.91	0.88	0.90	0.84	0.81	4.22	-2.02	1.49	No
<i>B. cereus</i>												
pMIC	2	0.287	1.2E-09	0.83	0.82	0.82	0.79	0.78	1.67	-3.34	1.15	p-MSoPhITC
	3	0.240	1.2E-10	0.89	0.87	0.84	0.85	0.83	1.21	-2.33	1.34	PITC
	4	<b>0.200</b>	<b>1.4E-11</b>	<b>0.93</b>	<b>0.91</b>	<b>0.90</b>	<b>0.89</b>	<b>0.87</b>	<b>2.98</b>	<b>-1.92</b>	<b>1.85</b>	p-MSoPhITC
	5	0.192	3.6E-11	0.94	0.92	0.88	0.90	0.88	4.87	-1.91	1.44	No
pGIR	2	0.403	1.6E-08	0.79	0.77	0.76	0.75	0.73	1.02	-2.39	1.60	PITC
	3	0.268	9.7E-12	0.91	0.90	0.85	0.87	0.85	1.52	-2.21	2.14	No
	4	<b>0.222</b>	<b>1.1E-12</b>	<b>0.94</b>	<b>0.93</b>	<b>0.92</b>	<b>0.91</b>	<b>0.89</b>	<b>1.54</b>	<b>-2.60</b>	<b>1.67</b>	No
	5	0.166	2.2E-14	0.97	0.96	0.97	0.95	0.93	1.88	-1.90	2.00	PITC
Criteria		< 0.300	< 0.05	> 0.6	$ R^2 - R_{adj}^2  < 0.3$	> 0.5	> 0.5; $R^2 - Q^2 < 0.3$	> 0.5	< 5	-3.0 < $\sigma < 3.0$		No
References		62	62	34	62	35	34, 62, 63	64, 65	66	67		33, 34

<sup>a</sup> k: number of descriptors; RMSE: standard error of residuals; R<sup>2</sup>: coefficient of determination; R<sup>2</sup><sub>adj</sub>: adjusted R<sup>2</sup>;  $\overline{R_m^2}$ : average modified R<sup>2</sup> (based on scaled activity values), the regression plots for calculating R<sup>2</sup><sub>m</sub> are in **Figure S5.2**; Q<sup>2</sup>: leave-one-out cross-validated coefficient of determination; Q<sup>2</sup><sub>adj</sub>: adjusted Q<sup>2</sup>; VIF<sub>max</sub>: maximum variance inflation factor;  $\sigma_{min}$ : minimum standardized residual;  $\sigma_{max}$ : maximum standardized residual; outlier: the presence of structural outlier (high leverage) and/or activity outlier (> 3.0 $\sigma$ ). The finally chosen models are shown in bold. The structural outliers are visualized in the applicability domains (**Figure S5.7**).



**Figure 5.3.** Observed vs predicted antibacterial activity (pMIC, p'GIR) of ITCs against *E. coli* (A-B) and against *B. cereus* (C-D).

### 5.3.3.2. QSAR models for *B. cereus*

The pMIC model for *B. cereus* (**Table 5.3**) indicated that the antibacterial activity of ITCs was positively correlated to van der Waals surface area of partial positive charges (*PEOE\_VSA+3*), hydrophilic-lipophilic balance (*vsurf\_HL1*), and surface rugosity (roughness) (*vsurf\_R*), but negatively correlated to global electrophilicity (*AM1\_Electrophilicity*). Although one might expect that partial positive charge is related to electrophilicity (electron deficient property), the descriptors related to both had low VIF values ( $< 5$ ) and their contribution to the model was significant ( $p$ -values  $< 0.05$ ). The p'GIR model for *B. cereus* indicated that the antibacterial activity of ITCs was positively correlated to molecular shape specified by principal moment of inertia PMI1/PMI3 (*npr1*), van der Waals surface area of partial negative charges (*PEOE\_VSA-1*), and hydrophilic volume (*vsurf\_W7*), but negatively correlated to hydrophilic integrity moment (*vsurf\_IW2*).



**Table 5.3.** The chosen MLR regression models for predicting antibacterial activity of ITCs.

Bacteria	Activity parameter	Descriptor	Coefficient	Standard error	p-value	VIF
<i>E. coli</i>	pMIC	TPSA	0.030	0.0028	$5.7 \times 10^{-10}$	2.24
		FCASA+	-1.000	0.105	$4.9 \times 10^{-9}$	4.26
		FCASA-	0.819	0.127	$2.2 \times 10^{-6}$	3.42
		vsurf_W1	0.001	0.00038	0.045	1.74
		Intercept	-2.240	0.286	$1.2 \times 10^{-7}$	–
	p'GIR	PM3_Eele	$9.1 \times 10^{-6}$	$1.0 \times 10^{-6}$	$1.6 \times 10^{-8}$	3.38
		PEOE_RPC+	-11.170	1.449	$1.5 \times 10^{-7}$	4.45
		npr2	-2.619	0.488	$2.5 \times 10^{-5}$	1.42
		vsurf_ID6	0.274	0.138	0.061	1.59
		Intercept	7.276	0.613	$8.8 \times 10^{-11}$	–
	pMIC	PEOE_VSA+3	0.040	0.005	$4.4 \times 10^{-8}$	2.98
		vsurf_HL1	6.413	0.826	$1.3 \times 10^{-7}$	1.14
		vsurf_R	2.802	0.599	0.00013	1.40
		AM1_Electrophilicity	-0.985	0.217	0.00018	2.63
		Intercept	-3.831	0.844	0.00018	–
	p'GIR	vsurf_IW2	-1.386	0.128	$7.6 \times 10^{-11}$	1.47
		npr1	2.622	0.274	$4.3 \times 10^{-9}$	1.29
		PEOE_VSA-1	0.019	0.003	$2.2 \times 10^{-6}$	1.54
		vsurf_W7	0.425	0.116	0.0033	1.24
		Intercept	1.401	0.154	$9.5 \times 10^{-9}$	–

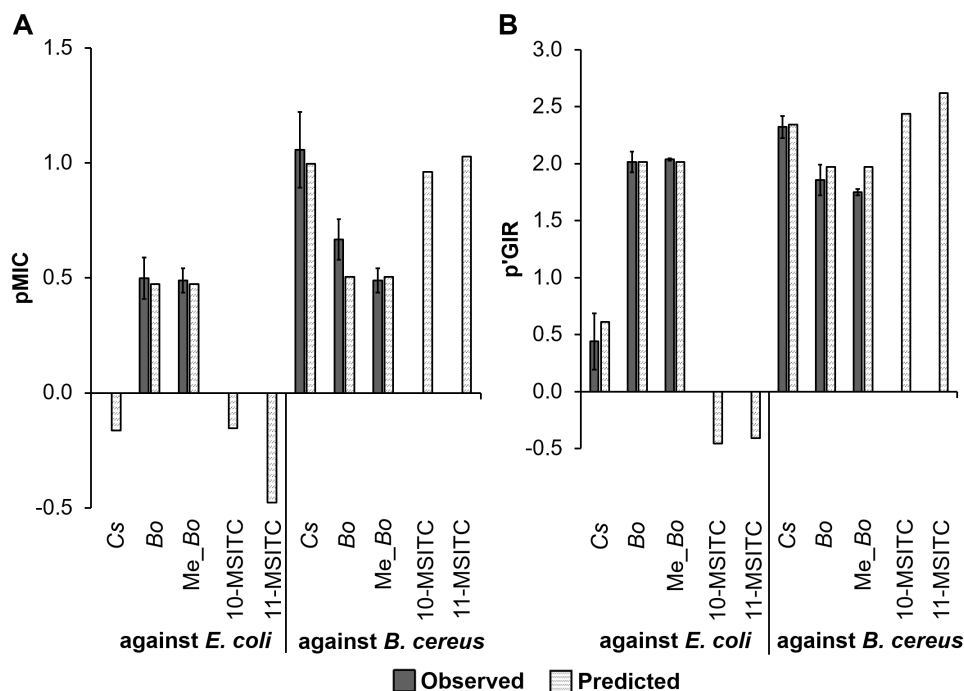
**Table 5.3** indicates that polarity, partial charge, reactivity, and molecular shape were important structural features of ITCs for imparting their antibacterial activity against *E. coli* and *B. cereus*. Molecular shape was more important for activity against *B. cereus* (*npr1*, *p*-value  $4.3 \times 10^{-9}$ ) than against *E. coli* (*npr2*, *p*-value  $2.5 \times 10^{-5}$ ), whereas reactivity was more important for activity against *E. coli* (*PM3\_Eele*, *p*-value  $1.6 \times 10^{-8}$ ) than against *B. cereus* (*AM1\_Electrophilicity*, *p*-value  $1.8 \times 10^{-4}$ ).

### 5.3.3.3. The application of the QSAR models to predict the antibacterial activity of ITC-rich extracts

The developed QSAR models (**Table 5.3**) for *B. cereus* and *E. coli* were used to predict the antibacterial activity of the ITC-rich *C. sativa* and *B. oleracea* extracts. MICs of the extracts ( $\mu\text{g/mL}$ ) presented in **Table 5.1** were transformed to the total concentration (mM) of ITCs in the extract. With the assumption that there was no interaction between ITCs in a mixture, the predicted antibacterial activity of ITC-rich extracts (pMIC and p'GIR) was calculated according to the contribution of each ITC in the extracts to the total antibacterial activity.

**Figure 5.4** shows that the predicted pMIC and p'GIR values of the ITC-rich *C. sativa* and *B. oleracea* extracts against *E. coli* and *B. cereus* matched to the

respective observed values. In the case of *C. sativa* ITC-rich extract against *E. coli*, the negative predicted pMIC shown in **Figure 5.4A** represents a MIC based on extract concentration of 3100 µg/mL, meaning that the predicted MIC was in line to the observed value (MIC > 1000 µg/mL). *C. sativa* ITC-rich extract contained abundantly two ITCs which were not in the training set, i.e. 10-MSITC and 11-MSITC, due to lack of standard compounds. The activity of 10-MSITC and 11-MSITC was predicted by the chosen models with 4 descriptors (**Table 5.3**). Their predicted activity was in line with the observed and predicted activity of *C. sativa* ITC-rich extract, especially against *B. cereus*, i.e. the susceptible bacterium towards long-chained MSITCs.



**Figure 5.4.** Observed vs predicted antibacterial activity (pMIC, **A**; p'GIR, **B**) of ITC-rich mixtures and predicted antibacterial activity of 10-MSITC and 11-MSITC against *E. coli* and *B. cereus*. Cs: *C. sativa* ITC-rich extract; Bo: *B. oleracea* ITC-rich extract; Me\_Bo: model *B. oleracea* ITC-rich extract. The bar for observed pMIC of Cs against *E. coli* is absent due to MIC > 1000.0 µg/mL (the highest tested extract concentration). The bars for observed pMIC and p'GIR of 10-MSITC and 11-MSITC against *E. coli* and *B. cereus* are absent due to lack of pure compounds for testing, but these were abundantly present in Cs. The error bars represent the standard deviation with three biological independent repetitions.

The largest difference between the observed and the predicted values in **Figure 5.4** was perceived for pMIC of *B. oleracea* ITC-rich extract against *B. cereus* (0.668 vs 0.504, respectively, equaled to extract concentration of 750 µg/mL and

989 µg/mL, respectively). Other minor compounds present in the natural extract might contribute to the antimicrobial activity. Therefore, a model extract containing only ITCs, i.e. absent of other potential non-ITC compounds, was made to mimic the *B. oleracea* ITC-rich extract. MIC and GIR values of the model extract were comparable to those of the natural extract (**Table 5.1**). Only a slightly lower activity against *B. cereus* was found for the model extract (MIC 1000 µg/mL) in comparison with the natural extract (MIC 750 µg/mL), but similar to the predicted activity (MIC 989 µg/mL). This confirms that the antibacterial activity of the ITC-rich natural extract against both *E. coli* and *B. cereus* is mainly due to the ITCs and that our QSAR models are able to predict well the activity of both natural ITC-rich mixtures and model ITC mixtures.

## 5.4. Discussion

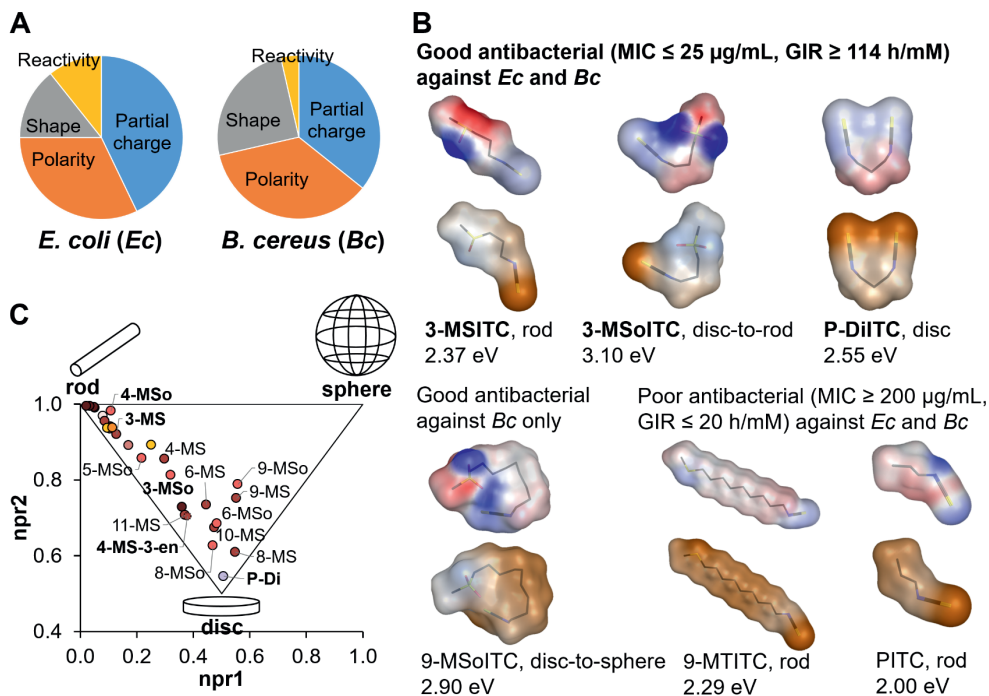
In this QSAR study, partial charge, polarity, molecular shape, and reactivity were the four main (physico)chemical properties determining the antibacterial activity of ITCs against both Gram<sup>-</sup> *E. coli* and Gram<sup>+</sup> *B. cereus* (**Figure 5.5A**, **Tables S5.5-S5.6**).

### 5.4.1. The importance of partial charge

Electrostatic (related to partial charges) surface maps of representative good and poor antibacterial ITCs are depicted in **Figure 5.5B** (red-blue surface). It demonstrates that ITCs with strong electrostatic regions (e.g. 3-MSITC, 3-MSoITC, 9-MSoITC) have antibacterial activity, either against both bacteria or against Gram<sup>+</sup> *B. cereus*. In contrast, ITCs without strong electrostatic regions (e.g. 9-MTITC, PITC) have no antibacterial activity, except the bifunctional ITC (i.e. P-DiITC, the exceptional behavior of this molecule will be discussed in section **5.4.5**).

### 5.4.2. The importance of polarity

Polarity related descriptors are frequently used in our QSAR models for ITCs (**Figure 5.5A**) and other QSAR models for other classes of antimicrobial compounds.<sup>10,31,37,38</sup> Most active ITCs have distinct hydrophilic and hydrophobic regions (**Figure 5.5B**, orange-light blue surface). The shorter the chain length, the more distinct the hydrophilic and hydrophobic regions (e.g. 3-MSoITC vs 9-MSoITC). In our study, only ITCs with short chain length, thus more distinctive hydrophilic and hydrophobic regions, exerted activity against both Gram<sup>-</sup> *E. coli* and Gram<sup>+</sup> *B. cereus*. ITCs with evenly distributed hydrophobicity (e.g. 9-MTITC, PITC) showed poor antibacterial activity against both bacteria.



**Figure 5.5.** Important physicochemical properties of ITCs for imparting their antimicrobial activity. Frequency of descriptors related to a physicochemical property (partial charge, polarity, molecular shape, or reactivity) used in the models with 2-5 descriptors for *E. coli* (left) and *B. cereus* (right) (A). The physicochemical classification of descriptors is in **Table S5.6**. Surface maps of electrostatic regions (blue: partial negative charge; red: partial positive charge) and hydrophobic/hydrophilic regions (yellow: hydrophobic; light blue: hydrophilic) of some representative ITCs (B). 3-MSITC: 3-(methylsulfinyl)propyl ITC; 3-MSolTC: 3-(methylsulfonyl)propyl ITC; P-DiITC: 1,3-propylene diisothiocyanate; 9-MSolTC: 9-(methylsulfonyl)nonyl ITC; 9-MTITC: 9-(methylthio)nonyl ITC; PITC: propyl ITC. The numbers (eV) underneath the names of ITCs represent the *AM1\_Electrophilicity* values. Molecular shape distribution of ITCs in the triangular npr (normalized PMI – principal moment of inertia – ratios) shape space according to Sauer & Schwarz<sup>39</sup> and Wirth *et al.*<sup>40</sup> (C). Different subclasses of ITCs are indicated by different colors according to those in **Figure 5.1**. The names of ITCs are represented as the abbreviation of their side chain. ITCs in bold face were good antibacterials (GIR  $\geq 114$  h/mM, MIC  $\leq 25$   $\mu\text{g/mL}$ ) against both *E. coli* and *B. cereus*, whereas ITCs in light face were good antibacterials only against *B. cereus*.

Polarity as a main physicochemical property for antimicrobial compounds often links to the polarity of the microbial cell envelope components, important for uptake of molecules.<sup>41-43</sup> High polarity is desirable for good antibacterials against Gram<sup>-</sup> *E. coli*, reflected by *TPSA* (*p*-value  $5.7 \times 10^{-10}$ ) and *vsurf\_W1* (*p*-value  $3.8 \times 10^{-4}$ ) (**Figure S5.8**). The nonspecific porins in the outer membrane of Gram<sup>-</sup>

bacteria allow small (< 600 Da) and hydrophilic molecules to pass,<sup>44</sup> and are often reported to be the importer for small and hydrophilic antimicrobial molecules.<sup>43,45-47</sup> As in our study short-chained ITCs with sulfinyl and sulfonyl groups (MSITCs and MSoITCs, respectively) had good antibacterial activity, whereas long-chained analogues did not, we suggest that the entry pathway of ITCs into Gram<sup>-</sup> *E. coli* cells is via the nonspecific porins. Further studies are required to confirm this hypothesis by using *E. coli* mutant strains lacking of the nonspecific porins.<sup>48,49</sup> In contrast, the long-chained MSITCs and MSoITCs were good antibacterials against *B. cereus*. This might be because the cell envelope of Gram<sup>+</sup> bacteria generally has less restriction for influx of molecules in comparison to the cell envelope of Gram<sup>-</sup> bacteria characterized by the presence of impermeable lipopolysaccharides.<sup>41</sup> Furthermore, the long-chained MSITCs and MSoITCs might passively diffuse through the cytoplasmic membrane of Gram<sup>+</sup> *B. cereus*. Moreover, our QSAR models for *B. cereus* agree with QSAR models of 1,4-benzoxazine-3-ones for Gram<sup>+</sup> bacteria, in which hydrophilic integrity moment and hydrophilic volume descriptors were important.<sup>31</sup>

#### 5.4.3. The importance of molecular shape

Molecular shape was often used in our models for both Gram<sup>-</sup> *E. coli* and Gram<sup>+</sup> *B. cereus* (**Figure 5.5A**). Various studies have revealed the importance of shape for interaction of an antimicrobial with the bacterial membrane and intracellular targets.<sup>39,50,51</sup> Moreover, modification of molecular shape of antibiotics altered their spectrum of activity.<sup>43</sup> In our models, the shape descriptors *npr1* and *npr2* were correlated to the activity against *B. cereus* and *E. coli*, respectively. The combinatorial *npr1* and *npr2* descriptor values in the triangle graph reflect the molecular shape (rod, sphere, or disc) as shown in **Figure 5.5C**.<sup>39,40</sup> For good antibacterial activity against *E. coli*, ITCs with rod-like shapes are desirable (**Figure 5.5B-C**), except for P-DiITC (disc-like). In contrast, for good antibacterial activity against *B. cereus*, ITCs with disc- or rod-like shapes are desirable. Our findings support previous QSAR study of 1,4-benzoxazin-3-ones that rod-like rather than sphere-like shape is desirable for good antibacterial activity against Gram<sup>-</sup> bacteria, whereas disc-like or rod-like shape is desirable against Gram<sup>+</sup> bacteria.<sup>31</sup>

#### 5.4.4. The importance of reactivity

Reactivity was an important physicochemical property for ITCs antimicrobial activity against Gram<sup>-</sup> *E. coli* and Gram<sup>+</sup> *B. cereus* (**Figure 5.5A**). Our study supports a previous QSAR study of benzenic ITCs as antibacterials (against *E. coli*),<sup>52</sup> QSAR studies of nitrogen-containing antimicrobial compounds,<sup>28,37,53</sup> and toxicological QSAR studies of ITCs and other electrophilic compounds,<sup>54-57</sup> where reactivity related descriptors are important in the models. The reactivity of ITCs is mainly due to the electrophilic carbon of the -N=C=S group. The substituent in the side chains varies the global electrophilicity ( $\omega^0$ , eV) of ITCs more than the

chain length does (e.g. 3-MSITC,  $\omega^o = 2.37$  eV; 3-MSoITC,  $\omega^o = 3.10$  eV; 9-MSoITC,  $\omega^o = 2.90$  eV). The electrophilic carbon is suggested to be essential for antimicrobial activity of ITCs because of its capability of impairing functions of proteins essential for cell growth and metabolism by forming covalent linkage to nucleophilic groups (particularly thiol,  $-SH$ ) in the active site of proteins.<sup>7,58</sup>

#### 5.4.5. The bifunctional ITC

P-DiITC, the bifunctional ITC, had remarkably high antimicrobial activity against both bacteria (MIC 6.3-9.4  $\mu\text{g/mL}$ , 0.04-0.06 mM), much higher than the activity of the monofunctional analogue (PITC, MIC > 200.0  $\mu\text{g/mL}$ , > 1.98 mM). A previous study showed that bifunctional ITC groups improved the activity against Gram<sup>+</sup> *B. cereus* (e.g. for two identical compounds except for the number of ITC groups, MIC<sub>bi</sub> 0.5  $\mu\text{g/mL}$ , MIC<sub>mono</sub> 16  $\mu\text{g/mL}$ ) and against Gram<sup>-</sup> *E. coli* (MIC<sub>bi</sub> 8  $\mu\text{g/mL}$ , MIC<sub>mono</sub> 64  $\mu\text{g/mL}$ ).<sup>59</sup> The enhanced antimicrobial activity of P-DiITC can be explained by twice higher topological polar surface area compared to PITC (**Figure S5.8A**). Furthermore, as the  $-N=C=S$  group is the site for nucleophilic attacks, P-DiITC has two electrophilic sites for the attack.

#### 5.4.6. QSAR models predict antibacterial activity of ITC-rich mixtures well

The antimicrobial activity of *B. oleracea* ITC-rich extract is promising as it has activity against both Gram<sup>-</sup> *E. coli* and Gram<sup>+</sup> *B. cereus* with MIC 750-1000  $\mu\text{g/mL}$ , whereas other natural extracts are often effective only against Gram<sup>+</sup> bacteria or require higher concentrations (2,500-10,000  $\mu\text{g/mL}$ ) to be also effective against Gram<sup>-</sup> bacteria.<sup>60</sup> The antimicrobial activity of *C. sativa* ITC-rich extract against Gram<sup>+</sup> *B. cereus* is also promising (MIC 188  $\mu\text{g/mL}$ ) in comparison with other natural extracts (MIC  $\geq 315$   $\mu\text{g/mL}$ ).<sup>60,61</sup> The developed QSAR models were able to predict the antibacterial activity of these two ITC-rich extracts well, with one of the extracts containing ITCs (in high abundance), which were not in the training set. This indicates that the developed models can potentially be used to predict the activity of (natural) mixtures of ITCs and untested ITCs.

This study was the first QSAR study of ITCs as antibacterials ( $n = 26$ ) covering various aliphatic and benzenic ITCs from 9 subclasses against Gram<sup>-</sup> and Gram<sup>+</sup> bacteria. Models with two activity parameters (pMIC and p'GIR) were developed with good internal predictivity ( $Q^2 \geq 0.83$ ,  $Q^2_{adj} \geq 0.80$ ). Models built by p'GIR are recommended for future QSAR studies on antimicrobial compounds, as imputation of missing data is no longer needed. Although the pMIC and p'GIR models used different descriptors for each bacterium, they supported similar physicochemical properties. Polarity, shape, partial charge, and reactivity are the key physicochemical properties of ITCs imparting their antibacterial activity. The models can be applied to predict antibacterial activity of new ITCs and ITC-rich

mixtures. ITCs are promising antimicrobial candidates to meet the consumers' demand for natural preservatives active against Gram<sup>-</sup> and Gram<sup>+</sup> bacteria.

### **5.5. Funding source**

The authors are grateful to Indonesia Endowment Fund for Education (LPDP), Ministry of Finance of Republic Indonesia, to financially support PhD study of SA.

The authors declare no competing financial interest.

## 5.6. References

1. Abdel-Aziz, S. M.; Aeron, A.; Kahil, T. A., Health benefits and possible risks of herbal medicine. In *Microbes in Food and Health*, Garg, N.; Abdel-Aziz, S. M.; Aeron, A., Eds. Springer International Publishing: Cham, **2016**; pp 97-116.
2. Michael, C. A.; Dominey-Howes, D.; Labbate, M., The antimicrobial resistance crisis: Causes, consequences, and management. *Front. Public Health* **2014**, *2*, 145.
3. Windels, E. M.; Michiels, J. E.; Fauvart, M.; Wenseleers, T.; Van den Bergh, B.; Michiels, J., Bacterial persistence promotes the evolution of antibiotic resistance by increasing survival and mutation rates. *ISME J.* **2019**, *13*, 1239-1251.
4. Abreu, A. C.; Borges, A.; Simões, L. C.; Saavedra, M. J.; Simões, M., Antibacterial activity of phenyl isothiocyanate on *Escherichia coli* and *Staphylococcus aureus*. *Med. Chem.* **2013**, *9*, 756-761.
5. Andini, S.; Araya-Cloutier, C.; Waardenburg, L.; den Besten, H. M. W.; Vincken, J. P., The interplay between antimicrobial activity and reactivity of isothiocyanates. Accepted in *LWT-Food Sci. Technol.* **2020**.
6. Bednarek, P.; Pislewska-Bednarek, M.; Svatos, A.; Schneider, B.; Doubsky, J.; Mansurova, M.; Humphry, M.; Consonni, C.; Panstruga, R.; Sanchez-Vallet, A.; Molina, A.; Schulze-Lefert, P., A glucosinolate metabolism pathway in living plant cells mediates broad-spectrum antifungal defense. *Science (New York, N.Y.)* **2009**, *323*, 101-6.
7. Dufour, V.; Stahl, M.; Baysse, C., The antibacterial properties of isothiocyanates. *Microbiology (Reading, England)* **2015**, *161*, 229-43.
8. Halkier, B. A.; Gershenzon, J., Biology and biochemistry of glucosinolates. *Annu. Rev. Plant Biol.* **2006**, *57*, 303-33.
9. Nowicki, D.; Rodzik, O.; Herman-Antosiewicz, A.; Szalewska-Palasz, A., Isothiocyanates as effective agents against enterohemorrhagic *Escherichia coli*: Insight to the mode of action. *Sci. Rep.* **2016**, *6*, 22263.
10. Araya-Cloutier, C.; Vincken, J.-P.; van de Schans, M. G. M.; Hageman, J.; Schaftenaar, G.; den Besten, H. M. W.; Gruppen, H., QSAR-based molecular signatures of prenylated (iso)flavonoids underlying antimicrobial potency against and membrane-disruption in Gram positive and Gram negative bacteria. *Sci. Rep.* **2018**, *8*, 9267.
11. Dias, C.; Aires, A.; Saavedra, M. J., Antimicrobial activity of isothiocyanates from cruciferous plants against methicillin-resistant *Staphylococcus aureus* (MRSA). *Int. J. Mol. Sci.* **2014**, *15*, 19552-19561.
12. Dufour, V.; Alazzam, B.; Ermel, G.; Thepaut, M.; Rossero, A.; Tresse, O.; Baysse, C., Antimicrobial activities of isothiocyanates against *Campylobacter jejuni* isolates. *Front. Cell. Infect. Microbiol.* **2012**, *2*, 53.
13. Stotz, H. U.; Sawada, Y.; Shimada, Y.; Hirai, M. Y.; Sasaki, E.; Krischke, M.; Brown, P. D.; Saito, K.; Kamiya, Y., Role of camalexin, indole glucosinolates, and side chain modification of glucosinolate-derived isothiocyanates in defense of *Arabidopsis* against *Sclerotinia sclerotiorum*. *Plant J.* **2011**, *67*, 81-93.
14. Wilson, A. E.; Bergaentzlé, M.; Bindler, F.; Marchioni, E.; Lintz, A.; Ennahar, S., In vitro efficacies of various isothiocyanates from cruciferous vegetables as antimicrobial agents against foodborne pathogens and spoilage bacteria. *Food Control* **2013**, *30*, 318-324.
15. Aires, A.; Mota, V. R.; Saavedra, M. J.; Rosa, E. A.; Bennett, R. N., The antimicrobial effects of glucosinolates and their respective enzymatic hydrolysis products on bacteria isolated from the human intestinal tract. *J. Appl. Microbiol.* **2009**, *106*, 2086-95.
16. Haristoy, X.; Fahey, J. W.; Scholtus, I.; Lozniewski, A., Evaluation of the antimicrobial effects of several isothiocyanates on *Helicobacter pylori*. *Planta Med.* **2005**, *71*, 326-330.



17. Hawkins, D. M., The problem of overfitting. *J. Chem. Inf. Comput. Sci.* **2004**, *44*, 1-12.
18. Blažević, I.; Montaut, S.; Burčul, F.; Olsen, C. E.; Burow, M.; Rollin, P.; Agerbirk, N., Glucosinolate structural diversity, identification, chemical synthesis and metabolism in plants. *Phytochemistry* **2020**, *169*, 112100.
19. Andini, S.; Dekker, P.; Gruppen, H.; Araya-Cloutier, C.; Vincken, J.-P., Modulation of glucosinolate composition in Brassicaceae seeds by germination and fungal elicitation. *J. Agric. Food Chem.* **2019**, *67*, 12770-12779.
20. Andini, S.; Araya-Cloutier, C.; Sanders, M.; Vincken, J.-P., Simultaneous analysis of glucosinolates and isothiocyanates by RP-UHPLC-ESI-MS<sup>n</sup>. *J. Agric. Food Chem.* **2020**, *68*, 3121-3131.
21. Aryani, D. C.; den Besten, H. M. W.; Hazeleger, W. C.; Zwietering, M. H., Quantifying strain variability in modeling growth of *Listeria monocytogenes*. *Int. J. Food Microbiol.* **2015**, *208*, 19-29.
22. Huang, L.; Xiao, Y.-h.; Xing, X.-d.; Li, F.; Ma, S.; Qi, L.-l.; Chen, J.-h., Antibacterial activity and cytotoxicity of two novel cross-linking antibacterial monomers on oral pathogens. *Arch. Oral Biol.* **2011**, *56*, 367-373.
23. Li, F.; Weir, M. D.; Fouad, A. F.; Xu, H. H. K., Time-kill behaviour against eight bacterial species and cytotoxicity of antibacterial monomers. *J. Dent.* **2013**, *41*, 881-891.
24. Tsou, S. H.; Hu, S. W.; Yang, J. J.; Yan, M.; Lin, Y. Y., Potential oral health care agent from coffee against virulence factor of periodontitis. *Nutrients* **2019**, *11*.
25. Gindulyte, A.; Shoemaker, B. A.; Yu, B.; Fu, G.; He, J.; Zhang, J.; Chen, J.; Wang, J.; Han, L.; Thiessen, P. A.; He, S.; Bryant, S. H.; Kim, S.; Bolton, E. E., PubChem Substance and Compound databases. *Nucleic Acids Res.* **2015**, *44*, D1202-D1213.
26. Parr, R. G.; Pearson, R. G., Absolute hardness: companion parameter to absolute electronegativity. *J. Am. Chem. Soc.* **1983**, *105*, 7512-7516.
27. Parr, R. G.; Szentpály, L. v.; Liu, S., Electrophilicity index. *J. Am. Chem. Soc.* **1999**, *121*, 1922-1924.
28. Dolezal, R.; Soukup, O.; Malinak, D.; Savedra, R. M. L.; Marek, J.; Dolezalova, M.; Pasdiorova, M.; Salajkova, S.; Korabecny, J.; Honegr, J.; Ramalho, T. C.; Kuca, K., Towards understanding the mechanism of action of antibacterial *N*-alkyl-3-hydroxypyridinium salts: Biological activities, molecular modeling and QSAR studies. *Eur. J. Med. Chem.* **2016**, *121*, 699-711.
29. Khazaei, A.; Sarmasti, N.; Seyf, J. Y., Quantitative structure-activity relationship of the curcumin-related compounds using various regression methods. *J. Mol. Struct.* **2016**, *1108*, 168-178.
30. Gramatica, P., Principles of QSAR models validation: internal and external. *QSAR Comb. Sci.* **2007**, *26*, 694-701.
31. de Bruijn, W. J. C.; Hageman, J. A.; Araya-Cloutier, C.; Gruppen, H.; Vincken, J.-P., QSAR of 1,4-benzoxazin-3-one antimicrobials and their drug design perspectives. *Bioorg. Med. Chem.* **2018**, *26*, 6105-6114.
32. Hageman, J. A.; Engel, B.; de Vos, R. C. H.; Mumm, R.; Hall, R. D.; Jwanro, H.; Crouzillat, D.; Spadone, J. C.; van Eeuwijk, F. A., Robust and confident predictor selection in metabolomics. In *Statistical Analysis of Proteomics, Metabolomics, and Lipidomics Data Using Mass Spectrometry*, Datta, S.; Mertens, B. J. A., Eds. Springer International Publishing: Cham, **2017**; pp 239-257.
33. Gramatica, P., On the development and validation of QSAR models. In *Computational Toxicology*, 2012/10/23 ed.; Reisfeld, B.; Mayeno, A. N., Eds. Springer Science+Business Media, LLC: NY, **2013**; Vol. 2, pp 499-526.
34. Tropsha, A., Best practices for QSAR model development, validation, and exploitation. *Mol. Inf.* **2010**, *29*, 476-488.
35. Roy, K.; Chakraborty, P.; Mitra, I.; Ojha, P. K.; Kar, S.; Das, R. N., Some case studies on application of "r<sup>2</sup>m" metrics for judging quality of quantitative structure-activity relationship predictions: Emphasis on scaling of response data. *J. Comput. Chem.* **2013**, *34*, 1071-1082.

36. Xu, L.; Zhang, W.-J., Comparison of different methods for variable selection. *Anal. Chim. Acta* **2001**, *446*, 475-481.
37. Judge, V.; Narasimhan, B.; Ahuja, M.; Sriram, D.; Yogeewari, P.; De Clercq, E.; Pannecouque, C.; Balzarini, J., Isonicotinic acid hydrazide derivatives: synthesis, antimicrobial activity, and QSAR studies. *Med. Chem. Res.* **2012**, *21*, 1451-1470.
38. Maguna, F.; Okulik, N.; Castro, E. A., Quantitative structure-activity relationships of antimicrobial compounds. In *Handbook of Computational Chemistry*, Leszczynski, J.; Kaczmarek-Kedziera, A.; Puzyn, T.; Papadopoulos, M. G.; Reis, H.; Shukla, M. K., Eds. Springer International Publishing: Cham, **2017**; pp 2341-2357.
39. Sauer, W. H. B.; Schwarz, M. K., Molecular shape diversity of combinatorial libraries: A prerequisite for broad bioactivity. *J. Chem. Inf. Comput. Sci.* **2003**, *43*, 987-1003.
40. Wirth, M.; Volkamer, A.; Zoete, V.; Rippmann, F.; Michielin, O.; Rarey, M.; Sauer, W. H. B., Protein pocket and ligand shape comparison and its application in virtual screening. *J. Comput.-Aided Mol. Des.* **2013**, *27*, 511-524.
41. Denyer, S. P.; Maillard, J. Y., Cellular impermeability and uptake of biocides and antibiotics in Gram-negative bacteria. *J. Appl. Microbiol.* **2002**, *92 Suppl*, 35s-45s.
42. Lambert, P. A., Cellular impermeability and uptake of biocides and antibiotics in Gram-positive bacteria and mycobacteria. *J. Appl. Microbiol.* **2002**, *92*, 46S-54S.
43. Richter, M. F.; Drown, B. S.; Riley, A. P.; Garcia, A.; Shirai, T.; Svec, R. L.; Hergenrother, P. J., Predictive compound accumulation rules yield a broad-spectrum antibiotic. *Nature* **2017**, *545*, 299-304.
44. van den Berg, B., The FadL family: unusual transporters for unusual substrates. *Curr. Opin. Struct. Biol.* **2005**, *15*, 401-407.
45. Braun, V.; Bos, C.; Braun, M.; Killmann, H., Outer membrane channels and active transporters for the uptake of antibiotics. *J. Infect. Dis.* **2001**, *183 Suppl 1*, S12-6.
46. Nikaido, H., Molecular basis of bacterial outer membrane permeability revisited. *Microbiol. Mol. Biol. Rev.* **2003**, *67*, 593-656.
47. Ziervogel, Brigitte K.; Roux, B., The binding of antibiotics in OmpF porin. *Structure* **2013**, *21*, 76-87.
48. Huang, H.; Hancock, R. E., The role of specific surface loop regions in determining the function of the imipenem-specific pore protein OprD of *Pseudomonas aeruginosa*. *J. Bacteriol.* **1996**, *178*, 3085-3090.
49. Mortimer, P. G. S.; Piddok, L. J. V., The accumulation of five antibacterial agents in porin-deficient mutants of *Escherichia coli*. *J. Antimicrob. Chemother.* **1993**, *32*, 195-213.
50. Liu, L.; Fang, Y.; Wu, J., Flexibility is a mechanical determinant of antimicrobial activity for amphipathic cationic  $\alpha$ -helical antimicrobial peptides. *BBA - Biomembranes* **2013**, *1828*, 2479-2486.
51. Reisser, S.; Strandberg, E.; Steinbrecher, T.; Ulrich, A. S., 3D hydrophobic moment vectors as a tool to characterize the surface polarity of amphiphilic peptides. *Biophys. J.* **2014**, *106*, 2385-94.
52. Valchová, D.; Drobica, L., Some relationships between biological activity and physico-chemical properties of monosubstituted phenylisothiocyanates. *Collect. Czech. Chem. Commun.* **1966**, *31*, 997-1008.
53. Debeljak, Ž.; Škrbo, A.; Jasprica, I.; Mornar, A.; Plečko, V.; Banjanac, M.; Medić-Šarić, M., QSAR study of antimicrobial activity of some 3-nitrocoumarins and related compounds. *J. Chem. Inf. Model.* **2007**, *47*, 918-926.
54. Borek, V.; Elbersson, L. R.; McCaffrey, J. P.; Morra, M. J., Toxicity of isothiocyanates produced by glucosinolates in Brassicaceae species to black vine weevil eggs. *J. Agric. Food Chem.* **1998**, *46*, 5318-5323.
55. Hansch, C.; Hoekman, D.; Gao, H., Comparative QSAR: Toward a deeper understanding of chemicobiological interactions. *Chem. Rev.* **1996**, *96*, 1045-1075.
56. Peterson, C. J.; Tsao, R.; Coats, J. R., Glucosinolate aglucones and analogues: Insecticidal properties and a QSAR. *Pestic. Sci.* **1998**, *54*, 35-42.

57. Schultz, T. W.; Cronin, M. T. D.; Walker, J. D.; Aptula, A. O., Quantitative structure–activity relationships (QSARs) in toxicology: A historical perspective. *J. Mol. Struct.: THEOCHEM* **2003**, 622, 1-22.
58. Luciano, F. B.; Holley, R. A., Enzymatic inhibition by allyl isothiocyanate and factors affecting its antimicrobial action against *Escherichia coli* O157:H7. *Int. J. Food Microbiol.* **2009**, 131, 240-5.
59. Kurepina, N.; Kreiswirth, B. N.; Mustaev, A., Growth-inhibitory activity of natural and synthetic isothiocyanates against representative human microbial pathogens. *J. Appl. Microbiol.* **2013**, 115, 943-954.
60. Gonelimali, F. D.; Lin, J.; Miao, W.; Xuan, J.; Charles, F.; Chen, M.; Hatab, S. R., Antimicrobial properties and mechanism of action of some plant extracts against food pathogens and spoilage microorganisms. *Front. Microbiol.* **2018**, 9.
61. Araya-Cloutier, C.; den Besten, H. M. W.; Aisyah, S.; Gruppen, H.; Vincken, J.-P., The position of prenylation of isoflavonoids and stilbenoids from legumes (Fabaceae) modulates the antimicrobial activity against Gram positive pathogens. *Food Chem.* **2017**, 226, 193-201.
62. Veerasamy, R.; Rajak, H.; Jain, A.; Sivadasan, S.; Christopher, P. V.; Agrawal, R. K., Validation of QSAR models - Strategies and importance. *Int. J. Drug Des. Discov.* **2011**, 2, 511-519.
63. Leach, A. R., *Molecular modelling: Principles and applications*. Prentice Hall: NY, **2001**.
64. de Assis, T. M.; Gajo, G. C.; de Assis, L. C.; Garcia, L. S.; Silva, D. R.; Ramalho, T. C.; da Cunha, E. F., QSAR models guided by molecular dynamics applied to human glucokinase activators. *Chem. Biol. Drug Des.* **2016**, 87, 455-66.
65. Gajo, G. C.; de Assis, T. M.; Assis, L. C.; Ramalho, T. C.; da Cunha, E. F. F., Quantitative structure-activity relationship studies for potential rho-associated protein kinase inhibitors. *J. Chem.* **2016**, 2016, 12.
66. Dolatabadi, M.; Nekoei, M.; Banaei, A., Prediction of antibacterial activity of pleuromutilin derivatives by genetic algorithm–multiple linear regression (GA–MLR). *Monatsh. Chem.* **2010**, 141, 577-588.
67. Roy, K.; Kar, S.; Ambure, P., On a simple approach for determining applicability domain of QSAR models. *Chemom. Intell. Lab. Syst.* **2015**, 145, 22-29.

## 5.7. Supplementary information

### 5.7.1. GSL and ITC compositions of the (hydrolysed) Brassicaceae seed extracts

GSL and ITC composition in the extracts were analysed simultaneously based on our recently developed LC-MS method.<sup>1</sup> In this study, we confirmed that upon myrosinase incubation at 50 °C for 4 h, all GSLs which were present in the seed extracts were hydrolysed (**Figure S5.4**). The GSL compositions before hydrolysis are presented in **Table S5.2** and **Table S5.3**.

#### 5.7.1.1. GSL compositions

Seeds from 5 Brassicaceae species were studied: *S. alba*, *B. napus*, *B. juncea*, *B. oleracea*, and *C. sativa*. In total, 26 GSLs were tentatively annotated; 12 GSLs were confirmed by the authentic standards listed in section **5.2.1**. The 26 GSLs belonged to *x*-(methylthio)alkyl (3), *x*-(methylsulfinyl)alkyl (6), alkenyl (3), hydroxylated alkenyl (2), acylated alkenyl (1), alkyl (2), unclassified aliphatic (1), benzenic (3), acylated benzenic (1), and indolic (4) subclasses (**Table S5.2**). The most abundant GSLs were *p*-OH-BGSL (30 mg GE/g DW) in *S. alba*, (*R*)-2-OH-BuGSL (2 mg GE/g DW) in *B. napus*, BuGSL (24 mg GE/g DW) and AGSL (3 mg GE/g DW) in *B. juncea*, 4-MSGSL (13 mg GE/g DW), 3-MSGSL (6 mg GE/g DW), and 4-MTGSL (4 mg GE/g DW) in *B. oleracea*, and 10-MSGSL (19 mg GE/g DW), 9-MSGSL (6 mg GE/g DW), and 11-MSGSL (5 mg GE/g DW) in *C. sativa*. The compositions of GSLs in  $\mu\text{M}$  for 1 mg/mL extract are presented in **Table S5.3**.

GSL compositions of *S. alba*, *B. napus*, and *B. juncea* obtained in this study were comparable to those obtained in the previous study.<sup>2</sup> *B. oleracea* and *C. sativa* were chosen for their (methylsulfinyl)alkyl GSL (MSGSLs) content; *C. sativa* was rich in the long-chained MSGSLs, whereas *B. oleracea* was rich in the short-chained MSGSLs.

#### 5.7.1.2. ITC compositions

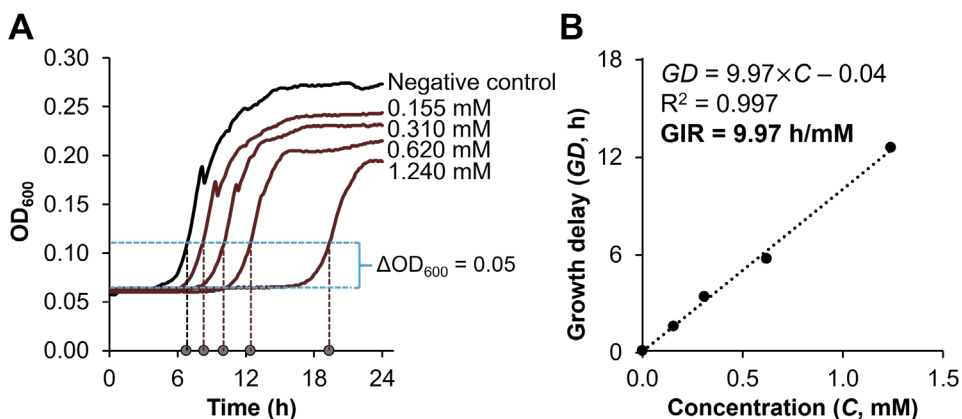
After hydrolysis with myrosinase, *S. alba* contained 6.6  $\mu\text{M}$  *p*-OH-BITC (**Table S5.3**). It supports previous studies which reported that *p*-OH-BGSL was hydrolysed forming various products, e.g. *p*-OH-BITC (minority) and *p*-OH-benzyl alcohol (majority).<sup>1,3</sup>

After hydrolysis, *B. napus* contained 20.5  $\mu\text{M}$  BuITC, which was in a comparable amount of BuGSL before hydrolysis. The majority GSL in *B. napus*, i.e. (*R*)-2-OH-BuGSL, is known to not form ITC.<sup>4</sup>

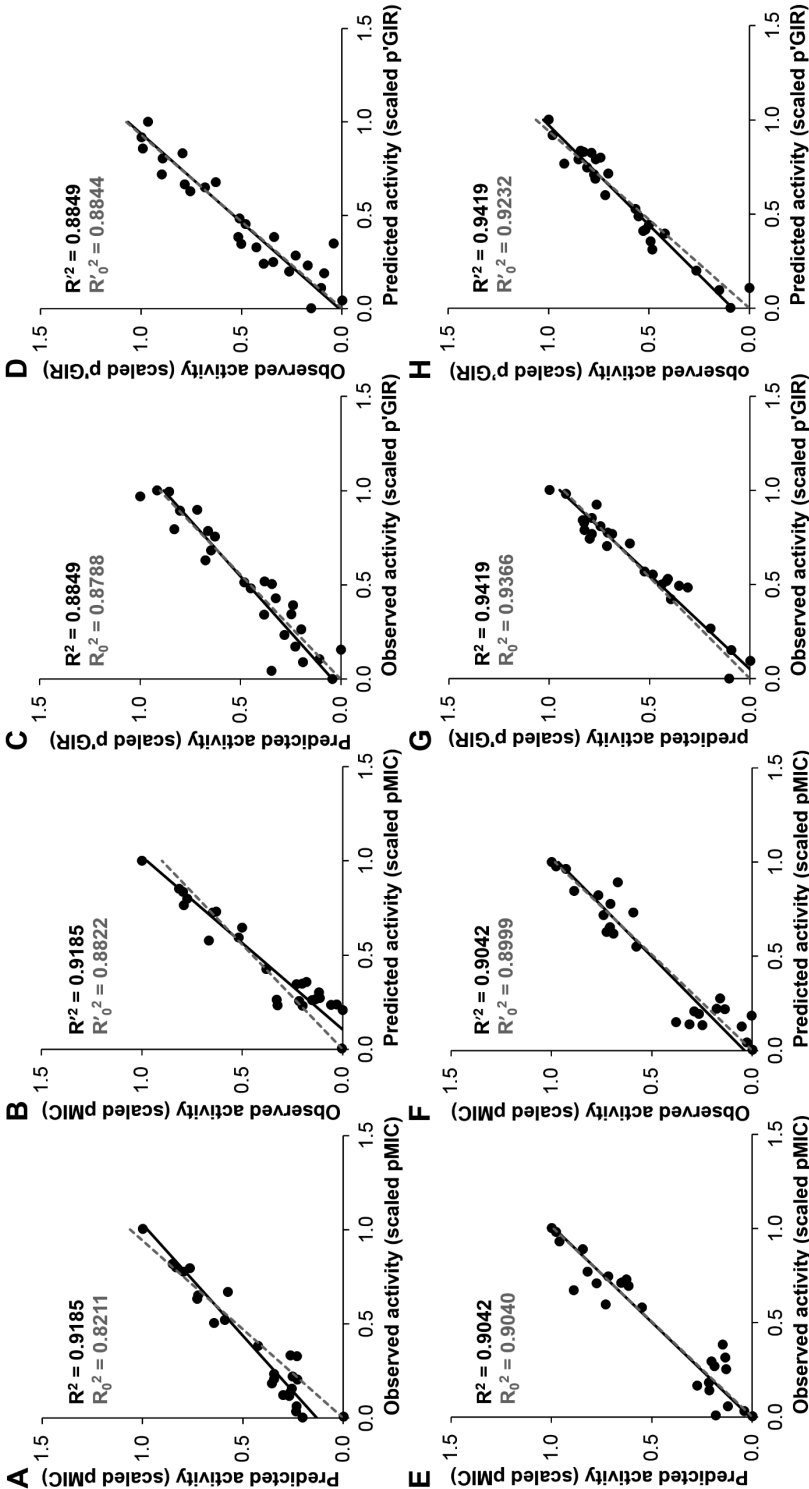
After hydrolysis, *B. juncea* contained 390.8  $\mu\text{M}$  BuITC and 48.7  $\mu\text{M}$  AITC, *B. oleracea* contained 173.3  $\mu\text{M}$  4-MSITC, 78.7  $\mu\text{M}$  3-MSITC, and 51.0  $\mu\text{M}$  4-MTITC, and *C. sativa* contained 322.5  $\mu\text{M}$  10-MSITC, 98.8  $\mu\text{M}$  9-MSITC, and 75.0  $\mu\text{M}$  11-MSITC (**Table S5.4**). Compared with the composition of GSLs (**Table S5.3**), the concentrations of ITCs were comparable to the concentrations of the corresponding

GSLs. Additionally, acylated GSL, i.e. 6'-*O*-sinapoyl(or isomer)-3-butenyl GSL, was not hydrolysed by the myrosinase and still present in the extracts after hydrolysis.

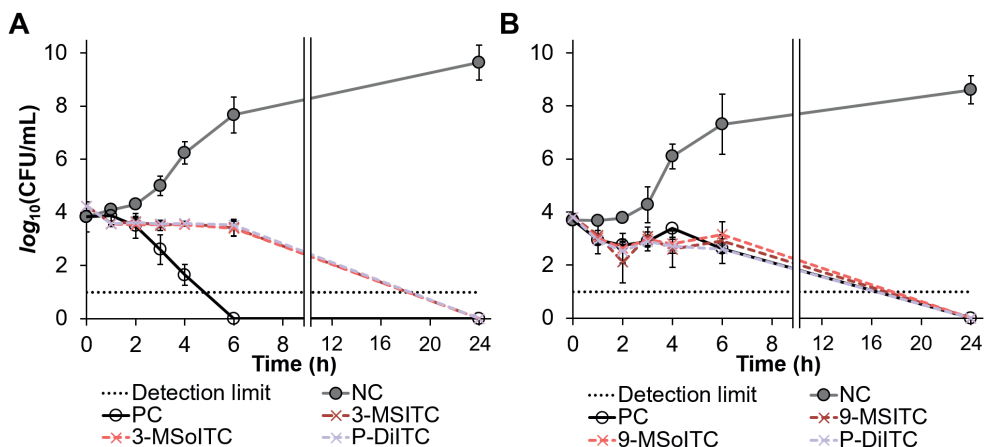
### 5.7.2. Supplementary figures



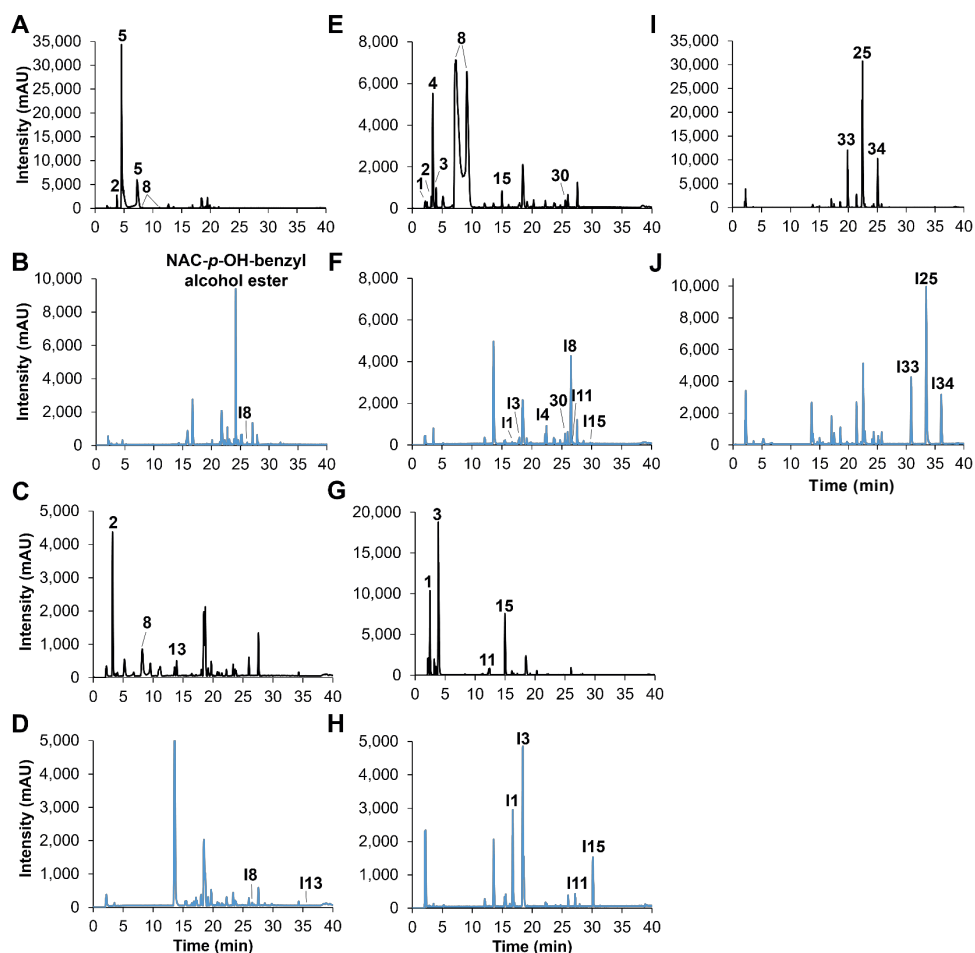
**Figure S5.1.** Determination of growth inhibitory response (GIR, h/mM). Time points indicated by grey-filled bullets are the TTD, which is defined as the time when the OD<sub>600</sub> is increased by 0.05 unit (**A**). These plots were taken from an experiment with 4-(methylthio)butyl ITC (4-MTITC). GIR is defined as the slope of the plot of growth delay (h) against concentration (mM) (**B**). Growth delay is defined as the difference between TTD in the presence of an antimicrobial compound and TTD in the absence of any antimicrobial compound (the negative control).



**Figure S5.2.** Scaled observed vs predicted activity of ITCs against *E. coli* (A-B, pMIC; C-D, pGIR) and *B. cereus* (E-F, pMIC; G-H, pGIR) calculated by the chosen models (Table 5.3). Plots were used for calculation of  $\overline{R_m^2}$ , where  $R^2$  and  $R_0^2$  represent the correlation coefficients obtained after switching the x and y axes with and without intercept, respectively.

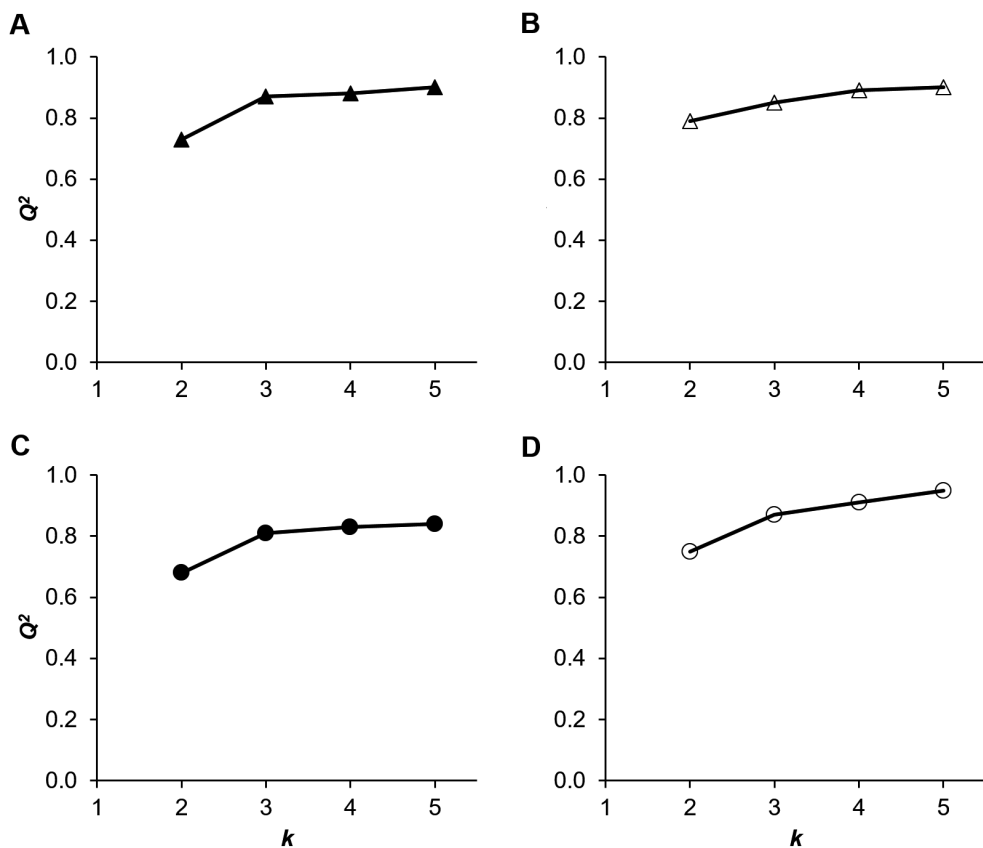


**Figure S5.3.** Killing kinetics of good antibacterial ITCs at their MBC against *E. coli* (A) and *B. cereus* (B), in comparison with the negative control (NC) and the positive control (PC: ampicillin 1.5  $\mu\text{g/mL}$  for *E. coli*, 15  $\mu\text{g/mL}$  for *B. cereus*). 3-MSITC: 3-(methylsulfinyl)propyl ITC; 3-MSoITC: 3-(methylsulfonyl)propyl ITC; P-DiITC: 1,3-propylene diisothiocyanate; 9-MSITC: 9-(methylsulfinyl)nonyl ITC; 9-MSoITC: 9-(methylsulfonyl)nonyl ITC. Data are means of two independent biological repetitions with standard deviation bars. Dotted black line represents the detection limit of cell count; when there was no colony at the lowest dilution factor in the agar plate, the  $\log_{10}(\text{CFU/mL})$  was assumed as null.

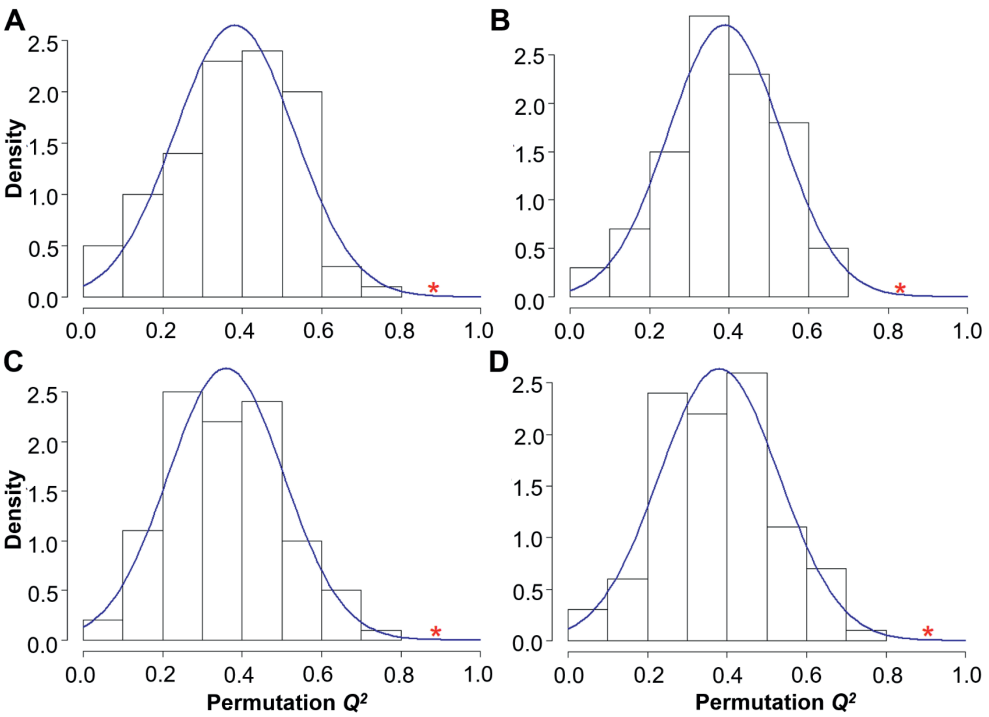


**Figure S5.4.** NI-MS chromatograms of seed extract of *S. alba* before (A) and after hydrolysis (B), *B. napus* before (C) and after hydrolysis (D), *B. juncea* before (E) and after hydrolysis (F), *B. oleracea* before (G) and after hydrolysis (H), and *C. sativa* before (I) and after hydrolysis (J). Extracts 5 mg/mL were hydrolysed simultaneously with NAC derivatization. All GSL peaks were absent after hydrolysis, except the long-chained MSGSL, i.e. 9-MSGSL, 10-MSGSL, and 11-MSGSL, in *C. sativa* seed extract with less than 1% left. The numbering of GSL peaks is according to Table S5.2, and the numbering of NAC-ITC peaks is according to Table S5.4.

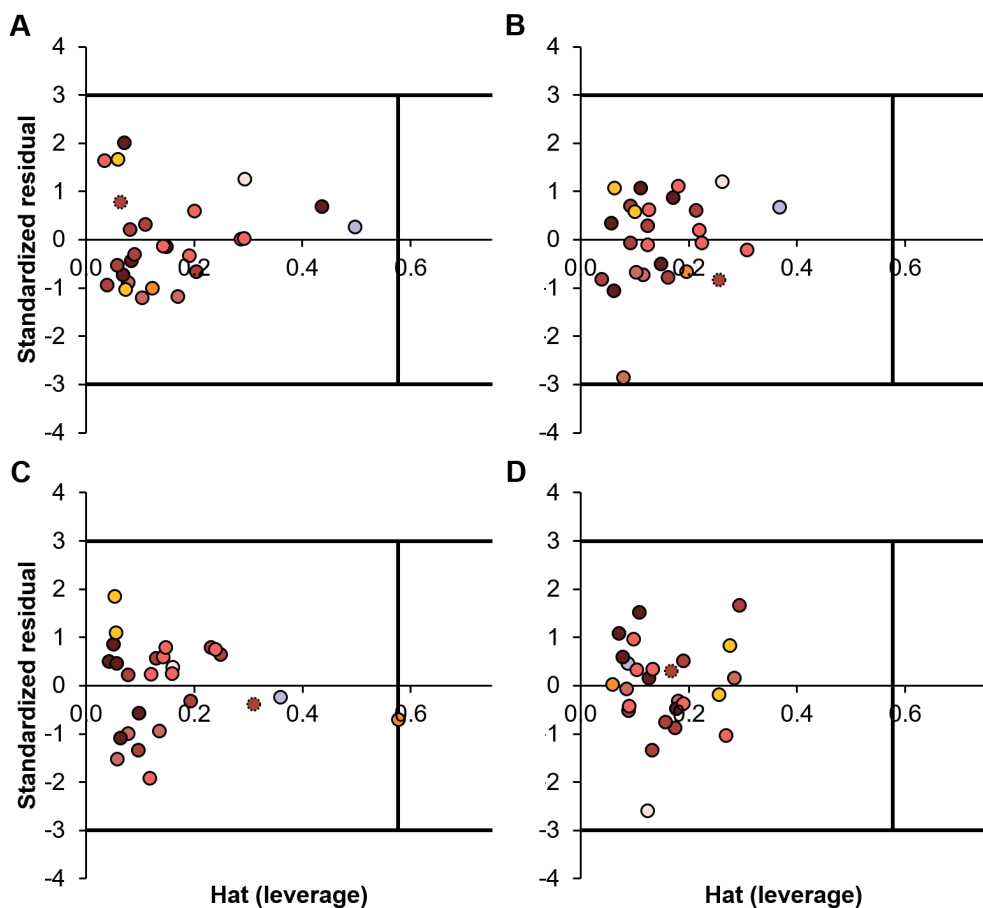




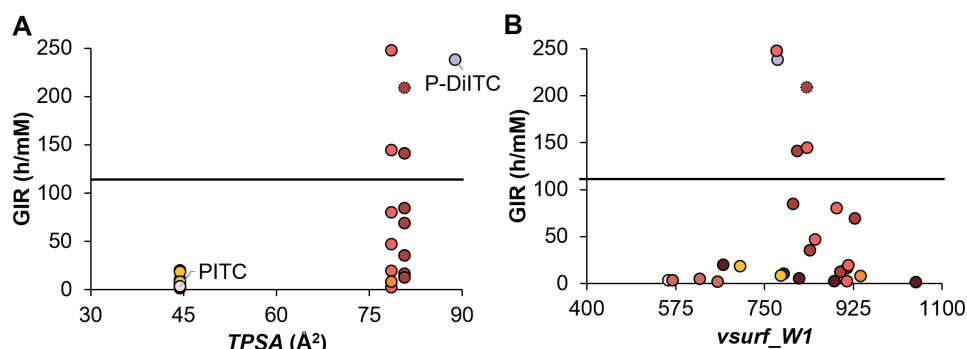
**Figure S5.5.** The leave-one-out cross-validated coefficient of determination ( $Q^2$ ) of the models obtained with different number of descriptors ( $k$ ). Models with pMIC for *E. coli* (A) and *B. cereus* (B), models with p'GIR for *E. coli* (C) and *B. cereus* (D).



**Figure S5.6.** Permutation tests for models with 4 descriptors for *E. coli* (pMIC, **A**; p'GIR, **B**) and *B. cereus* (pMIC, **C**; p'GIR, **D**). Red asterisks represent the actual  $Q^2$  values of the developed models (**Table 5.2**, in boldface).



**Figure S5.7.** Applicability domains (Williams plot) of the selected linear regression models for *E. coli* with pMIC (A) and p'GIR (B), and for *B. cereus* with pMIC (C) and p'GIR (D). The different colours refer to the different subclasses of ITCs according to Figure 5.1.



**Figure S5.8.** Polarity related descriptors used in *E. coli* models: *TPSA* (A) and *vsurf\_W1* (B) in relation to the antibacterial activity (GIR) of ITCs. The color codes refer to those in **Figure 5.1**. ITCs above the boldface horizontal line were considered as good antibacterials.

### 5.7.3. Supplementary tables

**Table S5.1.** List of molecular descriptors calculated by MOE and used in the QSAR analysis.

No.	Descriptor	Class	Description
1	<i>AM1_dipole</i>	i3D	Dipole moment calculated using the AM1 Hamiltonian (MOPAC)
2	<i>AM1_Electrophilicity</i>	i3D	Global electrophilicity calculated from AM1_HOMO and AM1_LUMO using the PM3 Hamiltonian
3	<i>AM1_HF</i>	i3D	Heat of formation (kcal/mol) calculated using the AM1 Hamiltonian
4	<i>AM1_HOMO</i>	i3D	Energy (eV) of the highest occupied molecular orbital calculated using the AM1 Hamiltonian
5	<i>AM1_LUMO</i>	i3D	Energy (eV) of the lowest unoccupied molecular orbital calculated using the AM1 Hamiltonian
6	<i>ASA-</i>	i3D	Water accessible surface area of all atoms with negative partial charge
7	<i>ASA_H</i>	i3D	Water accessible surface area of all hydrophobic ( $ q_i  < 0.2$ ) atoms
8	<i>bpol</i>	2D	Sum of the absolute value of the difference between atomic polarizabilities of all bonded atoms in the molecule
9	<i>b_1rotN</i>	2D	Number of rotatable single bonds. A bond is rotatable if it is not in a ring, and neither atom of the bond is such that $(d_i + h_i) < 2$ where the fraction of rotatable single bonds can be calculated with $(b\_1rotN / b\_count)$
10	<i>b_ar</i>	2D	Number of aromatic bonds
11	<i>b_double</i>	2D	Number of double bonds
12	<i>CASA+</i>	i3D	Positive charge weighted surface area, ASA+ times max ( $q_i > 0$ )
13	<i>CASA-</i>	i3D	Negative charge weighted surface area, ASA- times max ( $q_i < 0$ )

No.	Descriptor	Class	Description
14	<i>DASA</i>	i3D	Absolute difference in surface area of the atoms with a negative partial charge and a positive partial charge: the difference between ASA+ and ASA-.
15	<i>dens</i>	i3D	Mass density: molecular weight divided by van der Waals volume as calculated in the vol descriptor
16	<i>dipole</i>	i3D	Dipole moment calculated from the partial charges of the molecule
17	<i>FASA+</i>	i3D	Fractional positive accessible surface area
18	<i>FASA-</i>	i3D	Fractional negative accessible surface area
19	<i>FASA_H</i>	i3D	Fractional hydrophobic surface area: Fractional ASA_H calculated as ASA_H / ASA
20	<i>FASA_P</i>	i3D	Fractional polar surface area: Fractional ASA_P calculated as ASA_P / ASA
21	<i>FCASA+</i>	i3D	Fractional charge-weighted positive surface area: Fractional CASA+ calculated as CASA+ / ASA
22	<i>FCASA-</i>	i3D	Fractional charge-weighted negative surface area: Fractional CASA- calculated as CASA- / ASA
23	<i>glob</i>	i3D	Molecular globularity for which a value of 1 indicates a perfect sphere and a value of 0 indicates a two- or one-dimensional object
24	<i>KierFlex</i>	2D	Kier molecular flexibility index: (KierA1) (KierA2) / <i>n</i> with <i>n</i> : number of compounds
25	<i>logP(o/w)</i>	2D	Log octanol/water partition coefficient
26	<i>logS</i>	2D	Log of the aqueous solubility (mol/L)
27	<i>MNDO_dipole</i>	i3D	The dipole moment calculated using the MNDO Hamiltonian.
28	<i>MNDO_Electrophilicity</i>	i3D	Global electrophilicity calculated based on PM3 Hamiltonian and chemical potential
29	<i>MNDO_HF</i>	i3D	Heat formation (kcal/mol) calculated using the MNDO Hamiltonian
30	<i>MNDO_HOMO</i>	i3D	The energy (eV) of the Highest Occupied Molecular Orbital calculated using the MNDO Hamiltonian
31	<i>MNDO_LUMO</i>	i3D	The energy (eV) of the Lowest Unoccupied Molecular Orbital calculated using the MNDO Hamiltonian
32	<i>mr</i>	2D	Molecular refractivity.
33	<i>npr1</i>	i3D	Normalized principal moment of inertia ratio (1) (pmi1 / pmi3)
34	<i>npr2</i>	i3D	Normalized principal moment of inertia ratio (2) (pmi2 / pmi3)
35	<i>Partial charge on N atom of -N=C=S</i>	2D	Partial charge on the nitrogen atom of the ITCs' (-N=C=S) part obtained by energy minimization and conformation search with MOE
36	<i>Partial charge on C atom of -N=C=S</i>	2D	Partial charge on the carbon atom of the ITCs' (-N=C=S) part obtained by energy minimization and conformation search with MOE
37	<i>PEOE_RPC+</i>	2D	Relative positive partial charge: the largest positive qi divided by the sum of the positive qi.

No.	Descriptor	Class	Description
38	<i>PEOE_RPC-</i>	2D	Relative negative partial charge: the smallest negative $q_i$ divided by the sum of the negative $q_i$
39	<i>PEOE_VSA+0</i>	2D	Sum of $v_i$ , the van der Waals surface area of atom $i$ , where $q_i$ , the partial charge of atom $i$ , is in the range [0.00,0.05] kcal/mol.
40	<i>PEOE_VSA+1</i>	2D	Sum of $v_i$ , the van der Waals surface area of atom $i$ , where $q_i$ , the partial charge of atom $i$ , is in the range [0.05,0.10] kcal/mol.
41	<i>PEOE_VSA+3</i>	2D	Sum of $v_i$ , the van der Waals surface area of atom $i$ , where $q_i$ , the partial charge of atom $i$ , is in the range [0.15,0.20] kcal/mol.
42	<i>PEOE_VSA-0</i>	2D	Sum of $v_i$ , the van der Waals surface area of atom $i$ , where $q_i$ , the partial charge of atom $i$ , is in the range [-0.05,0.00] kcal/mol.
43	<i>PEOE_VSA-1</i>	2D	Sum of $v_i$ , the van der Waals surface area of atom $i$ , where $q_i$ , the partial charge of atom $i$ , is in the range [-0.10,-0.05] kcal/mol.
44	<i>PEOE_VSA_FHYD</i>	2D	Fractional hydrophobic van der Waals surface area. This is the sum of the $v_i$ such that $ q_i $ is less than or equal to 0.2 divided by the total surface area.
45	<i>PEOE_VSA_FNEG</i>	2D	Fractional negative van der Waals surface area. This is the sum of the $v_i$ such that $q_i$ is negative, divided by the total surface area.
46	<i>PEOE_VSA_FPOL</i>	2D	Fractional polar van der Waals surface area. This is the sum of the $v_i$ such that $ q_i $ is greater than 0.2 divided by the total surface area.
47	<i>PEOE_VSA_FPOS</i>	2D	Fractional positive van der Waals surface area. This is the sum of the $v_i$ such that $q_i$ is non-negative divided by the total surface area.
48	<i>PEOE_VSA_HYD</i>	2D	Total hydrophobic van der Waals surface area. This is the sum of the $v_i$ such that $ q_i $ is less than or equal to 0.2.
49	<i>PEOE_VSA_NEG</i>	2D	Total negative van der Waals surface area which refers to the sum of $v_i$ such that $q_i$ is negative.
50	<i>PEOE_VSA_POL</i>	2D	Total polar van der Waals surface area. This is the sum of the $v_i$ such that $ q_i $ is greater than 0.2.
51	<i>PEOE_VSA_POS</i>	2D	Total positive van der Waals surface area. This is the sum of the $v_i$ such that $q_i$ is non-negative.
52	<i>petitjeanSC</i>	2D	Petitjean graph Shape Coefficient: (diameter - radius) / radius
53	<i>PM3_dipole</i>	i3D	The dipole moment calculated using the PM3 Hamiltonian.
54	<i>PM3_E</i>	i3D	Total energy (kcal/mol) calculated using the PM3 Hamiltonian.
55	<i>PM3_Eele</i>	i3D	Electronic energy (kcal/mol) calculated using the PM3 Hamiltonian.

No.	Descriptor	Class	Description
56	<i>PM3_Electrophilicity</i>	i3D	Global electrophilicity calculated based on PM3 Hamiltonian and chemical potential
57	<i>PM3_HOMO</i>	i3D	The energy (eV) of the Highest Occupied Molecular Orbital calculated using the PM3 Hamiltonian.
58	<i>PM3_LUMO</i>	i3D	The energy (eV) of the Lowest Unoccupied Molecular Orbital calculated using the PM3 Hamiltonian.
59	<i>radius</i>	2D	If $r_i$ is the largest matrix entry in row $i$ of the distance matrix $D$ , then the radius is defined as the smallest of the $r_i$ .
60	<i>rgyr</i>	i3D	Radius of gyration.
61	<i>rings</i>	2D	Number of rings
62	<i>RPC+</i>	2D	Relative positive partial charge.
63	<i>RPC-</i>	2D	Relative negative partial charge.
64	<i>SlogP_VSA5</i>	2D	Sum of $v_i$ , accessible van der Waals surface area, such that $L_i$ , contribution to $\log P(o/w)$ for atom $i$ , is in range [0.15,0.20].
65	<i>SlogP_VSA7</i>	2D	Sum of $v_i$ , accessible van der Waals surface area, such that $L_i$ , contribution to $\log P(o/w)$ for atom $i$ , is in range [0.25,0.30].
66	<i>SlogP_VSA8</i>	2D	Sum of $v_i$ , accessible van der Waals surface area, such that $L_i$ , contribution to $\log P(o/w)$ for atom $i$ , is in range [0.30,0.40]
67	<i>std_dim2</i>	i3D	Standard dimension 2: the square root of the second largest eigenvalue of the covariance matrix of the atomic coordinates. Depends on the structure connectivity and conformation
68	<i>std_dim3</i>	i3D	Standard dimension 3: the square root of the third largest eigenvalue of the covariance matrix of the atomic coordinates, depending on the structure connectivity and conformation
69	<i>TPSA</i>	2D	Topological polar surface area ( $\text{\AA}^2$ ) calculated using group contributions to approximate the polar surface area from connection table information only
70	<i>VSA</i>	i3D	Van der Waals surface area ( $\text{\AA}^2$ )
71	<i>vsa_hyd</i>	2D	Approximation to the sum of VdW surface areas of hydrophobic atoms ( $\text{\AA}^2$ )
72	<i>vsurf_A</i>	i3D	Amphiphilic moment (ratio hydrophobic over hydrophilic surface area)
73	<i>vsurf_D1</i>	i3D	Hydrophobic volume at an interaction energy -0.2 kcal/mol
74	<i>vsurf_D2</i>	i3D	Hydrophobic volume at an interaction energy -0.4 kcal/mol
75	<i>vsurf_D3</i>	i3D	Hydrophobic volume at an interaction energy -0.6 kcal/mol
76	<i>vsurf_D4</i>	i3D	Hydrophobic volume at an interaction energy -0.8 kcal/mol

No.	Descriptor	Class	Description
77	<i>vsurf_D5</i>	i3D	Hydrophobic volume at an interaction energy -1.0 kcal/mol
78	<i>vsurf_D6</i>	i3D	Hydrophobic volume at an interaction energy -1.2 kcal/mol
79	<i>vsurf_D7</i>	i3D	Hydrophobic volume at an interaction energy -1.4 kcal/mol
80	<i>vsurf_D8</i>	i3D	Hydrophobic volume at an interaction energy -1.6 kcal/mol
81	<i>vsurf_EDmin1</i>	i3D	Lowest hydrophobic energy
82	<i>vsurf_EDmin2</i>	i3D	2nd lowest hydrophobic energy
83	<i>vsurf_EDmin3</i>	i3D	3rd lowest hydrophobic energy
84	<i>vsurf_EWmin1</i>	i3D	Lowest hydrophilic energy
85	<i>vsurf_EWmin2</i>	i3D	2nd lowest hydrophilic energy
86	<i>vsurf_EWmin3</i>	i3D	3rd lowest hydrophilic energy
87	<i>vsurf_G</i>	i3D	Surface globularity
88	<i>vsurf_HB1</i>	i3D	H-bond donor capacity at -0.2
89	<i>vsurf_HB2</i>	i3D	H-bond donor capacity at -0.5 kcal/mol
90	<i>vsurf_HL1</i>	i3D	First hydrophilic-lipophilic balance
91	<i>vsurf_ID1</i>	i3D	Hydrophobic integy moment at -0.2 kcal
92	<i>vsurf_ID2</i>	i3D	Hydrophobic integy moment at -0.4 kcal
93	<i>vsurf_ID3</i>	i3D	Hydrophobic integy moment at -0.6 kcal
94	<i>vsurf_ID4</i>	i3D	Hydrophobic integy moment at -0.8 kcal
95	<i>vsurf_ID5</i>	i3D	Hydrophobic integy moment at -1.0 kcal
96	<i>vsurf_ID6</i>	i3D	Hydrophobic integy moment at -1.2 kcal
97	<i>vsurf_ID7</i>	i3D	Hydrophobic integy moment at -1.4 kcal
98	<i>vsurf_ID8</i>	i3D	Hydrophobic integy moment at -1.6 kcal
99	<i>vsurf_IW1</i>	i3D	Hydrophilic integy moment at -0.2 kcal
100	<i>vsurf_IW2</i>	i3D	Hydrophilic integy moment at -0.5 kcal
101	<i>vsurf_IW3</i>	i3D	Hydrophilic integy moment at -1.0 kcal
102	<i>vsurf_IW4</i>	i3D	Hydrophilic integy moment at -2.0 kcal
103	<i>vsurf_IW5</i>	i3D	Hydrophilic integy moment at -3.0 kcal
104	<i>vsurf_IW6</i>	i3D	Hydrophilic integy moment at -4.0 kcal
105	<i>vsurf_IW7</i>	i3D	Hydrophilic integy moment at -5.0 kcal
106	<i>vsurf_R</i>	i3D	Surface rugosity (roughness)
107	<i>vsurf_W1</i>	i3D	Hydrophilic volume at -0.2 kcal/mol
108	<i>vsurf_W2</i>	i3D	Hydrophilic volume at -0.5 kcal/mol
109	<i>vsurf_W3</i>	i3D	Hydrophilic volume at -1.0 kcal/mol
110	<i>vsurf_W5</i>	i3D	Hydrophilic volume at -3.0 kcal/mol
111	<i>vsurf_W6</i>	i3D	Hydrophilic volume at -4.0 kcal/mol
112	<i>vsurf_W7</i>	i3D	Hydrophilic volume at -5.0 kcal/mol
113	<i>vsurf_Wp1</i>	i3D	Polar volume at -0.2 kcal/mol
114	<i>vsurf_Wp3</i>	i3D	Polar volume at -1.0 kcal/mol
115	<i>Weight</i>	2D	Molecular weight, including implicit hydrogens (g/mol)



**Table S5.2.** GSL composition (mg GE/g DW) in *S. alba* (Sa), *B. napus* (Bn), *B. juncea* (Bj), *B. oleracea* (Bo), and *C. sativa* (Cs) seeds.

Peak no. <sup>a</sup>	GSL	Content (mg GE/g DW)				
		Sa	Bn	Bj	Bo	Cs
11	3-(Methylthio)propyl	n.d.	n.d.	0.12 ± 0.01	0.94 ± 0.08	n.d.
15	4-(Methylthio)butyl	0.00 ± 0.00	0.02 ± 0.00	0.43 ± 0.04	3.83 ± 0.73	0.00 ± 0.00
21	5-(Methylthio)pentyl	n.d.	0.01 ± 0.01	0.02 ± 0.01	0.01 ± 0.01	n.d.
<b>Sub-total MTalkyl GSLs</b>		<b>0.00 ± 0.00</b>	<b>0.04 ± 0.01</b>	<b>0.56 ± 0.06</b>	<b>4.78 ± 0.81</b>	<b>0.00 ± 0.00</b>
1	3-(Methylsulfinyl)propyl	n.d.	n.d.	0.19 ± 0.02	5.64 ± 0.93	0.00 ± 0.00
3	4-(Methylsulfinyl)butyl	0.00 ± 0.00	0.05 ± 0.01	0.55 ± 0.01	12.85 ± 3.33	0.01 ± 0.00
6	5-(Methylsulfinyl)pentyl	n.d.	0.10 ± 0.01	0.05 ± 0.00	0.06 ± 0.02	n.d.
33	9-(Methylsulfinyl)nonyl	n.d.	n.d.	n.d.	n.d.	5.95 ± 0.87
25	10-(Methylsulfinyl)decyl	n.d.	n.d.	n.d.	n.d.	18.69 ± 2.31
34	11-(Methylsulfinyl)undecyl	n.d.	n.d.	n.d.	n.d.	5.35 ± 0.59
<b>Sub-total MSalkyl GSLs</b>		<b>0.00 ± 0.00</b>	<b>0.15 ± 0.01</b>	<b>0.79 ± 0.03</b>	<b>18.56 ± 4.27</b>	<b>30.00 ± 3.77</b>
4	Allyl	0.01 ± 0.01	0.00 ± 0.00	2.94 ± 0.23	0.32	0.00 ± 0.00
8	3-Butenyl	0.18 ± 0.01	0.90 ± 0.08	23.69 ± 3.25	0.24	n.d.
13	4-Pentenyl	n.d.	0.11 ± 0.01	0.02 ± 0.01	n.d.	n.d.
<b>Sub-total alkenyl GSLs</b>		<b>0.19 ± 0.02</b>	<b>1.02 ± 0.09</b>	<b>26.65 ± 3.49</b>	<b>0.56 ± 0.10</b>	<b>0.00 ± 0.00</b>
2	(R)-2-OH-3-Butenyl	0.80 ± 0.09	1.92 ± 0.11	0.28 ± 0.03	0.81 ± 0.02	n.d.
7	2-OH-4-Pentenyl	n.d.	0.05 ± 0.01	n.d.	n.d.	n.d.
<b>Sub-total OH-alkenyl GSLs</b>		<b>0.80 ± 0.09</b>	<b>1.97 ± 0.12</b>	<b>0.28 ± 0.03</b>	<b>0.81 ± 0.20</b>	<b>n.d.</b>
30	6'-O-Sinapoyl(or isomer)-3-butenyl	0.00 ± 0.00	0.02 ± 0.00	0.29 ± 0.03	n.d.	n.d.
<b>Sub-total sinapoyl alkenyl GSLs</b>		<b>0.00 ± 0.00</b>	<b>0.02 ± 0.00</b>	<b>0.55 ± 0.06</b>	<b>n.d.</b>	<b>n.d.</b>
16	Pentyl GSL or isomer	n.d.	0.00 ± 0.00	0.06 ± 0.01	0.16 ± 0.02	n.d.
23	Hexyl GSL or isomer	0.00 ± 0.00	0.01 ± 0.00	0.12 ± 0.01	0.18 ± 0.02	n.d.
<b>Sub-total alkyl GSLs</b>		<b>0.00 ± 0.00</b>	<b>0.01 ± 0.00</b>	<b>0.17 ± 0.02</b>	<b>0.34 ± 0.04</b>	<b>n.d.</b>
10	Unclassified aliphatic GSL	n.d.	n.d.	n.d.	0.09 ± 0.16	n.d.
<b>Total aliphatic GSLs</b>		<b>1.00 ± 0.11</b>	<b>3.21 ± 0.24</b>	<b>29.01 ± 3.69</b>	<b>25.13 ± 5.58</b>	<b>30.01 ± 3.78</b>
5	p-OH-Benzyl	30.49 ± 4.25	n.d.	n.d.	0.01 ± 0.01	n.d.
26	6'-O-Sinapoyl(or isomer)-p-OH-benzyl	0.01 ± 0.00	n.d.	n.d.	n.d.	n.d.
14	Benzyl	0.01 ± 0.00	n.d.	0.01 ± 0.00	0.01 ± 0.01	n.d.
20	Phenethyl	n.d.	0.05 ± 0.01	0.01 ± 0.00	0.03 ± 0.01	n.d.
<b>Total benzenic GSLs</b>		<b>30.49 ± 4.25</b>	<b>0.05 ± 0.01</b>	<b>0.02 ± 0.00</b>	<b>0.04 ± 0.02</b>	<b>n.d.</b>
17	Indol-3-ylmethyl (I3M)	0.05 ± 0.01	0.10 ± 0.04	0.08 ± 0.01	0.24 ± 0.02	n.d.
9	4-OH-I3M	n.d.	0.20 ± 0.06	0.02 ± 0.02	0.43 ± 0.48	n.d.
22	4-OCH <sub>3</sub> -I3M	n.d.	n.d.	0.08 ± 0.02	0.04 ± 0.01	n.d.
24	N-OCH <sub>3</sub> -I3M	0.01 ± 0.00	0.02 ± 0.00	0.01 ± 0.00	0.15 ± 0.04	n.d.
<b>Total indolic GSLs</b>		<b>0.07 ± 0.01</b>	<b>0.32 ± 0.10</b>	<b>0.20 ± 0.05</b>	<b>0.86 ± 0.55</b>	<b>n.d.</b>
<b>Total GSLs</b>		<b>31.56 ± 4.26</b>	<b>3.58 ± 0.30</b>	<b>29.23 ± 3.70</b>	<b>26.03 ± 6.04</b>	<b>30.01 ± 3.78</b>

<sup>a</sup> The (tentative) annotation including the peak numbers are according to Andini *et al.*<sup>2</sup> The tentative annotation of 9-(methylsulfinyl)nonyl GSL (33) and 11-(methylsulfinyl)undecyl GSL (34), found in *C. sativa*, was based on the fragmentation pattern of x-(methylsulfinyl)alkyl GSLs. Good to note that the peak numbers were in line with the elution order, except for 9-(methylsulfinyl)nonyl GSL (33) which eluted earlier than 10-(methylsulfinyl)decyl GSL (25).

**Table S5.3.** GSL composition ( $\mu\text{M}$ ) in 1 mg/mL extracts of *S. alba* (Sa), *B. napus* (Bn), *B. juncea* (Bj), *B. oleracea* (Bo), and *C. sativa* (Cs) seeds.

Peak no.	GSL	Concentration ( $\mu\text{M}$ ) in 1 mg/mL extract				
		Sa	Bn	Bj	Bo	Cs
11	3-(Methylthio)propyl	n.d.	n.d.	1.86 $\pm$ 0.24	10.69 $\pm$ 1.23	n.d.
15	4-(Methylthio)butyl	0.03 $\pm$ 0.02	0.52 $\pm$ 0.10	6.62 $\pm$ 0.69	58.82 $\pm$ 4.08	0.10 $\pm$ 0.02
21	5-(Methylthio)pentyl	n.d.	0.29 $\pm$ 0.13	0.26 $\pm$ 0.09	0.21 $\pm$ 0.11	n.d.
<b>Sub-total MTalkyl GSLs</b>		0.03 $\pm$ 0.02	0.81 $\pm$ 0.23	8.74 $\pm$ 1.01	74.13 $\pm$ 5.50	0.10 $\pm$ 0.02
1	3-(Methylsulfinyl)propyl	n.d.	n.d.	2.86 $\pm$ 0.31	86.58 $\pm$ 5.55	0.10 $\pm$ 0.03
3	4-(Methylsulfinyl)butyl	0.08 $\pm$ 0.01	1.09 $\pm$ 0.17	8.19 $\pm$ 0.16	189.35 $\pm$ 25.78	0.26 $\pm$ 0.10
6	5-(Methylsulfinyl)pentyl	n.d.	1.96 $\pm$ 0.10	0.78 $\pm$ 0.02	0.96 $\pm$ 0.35	n.d.
33	9-(Methylsulfinyl)nonyl	n.d.	n.d.	n.d.	n.d.	105.75 $\pm$ 8.24
25	10-(Methylsulfinyl)decyl	n.d.	n.d.	n.d.	n.d.	323.67 $\pm$ 21.72
34	11-(Methylsulfinyl)undecyl	n.d.	n.d.	n.d.	n.d.	90.46 $\pm$ 6.94
<b>Sub-total MSalkyl GSLs</b>		0.08 $\pm$ 0.01	3.05 $\pm$ 0.27	11.83 $\pm$ 0.49	276.89 $\pm$ 31.69	520.25 $\pm$ 37.01
4	Allyl	0.27 $\pm$ 0.17	0.08 $\pm$ 0.01	53.41 $\pm$ 4.12	5.74 $\pm$ 0.65	0.06 $\pm$ 0.00
8	3-Butenyl	4.30 $\pm$ 0.25	21.46 $\pm$ 1.80	414.18 $\pm$ 56.89	4.18 $\pm$ 0.03	n.d.
13	4-Pentenyl	n.d.	2.68 $\pm$ 0.29	0.33 $\pm$ 0.12	n.d.	n.d.
<b>Sub-total alkenyl GSLs</b>		4.57 $\pm$ 0.42	24.22 $\pm$ 2.10	467.92 $\pm$ 61.13	9.93 $\pm$ 0.67	0.06 $\pm$ 0.00
2	(R)-2-OH-3-Butenyl	18.03 $\pm$ 2.04	43.73 $\pm$ 2.39	4.72 $\pm$ 0.53	13.39 $\pm$ 1.54	n.d.
7	2-OH-4-Pentenyl	n.d.	1.08 $\pm$ 0.30	n.d.	n.d.	n.d.
<b>Sub-total OH-alkenyl GSLs</b>		18.03 $\pm$ 2.04	44.81 $\pm$ 2.69	4.72 $\pm$ 0.53	13.39 $\pm$ 1.54	n.d.
30	6'-O-Sinapoyl(or isomer)-3-butenyl	0.03 $\pm$ 0.01	0.24 $\pm$ 0.06	3.26 $\pm$ 0.32	0.00 $\pm$ 0.00	n.d.
<b>Sub-total sinapoyl alkenyl GSLs</b>		0.03 $\pm$ 0.01	0.24 $\pm$ 0.06	3.26 $\pm$ 0.32	0.00 $\pm$ 0.00	n.d.
16	Pentyl GSL or isomer	n.d.	0.00 $\pm$ 0.01	0.95 $\pm$ 0.10	2.67 $\pm$ 0.14	n.d.
23	Hexyl GSL or isomer	0.01 $\pm$ 0.00	0.12 $\pm$ 0.00	1.96 $\pm$ 0.21	2.99 $\pm$ 0.16	n.d.
<b>Sub-total alkyl GSLs</b>		0.01 $\pm$ 0.00	0.13 $\pm$ 0.01	2.91 $\pm$ 0.31	5.66 $\pm$ 0.30	n.d.
10	Unclassified aliphatic GSL	n.d.	n.d.	n.d.	1.40 $\pm$ 2.43	n.d.
<b>Total aliphatic GSLs</b>		<b>22.78 <math>\pm</math> 2.50</b>	<b>73.40 <math>\pm</math> 5.39</b>	<b>502.33 <math>\pm</math> 64.11</b>	<b>381.40 <math>\pm</math> 42.13</b>	<b>520.41 <math>\pm</math> 37.04</b>
5	<i>p</i> -OH-Benzyl	630.29 $\pm$ 87.89	n.d.	n.d.	0.10 $\pm$ 0.17	n.d.
26	6'-O-Sinapoyl(or isomer)- <i>p</i> -OH-benzyl	0.18 $\pm$ 0.00	n.d.	n.d.	n.d.	n.d.
14	Benzyl	0.11 $\pm$ 0.02	n.d.	0.10 $\pm$ 0.02	0.11 $\pm$ 0.09	n.d.
20	Phenethyl	n.d.	1.00 $\pm$ 0.32	0.24 $\pm$ 0.03	0.42 $\pm$ 0.04	n.d.
<b>Total benzenic GSLs</b>		<b>630.40 <math>\pm</math> 87.91</b>	<b>1.00 <math>\pm</math> 0.32</b>	<b>0.34 <math>\pm</math> 0.05</b>	<b>0.64 <math>\pm</math> 0.30</b>	<b>n.d.</b>
17	Indol-3-ylmethyl (I3M)	1.03 $\pm$ 0.19	1.96 $\pm$ 0.78	1.10 $\pm$ 0.13	3.55 $\pm$ 0.33	n.d.
9	4-OH-I3M	n.d.	3.91 $\pm$ 1.22	0.33 $\pm$ 0.31	5.61 $\pm$ 5.61	n.d.
22	4-OCH <sub>3</sub> -I3M	n.d.	n.d.	1.18 $\pm$ 0.27	0.49 $\pm$ 0.01	n.d.
24	<i>N</i> -OCH <sub>3</sub> -I3M	0.24 $\pm$ 0.01	0.35 $\pm$ 0.01	0.21 $\pm$ 0.02	2.02 $\pm$ 0.30	n.d.
<b>Total indolic GSLs</b>		<b>1.27 <math>\pm</math> 0.02</b>	<b>6.22 <math>\pm</math> 2.02</b>	<b>2.82 <math>\pm</math> 0.73</b>	<b>11.68 <math>\pm</math> 6.25</b>	<b>n.d.</b>
<b>Total GSLs</b>		<b>654.45 <math>\pm</math> 85.56</b>	<b>80.61 <math>\pm</math> 7.02</b>	<b>505.49 <math>\pm</math> 63.21</b>	<b>393.72 <math>\pm</math> 40.01</b>	<b>520.41 <math>\pm</math> 37.04</b>

**Table S5.4.** ITC composition in the hydrolysed extracts of *S. alba* (Sa), *B. napus* (Bn), *B. juncea* (Bj), *B. oleracea* (Bo), and *C. sativa* (Cs) seeds.

Peak no.	ITC	Concentration ( $\mu\text{M}$ ) in 1 mg/mL extract				
		Sa	Bn	Bj	Bo	Cs
I11	3-MTITC	n.d.	n.d.	2.03 $\pm$ 0.77	8.17 $\pm$ 0.28	n.d.
I15	4-MTITC	n.d.	n.d.	5.32 $\pm$ 1.67	51.03 $\pm$ 10.91	n.d.
I21	5-MTITC	n.d.	n.d.	n.d.	0.16 $\pm$ 0.09	n.d.
<b>Sub-total MTalkyl ITCs</b>		n.d.	n.d.	7.35 $\pm$ 2.43	59.36 $\pm$ 11.28	n.d.
I1	3-MSITC	n.d.	n.d.	2.76 $\pm$ 0.27	78.70 $\pm$ 4.60	0.16 $\pm$ 0.02
I3	4-MSITC	n.d.	1.55 $\pm$ 0.49	8.76 $\pm$ 0.71	173.30 $\pm$ 27.01	0.53 $\pm$ 0.44
I6	5-MSITC	n.d.	1.74 $\pm$ 0.11	0.90 $\pm$ 0.05	0.91 $\pm$ 0.14	0.03 $\pm$ 0.00
I33	9-MSITC	n.d.	n.d.	n.d.	n.d.	98.83 $\pm$ 2.75
I25	10-MSITC	n.d.	n.d.	n.d.	n.d.	322.45 $\pm$ 13.83
I34	11-MSITC	n.d.	n.d.	n.d.	n.d.	75.00 $\pm$ 8.34
<b>Sub-total MSalkyl ITCs</b>		n.d.	3.29 $\pm$ 0.60	12.42 $\pm$ 1.03	252.91 $\pm$ 31.74	497.00 $\pm$ 22.96
I4	AITC	n.d.	0.26 $\pm$ 0.37	48.70 $\pm$ 9.07	5.41 $\pm$ 2.55	0.40 $\pm$ 0.28
I8	BulTC	3.69 $\pm$ 0.66	20.51 $\pm$ 0.14	390.84 $\pm$ 48.92	3.31 $\pm$ 0.47	n.d.
I13	PeITC	n.d.	1.57 $\pm$ 0.40	0.13 $\pm$ 0.08	n.d.	n.d.
<b>Sub-total alkenyl ITCs</b>		3.69 $\pm$ 0.66	22.34 $\pm$ 0.91	439.67 $\pm$ 52.07	8.72 $\pm$ 3.02	0.40 $\pm$ 0.28
I16	Pentyl ITC	n.d.	n.d.	0.39 $\pm$ 0.06	2.11 $\pm$ 1.21	n.d.
I23	Hexyl ITC	n.d.	n.d.	0.25 $\pm$ 0.06	0.35 $\pm$ 0.10	n.d.
<b>Sub-total alkyl ITCs</b>		n.d.	n.d.	0.64 $\pm$ 0.11	2.46 $\pm$ 1.30	n.d.
<b>Sub-total aliphatic ITCs</b>		3.69 $\pm$ 0.66	25.63 $\pm$ 1.54	460.08 $\pm$ 52.21	323.45 $\pm$ 34.91	497.40 $\pm$ 23.12
I5	<i>p</i> -OH-BITC	6.55 $\pm$ 3.99	n.d.	n.d.	n.d.	n.d.
I14	BITC	n.d.	n.d.	n.d.	n.d.	n.d.
I20	PhEITC	n.d.	1.07 $\pm$ 0.03	0.40 $\pm$ 0.01	0.65 $\pm$ 0.22	n.d.
<b>Sub-total benzenic ITCs</b>		6.55 $\pm$ 3.99	1.07 $\pm$ 0.03	0.40 $\pm$ 0.01	0.65 $\pm$ 0.22	n.d.
<b>Total ITCs</b>		10.24 $\pm$ 4.36	26.70 $\pm$ 1.53	460.48 $\pm$ 52.21	324.10 $\pm$ 34.91	497.40 $\pm$ 23.12

**Table S5.5.** The multiple linear regression models obtained using genetic algorithm-selection of variables for predicting antibacterial activity of isothiocyanates against *B. cereus* and *E. coli*. The finally chosen models are highlighted in bold face.

Bacteria	k	Model
<i>E. coli</i>	2	pMIC = 1.606 + -6.872 * <i>PEOE_VSA_FNEG</i> + 0.008 * <i>ASA-</i>
	3	pMIC = -1.706 + -0.903 * <i>FCASA+</i> + 0.787 * <i>FCASA-</i> + 0.031 * <i>TPSA</i>
	4	<b>pMIC = -2.240 + -1.000 * <i>FCASA+</i> + 0.819 * <i>FCASA-</i> + 0.030 * <i>TPSA</i> + 0.001 * <i>vsurf_W1</i></b>
	5	pMIC = -2.795 + 0.033 * <i>TPSA</i> + -1.012 * <i>FCASA+</i> + 0.431 * <i>MNDO_Electrophilicity</i> + 0.347 * <i>vsurf_ID8</i> + 0.520 * <i>npr1</i>
<i>E. coli</i>	2	p'GIR = 4.762 + -8.479 * <i>PEOE_RPC+</i> + -0.016 * <i>vsurf_hyd</i>
	3	p'GIR = 7.742 + -12.78 * <i>PEOE_RPC+</i> + 9.75E-06 * <i>PM3_Eele</i> + -2.259 * <i>npr2</i>
	4	<b>p'GIR = 7.276 + -11.17 * <i>PEOE_RPC+</i> + 9.10E-06 * <i>PM3_Eele</i> + -2.619 * <i>npr2</i> + 0.274 * <i>vsurf_ID6</i></b>
	5	p'GIR = 4.804 + -5.035 * <i>PEOE_RPC+</i> + -0.920 * <i>FCASA+</i> + -1.770 * <i>npr2</i> + 0.426 * <i>vsurf_ID7</i> + -0.274 * <i>vsurf_IW4</i>
<i>B. cereus</i>	2	pMIC = -2.102 + 0.814 * <i>std_dim2</i> + 0.022 * <i>TPSA</i>
	3	pMIC = 0.117 + 1.244 * <i>std_dim2</i> + 5.350 * <i>PEOE_VSA_FNEG</i> + 0.005 * <i>ASA-</i>
	4	<b>pMIC = -3.831 + 0.040 * <i>PEOE_VSA+3</i> + 2.802 * <i>vsurf_R</i> + 6.413 * <i>vsurf_HL1</i> + -0.985 * <i>AM1_Electrophilicity</i></b>
	5	pMIC = -3.778 + 0.027 * <i>PEOE_VSA+3</i> + 0.977 * <i>npr1</i> + -6.164 * <i>PEOE_RPC+</i> + 5.304 * <i>PEOE_VSA_FHYD</i> + -0.191 * <i>vsurf_IW7</i>
<i>B. cereus</i>	2	p'GIR = -0.196 + -2.950 * <i>RPC-</i> + 0.040 * <i>TPSA</i>
	3	p'GIR = 1.657 + 0.018 * <i>PEOE_VSA-1</i> + 3.015 * <i>npr1</i> + -1.399 * <i>vsurf_IW2</i>
	4	<b>p'GIR = -1.401 + 0.019 * <i>PEOE_VSA-1</i> + 2.622 * <i>npr1</i> + 0.425 * <i>vsurf_W7</i> + -1.386 * <i>vsurf_IW2</i></b>
	5	p'GIR = 1.815 + 0.015 * <i>PEOE_VSA-1</i> + 2.469 * <i>npr1</i> + -1.264 * <i>vsurf_IW2</i> + 0.647 * <i>vsurf_W7</i> + -1.715 * <i>RPC-</i>

**Table S5.6.** Physicochemical classification of descriptors used in the best QSAR models.

<i>k</i>	Descriptor	Physicochemical property	<i>k</i>	Descriptor	Physicochemical property
<b><i>E. coli</i> - pMIC model</b>			<b><i>B. cereus</i> - pMIC model</b>		
2	PEOE_VSA_FNEG	Partial charge	2	std_dim2	Molecular shape
2	ASA-	Partial charge	2	TPSA	Polarity
3	FCASA-	Partial charge	3	std_dim2	Molecular shape
3	FCASA+	Partial charge	3	PEOE_VSA_FNEG	Partial charge
3	TPSA	Polarity	3	ASA-	Partial charge
4	FCASA-	Partial charge	4	PEOE_VSA+3	Partial charge
4	FCASA+	Partial charge	4	vsurf_R	Molecular shape
4	TPSA	Polarity	4	vsurf_HL1	Polarity
4	vsurf_W1	Polarity	4	AM1_Electrophilicity	Reactivity
5	TPSA	Polarity	5	PEOE_VSA+3	Partial charge
5	FCASA+	Partial charge	5	npr1	Molecular shape
5	MNDO_Electrophilicity	Reactivity	5	PEOE_RPC+	Partial charge
5	vsurf_ID8	Polarity	5	PEOE_VSA_FHYD	Polarity
5	npr1	Molecular shape	5	vsurf_IW7	Polarity
<b><i>E. coli</i> – p'GIR model</b>			<b><i>B. cereus</i> – p'GIR model</b>		
2	PEOE_RPC+	Partial charge	2	RPC-	Partial charge
2	vsa_hyd	Polarity	2	TPSA	Polarity
3	PEOE_RPC+	Partial charge	3	PEOE_VSA-1	Partial charge
3	PM3_Eele	Reactivity	3	npr1	Molecular shape
3	npr2	Molecular shape	3	vsurf_IW2	Polarity
4	PEOE_RPC+	Partial charge	4	PEOE_VSA-1	Partial charge
4	PM3_Eele	Reactivity	4	npr1	Molecular shape
4	npr2	Molecular shape	4	vsurf_IW2	Polarity
4	vsurf_ID6	Polarity	4	vsurf_W7	Polarity
5	PEOE_RPC+	Partial charge	5	PEOE_VSA-1	Partial charge
5	FCASA+	Partial charge	5	npr1	Molecular shape
5	npr2	Molecular shape	5	vsurf_IW2	Polarity
5	vsurf_ID7	Polarity	5	vsurf_W7	Polarity
5	vsurf_IW4	Polarity	5	RPC-	Partial charge

#### 5.7.4. Supplementary references

- Andini, S.; Araya-Cloutier, C.; Sanders, M.; Vincken, J.-P., Simultaneous analysis of glucosinolates and isothiocyanates by RP-UHPLC-ESI-MS<sup>n</sup>. *J. Agric. Food Chem.* **2020**, *68*, 3121-3131.
- Andini, S.; Dekker, P.; Gruppen, H.; Araya-Cloutier, C.; Vincken, J.-P., Modulation of glucosinolate composition in Brassicaceae seeds by germination and fungal elicitation. *J. Agric. Food Chem.* **2019**, *67*, 12770-12779.
- Buskov, S.; Hasselstrøm, J.; Olsen, C. E.; Sørensen, H.; Sørensen, J. C.; Sørensen, S., Supercritical fluid chromatography as a method of analysis for the determination of 4-hydroxybenzylglucosinolate degradation products. *J. Biochem. Biophys. Methods* **2000**, *43*, 157-174.
- Greer, M. A., Isolation from rutabaga seed of progoitrin, the precursor of the naturally occurring antithyroid compound, goitrin (L-5-vinyl-2-thiooxazolidone). *J. Am. Chem. Soc.* **1956**, *78*, 1260-1261.



# CHAPTER

# 6

---

## General Discussion

---

As described in the **General Introduction**, glucosinolates (GSLs) and myrosinase are part of the defense mechanism of the plant family of Brassicaceae, and the forth-coming isothiocyanates (ITCs) have antimicrobial activity. ITCs have potential to be utilized as natural antimicrobials against pathogens and food spoilage microorganisms, which might contribute to meet the need of healthcare systems for novel antimicrobials and to meet the consumer demands for natural preservatives. Because of the large discrepancy in the antimicrobial activity of ITCs between studies, incomplete data on the antimicrobial activity of ITCs against pathogens and food spoilage microorganisms, and the lack of data on the antimicrobial activity of long-chained ITCs, a systematic investigation on the antimicrobial activity and the quantitative structure-activity relationships of ITCs was performed. Due to the electrophilicity of ITCs, the effect of the nucleophile-richness of growth media was considered in the antimicrobial assays as well. In this chapter, the following aspects are further elaborated: (i) the different approaches in compositional analysis and antimicrobial assays used in this thesis, (ii) the evaluation of the simultaneous germination and fungal elicitation protocol for Brassicaceae seeds to modulate the composition of GSLs, (iii) the main findings regarding the antimicrobial activity of ITCs, (iv) hints for the mode of action of ITCs, and (v) the prospects of ITCs as natural antimicrobial candidates.

## 6.1. Considerations to the analytical protocols used in this thesis

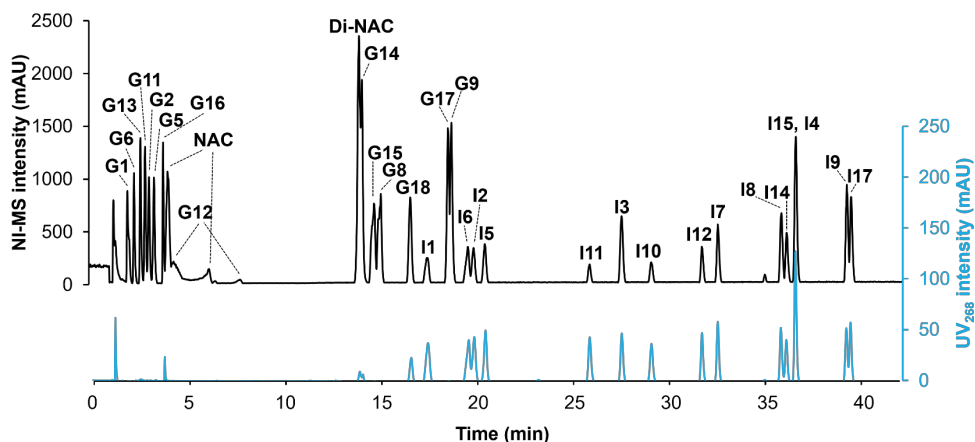
### 6.1.1. Quantification of GSLs and ITCs based on NI-MS signals

In this thesis, the compositional analysis of GSLs and ITCs (as *N*-acetyl-L-cysteine derivatives, i.e. NAC-ITCs) was developed by using NI-MS signals (**Chapter 3**), instead of UV signals which were often employed in previous studies.<sup>1-5</sup> Here, a comparison of NI-MS-based quantification and UV-based quantification methods is presented in **Table 6.1**. The NI-MS-based quantification was done by relating the base peak area of an analyte at its mass-to-charge ratio ( $m/z$ ) to the calibration curve of its reference compound. The UV-based quantification was done by relating peak area of an analyte at 234 nm for GSLs or 268 nm for NAC-ITCs to the calibration curve of its reference compound. The NI-MS-based quantification has several advantages: (i) the analysis of many GSLs without a specific UV absorption maximum ( $\lambda_{\max}$ ) in mixtures is possible, (ii) co-elution, when analyzing plant extracts,<sup>6</sup> is not an issue, (iii) the analysis has a higher (at least 5-fold) sensitivity than the UV-based analysis (**Figure 6.1**), (iv) the analysis has a lower experimental error, especially for analyzing GSLs (up to 8.1%), than the UV-based (up to 26.2%) (**Table 6.1**). The experimental error was obtained from experiments using reference compounds and defined as the absolute difference between the measured concentration and the known concentration in the standard solution. A common limitation of MS-based quantification is the variation in ionization efficiency of molecules, reflected in relative response factors (RRF) that can range from 0.44-1.39 for GSLs and from 0.44-3.62 for NAC-ITCs (**Table 6.1**). Furthermore, the ionization efficiency can be influenced by the configuration of the MS instrument, the experimental conditions (e.g. solvent), and matrix components.<sup>7-8</sup> This emphasizes the importance of employing reference compounds and spiked experiments as a routine check for the chromatographic system.

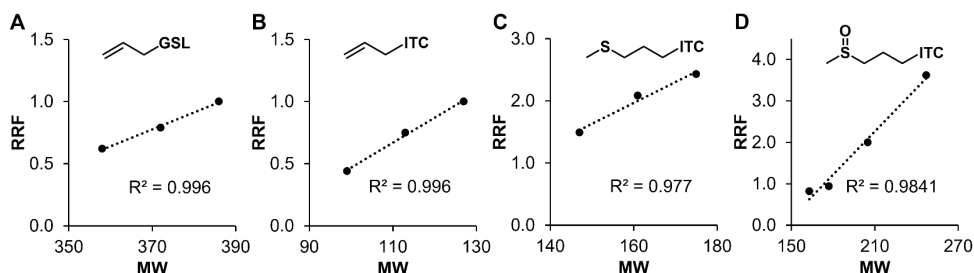
In literature, UV-based RRF of GSLs are often calculated relative to allyl GSL (**G11**),<sup>9-10</sup> whereas UV-based RRF of ITCs is to a lesser extent available and calculated relative to heptyl ITC.<sup>11</sup> Allyl GSL is ubiquitous, however, the corresponding allyl ITC is unstable upon storage.<sup>12</sup> In contrast, heptyl ITC is stable, but the presence of the corresponding heptyl GSL has never been evidenced.<sup>13</sup> MS-based RRF of GSLs and ITCs in this thesis was for the first time determined, because of the advantages of MS-based quantification described above. Here, the RRF was calculated relative to 4-pentenyl GSL (**G14**) for GSLs and 4-pentenyl ITC (**I14**) for ITCs because of their ubiquity and stability.<sup>12,14</sup> RRF is the ratio of slopes of the calibration curves of a GSL or an ITC relative to those of **G14** or **I14**. RRF in **Table 6.1** can be used for studies which have a limited set of GSL and ITC reference compounds. Furthermore, the RRF can be used for quantification of GSLs



and ITCs without reference and RRF. In the case where the RRF of only one compound from the same subclass as the target compound is known, this RRF can be used to calculate the RRF of the target compound by employing a correction factor comprising of the ratio of molecular weight (MW) of the target compound to the MW of the compound from the same subclass with known RRF. **Table 6.1** indicates a positive correlation between RRF and MW for GSLs and ITCs within a subclass. **Figure 6.2** specifies that the correlation is linear ( $R^2 > 0.97$ ) for subclasses alkenyl GSL, alkenyl ITC, x-(methylthio)alkyl ITC (MTITC), and x-(methylsulfinyl)alkyl ITC (MSITC). For the other subclasses, linear correlation could not be shown as there were less than 3 data points. In another case where there is a series of compounds within the same subclass, the RRF of a target compound can be predicted by using the linear regression plot of RRF against MW (**Figure 6.2**). Overall, quantification of ITCs and GSLs without reference compounds, but within the subclasses, should consider the molecular weight.



**Figure 6.1.** RP-UHPLC chromatograms using NI-MS signal (black) and UV signals (blue) at 268 nm of 14 GSLs and 15 NAC-ITCs at 30  $\mu$ M.



**Figure 6.2.** Linear correlation between molecular weight (MW) and relative response factor (RRF) of the alkenyl GSL subclass (A), alkenyl ITC subclass (B), x-(methylthio)alkyl ITC subclass (C), and x-(methylsulfinyl)alkyl ITC subclass (D). The structures shown are a representative of each subclass.

**Table 6.1.** Comparison of NI-MS-based and UV-based quantification methods for the analysis of GSLs and ITCs (as NAC-ITCs).

No. <sup>a</sup>	Compound	<i>m/z</i>	<i>t</i> R (min)	RRF <sup>b</sup>	Quantification method based on	
					NI-MS <sup>c</sup> , μM (% error) <sup>d</sup>	UV <sup>e</sup> , μM (% error)
GSL						
G1	3-(Methylsulfinyl)propyl	422	1.99	0.55	27.56 (8.1)	34.34 (14.5)
G2	4-(Methylsulfinyl)butyl	436	3.11	0.62	28.98 (3.4)	29.32 (2.3)
G5	4-(Methylsulfinyl)-3-butenyl	434	3.36	0.64	28.95 (3.5)	29.34 (2.2)
G6	3-(Methylsulfonyl)propyl	438	2.33	0.44	28.02 (6.6)	29.80 (0.7)
G8	4-(Methylthio)butyl	420	15.08	0.98	29.92 (0.3)	26.24 (12.5)
G9	5-(Methylthio)pentyl	434	18.73	1.39	29.53 (1.6)	Coeluted with G17
G11	Allyl	358	2.90	0.62	28.49 (5.0)	29.40 (2.0)
G12	3-Butenyl	372	7.82	0.79	32.21 (7.4)	32.49 (8.3)
G14	4-Pentenyl	386	14.05	1.00	30.65 (2.2)	Coeluted with Di-NAC
G13	( <i>R</i> )-2-OH-3-Butenyl	388	2.67	0.59	28.92 (3.6)	28.96 (3.5)
G15	Benzyl	408	14.72	1.06	30.71 (2.4)	28.05 (6.5)
G17	Phenethyl	422	18.54	1.16	30.75 (2.5)	Coeluted with G9
G16	<i>p</i> -OH-Benzyl	424	3.83	0.54	29.53 (1.6)	22.13 (26.2)
G18	Indol-3-ylmethyl	447	16.59	0.75	30.06 (0.2)	30.45 (1.5)
NAC-ITC						
I1	3-(Methylsulfinyl)propyl	325	17.53	0.82	29.00 (3.3)	29.55 (1.5)
I2	4-(Methylsulfinyl)butyl	339	19.88	0.94	28.09 (6.4)	29.33 (2.2)
I3	6-(Methylsulfinyl)hexyl	367	27.51	2.00	29.10 (3.0)	28.82 (3.9)
I4	9-(Methylsulfinyl)nonyl	409	36.53	3.62	28.60 (4.7)	Coeluted with I15
I5	4-(Methylsulfinyl)-3-butenyl	337	20.44	0.96	30.71 (2.4)	28.95 (3.5)
I6	3-(Methylsulfonyl)propyl	341	19.60	1.11	29.90 (0.3)	29.57 (1.4)
I7	3-(Methylthio)propyl	309	32.49	1.49	27.95 (6.8)	28.68 (4.4)
I8	4-(Methylthio)butyl	323	35.78	2.08	27.81 (7.3)	28.88 (3.7)
I9	5-(Methylthio)pentyl	337	39.15	2.43	27.83 (7.2)	29.06 (3.1)
I10	Propyl	263	29.04	0.70	28.26 (5.8)	28.44 (5.2)
I11	Allyl	261	25.87	0.44	29.20 (2.7)	28.37 (5.4)
I12	3-Butenyl	275	31.66	0.75	28.26 (5.8)	28.62 (4.6)
I14	4-Pentenyl	289	36.04	1.00	30.20 (0.7)	28.88 (3.7)
I15	Benzyl	311	36.53	1.32	28.51 (5.0)	Coeluted with I4
I17	Phenethyl	325	39.38	1.81	29.22 (2.6)	29.1 (3.0)

<sup>a</sup> Compound number is according to that in **Chapter 3**. Compounds are grouped per subclass as indicated by the grey or white shading.

<sup>b</sup> Relative response factors (RRF) based on NI-MS based quantification of GSLs are relative to 4-pentenyl GSL (**G14**), whereas those of ITCs are relative to 4-pentenyl ITC (**I14**).

<sup>c</sup> NI-MS signals at base peak of the *m/z* of the compound.

<sup>d</sup> Experimental error: the absolute difference between the measured concentration and the known concentration added (30 μM).

<sup>e</sup> UV signals at 234 nm for GSLs, UV at 268 nm for NAC-ITCs.

Furthermore, in this thesis the LC-MS analysis of GSLs and ITCs was successfully applied to monitor *in vitro* enzymatic conversion of many GSLs to ITCs simultaneously in one run (**Chapter 3**). The enzymatic process was performed along with NAC-derivatization of ITCs. The simultaneous analysis increased efficiency as it did not require ITC extraction. The solvent IPA 25% (in buffer pH 7) dissolved both GSLs and ITCs well. Additionally, this LC-based analytical method for simultaneous analysis of GSLs and ITCs can minimize under- or overestimation of ITCs (e.g. AITC, 3-BuITC, 4-MSITC), as would occur in GC analysis.<sup>15-16</sup>

### 6.1.2. Choice of growth media in antibacterial assays of ITCs

One of the main findings in **Chapter 4** was that the activity of antibacterial ITCs was notably lower in nucleophile-rich growth media (i.e. tryptone soy broth, TSB) than in nucleophile-poor growth media (i.e. 5-10× diluted TSB). The difference was up to a factor of 4-16. Since the nucleophile-richness of growth media was taken into account in this thesis, the antibacterial activity presented as MIC in **Chapters 4** and **5** is differentiated from that in previous studies (see **Chapter 1**). The intrinsic antibacterial activity of ITCs reported in previous studies is likely to be underestimated. The underestimation of the antimicrobial activity of ITCs evaluated in undefined rich media (brain heart infusion, BHI; lysogeny broth, LB) reported in literature,<sup>17-18</sup> using a similar broth microdilution assay as in this thesis, can be a factor of 3-14, compared to the antimicrobial activity in the nucleophile-poor TSB (**Chapter 4**). The amino acid sources provided by BHI (1 L) consist of 10 g peptone, 5 g beef heart infusion, and 12.5 g calf brain infusion. The amino acid sources provided by LB (1 L) consist of 10 g tryptone and 5 g yeast extract. The estimated total amino acid contents in BHI and LB were 17 mg/mL and 11-12 mg/mL, respectively.<sup>19-20</sup> Due to lack of data on the total amino acid composition of calf brain (or alike) infusion, it was assumed to be equal to that of beef heart infusion. Based on the total amino acid contents, BHI and LB are considered to be as nucleophile-rich as TSB (14 mg/mL, **Chapter 4**). According to findings in **Chapter 4** and a previous study,<sup>18</sup> the total amino acid content in growth media for being considered nucleophile-rich is > 1.5 mg/mL or 20 mM.

Another important finding in **Chapter 4** was that total Cys residue content (0.05 mg/mL) in nucleophile-rich TSB was similar to that in nucleophile-poor RPMI 1640. The total Cys residue content in BHI and LB was approximately 0.07 and 0.05-0.06 mg/mL, respectively.<sup>19-20</sup> The total Cys residue contents in TSB, BHI, and LB were the lowest among other amino acid residues. This implies that when Cys content is low, other amino acids contribute more to the nucleophilicity of growth media.

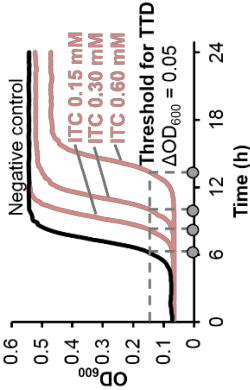
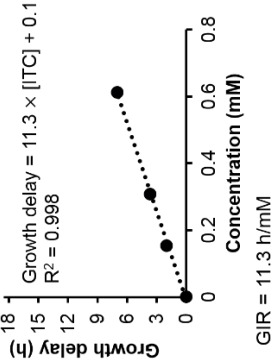
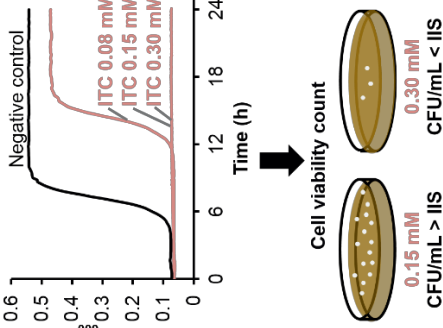
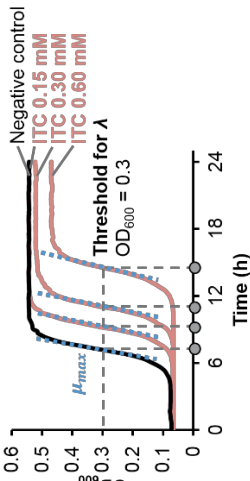
### 6.1.3. Antibacterial activity parameters for QSAR studies

The QSAR study in this thesis (**Chapter 5**) used two kinds of antibacterial activity parameters: minimum inhibitory concentration (MIC, in mM, as pMIC) and growth inhibitory response (GIR, in h/mM, as p'GIR). The comparison between GIR and MIC, as well as I<sub>AE</sub> (antimicrobial efficacy index, see further) is summarized in **Table 6.2**. MIC has been the standard used in the field of antimicrobials to define the potency of a compound.<sup>21-22</sup> However, it is often found that a defined MIC of compounds, including ITCs, cannot be determined due to their low activity and/or solubility. Meanwhile, microbial growth can still be delayed (i.e. higher time-to-detection, TTD) along with increasing compound concentrations. In this case, another antimicrobial activity parameter can describe the activity of a compound better than MIC.

Time-to-detection is used as a microbial growth parameter when growth is monitored through turbidity (OD<sub>600</sub>) measurement.<sup>23-26</sup> TTD is defined as the time point where the OD<sub>600</sub> has increased by 0.05 or 0.10.<sup>23-26</sup> In this thesis 0.05 was used, following previous studies in the Laboratory of Food Chemistry.<sup>23,27</sup> Based on TTD and compound concentration, another antimicrobial activity parameter, i.e. GIR (h/mM), was defined as the slope of the plot of growth delay (h) against concentration (mM) of the compound (**Chapter 5**). The plot was linear ( $R^2 > 0.98$ ) within the boundaries of the incubation period. Overall, GIR is able to indicate the antimicrobial activity of all compounds, regardless of their potency.

The higher the GIR value, the better the antimicrobial activity of a compound. This is opposite to MIC: the lower the MIC value, the better the antimicrobial activity of a compound. GIR for a compound with a good antimicrobial activity was found to be  $\geq 114$  h/mM, moderate activity 20-114 h/mM, and poor activity  $\leq 20$  h/mM (**Chapter 5**). For ITCs (**Chapters 4 and 5**) and other natural antimicrobial compounds,<sup>28</sup> the corresponding MIC values were  $\leq 25$   $\mu\text{g/mL}$ , 25-100  $\mu\text{g/mL}$ , and  $> 100$   $\mu\text{g/mL}$ , respectively. A defined MIC often cannot be determined for many compounds due to limited solubility. In contrast, GIR can indicate a reasonably precise antimicrobial activity value for such compounds. In addition, determination of MIC in literature varies; it can be either based on only OD<sub>600</sub> or on OD<sub>600</sub> and cell viability count.<sup>17,29-30</sup> According to the clinical authority (CLSI), MIC is determined based on OD<sub>600</sub>.<sup>31</sup> Nevertheless, OD<sub>600</sub> measurement has a higher detection limit ( $10^6$  CFU/mL) compared to cell viability count (10 CFU/mL). In this thesis, MIC was determined specifically based on the cell viability count.

Table 6.2. Comparison between GIR, MIC, and I<sub>AE</sub>.

Aspect	GIR	MIC	I <sub>AE</sub> <sup>22</sup>
Determination	<div><p>Graph of OD<sub>600</sub> vs Time (h) for TTD. Curves for ITC 0.15 mM, 0.30 mM, and 0.60 mM. Threshold for TTD is ΔOD<sub>600</sub> = 0.05.</p></div> <div><p>Graph of Growth delay (h) vs Concentration (mM). Data points show a linear relationship with a dotted line fit. GIR = 11.3 h/mM.</p></div>	<div><p>Graph of OD<sub>600</sub> vs Time (h) for MIC. Curves for ITC 0.08 mM, 0.15 mM, and 0.30 mM. Cell viability count is shown with CFU/mL &gt; IIS and CFU/mL &lt; IIS.</p></div>	<div><p>Graph of OD<sub>600</sub> vs Time (h) for I<sub>AE</sub>. Curves for ITC 0.15 mM, 0.30 mM, and 0.60 mM. Threshold for λ is OD<sub>600</sub> = 0.3.</p></div> <div><math display="block">I_{AE} = \frac{\lambda_C}{\lambda_0} \times \frac{\sigma_{max,0}}{\sigma_{max,C}} \times \frac{\mu_{max,0}}{\mu_{max,C}}</math><p>λ = the time when OD<sub>600</sub> reaches 0.3 σ<sub>max</sub> = maximum population, referred to maximum OD<sub>600</sub> at the end of log phase μ<sub>max</sub> = maximum growth rate, referred to the first derivative of OD<sub>600</sub> over time at the inflection point C and 0 refer to ITC at concentration C and 0 (negative control), respectively I<sub>AE</sub> calculation is repeated for 3 concentrations of an ITC, and the final I<sub>AE</sub> is the average</p><math display="block">\overline{I_{AE}} = \frac{I_{AE}(0.15 \text{ mM}) + I_{AE}(0.30 \text{ mM}) + I_{AE}(0.60 \text{ mM})}{3} = \frac{1.3 + 1.6 + 3.1}{3} = 2.0</math></div>
Unit	time/molar-based concentration, e.g. h/mM	concentration, e.g. μg/mL (common), mM	-
Interpretability	straightforward	straightforward	concentration dependent
Activity scale	good, GIR ≥ 114 h/mM; moderate, GIR 20-114 h/m; low, GIR ≤ 20 h/mM	good, MIC ≤ 25 μg/mL; moderate, MIC 25-100 μg/mL; low, MIC > 100 μg/mL	active, I <sub>AE</sub> > 1.00
Applicability	not limited to compound solubility	limited to compound solubility	not limited to compound solubility

As the antimicrobial potency of a compound is a matter of concentration, it is easy to interpret GIR as well as MIC, whether a compound has a good, moderate, or low antimicrobial activity. This is not the case for the other activity parameter, i.e. antimicrobial efficacy index ( $I_{AE}$ ),<sup>32</sup> as it does not integrate the concentration in its formula.  $I_{AE}$  of a compound is determined by taking the average of  $I_{AE}$  of that compound at three concentrations. As  $I_{AE}$  varies by concentration, the average  $I_{AE}$  of a compound differs if another series of concentrations is used. Meanwhile, an unbiased comparison of antimicrobial activity of compounds is a prerequisite, for instance in (Q)SAR studies. For  $I_{AE}$ , this can only be done if all compounds are tested under the same condition, including the concentration series which is used. For a very potent compound,  $I_{AE}$  at certain concentrations may turn out to be undefined as  $\lambda_C$  (equivalent to TTD with an  $OD_{600}$  threshold of 0.3) goes to over the maximum incubation period, e.g. 24 h, and  $\mu_{max,C}$  (the growth rate) is zero. This suggests that it is hard to classify the antimicrobial potency of compounds by using  $I_{AE}$  as an antimicrobial activity parameter.

Overall, GIR is recommended to use in the future as an antimicrobial activity parameter, which can accurately determine the antimicrobial activity of poor to good antimicrobial compounds. For research purposes GIR can provide a more complete insight into the (Q)SAR of antimicrobials than MIC and  $I_{AE}$ .

## 6.2. How to get ITC-rich extracts from nature?

### 6.2.1. Separate extraction and hydrolysis of GSLs from Brassicaceae seeds

An approach to get ITC-rich extracts from Brassicaceae was suggested in **Chapter 3** and applied in **Chapter 5** where the antimicrobial activity of the ITC-rich extracts was determined and predicted. In **Chapters 4** and **5**, a number of ITCs showed promising antimicrobial activity. They can be obtained from nature, meaning that they are released from GSLs. In this thesis, the GSLs already abundantly present in the particular seeds were extracted under conditions where myrosinase was deactivated. Afterwards, myrosinase was applied *in vitro* to the extract. GSLs were fully hydrolyzed, but not only ITCs were formed (see **Chapter 1**). This *in vitro* enzymatic degradation of GSLs yielded 80-96% ITCs (**Chapters 3** and **5**) from ITC-forming GSLs. Meanwhile, the common approach in literature applies the *in situ* enzymatic degradation of GSLs by water extraction, yielding only up to 45% ITCs.<sup>33</sup> During the *in situ* enzymatic degradation, ITCs and non-ITC degradation products, such as nitriles and epithionitriles, mainly due to the activity of endogenous specifier proteins, were released.<sup>33-38</sup> Besides, under this aqueous condition, co-extraction of potential nucleophiles, particularly glutathione as the major thiol compound in plants<sup>39-40</sup> or amino acids, such as cysteine, can occur, and these nucleophiles (**Chapter 4**) will react with ITCs. In contrast, under absolute MeOH condition, co-extraction of potential nucleophiles can be minimized.

It is known that all amino acids lose solubility in aqueous solvents with over 50% v/v ethanol.<sup>41</sup> Considering the polarity of 50% v/v aqueous ethanol, it can be assumed that all amino acids and small peptides (e.g. glutathione) are insoluble in absolute MeOH. In conclusion, to obtain the optimum amount of ITCs from nature, the approach consisting of separate extraction and *in vitro* hydrolysis of GSLs from Brassicaceae seeds is recommended.

### 6.2.2. Fungal elicitation not suitable to increase content of precursors of ITCs

As described in **Chapter 2**, germination activated biosynthesis of *p*-OH-benzyl GSL in *Sinapis alba*, acylated alkenyl GSLs in *Brassica napus* and *B. juncea*, and indolic GSLs in all three species. Simultaneous germination and fungal elicitation, regardless of the pathogenicity of the fungi, did not increase further the accumulation of GSLs in Brassicaceae seedlings. Furthermore, hardly any new GSL subclasses were formed upon fungal elicitation. The main GSLs induced were not precursors of the best antimicrobial ITCs. In **Chapter 4**, it became clear that MSITC and MSoITC were the promising antimicrobial subclasses against Gram<sup>-</sup> bacteria, Gram<sup>+</sup> bacteria, and fungi. It can be concluded that simultaneous germination and *Rhizopus* elicitation, which successfully boosted the accumulation of prenylated isoflavonoids and stilbenoids in Leguminosae,<sup>42</sup> could not be extrapolated to boost the accumulation of GSLs in Brassicaceae.

## 6.3. ITCs as antimicrobials

This thesis confirms that ITCs are a group of potential broad spectrum antimicrobials, i.e. effective against Gram<sup>-</sup> bacteria, Gram<sup>+</sup> bacteria, and fungi (**Chapter 4**). In particular, this thesis revealed many other ITCs with good antimicrobial activity (MIC  $\leq$  25  $\mu$ g/mL) than the most extensively studied ones (AITC, BITC, PhEITC, and 4-MSITC, see **Chapter 1**). MSITC and MSoITC are among the most effective ITC subclasses, which can be naturally obtained (**Chapters 4 and 5**). The short-chained MSITC and MSoITC are good antimicrobials against Gram<sup>-</sup> bacteria, Gram<sup>+</sup> bacteria, and fungi, whereas the long-chained ones are good antimicrobials against Gram<sup>+</sup> bacteria and fungi. ITCs are more potent than other natural antimicrobials (e.g. thymol, eugenol, MIC > 1000  $\mu$ g/mL; chlorogenic acid, ferulic acid, MIC > 500  $\mu$ g/mL).<sup>43-44</sup> Another class of phenolic compounds, namely prenylated isoflavonoids, were potent against Gram<sup>+</sup> bacteria, with the lowest MIC of 6.3  $\mu$ g/mL.<sup>29</sup> The antimicrobial activity of ITCs was dependent on the nucleophile content of the growth media, with the lowest MIC of 9.4  $\mu$ g/mL against Gram<sup>+</sup> bacteria and 25  $\mu$ g/mL against Gram<sup>-</sup> bacteria in nucleophile-poor growth media (**Chapters 4 and 5**). Meanwhile, the bifunctional ITC was the most effective against both Gram<sup>+</sup> (MIC = 6.3  $\mu$ g/mL) and Gram<sup>-</sup> bacteria (MIC = 9.4  $\mu$ g/mL); this ITC can only be synthetically obtained (**Chapter 5**). Against Gram<sup>-</sup> bacteria, the activity of prenylated isoflavonoids was dependent on efflux pump

inhibitors (EPI), with the lowest MIC of 10 µg/mL in the presence of EPI.<sup>29</sup> The activity of ITCs against Gram<sup>-</sup> bacteria did not require EPI.

### 6.3.1. Future QSAR studies of antimicrobial ITCs

In **Chapter 5**, the main physicochemical properties of ITCs defining antimicrobial activity against Gram<sup>-</sup> *E. coli* and Gram<sup>+</sup> *Bacillus cereus* (partial charge, polarity, reactivity, and shape) were established based on a QSAR study. **Table 6.3** presents 54 ITCs (**1-54**) of various subclasses, comprising those which can be naturally obtained as well as synthetic representatives. Structures of the ITCs are displayed in **Figure 6.3**.

ITCs **1-26** were used in the training set in the QSAR modeling in **Chapter 5**. These 26 ITCs covered quite a number (9) of ITC subclasses. One of the main findings in **Chapter 5** was that the QSAR models had high internal prediction ability (leave-one-out cross validation  $Q^2 > 0.80$ ). Because of the relatively small dataset size, the dataset in the QSAR study in **Chapter 5** was not split into training set and test set. Test set is used for external validation, which is the final step in QSAR modeling to confirm the prediction ability of the models.<sup>45-47</sup> In **Chapter 5**, in complementary to the internal validation, the prediction ability of the models were examined by comparing the observed activity and predicted activity of ITC-rich Brassicaceae extracts. The QSAR models were able to predict the activity of ITC-rich Brassicaceae extracts, including the extract containing external ITCs (**36** and **37**), i.e. ITCs not in the training set.

ITCs **27-54** are candidates of external ITCs to be considered for future QSAR studies. All the compounds were within the applicability domain of the four selected QSAR models in **Chapter 5**. Since antimicrobial activity of the external ITCs against *E. coli* or *B. cereus* in nucleophile-poor TSB has never been experimentally determined, the applicability domains were built based on the chemical space (i.e. descriptors) only, and not on the response space (i.e. antimicrobial activity).<sup>48</sup>

The predicted activity (GIR, **Table 6.3**) of the majority of the external ITCs followed the trends in **Chapter 5**. The short-chained (C2-C4) ITCs containing sulfinyl or sulfonyl group had good predicted antimicrobial activity ( $GIR_{pre} \geq 114$  h/mM) against both Gram<sup>-</sup> *E. coli* and Gram<sup>+</sup> *B. cereus*, whereas the long-chained (C5-C11) analogues had good predicted activity against Gram<sup>+</sup> *B. cereus*. Furthermore, regardless of the side chain length, alkyl ITCs, alkenyl ITCs, methylthio (MT)-containing ITCs, and sulfonyl benzenic ITCs generally had low predicted activity ( $GIR_{pre} \leq 20$  h/mM). Additionally, the presence of an oxo group in the side chain does not seem to improve the antimicrobial activity of ITCs. These predictions can guide researchers in deciding which ITCs have potentially good antimicrobial activity, worth further investigation.



**Table 6.3.** Internal ITCs (1-26) used in the training set of QSAR study in **Chapter 5** and external ITCs (27-54) within the applicability domains, built using the standardization approach,<sup>48</sup> of the selected QSAR models in **Chapter 5**, to be considered for future studies.

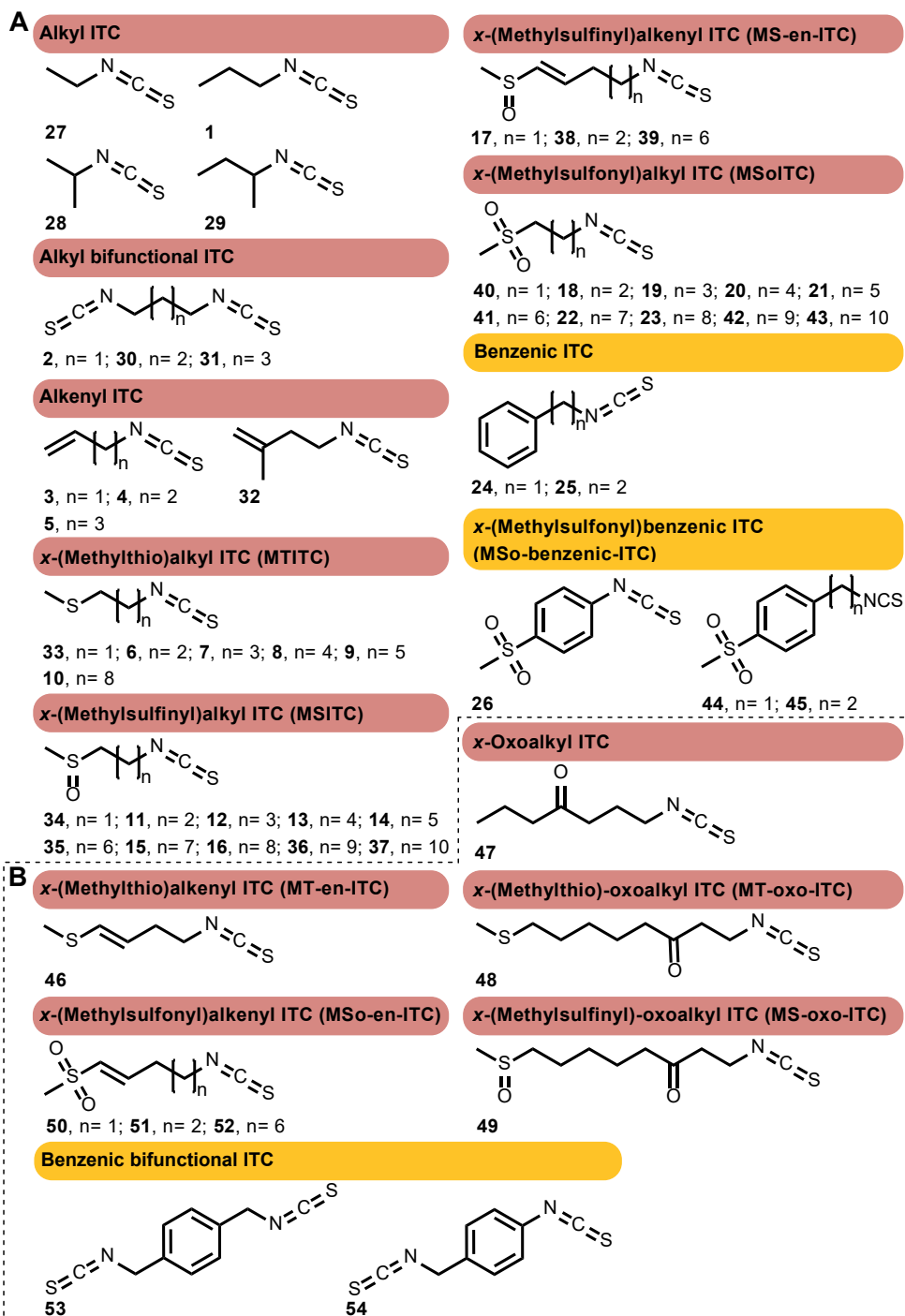
ID	ITC	N/S <sup>a</sup>	Ref. <sup>b</sup>	Predicted GIR (h/mM)	
				Ec <sup>c</sup>	Bc
Subclass Alkyl ITC					
1	Propyl ITC (PITC)	S	-	1	2
Subclass Alkyl bifunctional ITC					
2	1,3-Propylene diisothiocyanate (P-DiITC)	S	-	157	427
Subclass Alkenyl ITC					
3	Allyl ITC (AITC)	N	49-52	5	3
4	3-Butenyl ITC (BuITC)	N	49,51,53-54	7	2
5	4-Pentenyl ITC (PeITC)	N	51,55-56	9	1
Subclass MTITC					
6	3-(Methylthio)propyl ITC (3-MTITC)	N	57	11	23
7	4-(Methylthio)butyl ITC (4-MTITC)	N	49-50,58-61	5	7
8	5-(Methylthio)pentyl ITC (5-MTITC)	N	61-64	4	9
9	6-(Methylthio)hexyl ITC (6-MTITC)	N	61,65-67	4	14
10	9-(Methylthio)nonyl ITC (9-MTITC)	N	68-69	2	12
Subclass MSITC					
11	3-(Methylsulfinyl)propyl ITC (3-MSITC)	N	49-50,60,67,70-73	117	179
12	4-(Methylsulfinyl)butyl ITC (4-MSITC)	N	49-50,60,67,72,74-75	136	89
13	5-(Methylsulfinyl)pentyl ITC (5-MSITC)	N	60,62,76-79	45	107
14	6-(Methylsulfinyl)hexyl ITC (6-MSITC)	N	60-61,67,76,80-81	58	191
15	8-(Methylsulfinyl)octyl ITC (8-MSITC)	N	51,61,82-83	17	232
16	9-(Methylsulfinyl)nonyl ITC (9-MSITC)	N	61,83-85	8	152
Subclass MS-en-ITC					
17	4-(Methylsulfinyl)-3-butenyl ITC (4-MS-3-en-ITC)	N	49,60,86-88	349	104
Subclass MSolTC					
18	3-(Methylsulfonyl)propyl ITC (3-MSolTC)	N	67,89	219	243
19	4-(Methylsulfonyl)butyl ITC (4-MSolTC)	N	67	73	120
20	5-(Methylsulfonyl)pentyl ITC (5-MSolTC)	S	-	54	133
21	6-(Methylsulfonyl)hexyl ITC (6-MSolTC)	N	90-91	50	227
22	8-(Methylsulfonyl)octyl ITC (8-MSolTC)	N	51,83,92-94	20	178
23	9-(Methylsulfonyl)nonyl ITC (9-MSolTC)	N	83,92-94	3	756
Subclass Benzenic ITC					
24	Benzyl ITC (BITC)	N	49,60,95	9	30
25	Phenethyl ITC (PhEITC)	N	49-50,95	6	13
Subclass MSo-benzenic-ITC					
26	<i>p</i> -(Methylsulfonyl)phenyl ITC ( <i>p</i> -MSoPhITC)	S	-	12	17
Subclass Alkyl ITC					
27	Ethyl ITC (EITC)	N	96	1	1
28	Isopropyl ITC (iPITC)	N	97	1	1
29	<i>sec</i> -Butyl ITC (sButyl ITC)	N	98	1	1
Subclass Alkyl bifunctional ITC					
30	1,4-Butane diisothiocyanate (butyl-DiITC)	S	-	6	685
31	1,5-Pentane diisothiocyanate (pentyl-DiITC)	S	-	30	371

ID	ITC	N/S <sup>a</sup>	Ref. <sup>b</sup>	Predicted GIR (h/mM)	
				Ec <sup>c</sup>	Bc
Subclass Alkenyl ITC					
32	3-Methyl-3-butenyl ITC (3-M-3-BuITC)	N	99	6	2
Subclass MTITC					
33	2-(Methylthio)ethyl ITC (2-MTITC)*	S	-	5	10
Subclass MSITC					
34	2-(Methylsulfinyl)ethyl ITC (2-MSITC)	N	100	279	105
35	7-(Methylsulfinyl)heptyl ITC (7-MSITC)	N	51,101-103	48	94
36	10-(Methylsulfinyl)decyl ITC (10-MSITC)	N	51,84,104	3	280
37	11-(Methylsulfinyl)undecyl ITC (11-MSITC)	N	84,103,105	3	425
Subclass MS-en-ITC					
38	5-(Methylsulfinyl)-4-pentenyl ITC (5-MS-4-en-ITC)*	S	-	74	283
39	9-(Methylsulfinyl)-8-nonenyl ITC (9-MS-8-en-ITC)*	S	-	12	52
Subclass MSolTC					
40	2-(Methylsulfonyl)ethyl ITC (2-MSolTC)*	S	-	154	431
41	7-(Methylsulfonyl)heptyl ITC (7-MSolTC)*	S	-	22	230
42	10-(Methylsulfonyl)decyl ITC (10-MSolTC)	N	83,93,95	2	316
43	11-(Methylsulfonyl)undecyl ITC (11-MSolTC)*	S	-	2	155
Subclass MSo-benzenic-ITC					
44	p-(Methylsulfonyl)benzyl ITC (p-MSoBITC)	S	-	8	22
45	p-(Methylsulfonyl)phenethyl ITC (p-MSoPhEITC)	S	-	3	33
Subclass MT-en-ITC					
46	4-(Methylthio)-3-butenyl ITC (4-MT-3-en-ITC)	N	49,60,106-109	17	3
Subclass x-Oxoalkyl ITC					
47	4-Oxo-heptyl ITC (4-oxo-HITC)	N	110	7	14
Subclass MT-oxo-ITC					
48	8-(Methylthio)-3-oxooctyl ITC (8-MT-3-oxo-ITC)	N	111	3	49
Subclass MS-oxo-ITC					
49	8-(Methylsulfinyl)-3-oxooctyl ITC (8-MS-3-oxo-ITC)	N	111	23	83
Subclass MSo-en-ITC					
50	4-(Methylsulfonyl)-3-butenyl ITC (4-MSo-3-en-ITC)*	S	-	113	121
51	5-(Methylsulfonyl)-4-pentenyl ITC (5-MSo-4-en-ITC)*	S	-	49	623
52	9-(Methylsulfonyl)-8-nonenyl ITC (9-MSo-8-en-ITC)*	S	-	4	401
Subclass benzenic bifunctional ITC					
53	1,4-Bis(ITCmethyl)benzene (p-methyl-ITC-BITC)	S	-	20	385
54	1-ITC-4-(ITCmethyl)benzene (p-ITC-BITC)	S	-	12	77

<sup>a</sup> N stands for natural (i.e. ITCs whose precursor GSLs have been identified unambiguously in plants); S stands for synthetic (i.e. ITCs whose precursor GSLs have not been identified unambiguously in plants, although some of the GSLs can theoretically be biosynthesized in plants, e.g. those indicated by the (\*) symbol, or ITCs whose precursor GSLs cannot be biosynthesized in plants).

<sup>b</sup> References for the botanical sources of their GSL precursors. The natural occurrence of ITCs was confirmed.<sup>1,13</sup>

<sup>c</sup> *Ec* stands for *E. coli*; *Bc* stands for *B. cereus*.



**Figure 6.3.** Natural and synthetic ITCs belonging to the subclasses in the training set (A) and outside the training set (B). Bold-face numbers refer to the compound ID in **Table 6.3**.

As GIR is for the first time introduced in this thesis (**Chapter 5**), GIR of external ITCs is not available in literature. It is also not possible to calculate GIR from the data available in literature. In contrast, as a well-known antimicrobial activity parameter, MIC of several external ITCs are available in literature. **Table 6.4** shows the experimental and predicted MIC values of few external ITCs against *E. coli* and *B. cereus*. It should be emphasized that the experimental MIC values were obtained from previous studies using nucleophile-rich TSB (undiluted TSB).<sup>18,30</sup> Meanwhile, the predicted MIC values were calculated by employing the selected pMIC models in **Chapter 5** which were based on the antimicrobial assays using nucleophile-poor TSB (see section **6.1.2**). The activity of ITCs **30**, **31**, and **54** against *E. coli* were predicted as a good activity, which was higher than the experimentally determined ones (low to moderate activity).<sup>30</sup> Furthermore, the predicted MIC values of ITCs **30**, **31**, **53**, and **54** against *B. cereus* were higher than the experimental ones, but they were in the same activity potency class (good activity), except **54** (moderate activity). Considering the finding in **Chapter 4** that the activity can be improved up to 16-fold in nucleophile-poor TSB, the difference between the experimental and predicted MIC values can be because of the different nucleophile richness of the growth media which were used. In addition, it might be due to insufficient (only one) bifunctional ITC representative in the training set. Overall, the QSAR models developed in **Chapter 5** possibly have good external prediction ability for ITCs which possess structural features captured in the training set.

**Table 6.4.** Experimental and predicted activity (MIC,  $\mu\text{g/mL}$ ) of few external ITCs against *E. coli* (*Ec*) and *B. cereus* (*Bc*).

ID <sup>a</sup>	Compound	Experimental MIC ( $\mu\text{g/mL}$ ) <sup>b</sup>		Ref.	Predicted MIC ( $\mu\text{g/mL}$ )	
		<i>Ec</i>	<i>Bc</i>		<i>Ec</i>	<i>Bc</i>
<b>28</b>	iPITC	810	-	18	358	237
<b>30</b>	Butyl-DiITC	>64	2	30	11	19
<b>31</b>	Pentyl-DiITC	>64	2	30	18	9
<b>53</b>	<i>p</i> -methyl-ITC-BITC	8	0.5	30	10	18
<b>54</b>	<i>p</i> -ITC-BITC	64	2	30	5	27

<sup>a</sup> Compound ID refers to that in **Table 6.3**.

<sup>b</sup> The experimental MIC values of ITCs were obtained from assays using nucleophile-rich TSB (undiluted TSB).<sup>18,30</sup> The predicted MIC values were obtained from the pMIC models in **Chapter 5** using nucleophile-poor TSB (10 $\times$  diluted TSB).

Future QSAR studies should be directed towards the external validation and the application of the models to predict the activity of natural ITC-rich extracts for application as natural food preservatives. Additionally, based on the findings in **Chapter 4** showing that ITCs were effective against various microorganisms, QSAR studies of ITCs against other microbial species, e.g. *A. niger* (as spores) and *S. cerevisiae*, are recommended.

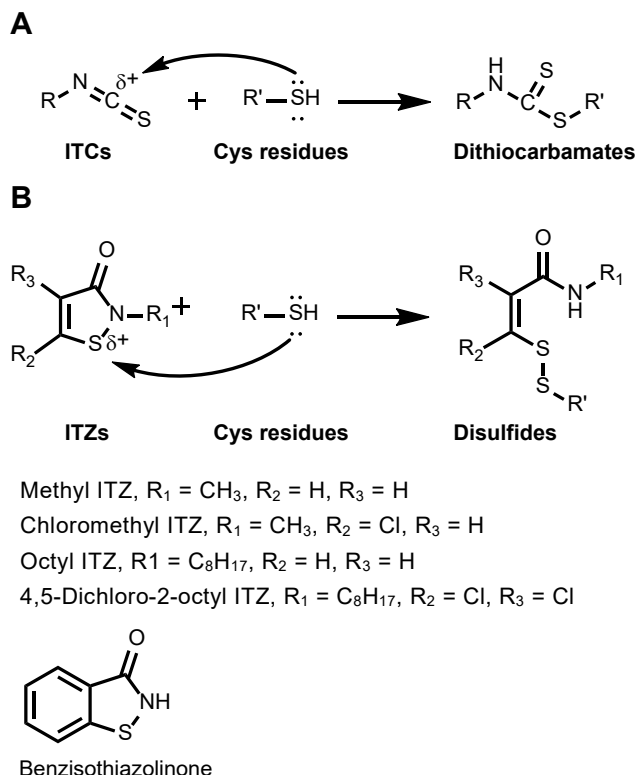
### 6.3.2. Hints for the mode of action

All ITCs have the same functional group  $-N=C=S$ , which is electrophilic. This functional group makes ITCs reactive towards nucleophiles and postulated to be the key structural feature for interaction with the intracellular targets.<sup>112-115</sup>

**Chapters 4 and 5** indicated that not all ITCs exerted antimicrobial activity. This suggests that the main physicochemical property for defining antimicrobial activity of ITCs is not only electrophilicity, but also polarity, partial charge surface area, and molecular shape (**Chapter 5**). These important physicochemical properties affect all the processes (e.g. cell entry, residence time in the cell, reaching the target) for ITCs to finally interact with their target in the microbe to exert their antimicrobial activity.

Cell wall architecture of Gram<sup>-</sup> bacteria is different from that of Gram<sup>+</sup> bacteria, whereas cell wall architecture of Gram<sup>+</sup> bacteria and fungi are alike (see **Chapter 1**). The entry pathway for ITCs in Gram<sup>-</sup> bacteria is possibly through water-filled porins present in the outer membrane. It is of interest to investigate ITC activity by using mutant strains lacking of porins, living without any substantial metabolic disorder, to confirm this hypothesis.<sup>116-117</sup> Additionally, ITCs are insignificantly affected by the efflux pumps (**Chapter 4**). Meanwhile, the entry pathway for ITCs in Gram<sup>+</sup> bacteria and fungi is suggested via passive diffusion through the permeable cell wall and cell membrane, likewise for other antimicrobials.<sup>118-119</sup>

ITCs are effective antimicrobials, not only against bacteria (prokaryotic cells), but also against fungi (eukaryotic cells). Besides, ITCs have been studied extensively for their mode of action in eukaryotic cells, such as human cell lines, for their capacity to kill cancer cells.<sup>120-121</sup> AITC, 4-MSITC, BITC, and PhEITC were able to cross eukaryotic cell membranes,<sup>122</sup> although these membranes contain proteins with thiol groups.<sup>123</sup> A proteomic study indicated that more than 30 proteins in a human lung cancer cell line were bound to 4-MSITC and PhEITC via dithiocarbamation (**Figure 6.4A**).<sup>124</sup> Those proteins include redox-regulating proteins, e.g. thioredoxins, NADH dehydrogenase.<sup>124</sup> Such a proteomic study by incubating microbial cells with radioactive-labelled ITCs could be one possible approach to gain further mechanistic insight of the antimicrobial action of ITCs. Another study indicated that 4-MSITC and 4-MSoITC caused GSH depletion in various eukaryotic cells, e.g. human and rat cell lines.<sup>80</sup> GSH depletion might cause an induction of ROS generation, which can change the redox state of the cells.<sup>121,125</sup> Interestingly, these two (subclasses of) ITCs were among the most potent antimicrobials (**Chapters 4 and 5**). The mode of action of ITCs in eukaryotic cells might be extrapolated to other eukaryotic cells (i.e. fungi) as well as prokaryotic cells.

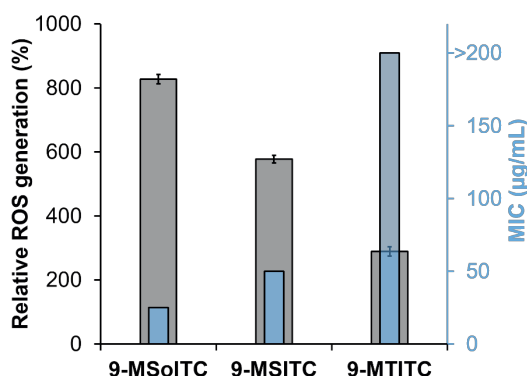


**Figure 6.4.** Reaction schemes of ITC (**A**) and ITZ (**B**) electrophiles with thiol nucleophiles. The electrophilic atoms are denoted with  $\delta+$ .

Preliminary experiments from this thesis on ROS generation in *B. cereus* ATCC14579, one of the most susceptible microorganisms tested towards ITCs (**Chapter 4**), was performed by pre-treating the cells with 2'-7'-dichlorofluorescein diacetate (DCFDA) and measuring fluorescence upon incubation in the absence and in the presence of ITCs. 9-MSoITC, 9-MSITC, and 9-MTITC were tested as a representative of ITCs having a good, moderate, and low antimicrobial activity in nucleophile-rich TSB, respectively (**Chapter 4**). **Figure 6.5** shows that at its MIC 9-MSoITC caused the largest ROS increase (8-fold, compared to the negative control), followed by 9-MSITC (6-fold). At 200  $\mu\text{g/mL}$ , 9-MTITC only caused a 3-fold ROS increase. This indicated that antimicrobial ITCs increased ROS generation remarkably.

ITCs might elevate ROS levels in *Bacillus* by reacting with high-molecular-weight (HMW) thiol molecules, e.g. NADH dehydrogenase and thioredoxin, as mentioned above.<sup>124,126</sup> Prokaryotic and eukaryotic dehydrogenases are specific enzymes inhibited by isothiazolinones (ITZs).<sup>127-131</sup> ITZs are another class of electrophilic antimicrobials (**Figure 6.4B**), which receive much research and industrial interest.<sup>131-136</sup> ITZs have *AM1\_electrophilicity* values in the range of

those of ITCs (1.91–3.62 eV). ITCs and ITZs are hypothesized to share a similar mode of antimicrobial action. Another study found that 4-MSITC and PhEITC inhibited DNA/RNA synthesis in various Gram<sup>−</sup> and Gram<sup>+</sup> bacteria.<sup>115</sup> Thioredoxin reductase, an enzyme required for DNA synthesis, could be inhibited by ITCs, as shown in an *in vitro* study.<sup>114</sup> Furthermore, ITCs might elevate ROS levels in *Bacillus* by reacting with low-molecular-weight (LMW) thiol molecules, e.g. bacillithiol (BSH, an analogue GSH in *Bacillus*) and/or other LMW thiol molecules. These LMW thiol molecules are responsible for keeping the redox balance inside the cells.<sup>126,137</sup> Overall, dithiocarbamation (**Figure 6.4A**) seems to be the mechanism of ITCs reacting with microbial targets. This needs to be substantiated in future studies, including *in vivo* studies.



**Figure 6.5.** ROS generation in *B. cereus* ATCC14579 upon exposure to ITCs at MIC for 9-MSolITC (25 μg/mL) and 9-MSITC (50 μg/mL), and 200 μg/mL for 9-MTITC (MIC > 200 μg/mL), relative to the negative control (inoculum without ITCs or antimicrobials). The measurement was performed after 24 h incubation at 30 °C in nucleophile-rich TSB. The ROS generation assay was performed according to the instructions provided by Abcam (Cambridge, UK).

## 6.4. Prospects

### 6.4.1. Brassicaceae seeds as source of natural preservatives

The seeds of Brassicaceae are of interest as source of natural preservatives. *B. oleracea* (broccoli), one of the most widely studied *Brassica* species, is rich in short-chained MSGSL, particularly C4.<sup>138–143</sup> *C. sativa* (German sesame) is rich in long-chained MSGSL, particularly C9–11.<sup>84,104,144</sup> *Erysimum allionii* (wallflower) is rich in short-chained MSoGSL, particularly C3–4,<sup>68</sup> whereas *Rorippa indica* (yellowcress) is rich in long-chained MSoGSL, particularly C8–9.<sup>145</sup> Based on results in **Chapters 4** and **5**, *B. oleracea* and *E. allionii* can be potential sources for natural preservatives against Gram<sup>−</sup> bacteria, Gram<sup>+</sup> bacteria, and fungi, whereas *C. sativa* and *R. indica* can be potential sources for natural preservatives against Gram<sup>+</sup> bacteria and fungi.

### 6.4.2. Types of application

Based on findings in **Chapters 3** and **4**, the application of ITCs should consider their reactivity towards thiol groups (including Cys) as well as other amino-acid nucleophiles in the matrix. This reactivity is affected by pH and temperature. Low pH and temperature are beneficial for the stability of ITCs. Food products with low pH and stored in a refrigerator, such as fruit juices and tomato sauces, would be best suited for application of ITCs. Conditions with relatively low content of protein, peptides, and amino acids, e.g. the aforementioned fruit-based products, would be more suitable for ITCs than conditions with relatively high content of such components, e.g. legume seeds and animal-based products.<sup>146</sup> The concentration of ITCs required to warrant their effective antimicrobial activity must overcome the influence of the background concentration of thiol groups and other nucleophiles.

ITCs might be suitable for prolonging the open shelf life (i.e. secondary shelf life<sup>147</sup>) of food products. Once the products are opened and microorganisms start to grow, ITCs can exert their antimicrobial activity. Under the microbial physiological pH, ITCs can readily react with their microbial targets.

### 6.4.3. Pungency, bitterness, and toxicity of ITCs

The application of ITCs in food products should be done with caution because of their pungency<sup>148-149</sup> and toxicity,<sup>150-151</sup> whereas the application of the GSL precursors and myrosinase should be employed with caution because of GSL bitterness.<sup>152-154</sup> TRPA1 (transient receptor potential ankyrin 1), responsible for pungency, was *in vitro* activated by alkenyl ITCs, MTITCs, and benzenic ITCs (EC<sub>50</sub> 0.25-0.58  $\mu$ M, equal to 37-110  $\mu$ g/mL, which was within the range of concentrations where moderate antimicrobials exert their activity).<sup>149</sup> The -N=C=S moiety was likely the predominant contributor to TRPA1-activating ability of ITCs.<sup>149</sup> It is speculated that the most antimicrobial ITC subclasses (i.e. MSITC and MSoITC, **Chapters 4** and **5**) have an EC<sub>50</sub> for the *in vitro* activation of TRPA1 within the range of that of other ITC subclasses. Organoleptic tests of ITCs in food application should be performed to evaluate whether or not ITCs in food application are perceived to be pungent and, thus, hinder or support their application. Allyl GSL, 3-butenyl GSL, are associated with bitter taste of *Brassica* vegetables,<sup>152-154</sup> whereas other GSLs, e.g. 4-MSGSL, are consistently noted for the lack of association with bitter taste.<sup>155-157</sup> Therefore, it is speculated that the application of MSGSLs and MSoGSLs as the source of potential antimicrobial MSITCs and MSoITCs would not be hindered by bitterness.

Based on a previous study in rats, a no-observed-adverse-effect level (NOAEL) for AITC was defined as 12 mg/kg body weight (bw)/day.<sup>158</sup> The mean daily total exposure to AITC from natural occurrence in food, used as a flavoring agent and as an antimicrobial agent, is estimated to be 0.027-0.084 mg/kg bw/day,<sup>159</sup> which is more than 140 fold lower than the NOAEL. This indicates that AITC can be considered safe as a natural food preservative. Some other ITCs, e.g. BITC and P-



DiITC (a bifunctional ITC studied in **Chapter 5**), were found to be at least 4 times more toxic than AITC.<sup>150-151</sup> Furthermore, the toxic dose of 4-MSITC in mice was relatively high, i.e. 192 mg/kg bw.<sup>160</sup> With the findings in **Chapter 5** (MIC of 4-MSITC in nucleophile-poor growth media was 25 µg/mL against *B. cereus* and 50 µg/mL against *E. coli*), if 4-MSITC would be applied as antimicrobial agent at 50 µg/mL, this concentration is translated to 50 µg/g food product. Assuming that the food product is fruit juice and one portion is one cup (250 g), if one consumes 1 cup of fruit juice, the intake of 4-MSITC would be 12.5 mg. Assuming the body weight of 60 kg, the concentration of 4-MSITC taken up was 0.21 mg/kg bw, which is far (> 900 fold) below the toxic dose. It can be speculated that MSITCs, as well as MSoITCs, would be safe antimicrobial candidates for food preservatives.

#### 6.4.4. Potential synergism with other antimicrobial compounds

In addition to the potential application of ITCs as food preservatives, ITCs might have potential in clinical applications. Combination of different antimicrobial compounds with different mode of action is a strategy to combat diseases caused by microorganisms. Among the few studies on the use of ITCs in combination with traditional antibiotics against Gram<sup>-</sup> and Gram<sup>+</sup> bacteria,<sup>161-164</sup> only one study<sup>162</sup> clearly reported synergism (fractional inhibitory concentration index, FICI < 0.36) between the ITC (i.e. AITC) and the antibiotics (i.e. ampicillin, erythromycin, bacitracin) against Gram<sup>-</sup> *S. Typhimurium* and Gram<sup>+</sup> *Streptococcus pyogenes* and *S. aureus*. FICI characterizes interactions between antimicrobials (FICI ≤ 0.5 synergism, FICI > 0.5 additive, FICI > 1.0 indifferent, and FICI > 4.0 antagonism).<sup>165-166</sup> FICI is the sum of FIC of each antimicrobial. FIC of each antimicrobial is the ratio of MIC of the antimicrobial in combination to MIC of the antimicrobial alone.<sup>167-168</sup> The previous studies of combination of ITCs and antibiotics included only few ITCs, namely AITC, BITC, PhEITC, and *p*-OH-PhEITC. Further studies are needed to explore the potential synergism of the most active ITCs (MSITCs and MSoITCs, **Chapters 4** and **5**) with antibiotics against (antimicrobial resistant) pathogens. In addition to the potential synergism with antibiotics, ITCs might work synergistically with traditional food preservatives, such as sorbic acid. The widely known mode of action of sorbic acid is the reduction of intracellular pH.<sup>169-170</sup> Sorbic acid can be an effective antimicrobial under acidic pH conditions up to pH 6.5.<sup>170</sup>

In conclusion, the low MIC values, broad spectrum of activity, and presumed low toxicity of ITCs suggest that ITCs are potential natural antimicrobial compounds. The mode of action of ITCs needs to be revealed. Moreover, the potential synergisms with antibiotics as well as other food preservatives are intriguing topics for future studies. Additionally, due to the "well-known" pungent character of ITCs, sensory evaluation of ITCs in real food application needs to be thoroughly done.

## 6.5. References

1. Blažević, I.; Montaut, S.; Burčul, F.; Olsen, C. E.; Burow, M.; Rollin, P.; Agerbirk, N., Glucosinolate structural diversity, identification, chemical synthesis and metabolism in plants. *Phytochemistry* **2020**, *169*, 112100.
2. Budnowski, J.; Hanschen, F. S.; Lehmann, C.; Haack, M.; Brigelius-Flohé, R.; Kroh, L. W.; Blaut, M.; Rohn, S.; Hanske, L., A derivatization method for the simultaneous detection of glucosinolates and isothiocyanates in biological samples. *Anal. Biochem.* **2013**, *441*, 199-207.
3. Gonda, S.; Kiss-Szikszai, A.; Szűcs, Z.; Nguyen, N. M.; Vasas, G., Myrosinase compatible simultaneous determination of glucosinolates and allyl isothiocyanate by capillary electrophoresis micellar electrokinetic chromatography (CE-MEKC). *Phytochem. Anal.* **2016**, *27*, 191-198.
4. Tsao, R.; Yu, Q.; Potter, J.; Chiba, M., Direct and simultaneous analysis of sinigrin and allyl isothiocyanate in mustard samples by high-performance liquid chromatography. *J. Agric. Food Chem.* **2002**, *50*, 4749-53.
5. Vastenhout, K. J.; Tornberg, R. H.; Johnson, A. L.; Amolins, M. W.; Mays, J. R., High-performance liquid chromatography-based method to evaluate kinetics of glucosinolate hydrolysis by *Sinapis alba* myrosinase. *Anal. Biochem.* **2014**, *465*, 105-113.
6. Lee, J. G.; Bonnema, G.; Zhang, N.; Kwak, J. H.; de Vos, R. C.; Beekwilder, J., Evaluation of glucosinolate variation in a collection of turnip (*Brassica rapa*) germplasm by the analysis of intact and desulfo glucosinolates. *J Agric Food Chem* **2013**, *61* (16), 3984-93.
7. Kiontke, A.; Oliveira-Birkmeier, A.; Opitz, A.; Birkemeyer, C., Electrospray ionization efficiency is dependent on different molecular descriptors with respect to solvent pH and instrumental configuration. *PLoS ONE* **2016**, *11*, e0167502-e0167502.
8. Scalbert, A.; Brennan, L.; Fiehn, O.; Hankemeier, T.; Kristal, B. S.; van Ommen, B.; Pujos-Guillot, E.; Verheij, E.; Wishart, D.; Wopereis, S., Mass-spectrometry-based metabolomics: limitations and recommendations for future progress with particular focus on nutrition research. *Metabolomics* **2009**, *5*, 435-458.
9. Clarke, D. B., Glucosinolates, structures and analysis in food. *Anal. Methods* **2010**, *2*, 310-325.
10. Wathelet, J. P.; Iori, R.; Leoni, O.; Rollin, P.; Quinsac, A.; Palmieri, S., Guidelines for glucosinolate analysis in green tissues used for biofumigation. *Agroindustria* **2004**, *3*, 257-266.
11. Matthäus, B.; Fiebig, H. J., Simultaneous determination of isothiocyanates, indoles, and oxazolidinethiones in myrosinase digests of rapeseeds and rapeseed meal by HPLC. *J. Agric. Food Chem.* **1996**, *44*, 3894-3899.
12. Fahey, J. W.; Zalcmann, A. T.; Talalay, P., The chemical diversity and distribution of glucosinolates and isothiocyanates among plants. *Phytochemistry* **2001**, *56*, 5-51.
13. Agerbirk, N.; Olsen, C. E., Glucosinolate structures in evolution. *Phytochemistry* **2012**, *77*, 16-45.
14. Spinks, E. A.; Sones, K.; Fenwick, G. R., The quantitative analysis of glucosinolates in cruciferous vegetables, oilseeds and forage crops using high performance liquid chromatography. *Fette, Seifen, Anstrichm.* **1984**, *86*, 228-231.
15. Chen, C.-W.; Ho, C.-T., Thermal degradation of allyl isothiocyanate in aqueous solution. *J. Agric. Food Chem.* **1998**, *46*, 220-223.
16. Chiang, W. C. K.; Pusateri, D. J.; Leitz, R. E. A., Gas chromatography/mass spectrometry method for the determination of sulforaphane and sulforaphane nitrile in broccoli. *J. Agric. Food Chem.* **1998**, *46*, 1018-1021.
17. Ko, M. O.; Kim, M. B.; Lim, S. B., Relationship between chemical structure and antimicrobial activities of isothiocyanates from cruciferous vegetables against oral pathogens. *J. Microbiol. Biotechnol.* **2016**, *26*, 2036-2042.

18. Nowicki, D.; Rodzik, O.; Herman-Antosiewicz, A.; Szalewska-Palasz, A., Isothiocyanates as effective agents against enterohemorrhagic *Escherichia coli*: Insight to the mode of action. *Sci. Rep.* **2016**, *6*, 22263.
19. Oxoid Oxoid - Product detail: Laboratory preparations/biological extracts. [http://www.oxoid.com/UK/blue/prod\\_detail/prod\\_detail.asp?pr=LP0037&c=UK&lang=EN&minfo=Y&sec=1](http://www.oxoid.com/UK/blue/prod_detail/prod_detail.asp?pr=LP0037&c=UK&lang=EN&minfo=Y&sec=1) (accessed 17 February 2020).
20. Sezonov, G.; Joseleau-Petit, D.; D'Ari, R., *Escherichia coli* physiology in Luria-Bertani broth. *J. Bacteriol.* **2007**, *189*, 8746-8749.
21. Misra, R.; Sahoo, S. K., Chapter four - Antibacterial activity of doxycycline-loaded nanoparticles. In *Methods in Enzymology*, Düzgünes, N., Ed. Academic Press: **2012**; Vol. 509, pp 61-85.
22. Wagenlehner, F. M. E.; Kinzig-Schippers, M.; Sörgel, F.; Weidner, W.; Naber, K. G., Concentrations in plasma, urinary excretion and bactericidal activity of levofloxacin (500mg) versus ciprofloxacin (500mg) in healthy volunteers receiving a single oral dose. *Int. J. Antimicrob. Agents* **2006**, *28*, 551-559.
23. Araya-Cloutier, C.; Vincken, J. P.; van Ederen, R.; den Besten, H. M. W.; Gruppen, H., Rapid membrane permeabilization of *Listeria monocytogenes* and *Escherichia coli* induced by antibacterial prenylated phenolic compounds from legumes. *Food Chem.* **2018**, *240*, 147-155.
24. Aryani, D. C.; den Besten, H. M. W.; Hazeleger, W. C.; Zwietering, M. H., Quantifying strain variability in modeling growth of *Listeria monocytogenes*. *Int. J. Food Microbiol.* **2015**, *208*, 19-29.
25. Biesta-Peters, E. G.; Reij, M. W.; Joosten, H.; Gorris, L. G. M.; Zwietering, M. H., Comparison of two optical-density-based methods and a plate count method for estimation of growth parameters of *Bacillus cereus*. *Appl. Environ. Microbiol.* **2010**, *76* (5), 1399-1405.
26. Lambert, R. J. W.; Bidlas, E., An investigation of the Gamma hypothesis: A predictive modelling study of the effect of combined inhibitors (salt, pH and weak acids) on the growth of *Aeromonas hydrophila*. *Int. J. Food Microbiol.* **2007**, *115*, 12-28.
27. de Bruijn, W. J. C.; Araya-Cloutier, C.; Bijlsma, J.; de Swart, A.; Sanders, M. G.; de Waard, P.; Gruppen, H.; Vincken, J.-P., Antibacterial prenylated stilbenoids from peanut (*Arachis hypogaea*). *Phytochem. Lett.* **2018**, *28*, 13-18.
28. Gibbons, S., Anti-staphylococcal plant natural products. *Nat. Prod. Rep.* **2014**, *21*, 263-277.
29. Araya-Cloutier, C.; Vincken, J.-P.; van de Schans, M. G. M.; Hageman, J.; Schaftenaar, G.; den Besten, H. M. W.; Gruppen, H., QSAR-based molecular signatures of prenylated (iso)flavonoids underlying antimicrobial potency against and membrane-disruption in Gram-positive and Gram-negative bacteria. *Sci. Rep.* **2018**, *8*, 9267.
30. Kurepina, N.; Kreiswirth, B. N.; Mustaev, A., Growth-inhibitory activity of natural and synthetic isothiocyanates against representative human microbial pathogens. *J. Appl. Microbiol.* **2013**, *115*, 943-954.
31. CLSI, *Methods for dilution antimicrobial susceptibility test for bacteria that grow aerobically; approved standard - 9th edition*. Clinical and Laboratory Standard Institute: Wayne, PA, USA, **2012**.
32. Wilson, A. E.; Bergaentzlé, M.; Bindler, F.; Marchioni, E.; Lintz, A.; Ennahar, S., In vitro efficacies of various isothiocyanates from cruciferous vegetables as antimicrobial agents against foodborne pathogens and spoilage bacteria. *Food Control* **2013**, *30*, 318-324.
33. Hanschen, F. S.; Klopsch, R.; Oliviero, T.; Schreiner, M.; Verkerk, R.; Dekker, M., Optimizing isothiocyanate formation during enzymatic glucosinolate breakdown by adjusting pH value, temperature and dilution in *Brassica* vegetables and *Arabidopsis thaliana*. *Sci. Rep.* **2017**, *7*, 40807.
34. Bones, A. M.; Rossiter, J. T., The enzymic and chemically induced decomposition of glucosinolates. *Phytochemistry* **2006**, *67*, 1053-1067.

35. Liang, H.; Yuan, Q. P.; Dong, H. R.; Liu, Y. M., Determination of sulforaphane in broccoli and cabbage by high-performance liquid chromatography. *J. Food Compos. Anal.* **2006**, *19*, 473-476.
36. Matusheski, N. V.; Swarup, R.; Juvik, J. A.; Mithen, R.; Bennett, M.; Jeffery, E. H., Epithiospecifier protein from broccoli (*Brassica oleracea* L. ssp. *italica*) inhibits formation of the anticancer agent sulforaphane. *J. Agric. Food Chem.* **2006**, *54*, 2069-76.
37. Wilson, E. A.; Ennahar, S.; Zhao, M.; Bergaentzle, M.; Marchioni, E.; Bindler, F., Simultaneous determination of various isothiocyanates by RP-LC following precolumn derivatization with mercaptoethanol. *Chromatographia* **2011**, *73*, 137-142.
38. Wittstock, U.; Burow, M., Glucosinolate breakdown in *Arabidopsis*: Mechanism, regulation and biological significance. *The Arabidopsis Book / American Society of Plant Biologists* **2010**, *8*, e0134.
39. Anjum, N. A.; Umar, S.; Iqbal, M.; Ahmad, I.; Pereira, M. E.; Khan, N. A., Protection of growth and photosynthesis of *Brassica juncea* genotype with dual type sulfur transport system against sulfur deprivation by coordinate changes in the activities of sulfur metabolism enzymes and cysteine and glutathione production. *Russ. J. Plant Physiol.* **2011**, *58*, 892.
40. Ruiz, J. M.; Blumwald, E., Salinity-induced glutathione synthesis in *Brassica napus*. *Planta* **2002**, *214*, 965-9.
41. Bowden, N. A.; Sanders, J. P. M.; Bruins, M. E., Solubility of the proteinogenic  $\alpha$ -amino acids in water, ethanol, and ethanol-water mixtures. *J. Chem. Eng. Data* **2018**, *63*, 488-497.
42. Araya-Cloutier, C.; den Besten, H. M. W.; Aisyah, S.; Gruppen, H.; Vincken, J.-P., The position of prenylation of isoflavonoids and stilbenoids from legumes (Fabaceae) modulates the antimicrobial activity against Gram-positive pathogens. *Food Chem.* **2017**, *226*, 193-201.
43. Fu, L.; Lu, W. Q.; Zhou, X. M., Phenolic compounds and *in vitro* antibacterial and antioxidant activities of three tropic fruits: persimmon, guava, and sweetsop. *BioMed Res. Int.* **2016**, *2016*, 4287461.
44. van de Vel, E.; Sampers, I.; Raes, K., A review on influencing factors on the minimum inhibitor concentration of essential oils. *Crit. Rev. Food Sci. Nutr.* **2019**, *59*, 357-378.
45. Gramatica, P., Principles of QSAR models validation: internal and external. *QSAR Comb. Sci.* **2007**, *26*, 694-701.
46. Gramatica, P., On the development and validation of QSAR models. *Methods Mol. Biol.* **2013**, *930*, 499-526.
47. Tropsha, A., Best practices for QSAR model development, validation, and exploitation. *Mol. Inf.* **2010**, *29*, 476-488.
48. Roy, K.; Kar, S.; Ambure, P., On a simple approach for determining applicability domain of QSAR models. *Chemom. Intell. Lab. Syst.* **2015**, *145*, 22-29.
49. Ibrahim, N.; Allart-Simon, I.; De Nicola, G. R.; Iori, R.; Renault, J.-H.; Rollin, P.; Nuzillard, J.-M., Advanced NMR-based structural investigation of glucosinolates and desulfoglucosinolates. *J. Nat. Prod.* **2018**, *81*, 323-334.
50. Kuszniereicz, B.; Iori, R.; Piekarska, A.; Namiesnik, J.; Bartoszek, A., Convenient identification of desulfoglucosinolates on the basis of mass spectra obtained during liquid chromatography-diode array-electrospray ionisation mass spectrometry analysis: method verification for sprouts of different Brassicaceae species extracts. *J. Chromatogr. A* **2013**, *1278*, 108-15.
51. Olsen, C. E.; Huang, X.-C.; Hansen, C. I. C.; Cipollini, D.; Ørgaard, M.; Matthes, A.; Geu-Flores, F.; Koch, M. A.; Agerbirk, N., Glucosinolate diversity within a phylogenetic framework of the tribe *Cardamineae* (Brassicaceae) unraveled with HPLC-MS/MS and NMR-based analytical distinction of 70 desulfoglucosinolates. *Phytochemistry* **2016**, *132*, 33-56.

52. Sodhi, Y. S.; Mukhopadhyay, A.; Arumugam, N.; Verma, J. K.; Gupta, V.; Pental, D.; Pradhan, A. K., Genetic analysis of total glucosinolate in crosses involving a high glucosinolate Indian variety and a low glucosinolate line of *Brassica juncea*. *Plant Breed.* **2002**, *121*, 508-511.
53. Borgen, B. H.; Thangstad, O. P.; Ahuja, I.; Rossiter, J. T.; Bones, A. M., Removing the mustard oil bomb from seeds: transgenic ablation of myrosin cells in oilseed rape (*Brassica napus*) produces MINELESS seeds. *J. Exp. Bot.* **2010**, *61*, 1683-1697.
54. Kjær, A.; Jensen, R. B., Isothiocyanates III. The volatile of isothiocyanates in seeds of rape (*Brassica napus* L.). *Acta Chem. Scand.* **1953**, *7*, 1271-1275.
55. Kjær, A. J., R. B., Isothiocyanates XX. 4-Pentenyl isothiocyanate, a new mustard oil occurring as a glucoside (glucobrassicinapin) in nature. *Acta Chem. Scand.* **1956**, *10*, 1356-1371.
56. Millán, S.; Sampedro, M. C.; Gallejones, P.; Castellón, A.; Ibargoitia, M. L.; Goicolea, M. A.; Barrio, R. J., Identification and quantification of glucosinolates in rapeseed using liquid chromatography-ion trap mass spectrometry. *Anal. Bioanal. Chem.* **2009**, *394*, 1661-1669.
57. Kjær, A.; Gmelin, R.; Larsen, I., Isothiocyanates XII. 3-Methylthiopropyl isothiocyanate (ibervirin), a new naturally occurring mustard oil. *Acta Chem. Scand.* **1955**, *9*, 1143-1147.
58. Kjær, A.; Gmelin, R., Isothiocyanates XI. 4-Methylthiobutyl isothiocyanate, a new naturally occurring mustard oil. *Acta Chem. Scand.* **1955**, *9*, 542-544.
59. Leoni, O.; Iori, R.; Palmieri, S.; Esposito, E.; Menegatti, E.; Cortesi, R.; Nastruzzi, C., Myrosinase-generated isothiocyanate from glucosinolates: isolation, characterization and *in vitro* antiproliferative studies. *Bioorg. Med. Chem.* **1997**, *5*, 1799-806.
60. Maldini, M.; Foddai, M.; Natella, F.; Petretto, G. L.; Rourke, J. P.; Chessa, M.; Pintore, G., Identification and quantification of glucosinolates in different tissues of *Raphanus raphanistrum* by liquid chromatography tandem-mass spectrometry. *J. Food Compos. Anal.* **2017**, *61*, 20-27.
61. Montaut, S.; Montagut-Romans, A.; Chiari, L.; Benson, H. J., Glucosinolates in *Draba borealis* DC. (Brassicaceae) in a taxonomic perspective. *Biochem. Syst. Ecol.* **2018**, *78*, 31-34.
62. Blažević, I.; Radonić, A.; Mastelić, J.; Zekić, M.; Skočibušić, M.; Maravić, A., Glucosinolates, glycosidically bound volatiles and antimicrobial activity of *Aurinia sinuata* (Brassicaceae). *Food Chem.* **2010**, *121*, 1020-1028.
63. De Nicola, G. R.; Blažević, I.; Montaut, S.; Rollin, P.; Mastelić, J.; Iori, R.; Tatibouët, A., Glucosinolate distribution in aerial parts of *Degenia velebitica*. *Chem. Biodiversity* **2011**, *8*, 2090-2096.
64. Kjær, A.; Larsen, I.; Gmelin, R., Isothiocyanates XIV. 5-Methylthiopentyl isothiocyanate, a new mustard oil present in nature as a glucoside (glucoberteroin). *Acta Chem. Scand.* **1955**, *9*, 1311-1316.
65. Daxenbichler, M.; Van Etten, C.; Wolff, I., Notes-Identification of a new, naturally occurring, steam-volatile isothiocyanate from *Lesquerella lasiocarpa* seed. *J. Org. Chem.* **1961**, *26*, 4168-4169.
66. Ina, K.; Ina, H.; Ueda, M.; Yagi, A.; Kishima, I.,  $\omega$ -Methylthioalkyl isothiocyanates in wasabi. *Agric. Biol. Chem.* **1989**, *53*, 537-538.
67. Vaughn, S. F.; Berhow, M. A., Glucosinolate hydrolysis products from various plant sources: pH effects, isolation, and purification. *Ind. Crops Prod.* **2005**, *21*, 193-202.
68. Bennett, R. N.; Mellon, F. A.; Kroon, P. A., Screening crucifer seeds as sources of specific intact glucosinolates using ion-pair high-performance liquid chromatography negative ion electrospray mass spectrometry. *J. Agric. Food Chem.* **2004**, *52*, 428-38.
69. Hasapis, X.; J. MacLeod, A.; Moreau, M., Glucosinolates of nine Cruciferae and two Capparaceae species. *Phytochemistry* **1981**, *20*, 2355-2358.

70. Ciska, E.; Martyniak-Przybyszewska, B.; Kozłowska, H., Content of glucosinolates in cruciferous vegetables grown at the same site for two years under different climatic conditions. *J. Agric. Food Chem.* **2000**, *48*, 2862-7.
71. Jaki, B.; Sticher, O.; Veit, M.; Fröhlich, R.; Pauli, G. F., Evaluation of glucoiberin reference material from *Iberis amara* by spectroscopic fingerprinting. *J. Nat. Prod.* **2002**, *65*, 517-522.
72. Kore, A. M.; Spencer, G. F.; Wallig, M. A., Purification of the  $\omega$ -(methylsulfinyl)alkyl glucosinolate hydrolysis products: 1-isothiocyanato-3-(methylsulfinyl)propane, 1-isothiocyanato-4-(methylsulfinyl)butane, 4-(methylsulfinyl)butanenitrile, and 5-(methylsulfinyl)pentanenitrile from broccoli and *Lesquerella fendleri*. *J. Agric. Food Chem.* **1993**, *41*, 89-95.
73. Schultz, O.-E.; Gmelin, R., Das Senföglglukosid „Glukoiberin“ und der Bitterstoff „Ibamarin“ von *Iberis amara* L. (Schleifenblume). IX. Mitteilung über Senföglglukoside. *Arch. Pharm.* **1954**, *287*, 404-411.
74. Kiddle, G.; Bennett, R. N.; Botting, N. P.; Davidson, N. E.; Robertson, A. A. B.; Wallsgrove, R. M., High-performance liquid chromatographic separation of natural and synthetic desulphoglucosinolates and their chemical vadation by UV, NMR and chemical ionisation-MS methods. *Phytochem. Anal.* **2001**, *12*, 226-242.
75. Procházka, Ž., Isolation of sulforaphane from hoare cress (*Lepidium draba* L.). *Collect. Czech. Chem. Commun.* **1959**, *24*, 2429-2430.
76. Etoh, H.; Nishimura, A.; Takasawa, R.; Yagi, A.; Saito, K.; Sakata, K.; Kishima, I.; Ina, K.,  $\omega$ -Methylsulfinylalkyl isothiocyanates in wasabi, *Wasabia japonica* Matsum. *Agric. Biol. Chem.* **1990**, *54*, 1587-1589.
77. Kjær, A.; Gmelin, R., Isothiocyanates XIX. L(-)-5-Methylsulphinylpentyl isothiocyanate, the aglucone of a new naturally occurring glucoside (glucoalyssin). *Acta Chem. Scand.* **1956**, *10*, 1100-1110.
78. Schultz, O.-E.; Wagner, W., Glucoalyssin, ein neues Senföglglukosid aus *Alyssum*-Arten. *Z. Naturforsch. B* **1956**, *11*, 417.
79. Song, L.; Iori, R.; Thornalley, P. J., Purification of major glucosinolates from Brassicaceae seeds and preparation of isothiocyanate and amine metabolites. *J. Sci. Food Agric.* **2006**, *86*, 1271-1280.
80. Christensen, B. W.; Kjær, A., A mustard oil of *Hesperis matronalis* seed, 6-methylsulphinylhexyl isothiocyanate. *Acta Chem. Scand.* **1963**, 846-847.
81. Montaut, S.; Grandbois, J.; Righetti, L.; Barillari, J.; Iori, R.; Rollin, P., Updated glucosinolate profile of *Dithyrea wislizenii*. *J. Nat. Prod.* **2009**, *72*, 889-893.
82. Kjær, A. C., B., Isothiocyanates XXX. Glucohirsutin, a new naturally occurring glucoside furnishing 8-methylsulphinyl-octyl isothiocyanate on enzymic hydrolysis. *Acta Chem. Scand.* **1958**, *12*, 833-838.
83. Yamane, A.; Fujikura, J.; Ogawa, H.; Mizutani, J., Isothiocyanates as alleopathic compounds from *Rorippa indica* Hiern. (Cruciferae) roots. *J. Chem. Ecol.* **1992**, *18*, 1941-1954.
84. Berhow, M. A.; Polat, U.; Glinski, J. A.; Glensk, M.; Vaughn, S. F.; Isbell, T.; Ayala-Diaz, I.; Marek, L.; Gardner, C., Optimized analysis and quantification of glucosinolates from *Camelina sativa* seeds by reverse-phase liquid chromatography. *Ind. Crops Prod.* **2013**, *43*, 119-125.
85. Kjær, A.; Gmelin, R., Isothiocyanates XXIII. L(-)-9-Methylsulphinylnonyl isothiocyanate, a new mustard oil present as a glucoside (glucoarabin) in *Arabis* species. *Acta Chem. Scand.* **1956**, *10*, 1358-1359.
86. Iori, R.; Barillari, J.; Gallienne, E.; Bilardo, C.; Tatibouët, A.; Rollin, P., Thio-functionalised glucosinolates: Unexpected transformation of desulfoglucoraphenin. *Tetrahedron Lett.* **2008**, *49*, 292-295.
87. Kim, K. H.; Moon, E.; Kim, S. Y.; Choi, S. U.; Lee, J. H.; Lee, K. R., 4-Methylthio-butanyl derivatives from the seeds of *Raphanus sativus* and their biological evaluation on anti-inflammatory and antitumor activities. *J. Ethnopharmacol.* **2014**, *151*, 503-508.

88. Schmid, H.; Karrer, P., Über Inhaltsstoffe des Rettichs I. Über Sulforaphen, ein Senföl aus Rettichsamen (*Raphanus sativus* L. var. *alba*). *Helv. Chim. Acta* **1948**, *31*, 1017-1028.
89. Huang, X.; Renwick, J. A. A.; Sachdev-Gupta, K., A chemical basis for differential acceptance of *Erysimum cheiranthoides* by two *Pieris* species. *J. Chem. Ecol.* **1993**, *19*, 195-210.
90. Emam, S. S.; El-Moaty, H. I. A., Glucosinolates, phenolic acids and anthraquinones of *Isatis microcarpa* Boiss and *Pseuderucaria clavate* (Boiss&Reut.) family: Cruciferae. *J. Appl. Sci. Res.* **2009**, *5*, 2315-2322.
91. Rodman, J. E.; Chew, F. S., Phytochemical correlates of herbivory in a community of native and naturalized Cruciferae. *Biochem. Syst. Ecol.* **1980**, *8*, 43-50.
92. Agerbirk, N.; De Vos, M.; Kim, J. H.; Jander, G., Indole glucosinolate breakdown and its biological effects. *Phytochem. Rev.* **2008**, *8*, 101-120.
93. Daxenbichler, M. E.; Spencer, G. F.; Carlson, D. G.; Rose, G. B.; Brinker, A. M.; Powell, R. G., Glucosinolate composition of seeds from 297 species of wild plants. *Phytochemistry* **1991**, *30*, 2623-2638.
94. Fabre, N.; Bon, M.; Moulis, C.; Fouraste, I.; Stanislas, E., Three glucosinolates from seeds of *Brassica juncea*. *Phytochemistry* **1997**, *45*, 525-527.
95. Agerbirk, N.; Warwick, S. I.; Hansen, P. R.; Olsen, C. E., Sinapis phylogeny and evolution of glucosinolates and specific nitrile degrading enzymes. *Phytochemistry* **2008**, *69*, 2937-2949.
96. Kjær, A.; Larsen, I., Isothiocyanates IX. The occurrence of ethyl isothiocyanate in nature. *Acta Chem. Scand.* **1954**, *8*, 699-701.
97. Puntambekar, S. V., Mustard oils and mustard oil glucosides occurring in the seed kernels of *Putranjiva roxburghii* Wall. *Proceedings of the Indian Academy of Sciences - Section A* **1950**, *32*, 114-122.
98. Dauvergne, X.; Cérantola, S.; Salaün, S.; Magné, C.; Kervarec, N.; Bessières, M.-A.; Deslandes, E., General occurrence of the glucosinolate glucocochlearin within the Cochlearia genus. *Carbohydr. Res.* **2006**, *341*, 2166-2169.
99. Kjær, A.; Wagnières, W., 3-Methyl-3-butenylglucosinolate, a new isothiocyanate-producing thioglucoside. *Acta Chem. Scand.* **1965**, *19*, 1989-1991.
100. Reichelt, M.; Brown, P. D.; Schneider, B.; Oldham, N. J.; Stauber, E.; Tokuhisa, J.; Kliebenstein, D. J.; Mitchell-Olds, T.; Gershenzon, J., Benzoic acid glucosinolate esters and other glucosinolates from *Arabidopsis thaliana*. *Phytochemistry* **2002**, *59*, 663-71.
101. Agerbirk, N.; Olsen, C. E.; Cipollini, D.; Ørgaard, M.; Linde-Laursen, I.; Chew, F. S., Specific glucosinolate analysis reveals variable levels of epimeric glucobarbarins, dietary precursors of 5-phenyloxazolidine-2-thiones, in watercress types with contrasting chromosome numbers. *J. Agric. Food Chem.* **2014**, *62*, 9586-9596.
102. Gmelin, R.; Kjær, A.; Schuster, A.; Larsen, E.; Shimizu, A., Glucosinolates in seeds of *Sibara virginica* (L.) Rollins: Two new glucosinolates. *Acta Chem. Scand.* **1970**, *3031*-3037.
103. Spencer, G. F.; Daxenbichler, M. E., Gas chromatography-mass spectrometry of nitriles, isothiocyanates and oxazolidinethiones derived from cruciferous glucosinolates. *J. Sci. Food Agric.* **1980**, *31*, 359-367.
104. Kjær, A. G., R.; Jensen, R. B., Isothiocyanates XXI. (-)-10-Methylsulphinyldodecyl isothiocyanate, a new mustard oil present as a glucoside (glucocamelinin) in *Camelina* species. *Acta Chem. Scand.* **1956**, *10*, 1614-1619.
105. Kjær, A.; Schuster, A., Glucosinolates in seeds of *Neslia paniculata*. *Phytochemistry* **1972**, *11*, 3045-3048.
106. Barillari, J.; Cervellati, R.; Paolini, M.; Tatibouët, A.; Rollin, P.; Iori, R., Isolation of 4-methylthio-3-butenyl glucosinolate from *Raphanus sativus* sprouts (Kaiware Daikon) and its redox properties. *J. Agric. Food Chem.* **2005**, *53*, 9890-9896.
107. Blažević, I.; Mastelić, J., Glucosinolate degradation products and other bound and free volatiles in the leaves and roots of radish (*Raphanus sativus* L.). *Food Chem.* **2009**, *113*, 96-102.

108. Friis, P.; Kjær, A., 4-Methylthio-3-butenyl isothiocyanate, the pungent principle of radish root. *Acta Chem. Scand.* **1966**, *20*, 698-705.
109. Visentin, M.; Tava, A.; Iori, R.; Palmieri, S., Isolation and identification for trans-4-(methylthio)-3-butenyl glucosinolate from radish roots (*Raphanus sativus* L.). *J. Agric. Food Chem.* **1992**, *40*, 1687-1691.
110. Kjær, A.; Thomsen, H.; Hansen, S. E., Isothiocyanates XXXVIII. Glucocapangulin, a novel isothiocyanate-producing glucoside. *Acta Chem. Scand.* **1960**, *14*, 1226-1227.
111. Kjær, A.; Schuster, A., Glucosinolates in seeds of *Arabis hirsuta* (L.) Scop.: Some new, naturally derived isothiocyanates. *Acta Chemica Scandinavica* **1972**, *26*, 8-14.
112. Dufour, V.; Stahl, M.; Baysse, C., The antibacterial properties of isothiocyanates. *Microbiology (Reading, England)* **2015**, *161*, 229-43.
113. Dufour, V.; Stahl, M.; Rosenfeld, E.; Stintzi, A.; Baysse, C., Insights into the mode of action of benzyl isothiocyanate on *Campylobacter jejuni*. *Appl. Environ. Microbiol.* **2013**, *79*, 6958-6968.
114. Luciano, F. B.; Holley, R. A., Enzymatic inhibition by allyl isothiocyanate and factors affecting its antimicrobial action against *Escherichia coli* O157:H7. *Int. J. Food Microbiol.* **2009**, *131*, 240-5.
115. Nowicki, D.; Maciąg-Dorszyńska, M.; Bogucka, K.; Szalewska-Pałasz, A.; Herman-Antosiewicz, A., Various modes of action of dietary phytochemicals, sulforaphane and phenethyl isothiocyanate, on pathogenic bacteria. *Sci. Rep.* **2019**, *9*, 13677.
116. Huang, H.; Hancock, R. E., The role of specific surface loop regions in determining the function of the imipenem-specific pore protein OprD of *Pseudomonas aeruginosa*. *J. Bacteriol.* **1996**, *178*, 3085-3090.
117. Mortimer, P. G. S.; Piddok, L. J. V., The accumulation of five antibacterial agents in porin-deficient mutants of *Escherichia coli*. *J. Antimicrob. Chemother.* **1993**, *32*, 195-213.
118. De Nobel, J. G.; Barnett, J. A., Passage of molecules through yeast cell walls: A brief essay-review. *Yeast (Chichester, England)* **1991**, *7*, 313-23.
119. Lambert, P. A., Cellular impermeability and uptake of biocides and antibiotics in Gram-positive bacteria and mycobacteria. *J. Appl. Microbiol.* **2002**, *92*, 46S-54S.
120. Gamet-Payraastre, L.; Li, P.; Lumeau, S.; Cassar, G.; Dupont, M. A.; Chevolleau, S.; Gasc, N.; Tulliez, J.; Tercé, F., Sulforaphane, a naturally occurring isothiocyanate, induces cell cycle arrest and apoptosis in HT29 human colon cancer cells. *Cancer Res.* **2000**, *60*, 1426-1433.
121. Xiao, D.; Lew, K. L.; Zeng, Y.; Xiao, H.; Marynowski, S. W.; Dhir, R.; Singh, S. V., Phenethyl isothiocyanate-induced apoptosis in PC-3 human prostate cancer cells is mediated by reactive oxygen species-dependent disruption of the mitochondrial membrane potential. *Carcinogenesis* **2006**, *27*, 2223-34.
122. Tang, L.; Zhang, Y., Mitochondria are the primary target in isothiocyanate-induced apoptosis in human bladder cancer cells. *Mol. Cancer Ther.* **2005**, *4*, 1250-1259.
123. Syed, A.; Arora, N.; Buch, T. A.; Smith, E. A., The role of a conserved membrane proximal cysteine in altering  $\alpha$ PS2C $\beta$ PS integrin diffusion. *Phys. Biol.* **2016**, *13*, 066005.
124. Mi, L.; Hood, B. L.; Stewart, N. A.; Xiao, Z.; Govind, S.; Wang, X.; Conrads, T. P.; Veenstra, T. D.; Chung, F. L., Identification of potential protein targets of isothiocyanates by proteomics. *Chem. Res. Toxicol.* **2011**, *24*, 1735-43.
125. Zhang, Y.; Talalay, P., Mechanism of differential potencies of isothiocyanates as inducers of anticarcinogenic phase 2 enzymes. *Cancer Res.* **1998**, *58*, 4632-9.
126. Imber, M.; Pietrzyk-Brzezinska, A. J.; Antelmann, H., Redox regulation by reversible protein S-thiolation in Gram-positive bacteria. *Redox Biol.* **2019**, *20*, 130-145.
127. Chapman, J. S.; Diehl, M. A., Methylchloroisothiazolone-induced growth inhibition and lethality in *Escherichia coli*. *J. Appl. Bacteriol.* **1995**, *78*, 134-141.



128. Collier, P. J.; Austin, P.; Gilbert, P., Isothiazolone biocides: enzyme-inhibiting pro-drugs. *Int. J. Pharm.* **1991**, *74*, 195-201.
129. Czechowski, M.; Rossmore, H. W., The effect of selected industrial biocides on lactate metabolism in *Desulfovibrio desulfuricans*. *Dev. Ind. Microbiol.* **1981**, *22*, 797-804.
130. Haack, T. K.; Diehl, M. A.; Chapman, J. S. *Proclin™ 300 preservative for diagnostic reagents technical bulletin*; Rohm and Haas Co., Inc.: Philadelphia, **1992**.
131. Williams, T. M., The mechanism of action of isothiazolone biocides. *PowerPlant Chem.* **2007**, *9*, 14-22.
132. Chen, M.; Mudhar, R. In *Antimicrobial activity of organic wood preservatives against bio-deterioration fungi: minimum inhibitory concentration (MIC) via SPIRAL GRADIENT ENDPOINT (SGE) test*, 2018 American Wood Protection Association Proceeding, **2018**; pp 95-102.
133. Karsa, D. R., F.2 - Biocides. In *Handbook for Cleaning/Decontamination of Surfaces*, Johansson, I.; Somasundaran, P., Eds. Elsevier Science B.V.: Amsterdam, **2007**; pp 593-623.
134. Luna, B. L.; Garcia, J. A.; Huang, M.; Ewing, P. J.; Valentine, S. C.; Chu, Y. M.; Ye, Q. Z.; Xu, H. H., Identification and characterization of novel isothiazolones with potent bactericidal activity against multi-drug resistant *Acinetobacter baumannii* clinical isolates. *Int. J. Antimicrob. Agents* **2019**, *53*, 474-482.
135. Rushton, L.; Sass, A.; Baldwin, A.; Dowson, C. G.; Donoghue, D.; Mahenthiralingam, E., Key role for efflux in the preservative susceptibility and adaptive resistance of *Burkholderia cepacia* complex bacteria. *Antimicrob. Agents Chemother.* **2013**, *57*, 2972-2980.
136. Weiser, R.; Green, A. E.; Bull, M. J.; Cunningham-Oakes, E.; Jolley, K. A.; Maiden, M. C. J.; Hall, A. J.; Winstanley, C.; Weightman, A. J.; Donoghue, D.; Amezcua, A.; Connor, T. R.; Mahenthiralingam, E., Not all *Pseudomonas aeruginosa* are equal: strains from industrial sources possess uniquely large multireplicon genomes. *Microb. Genom.* **2019**, *5*, e000276.
137. Poole, L. B., The basics of thiols and cysteines in redox biology and chemistry. *Free Radical Biol. Med.* **2015**, *80*, 148-157.
138. Baenas, N.; García-Viguera, C.; Moreno, D. A., Biotic elicitors effectively increase the glucosinolates content in Brassicaceae sprouts. *J. Agric. Food Chem.* **2014**, *62*, 1881-1889.
139. Baenas, N.; Marhuenda, J.; Garcia-Viguera, C.; Zafrilla, P.; Moreno, D. A., Influence of cooking methods on glucosinolates and isothiocyanates content in novel cruciferous foods. *Foods (Basel, Switzerland)* **2019**, *8*, 257.
140. Barrameda-Medina, Y.; Blasco, B.; Lentini, M.; Esposito, S.; Baenas, N.; Moreno, D. A.; Ruiz, J. M., Zinc biofortification improves phytochemicals and amino-acidic profile in *Brassica oleracea* cv. Bronco. *Plant Sci.* **2017**, *258*, 45-51.
141. Hanschen, F. S.; Schreiner, M., Isothiocyanates, Nitriles, and epithionitriles from glucosinolates are affected by genotype and developmental stage in *Brassica oleracea* varieties. *Front. Plant Sci.* **2017**, *8*, 1095-1095.
142. Hassini, I.; Baenas, N.; Moreno, D. A.; Carvajal, M.; Boughanmi, N.; Martinez Ballesta, M. D. C., Effects of seed priming, salinity and methyl jasmonate treatment on bioactive composition of *Brassica oleracea* var. capitata (white and red varieties) sprouts. *J. Sci. Food Agric.* **2017**, *97*, 2291-2299.
143. Wang, J.; Yu, H.; Zhao, Z.; Sheng, X.; Shen, Y.; Gu, H., Natural variation of glucosinolates and their breakdown products in broccoli (*Brassica oleracea* var. italica) seeds. *J. Agric. Food Chem.* **2019**, *67*, 12528-12537.
144. Das, N.; Berhow, M. A.; Angelino, D.; Jeffery, E. H., *Camelina sativa* defatted seed meal contains both alkyl sulfanyl glucosinolates and quercetin that synergize bioactivity. *J. Agric. Food Chem.* **2014**, *62*, 8385-91.
145. Lin, L. Z.; Sun, J.; Chen, P.; Zhang, R. W.; Fan, X. E.; Li, L. W.; Harnly, J. M., Profiling of glucosinolates and flavonoids in *Rorippa indica* (Linn.) Hiern. (Cruciferae) by UHPLC-PDA-ESI/HRMS(n). *J. Agric. Food Chem.* **2014**, *62*, 6118-29.

146. Self nutrition data - know what you eat. <https://nutritiondata.self.com/> (accessed 21 April 2020).
147. Villalobos-Delgado, L. H.; Nevárez-Moorillon, G. V.; Caro, I.; Quinto, E. J.; Mateo, J., Chapter 4 - Natural antimicrobial agents to improve foods shelf life. In *Food Quality and Shelf Life*, Galanakis, C. M., Ed. Academic Press: **2019**; pp 125-157.
148. Bell, L.; Oloyede, O. O.; Lignou, S.; Wagstaff, C.; Methven, L., Taste and flavor perceptions of glucosinolates, isothiocyanates, and related compounds. *Mol. Nutr. Food Res.* **2018**, 62, e1700990.
149. Terada, Y.; Masuda, H.; Watanabe, T., Structure-activity relationship study on isothiocyanates: Comparison of TRPA1-activating ability between allyl isothiocyanate and specific flavor components of wasabi, horseradish, and white mustard. *J. Nat. Prod.* **2015**, 78, 1937-41.
150. Masutomi, N.; Toyoda, K.; Shibutani, M.; Niho, N.; Uneyama, C.; Takahashi, N.; Hirose, M., Toxic effects of benzyl and allyl isothiocyanates and benzyl-isoform specific metabolites in the urinary bladder after a single intravesical application to rats. *Toxicol. Pathol.* **2001**, 29, 617-22.
151. Schultz, T. W.; Comeaux, J. L., Structure-toxicity relationships for aliphatic isothiocyanates to *Tetrahymena pyriformis*. *Bull. Environ. Contam. Toxicol.* **1996**, 56, 638-642.
152. Engel, E.; Baty, C.; Le Corre, D.; Souchon, I.; Martin, N., Flavor-active compounds potentially implicated in cooked cauliflower acceptance. *J. Agric. Food Chem.* **2002**, 50, 6459-67.
153. Fenwick, G. R.; Griffiths, N. M.; Heaney, R. K., Bitterness in brussels sprouts (*Brassica oleracea* L. var. gemmifera): The role of glucosinolates and their breakdown products. *J. Sci. Food Agric.* **1983**, 34, 73-80.
154. van Doorn, H. E.; van der Kruk, G. C.; van Holst, G.-J.; Raaijmakers-Ruijs, N. C. M. E.; Postma, E.; Groeneweg, B.; Jongen, W. H. F., The glucosinolates sinigrin and progoitrin are important determinants for taste preference and bitterness of Brussels sprouts. *J. Sci. Food Agric.* **1998**, 78, 30-38.
155. Baik, H.-Y.; Juvik, J. A.; Jeffery, E. H.; Wallig, M. A.; Kushad, M.; Klein, B. P., Relating glucosinolate content and flavor of broccoli cultivars. *J. Food Sci.* **2003**, 68, 1043-1050.
156. Bell, L.; Methven, L.; Wagstaff, C., The influence of phytochemical composition and resulting sensory attributes on preference for salad rocket (*Eruca sativa*) accessions by consumers of varying TAS2R38 diplotype. *Food Chem.* **2017**, 222 (Supplement C), 6-17.
157. Traka, M.; Mithen, R., Glucosinolates, isothiocyanates and human health. *Phytochem. Rev.* **2009**, 8, 269-282.
158. NTP Carcinogenesis bioassay of allyl isothiocyanate (CAS no. 57-06-7) in F344/N rats and B6C3F1 mice (gavage study) TR 234; U.S. Department of Health and Human Services, Public Health Service, National Institute of Health: **1982**.
159. EFSA, Scientific Opinion on the safety of allyl isothiocyanate for the proposed uses as a food additive. (EFSA), E. F. S. A., Ed. Parma, Italy, **2010**.
160. Socala, K.; Nieoczym, D.; Kowalczyk-Vasilev, E.; Wyska, E.; Wlaż, P., Increased seizure susceptibility and other toxicity symptoms following acute sulforaphane treatment in mice. *Toxicol. Appl. Pharmacol.* **2017**, 326, 43-53.
161. Freitas, E.; Aires, A.; de Santos Rosa, E. A.; Saavedra, M. J., Antibacterial activity and synergistic effect between watercress extracts, 2-phenylethyl isothiocyanate and antibiotics against 11 isolates of *Escherichia coli* from clinical and animal source. *Lett. Appl. Microbiol* **2013**, 57, 266-73.
162. Palaniappan, K.; Holley, R. A., Use of natural antimicrobials to increase antibiotic susceptibility of drug resistant bacteria. *Int. J. Food Microbiol.* **2010**, 140, 164-8.
163. Saavedra, M. J.; Borges, A.; Dias, C.; Aires, A.; Bennett, R. N.; Rosa, E. S.; Simoes, M., Antimicrobial activity of phenolics and glucosinolate hydrolysis products and their synergy with streptomycin against pathogenic bacteria. *Med. Chem.* **2010**, 6, 174-83.

164. Tajima, H.; Kimoto, H.; Taketo, A., Specific Antimicrobial synergism of synthetic hydroxy isothiocyanates with aminoglycoside antibiotics. *Biosci., Biotechnol., Biochem.* **2001**, *65*, 1886-1888.
165. Fujita, K.-I.; Kubo, I., Naturally occurring antifungal agents against *Zygosaccharomyces bailii* and their synergism. *J. Agric. Food Chem.* **2005**, *53*, 5187-5191.
166. Odds, F. C., Synergy, antagonism and what the checkerboard puts between them. *J. Antimicrob. Chemother.* **2003**, *52*, 1.
167. Pillai, S. K.; Moellering, R. C.; Eliopoulos, G. M., Antimicrobial combinations. In *Antibiotics in Laboratory Medicine*, Lorian, V., Ed. Lippincott Williams & Wilkins: Philadelphia, PA, **2005**; p 851.
168. Vigil, A. L.-M.; Palou, E.; Parish, M. E.; Davidson, P. M., Methods for activity assay and evaluation of results. In *Antimicrobials in Food*, Davidson, P. M.; Sofos, J. N.; Branen, A. L., Eds. Taylor and Francis: Boca Raton, FL, **2005**; pp 659-680.
169. Brul, S.; Coote, P., Preservative agents in foods: Mode of action and microbial resistance mechanisms. *Int. J. Food Microbiol.* **1999**, *50*, 1-7.
170. Sofos, J. N.; Pierson, M. D.; Blocher, J. C.; Busta, F. F., Mode of action of sorbic acid on bacterial cells and spores. *Int. J. Food Microbiol.* **1986**, *3*, 1-17.



---

## Summary

---

The increased consumer awareness of health-associated risks of synthetic preservatives along with increasing antimicrobial resistance drive research towards exploring new natural antimicrobial compounds. The Brassicaceae plant family is a potential source of new antimicrobials, e.g. as food preservatives. These plants abundantly produce glucosinolates (GSLs), which serve as precursors of antimicrobial isothiocyanates (ITCs), formed upon contact of GSLs and myrosinase. GSLs as well as ITCs are structurally diverse, differing in side chain configuration. The main aim of this thesis research was to explore the potential of ITCs as natural antimicrobials. For this, the production, the analysis, the reactivity, and the (quantitative) structure-antimicrobial activity relationships ((Q)SAR) of ITCs were studied.

In **Chapter 1**, the structural diversity, the occurrence, and the analysis of GSLs and ITCs were described. Furthermore, approaches to modulate structural diversity and content of GSLs in Brassicaceae seeds were explained. Lastly, the state-of-the-art of ITCs as new natural antimicrobial candidates was reviewed, also by considering their reactivity (i.e. electrophilicity).

In **Chapter 2**, simultaneous fungal elicitation and germination of Brassicaceae seeds was studied as an attempt to increase content and structural diversity of GSLs. Compositional changes of aliphatic, benzenic, and indolic GSLs of *Sinapis alba*, *Brassica napus*, and *B. juncea* seeds by germination and fungal elicitation were determined. *Rhizopus oryzae* (non-pathogenic), *Fusarium graminearum* (non-pathogenic), and *F. oxysporum* (pathogenic) were employed. Thirty-one GSLs were detected by RP-UHPLC-PDA-ESI-MS<sup>n</sup>. Aromatic-acylated derivatives of 3-butenyl GSL, *p*-hydroxybenzyl GSL, and indol-3-ylmethyl GSL were for the first time tentatively annotated and confirmed not to be artefacts. Germination alone increased total GSL content in *S. alba*, mainly consisting of *p*-hydroxybenzyl GSL, by 2- to 3-fold. Meanwhile, germination alone did not significantly affect total GSL content in *B. napus* and *B. juncea*. Regardless of the pathogenicity of the fungi, fungal elicitation did not increase the content nor the structural diversity of GSLs further than what could be obtained by germination alone.

In **Chapter 3**, a new method to simultaneously analyze various GSLs and ITCs by RP-UHPLC-ESI-MS<sup>n</sup> was described. The method was validated for 14 GSLs and 15 ITCs. It involved derivatization of ITCs with *N*-acetyl-L-cysteine (NAC). The limits of detection were 0.4–1.6 µM for GSLs and 0.9–2.6 µM for NAC-ITCs. The analysis of *S. alba*, *B. napus*, and *B. juncea* extracts spiked with 14 GSLs and 15 ITCs indicated that the method generally had good intraday (≤10% RSD) and interday precisions (≤16% RSD). Recovery of the method did not differ for each extract and was within 71–110% for GSLs and 66–122% for NAC-ITCs. The method was able to monitor the enzymatic hydrolysis of standard GSLs to ITCs in mixtures. Furthermore, GSLs and ITCs were simultaneously determined in Brassicaceae plant extracts before and after *in vitro* myrosinase treatment.

In **Chapter 4**, the antimicrobial activity (minimum inhibitory concentration, MIC; minimum bactericidal/fungicidal concentration, MBC/MFC) of 10 ITCs against

pathogenic and food spoilage Gram<sup>-</sup> bacteria, Gram<sup>+</sup> bacteria, and fungi was determined. The activity of the long-chained (C9) 9-(methylthio)nonyl ITC (9-MTITC), 9-(methylsulfinyl)nonyl ITC (9-MSITC), and 9-(methylsulfonyl)nonyl ITC (9-MSoITC) was determined for the first time. Due to the electrophilicity of ITCs, the activity of ITCs was evaluated in nucleophile-rich and nucleophile-poor growth media. ITCs reacted with components in a nucleophile-rich growth medium at a rate of 39-141  $\mu\text{M}/\text{h}$ , depending on their side chain configuration and temperature. The reaction rates were lowered by a factor of 2-21 when using nucleophile-poor growth media. Consequently, the activity of ITCs was generally improved, with MSITC and MSoITC being the most positively affected (activity increased by a factor of  $> 4$ ). 9-MSITC and 9-MSoITC had good activity ( $\text{MIC} \leq 25 \mu\text{g}/\text{mL}$ ) against Gram<sup>+</sup> bacteria and fungi. The short-chained (C3) analogues had good activity against Gram<sup>+</sup> bacteria and Gram<sup>-</sup> bacteria.

ITCs exhibit different antimicrobial activity, depending on their structure.

**Chapter 5** aimed at determining QSAR-based physicochemical properties of ITCs important for their antimicrobial activity and developing QSAR models to predict the activity of ITCs as individual and in mixtures. Twenty-six ITCs covering 9 subclasses were tested against *Escherichia coli* and *Bacillus cereus*. MIC (mM) and growth inhibition response (GIR, h/mM) were determined and used to develop QSAR models. The most active ITC subclasses were bifunctional ITC, MSITC, and MSoITC. MIC of the most active ITCs was 9.4-25  $\mu\text{g}/\text{mL}$  against *E. coli* and 6.3-25  $\mu\text{g}/\text{mL}$  against *B. cereus*. Multiple linear regression models were proposed with a good fit ( $R^2_{adj}$  0.86-0.93) and high internal predictive power ( $Q^2_{adj}$  0.80-0.89). Partial charge, polarity, shape, and reactivity were key physicochemical properties for antibacterial activity of ITCs. Furthermore, ITC compositions and antibacterial activity of Brassicaceae ITC-rich extracts were determined. *B. oleracea* ITC-rich extract, mainly comprising of short-chained (C3, C4) MSITCs, had MIC 750-1000  $\mu\text{g}/\text{mL}$  against both bacteria, and *Camelina sativa* ITC-rich extract, mainly comprising of long-chained (C9, C10, C11) MSITCs, had MIC 188  $\mu\text{g}/\text{mL}$  against *B. cereus*. Moreover, based on the ITC compositional analysis, the models successfully predicted the antibacterial activity of these extracts.

In **Chapter 6**, the main findings of this thesis were discussed. The approaches in compositional analysis and antimicrobial assays used in this thesis were examined. Prospective external ITCs, to be tested for the external validation of the QSAR models, were given in detail with their predicted activity. Some hints on mode of action of ITCs based on important QSAR-based physicochemical properties and previous studies were elaborated for future studies. Finally, the prospects of ITCs as natural food preservatives, considering their electrophilicity, pungency and bitterness, toxicity, and potential synergisms with other antimicrobial compounds, were elaborated.

In conclusion, the newly developed simultaneous RP-UHPLC-ESI-MS<sup>n</sup> analysis of various GSLs and ITCs is useful to monitor the *in vitro* enzymatic degradation of GSLs to ITCs in complex mixtures. Furthermore, this study confirms that ITCs

from subclasses MSITC and MSoITC had potent antimicrobial activity and, therefore, might be potential new natural food preservatives, but their reactivity with food matrix components should be considered. Furthermore, the QSAR models developed in this thesis can be applied to predict antibacterial activity of new ITCs and (natural) mixtures of ITCs. Overall, ITCs are promising natural antimicrobial candidates worth further studies.



---

## **Acknowledgements**

---

I am deeply grateful for the accomplishment of my PhD thesis. I realize that it is not of my strength. Every person present in my life during the past five years has coloured my PhD journey and made it enjoyable up to this final stage. Words are not enough to express how I am grateful.

I would like to express my sincere gratitude to FCH leaders: Harry and Jean-Paul, for giving me the opportunity to do a PhD at FCH. Special thanks to Jean-Paul for remembering me when I was in Indonesia and reminding me in 2014 about my dream to come back to FCH to pursue a PhD. Your guidance, patience, knowledge, and hospitality (together with Marian) to me (and Febi) during these 5 years were highly appreciated. Your critical input for my thesis chapters has sharpened my analytical thinking and broadened my view. Thank you very much for having been my daily supervisor and my promotor and for leading FCH group. My co-promotor, Carla, I was grateful that you became actively involved in my PhD project since May 2019. Your input was really progressing my thesis writing. I also appreciate that you were accessible at almost any time I needed. Additionally, thanks for introducing me to phytolab and FCH MLII lab in my first months, as well as for supervising my students in my absence.

My sincere gratitude also goes to all my other co-authors. Mark, thank you for your expertise in LC-MS techniques and your patience that helped me in the method development, and for ordering goods. Heidy, thank you for your advice and insightful comments in the field of microbiology and food safety, for your patience, and for providing microbial strains needed for my research. Jos, thank you for your willingness to collaborate in the last part of my research. Your expertise in statistics and your fast response sped up the finalization of my QSAR chapter. Pieter, Leonie, Gijs, Bianca, thank you all for all your effort in understanding the topics and generating good results during your MSc or BSc thesis, and for giving input to the manuscripts.

I would like to thank other people from the laboratory of Food Microbiology: Tjakko and Marcel Tempelaars, our discussion gave me ideas how to proceed my microbiological experiments; Ingrid, thank you for your technical support in providing bacterial strains, for the chat we had in the kitchen, and for your careful observation on me and everyone working in the kitchen to ensure the safety of everyone; Judith, thank you for your technical and scientific support in providing me fungal strains and introducing me to CBS website. I also enjoyed our time together in Advanced Fermentation Science practical course. Thanks to Eddy for organizing the course that I had pleasant times supervising students in the course and for your always kind and smiling face whenever we met.

Special thanks to all other FCH staff and Smaaklessen colleagues, thanks for sharing your knowledge and making FCH a pleasant working environment. To Peter Wierenga, thank you so much for connecting me to the laboratory of Animal Nutrition and our discussion about Ellman assay and amino acid analysis. Thanks to Annemiek for your readiness to perform the Ellman assay for me. To phyto people: Carla, Wouter (also for introducing me to FCH at the start of my PhD

journey), Anne, Renske, Roelant, Sylvia, Zhibin, Junfeng, Judith, Sarah, Annemiek, Pimvisuth, thank you all for sharing your knowledge in our phytomeeting and for your effort to make our lab tidy. Sylvia, thanks for chat, tears, and laugh you shared with me. To Peter de Gijssel, thank you for the GC-MS introduction, although at the end I did not use it for my PhD thesis. To both Peter and René, thank you for your help with troubleshooting of Tecan and Spectramax, and for placing my orders in the absence of Mark. To Edwin and Wouter Lubbers, thank you for sharing your office while I was working with MOE. To Marlies, thank you for your hospitality inviting me for a dinner with your family and Yvonne. I was pleased to be your Indonesian translator. To Mirjam and Annelou, thank you that I had a fun time organizing FCH Lab Trip 2016 with you. To Yuxi and Ginny, we met for the first time during our MSc study. Thank you for welcoming me back in Wageningen in 2015 with a nice BBQ, for a Chinese hotpot, for sharing bedroom during PhD trip, and for encouragement. To Ying, although we did not meet each other on a daily basis, but we spent much time together during PhD trips. From there, I got to know you and we kept in touch to the last days you were in Wageningen. To activity committees, lab trip committees, and PhD trip committees, thank you all for your effort and time to make FCH members get to know each other better, to maintain FCH's good working atmosphere, and to broaden FCH PhD students' network and horizon. Dear Jolanda, thank you so much for arranging things (visa, residence permits, booking big rooms for VLAG Dutch lessons and other social activities, booking my defence date, etc) so organized and efficient.

Special thanks to dear Anne for sharing your life with me as well as your baking hobby. Thank you for your (and Graham's) time to accompany me (and Febi) exploring London and for staying with us while you visited Wageningen.

Many thanks to my former students: Frederike Wiggers, Pieter Dekker, Hidde Berg, Shilu Chen, Leonie Waardenburg, Sjoera Tjin A-Lim, Aldo Mendoza Santiago, Gijs Vreeke, Kirsty Wu, and Bianca Lay. Thank you for your interest and dedication in my research. I was pleased to supervise you and learn from you all.

My (former) officemates: Elisabetta, Milou (also for visiting your parents' farm), Gijs van Erven, Cynthia, Yvonne, Jolieke, Wander, Dana, Natalia, Sarah, thank you all for the chat, help, encouragement, foods and drinks we had together. To my female officemates, thanks a lot for personal stuff and tears we shared one another. Dear Cynthia, thank you (and Bas) for your hospitality inviting me and Febi to your apartment and for our Monday lunches.

I am also grateful for other colleagues and students I met in courses and for VLAG PhD council mates 2016-2018.

Many thanks to Naomi and Sarah for being my paranymphs, and to Karin for designing the cover of this thesis.

My sincere gratitude goes to Satya Wacana Christian University, Faculty of Science and Mathematics, Department of Chemistry, the first place where I learned about research and teaching. Many thanks for supporting me to do a PhD.

To all Indonesian PhD students and postdocs in Wageningen 2015-2020: ci Melli, bang Audrie, teh Ais, mba Ita, pak Yo (kak Asmi, Benaya), Riahna, Steven (Litha, Gavriel), mas Ludi (mba Lia, Lova, Levi), Belinda, mba Suparmi, mba Hikmah, mba Linda, mba Titis, mba Nila, mba Nuning, mas Yuda, mas Taufik, Alim, mas Ayusta, pak Eko (mba Andra), pak Dikky, teh Novi, kang Indra, dll, terima kasih untuk kebersamaan dan perhatiannya selama di Wageningen.

Kak Tini and Enid, thank you for helping Febi look for a job in Wageningen when we just arrived in this town. Special thanks to Enid for bringing Febi to Rumah Kita, that he got a voluntary job there. I am also grateful for our fellowship. Octovina (Andy, Manoach, Davitha) and bu Seska (Hannah) whom Febi met in Rumah Kita, your warm hospitality stays in our hearts. Bersyukur juga untuk pertemuan kita di dalam Persekutuan. Kak Uli en bang Mario, terima kasih untuk perhatian, kunjungan ke Wageningen, dan perayaan tahun baru 2016 bersama di Tiel. Jeremiah-Rosalinde-Caleb-Tabitha, Koos-Carolien-Tom-Tijs-Chrisje, thank you so much for sharing Christmas time, dinner time with us at your homes. Pak Frits, Simon Last, Hans-Griet-Femke, Pak Chrisjan-Bu Marieke-Ruth-Aaron-Harmen, thank you so much for your help and hospitality. Christine and Rebecca, thank you for sharing your life with me in the fellowship. Ruri, terima kasih sudah jauh-jauh dari Salatiga mengunjungi kami dan ikut retreat Paskah (EBR) bersama.

Syukur yang tak terkatakan untuk keluarga baru (ekkklesia) yang dianugerahkan-Nya di Wageningen: mas Anto, mba Ita, Ehre, Naomi medior, Hugo, Tya, Naomi, Karin, Fani, dan Beta. Fani dan Beta, semoga kita boleh dipertemukan-Nya lagi. Sungguh bersyukur untuk kehadiran Pak Anton dan Ibu Isti, untuk kasih, perhatian, dan dukungan yang terlihat maupun tak terlihat kepada kami. Bersyukur untuk pertemuan dengan ci Melli, bang Audrie, Mary, Marlin, Raka, Rocky, Fahrell, Hendy, Dian, Frances, Kevin, Julius, Yosi, Windy, Tiffany, Irene, Angela, Jessica, dll, di Persekutuan di Wageningen maupun EBR. Bersyukur untuk pertemuan dengan ci Anita, ko Johan, ci Lusi, ci Ahun, ko Dennis, ci Tannie, ko Khai Ming, ci Melisa, ko Yosia, ci Lili, ci Siany, ci Ros, ko Handri, ci Wiwi, Jaklyn, Robert, Vicky, bu Nawang, ci Siska, ci Veivei, ko Justin, ci Rina, ko Benji, ko Chandra, Devi, Rio, Jenny, Samantha, Adi, Gene, Bri, Ivan, Andre, Kartika, Fani, Selfina, dan semua anak-anak. Terima kasih untuk dukungan, semangat, perhatian, keceriaan, dan nasihatnya. Mengerjakan S3 menjadi terhibur dan dikuatkan.

Papa dan mama, pi dan mama, ko Yung, ce Lina, ce Ching, ko Yance, Sela, Daniel, Tata, Delin, Calvin, Yuli, Andy, dan semua sanak saudara di Indonesia, terima kasih banyak untuk dukungan dan perhatiannya. Mohon maaf kalau kami tidak bisa berada dekat. Semoga kita semua diberikan kekuatan, kesehatan, dan kesempatan untuk bisa bertemu kembali dalam keadaan yang lebih baik.

Febi Christian, terima kasih untuk suka duka dilalui bersama 5 tahun di Wageningen ini, untuk dukungan, perhatian, kesabaran, kesetiaan, dan kasih sayang. Semoga kasih dan sukacita ditambahkan-Nya dalam rumah tangga kita.

Silvia Andini

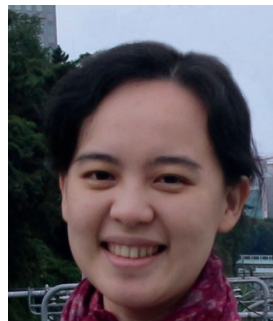
---

## **About the author**

---

## Curriculum vitae

Silvia Andini was born on April 21, 1988 in Curup, Indonesia. In 2005, she started her study in Chemistry at Satya Wacana Christian University (SWCU or UKSW), Salatiga, Indonesia, with a specialization in Food Chemistry in the last year of the study. Her bachelor thesis focused on the effect of light intensity on the color of bread naturally colored by carrot juice. In 2009, she graduated with honours and began to work as a teacher at SWCU. In 2011, she received a scholarship from Evangelischer Entwicklungsdienst, Germany, to pursue an MSc study in Food Technology with a specialization in Food Ingredient Functionality, Wageningen University, the Netherlands. Her thesis focused on the effect of germination and fungal elicitation on prenylated (iso)flavonoid compositions of 22 legume species. The thesis was performed at the Laboratory of Food Chemistry, Wageningen University. As part of her MSc study program, she did an industrial internship at Food Structuring group of FrieslandCampina Research, Deventer, the Netherlands, where she studied the effect of shear on milk fat crystallization. After graduating with honours in 2013, she recommence her work at SWCU as a lecturer. In 2015, she started her PhD research at the Laboratory of Food Chemistry. The results of her PhD research are presented in this thesis.



Contact: [silviaandini88@gmail.com](mailto:silviaandini88@gmail.com)

## List of publications

**Andini, Silvia**; Araya-Cloutier, Carla; Lay, Bianca; Vreeke, Gijs; Hageman, Jos; Vincken, Jean-Paul. 2020. QSAR-based physicochemical properties of isothiocyanate antimicrobials against Gram-negative and Gram-positive bacteria. *Submitted for publication*.

**Andini, Silvia**; Araya-Cloutier, Carla; Waardenburg, Leonie; den Besten, Heidy M. W.; Vincken, Jean-Paul. 2020. Isothiocyanates as natural broad-spectrum antimicrobials. *LWT-Food Science and Technology* 134: 109843.

**Andini, Silvia**; Araya-Cloutier, Carla; Sanders, Mark; Vincken, Jean-Paul. 2020. Simultaneous analysis of glucosinolates and isothiocyanates by RP-UHPLC-ESI-MS<sup>n</sup>. *Journal of Agricultural and Food Chemistry* 68(10): 3121-3131.

**Andini, Silvia**; Dekker, Pieter; Gruppen, Harry; Araya-Cloutier, Carla; Vincken, Jean-Paul. 2019. Modulation of glucosinolate composition in Brassicaceae seeds by germination and fungal elicitation. *Journal of Agricultural and Food Chemistry* 67(46): 12770-12779.

Aisyah, Siti; Vincken, Jean-Paul; **Andini, Silvia**; Mardiah, Zahara; Gruppen, Harry. 2016. Compositional changes in (iso)flavonoids and estrogenic activity of three edible *Lupinus* species by germination and *Rhizopus*-elicitation. *Phytochemistry* 122: 65-75.

Aisyah, Siti; Gruppen, Harry; **Andini, Silvia**; Bettonvil, Monique; Severing, Edouard; Vincken, Jean-Paul. 2016. Variation in accumulation of isoflavonoids in *Phaseoleae* seedlings elicited by *Rhizopus*. *Food Chemistry* 196: 694-701.

## Overview of completed training activities

### Discipline specific activities

#### Courses

Food and biorefinery enzymology	VLAG, Wageningen, 2015
Food fermentation	VLAG, Wageningen, 2016
Genetics and physiology of food associated microorganisms	VLAG, Wageningen, 2016
International chemical design and discovery course	CMBI, Nijmegen, 2016
Advanced food analysis <sup>a</sup>	VLAG, Wageningen, 2016
Introduction to R	VLAG, Wageningen, 2018
Applied statistics	VLAG, Wageningen, 2018
Chemometrics	VLAG, Wageningen, 2018

#### Conferences

Wageningen Indonesia Scientific Exposure 2017 <sup>a</sup>	WISE, Wageningen, 2017
Advances in phytochemical analysis (Trends in natural product research) <sup>b</sup>	PSE, Liverpool, 2018
Wageningen Indonesia Scientific Exposure 2019 <sup>b</sup>	WISE, Wageningen, 2019

### General courses

VLAG PhD week	VLAG, Baarlo, 2015
Project and time management	WGS, Wageningen, 2016
Philosophy and ethics of food science and technology	WGS, Wageningen, 2016
Scientific publishing	WGS, Wageningen, 2016
The essentials of scientific writing & presenting	WGS, Wageningen, 2017
Scientific writing	WGS, Wageningen, 2018

### Optionals

Research proposal preparation	FCH, Wageningen, 2015
PhD study trip 2016 <sup>a,b</sup>	FCH, Japan, 2017
PhD study trip 2018 <sup>a,b</sup>	FCH, Italy and Austria, 2018
BSc and MSc thesis student supervisions, presentations, and colloquia	FCH, Wageningen, 2015-2019
PhD presentations	FCH, Wageningen, 2015-2019
VLAG PhD council	VLAG, Wageningen, 2016-2018

---

<sup>a</sup> Poster presentation.

<sup>b</sup> Oral presentation.

Abbreviations: CMBI, Center for Molecular and Biomolecular Informatics. FCH, Laboratory of Food Chemistry, Wageningen University. PSE, Phytochemical Society of Europe. VLAG, Graduate School for Food Technology, Agrobiotechnology, Nutrition, and Health Sciences. WGS, Wageningen Graduate Schools.





The research described in this thesis was performed at the Laboratory of Food Chemistry, Wageningen University & Research, the Netherlands, with a financial support by Indonesia Endowment Fund for Education (LPDP), Ministry of Finance, Republic of Indonesia.

Financial support from Wageningen University for printing this thesis is gratefully acknowledged.

Lay out by Silvia Andini

Cover design by Karinska Eunike Muis and Silvia Andini

Printed by Digiforce-Proefschriftmaken.nl

Edition: 250 copies

Silvia Andini, 2020



